AD 255830

DISCLAIMER NOTICE

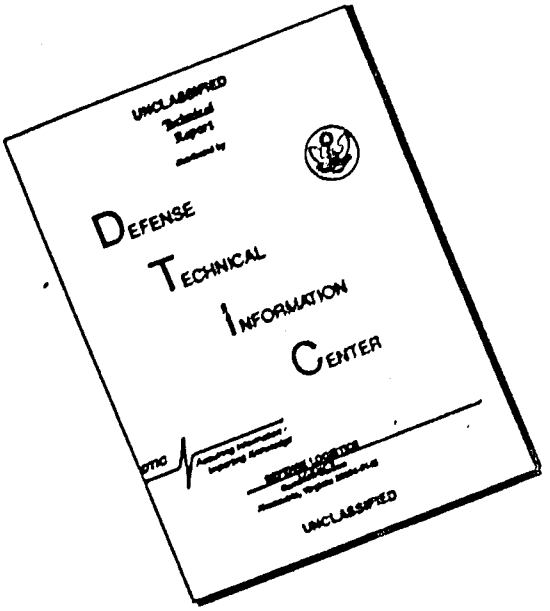

THIS DOCUMENT IS BEST QUALITY AVAILABLE. THE COPY FURNISHED TO DTIC CONTAINED A SIGNIFICANT NUMBER OF PAGES WHICH DO NOT REPRODUCE LEGIBLY.

SECOND SYMPOSIUM
ON
ADVANCED PROPULSION CONCEPTS

VOLUME I

OCTOBER 1963

BOSTON, MASSACHUSETTS


FILE CO
Return
AST
ARLINGTON
ARLINGTON
Attn
ASTI
MAY 12 1961
TIPDR
7161-3-1
XEROX

VOLUME I

PROCEEDINGS OF

SECOND SYMPOSIUM
ON
ADVANCED PROPULSION CONCEPTS

SPONSORED BY

AIR FORCE OFFICE
OF
SCIENTIFIC RESEARCH (ARDC)

AND

AVCO - EVERETT RESEARCH LABORATORY
A DIVISION OF AVCO CORPORATION

7 - 8 OCTOBER 1959
STATLER HILTON HOTEL, BOSTON, MASSACHUSETTS

These proceedings are published in three volumes. Volume I contains unclassified sessions; Volume II, sessions classified CONFIDENTIAL; Volume III, sessions classified SECRET - RESTRICTED DATA.

PREFACE

The Second Symposium on Advanced Propulsion Concepts was held at the Statler Hilton Hotel, Boston, Massachusetts, October 7 - 8, 1959. Co-sponsors were the Air Force Office of Scientific Research (ARDC) and the Avco-Everett Research Laboratory, a division of Avco Corporation. Chairmanship of the Symposium was shared by Lt. Colonel Paul G. Atkinson, USAF, Chief, Propulsion Research Division, Air Force Office of Scientific Research, and Dr. Mac C. Adams, Deputy Director, Avco-Everett Research Laboratory. Some 650 scientists, engineers and other technically qualified people attended.

The program was made up of seven technical sessions which included a wide range of subjects related to advanced propulsion systems, and an eighth session devoted to a panel discussion of "Progress in Propulsion." On the evening of October 7 a dinner meeting was held at the Statler Hilton Hotel. The guest of honor was Brig. General Homer A. Boushey, USAF, Director of Advanced Technology, United States Air Force. Professor Thomas Gold, Chairman of the Astronomy Department and Director of Radio Astronomy, Cornell University, was the guest speaker.

On behalf of the Air Force Office of Scientific Research and the Avco-Everett Research Laboratory, thanks are extended to all those individuals and agencies whose cooperation made this Second Symposium possible. Special appreciation goes to the authors who created the written material and presented it in person at the meeting, and to the participants in the various discussion periods for their patience and cooperation in editing their comments.

Thanks also are due to the following persons who helped in editing these proceedings and in preparing them for publication: Captain Russell G. Langlois, USAF, Air Force Office of Scientific Research; Mr. Vincent J. Coates, Jr., Miss Joan McGonagle and Mr. Joseph Spatola of the Avco-Everett Research Laboratory.

The proceedings are published in three volumes. Volume I contains unclassified sessions; Volume II, sessions classified CONFIDENTIAL; Volume III, sessions classified SECRET-RESTRICTED DATA.

TABLE OF CONTENTS

VOLUME I

VOLUME II

VOLUME III

SECOND SYMPOSIUM

ON

ADVANCED PROPULSION CONCEPTS

Address by

Brig. General Benjamin G. Holzman, USAF

Commander, Air Force Office of Scientific Research

It is with a great deal of pleasure that I take this opportunity to convey to you some of my thoughts and feelings on this, the Second Symposium on Advanced Propulsion Concepts.

Almost two years ago, on 11 December 1957, the Air Force Office of Scientific Research joined with the Rocketdyne Division of North American Aviation in holding the First Symposium on this subject. The Russians were good enough to insure wide interest in that symposium by firing Sputnik I. The fact that this was not a coincidence is now established by the successful firing of Lunik II to focus attention on this, the Second Symposium on Advanced Propulsion Concepts. The large turnout must be gratifying to the Russians.

The sole mission of my organization is the support of basic research, the purpose of which is to increase the Air Force capability by taking advantage of new ideas for the development of more effective weapon systems. Although we are concerned primarily with the understanding of basic principles, we find it useful to take stock, occasionally, of those to which the knowledge has been put and at the same time to get some idea as to which of the many unanswered questions should be tackled first. In other words I, for one, have no doubt but what the discussions of the next two days will further substantiate the reciprocal relationship between basic research and technological progress.

Tomorrow afternoon I will have a few words to say about the impact of progress in propulsion technology. Now, however, I would like to take just a few moments to point out the way in which basic research affects technological progress in propulsion. I will not belabor the idea that, without understanding, progress is at best extremely slow. Rather, I prefer to call your attention to specific cases.

You all know how the study of molecular bond energies led to the development of high energy chemical fuels and how the study of nuclear binding energies led to nuclear reactors. What all of you may not be aware of, however, is that the understanding of chemical kinetics and aerodynamics has increased flame speeds and stability to the point we are now able to consider the practicability of detonative combustion for hypersonic ramjets, and that the increased understanding of matter in the solid state has already pushed the temperature barrier back with more significant success yet to come. The development of photoelectric and thermoelectric energy converters can be directly attributed to the results of basic research in solid state physics. Finally, I would like to call your attention to the way in which basic studies of the properties and behavior of plasmas -- called by some, the fourth state of matter -- have stimulated creative minds to produce concepts with application possibilities ranging from thermonuclear reactors through energy converters to thrust devices.

These are but a few of the more obvious examples of the way in which understanding of phenomena leads to their utilization. I am sure that you can think of many more.

The Air Force Office of Scientific Research owes its existence to the fact that the Air Force is aware of the practical value of basic research. It is my hope that industry is equally aware of its value and will continue to join with us, as has AVCO and others, in the effort to make an environment in which penetrating analysis and definitive experimentation will flourish.

There is just one more thought that I would like to leave with you. As you listen to and partake in the discussions to follow, I am sure you will agree that we cannot afford the luxury of being skeptical of new ideas. Not only must we estimate the probability of successful application, we must also try to determine if the probability is small because of the limitations imposed by the state of the art or because of some well established natural laws. If it is the former, we must improve the state of the art. If it is the latter, we might well put our efforts elsewhere -- at least until the laws are repealed.

Certain key people are responsible for the symposium. I want to thank especially Dr. Arthur Kantrowitz and all of his staff, and Colonel Atkinson and Dr. Slawsky of my office, who made the technical arrangements for the program. I think they did a very fine job on this. I also want to thank Mr. Vincent J. Coates, Jr. of Avco-Everett Research Laboratory who is intimately involved with the arrangements. Two young ladies with good Irish names - Miss Joan McGonagle and Miss Anne O'Neill - are handling security and other matters in connection with this symposium and deserve our appreciation.

Thank you.

Address by

Lt. Colonel Paul G. Atkinson, USAF

Chief, Propulsion Research Division
Air Force Office of Scientific Research

Before proceeding with the technical sessions, I would like to make a few comments on the Second Symposium on Advanced Propulsion Concepts. The structure of the meeting, if you will note, is based upon concepts which have received a certain amount of engineering feasibility study. Some have been extensively treated. Not all have been established as feasible. By and large the concepts covered in this Symposium are past the purely hypothetical stage, however, and I think most of them are in the foreseeable future. We have not included in the agenda anything on stabilized free radicals. The consensus at this time is that we do not now have enough basic knowledge to establish their engineering feasibility as high energy propellants. However, the accelerated program which has been underway for three years has better defined the scientific problems which still have to be solved.

There are a number of studies underway on atmospheric free radicals for propulsion, and these at the present time indicate that this concept is marginal at best.

On solar ramjets, there was a study made a year or so ago, which I believe, concluded that on the basis of our present knowledge of structures, heat transfer, and solar energy conversion, this concept is not feasible.

Fusion propulsion appears to be some distance off, and in assembling an agenda we were not aware of any recent studies of the application of fusion to propulsion. Anti-gravity and anti-matter are certainly interesting possibilities, but we have not really been able to come to grips with them to date.

In planning the contents of this agenda, we felt that in the hypersonic air breathing area there are some new avenues opening which we would like to explore. We wanted to touch base with the large rocket effort, because certainly this is the backbone of the missile and space flight programs.

From the projects in synthesis of high energy solid propellants, we invited papers on two efforts which seem to offer ten percent better performance than conventional propellants and which are fairly far along. The tempo of activity in solid propellant research has recently increased, although much of it is still devoted to study of bond energies and the chemistry of high energy compounds.

In the field of high energy liquid propellants, we want to take a look at the exotics and the novel idea which has recently come down the road involving something other than the conventional fuel and oxidizer combination.

In the area of electrical propulsion, there are a variety of efforts underway including arc heaters, ion rockets, plasma accelerators, and charged colloids.

No consideration of the propulsion spectrum would be complete, of course, without looking at the possibilities of nuclear fission and the family of concepts

which are being investigated at this time. Nuclear fission is likewise pertinent to space power, and surveys in the space power session will cover both low power and high power sources.

After examining the state of propulsion science and technology, we have planned a philosophical look at propulsion from the point of view of research, development, and the operational commands, together with the economic frame of reference, the perspective of the historian, and that of the newsman.

"Space Research" by

Professor Thomas Gold

Chairman of the Astronomy Department, Director of Radio Astronomy
Cornell University

(Presented at Dinner Meeting of Second Symposium on Advanced Propulsion Concepts, 7 October, 1959)

Many people are aware of the great importance of rocketry and space research in terms of military power, in terms of national prestige, and from the point of view of the great amount of new knowledge that will be gathered about the nature and origin of the universe by these new techniques. This country and others too are aware of all this at the present time. Does this assure that the space age is coming? Can one be sure that very large sums of money will continue to be made available as they are needed for the massive technology to take us into space? Can we be sure that the attention will remain focused in this direction or will the interest wane before the main results are achieved?

The first Sputnik was a great prestige weapon. Whether we like it or not, the prestige stakes will get higher and higher as the space achievements increase: When the day comes that real expeditions of many people can be sent to the Moon or Mars, it will be a matter of great consequence to international politics which nation is then in the lead. Prestige is hardly the word to express the great influence in the psychological war of our day which such events will have. And psychological warfare tends to be the most important kind in the long run. I feel confident that the people of the United States will sense this situation and will be willing to follow the lead which the government will plainly recognize to be its obligation to give. So I think space research will continue at a high priority for a long time.

With the situation reasonably secure as I see it, science can thus look ahead to a long period of reaping the fruits of space technology. What will those be? A well known British astronomer, when asked about a year ago to advise concerning the future of space research, declared that the scientific prospects were confined to two subjects: Certain aspects of geodesy which, however, could be done more cheaply from the ground; and an examination of the ultraviolet spectrum of the sun which, however, cannot be done well from as unsuitable a platform as a rocket. That is all. I predict that this statement will one day be a most valuable collector's item.

My own view is about as far from that one as one can get. Rather than give you a survey of all the speculation concerning the discoveries that will be made - and I am sure you have often heard such speculations - I will discuss as an illustration just one particular subject. Let us see what kind of information we may expect that will solve the problem of the origin of the solar system.

The question of the origin of the solar system has been discussed more or less in modern terms for about 150 years now, and although it has become possible in recent times to limit the possibilities and to define the requirements of a theory very much more closely, a really definitive answer is still missing. Yet, there are many fascinating clues that spur one on, that seem to place the final answer not very far out of sight.

The first step in any discussion is usually how it should have come about that the great majority of the angular momentum of the system is concentrated in the planets which constitute only such a very small fraction of the mass. 0.1 per cent of the mass of the system, namely the planets, contain 98 per cent of the angular momentum. No change in these proportions can be envisaged as occurring once a planetary mass is in concentrated bodies and, of course, no change in the total angular momentum of the whole system can occur at all. The distribution of angular momentum is, therefore, clearly a consideration that refers to circumstances in an earlier epoch of the system before the condensation of the planets.

The Sun belongs to the class of stars that rotate slowly. There is quite a sharp division between the two classes, and the fast rotating stars possess an amount of angular momentum per unit mass which is of the same order as the mean in the solar system. In other words, if a star like the Sun had given most of its angular momentum to a planetary disc which subsequently developed into planets, one could suppose that it was initially in the class of fast rotators. This then gives the exciting possibility that all stars commence life as fast rotating ones and that the entire class which we now see by spectroscopic methods to be rotating slowly is in fact in possession of planetary systems.

When we discuss the ways in which stars might form out of the interstellar gas, we always arrive at the conclusion that they ought to be rotating very fast, and no way can be seen in which the slowly rotating stars could be set up directly. From this point of view, therefore, it would also be much preferable to think of the class of fast rotating stars as being the initial one.

If all the slowly rotating stars have planetary systems, this would imply a number of the order of 10^{10} planetary systems in our galaxy alone. In the hundreds of millions of other galaxies whose light reaches us in measurable amounts, there would be numbers of planetary systems of the order of 10^{18} or 10^{19}. Is there life on each one of them? Or on most of them? Or perhaps it is very unlikely for life to develop and it occurs on only one in a million of them, and then there are still 10^{12} places on which it has occurred. Who knows?

How could such a redistribution of angular momentum between the sun and a gaseous disc around it take place? We now understand that magnetic fields originating from the Sun could provide this coupling, and such a coupling would have the specific result of slowing up the Sun's polar regions more than the equatorial ones. This is just what is observed. Where space research comes into the picture here is in the attempt to see the magnetic coupling at work at the present time. It is true that by now only a small fraction of the gas remains in interplanetary space of the amount that must at one time have been present to make the

planets. Nevertheless, we would expect to see the magnetic coupling still occurring in this small remainder, and we might still recognize the tail end of the process at work now. This information would come from a measurement of the magnetic fields and the streaming velocities that now occur in the interplanetary gas. If the process were confirmed it would be a vital step in the understanding of the origin of the solar system and it would greatly strengthen the estimate of the probability that I have given concerning the enormous numbers of planetary systems that might exist in the universe.

That is what the investigations of the gas in the solar system might do to the origin theories. The investigation of the moon is probably the most important one for the understanding of the manner in which the condensation into solid objects occurred. We are familiar with the geologocial record on the earth describing the processes of erosion, mountain building, sedementation, and volcanism. So much has happened on the surface of the earth for such a long time that information about an earlier phase can no longer be found. On the moon the situation is quite different. There the processes that have shaped its present surface are slower by a very large factor, and the geology of the moon is likely to be a record of the history of the solar system. When the day comes that we can mount an expedition to go there and analyze the surface of the moon in detail, we shall be able to read this record. Long before then, from close approaches or instrumented landings, we shall get some very interesting individual items of information; but not, I think, the whole story that could be seen if one could walk over the countryside and pick up a piece here and there, or dig down a little way in places that look interesting, or do any of the many things that a geologist would do in a new region on the earth that he is investigating.

The investigation of Mars will be dominated by the problem of the origin of life. The work of Sinton has made it appear very probable that at least plant life exists on Mars and that the dark regions whose color changes seasonally derive their dark color from vegetation. When we can investigate samples of Martian life, we shall be able to see how similar or dissimilar it is to ours on earth. Will the molecules all show the same symmetries as they do on earth, or will the mirror images of the same molecules be represented there? In the former case, one might suspect a common origin for the life on Mars as on earth. In the latter, that would be definitely excluded. Perhaps other amino acids that do not occur in terrestrial life occur there, in which case again a different origin would be suspected.

So long as we only know of the occurrence of life on our own earth, we cannot really make a judgement of the probability of the origin of life. There might be billions and billions of other planets, but it might be thought it was only on ours on which this exceedingly unlikely event took place, and it is for that reason that we are here and not elsewhere. If we found that a rather similar form of life originated independently on Mars, we would have quite a different understanding of the probability of this event. If the original event was very unlikely, then why should it have occurred just on our neighbor?

The other possibility of an obviously similar form of life on Mars in which all the same molecular symmetries are found and all the same compounds are represented, would be equally exciting. This would clearly make a strong case for common origin and it would force us to look at mechanisms for transferring at least microbiological organisms without destruction from one planet to another. We might think in terms of some events in the solar system that could do it, or we might think on a yet grander scale of some way in which, perhaps very rarely, some contamination is distributed within the galaxy from one planetary system to another. The space travellers from other planetary systems are not likely to be coming here just now, but, did they leave behind an amoeba the last time they came a thousand million years ago?

The conclusions when this piece of space research has been done may well be that planets and life are common. How important would it be to know that? How much money, how much effort should be spent to secure this information? I personally cannot think of any kind of information that I would value more highly.

For the whole job one will, of course, want very much more than the kind of space payloads one is talking about at the present time. We shall want real space ships weighing perhaps hundreds of tons so that expeditions with all the equipment could go out. I am confident that this will one day be possible, and it seems to me that if one has this confidence, one might proceed in a different way with the technology. If it became known tomorrow that some other nation had launched a gigantic space ship with 30 people aboard to land on the moon and come back, but if no information was revealed as to how they had done it, I am quite certain that the influence on space technology would nevertheless be tremendous. One would suddenly be willing to proceed in a big way with the really large projects and one would attempt to leapfrog the slow step-by-step evolution of technology which is the common practice in engineering. Now, of course, we do not actually have this information, so we would not be entitled to stop a safe and gradual method. But, at the same time if we have confidence that the other will be done one day, perhaps we should start now with the gigantean schemes as well. Certainly they will be wanted and they will be built one day. The gains in starting these schemes sooner and therefore completing them sooner will be enormous.

ELECTRICAL PROPULSION CONCEPTS

CHAIRMAN

ROBERTSON YOUNGQUIST

ADVANCED RESEARCH PROJECTS AGENCY

DEPARTMENT OF DEFENSE

574071 O - 60 - 2

ROBERTSON YOUNGQUIST (Chairman)

This afternoon we will put our attention on a new class of advanced propulsion systems, a class of which first it might be said is so advanced that none has ever been built. This applies to some of the other systems we have heard of today, too, such as million-pound solid rockets. It might also be said that electrical rocket propulsion systems are so advanced that they can't even begin to lift their own weight, nor can they accelerate anything at more than one ten-thousandth of a g or so. This also sometimes applies to more conventional systems, when they do not work. It might be said thirdly that electrical rocket propulsion systems are so advanced that they will not work unless they are, essentially, out of the earth's atmosphere and into the vacuum of space. This, perhaps, is what makes them advanced in the different sense from other systems we have been hearing about and will hear about.

Despite these limitations, there do appear to be real potential uses for electrical propulsion devices, and we will hear to some extent this afternoon what these uses are. However, the main aims, I think, of the afternoon's session are to get acquainted with some of the kinds of electrical rocket propulsion thrust device concepts which have appeared, to get acquainted with their problems, and to get acquainted with their research and development status.

The class might be defined as propulsion devices in which electrical energy, supplied in some form, from some source, is employed to accelerate and eject matter which has been carried aboard the vehicle. This end between the source of energy and the, shall we call it, working fluid provides in practice one great virtue and one rather unfortunate deficiency in this class of propulsion. The virtue is that by being able to apply tremendous accelerating powers to small masses of matter, tremendous jet velocities or tremendous specific impulses can be achieved. And the deficiency, of course, is that in general the mass of the power supply unit which has to be carried with and propelled by our thrust device is orders of magnitude heavier than the thrust developed.

The kinds of electrical rocket thrust devices are numerous. I think a thumb-nail morphology might be helpful just to indicate that today we are only going to take a sample. First of all, you presumably can have as your expellant or working fluid practically anything--a liquid, a solid, a gas, or a plasma. Second, this matter may be accelerated thermodynamically (as by heating), electromagnetically, electrostatically, or by combinations of these. And, third, the cycle may be either continuous, intermittent, or fluctuating. This gives a rough idea of conceivable systems falling into this class.

THE ARC JET

by

GABRIEL M. GIANNINI

PLASMADYNE CORPORATION

ABSTRACT

Space flight propulsion studies definitely indicate that for practically all space missions electrically driven rockets offer a substantial saving in mass over chemical rockets.

Furthermore, if these studies are limited to satellites and Moon missions, they show that the most advantageous specific impulses are in the 2000-3000 second range. Thus, the arc jet becomes definitely suitable for this kind of application.

The following paper first presents the results of typical mission studies and subsequently outlines the analytical and experimental work conducted to develop the plasma jet as a means of propulsion.

The results of the various phases of the program are presented and discussed following the same chronological sequence in which they were obtained.

On the basis of these results a plasma-propelled space ship appears a feasible task.

INTRODUCTION

With the development of nuclear power and methods for the conversion of solar radiation to electrical power, immense quantities of energy have become available for the propulsion of space vehicles. Although this energy is available at relatively modest power levels, the total amount of energy obtainable is for practical purposes limited only by the life that can be built into the equipment. For example, a power plant weighing 10 lb/kw and capable of 1000 hours operation would in its lifetime produce 341,000 Btu/lb of power plant. This compares to 5800 Btu/lb available when energy is obtained by the combustion of hydrogen and oxygen. Notice that this comparison becomes more favorable as the operating time is increased.

To take advantage of these large amounts of energy, it is necessary to produce jet velocities that are much higher than can be obtained with chemical rocket engines. Otherwise, the large weight of propellant required would offset the advantage of the light weight energy source.

The arc jet is a promising device for this application. It consists of a chamber in which the propellant is heated by an electric arc followed by a nozzle in which the hot gas expands to form a high velocity jet.

High jet velocities are attainable because the temperature of the gas can be high and because a propellant of low molecular weight may be selected. The purpose of this paper is to report on some recent and contemplated developments in the arc jet field and to comment on the types of missions where the arc jet should find application.

APPLICATIONS

Any study to determine suitable applications for the arc jet must be re-evaluated as the development of competing propulsion systems proceeds. However, the rough studies that are possible at present provide valuable guidance. For simplicity, we will assume that the propulsion systems, complete except for propellant, have the same weight per unit of kinetic energy in the jet for all systems considered. For this paper, the weight will be taken as ten lb/jet kw. The range of specific impulses which can be obtained with good performance will be taken as up to 2000 seconds for the arc jet. For comparison, ideal chemical rockets are assumed to have a specific impulse of 400 seconds and to have no engine weight.

The simplest way to choose suitable applications for the arc jet is to look at some specific missions. Figure 1 shows performance for a series of satellite orbit changes. The vehicle starts at a circular orbit at 1.1 times the earth's radius and spirals out to orbits at various radial positions. This family is fairly representative of requirements that may be encountered in changing satellite orbits. The figure shows total initial vehicle weight as a ratio of payload weight plotted versus operating time required to complete the change in orbit. The word payload is used herein to mean all of the vehicle weight that is not included as part of the propulsion system. Each point on the curve was determined using the specific impulse necessary to minimize the weight ratio. The specific impulses used are identified by contour lines. Notice that the arc jet provides the lightest system for making the orbit change if the change must

be effected in 10 to 13 days, or less. If longer time periods may be used, some saving in weight may be realized by using higher specific impulses, provided devices are available to supply the higher jet velocities with performance comparable to the arc jet in other respects. Note that an arc jet system can result in a propulsion system weight which is about 35 per cent of the weight that would be required with an ideal chemical rocket. This assumes that the power plant is used only for the propulsion system and is therefore completely chargeable to it.

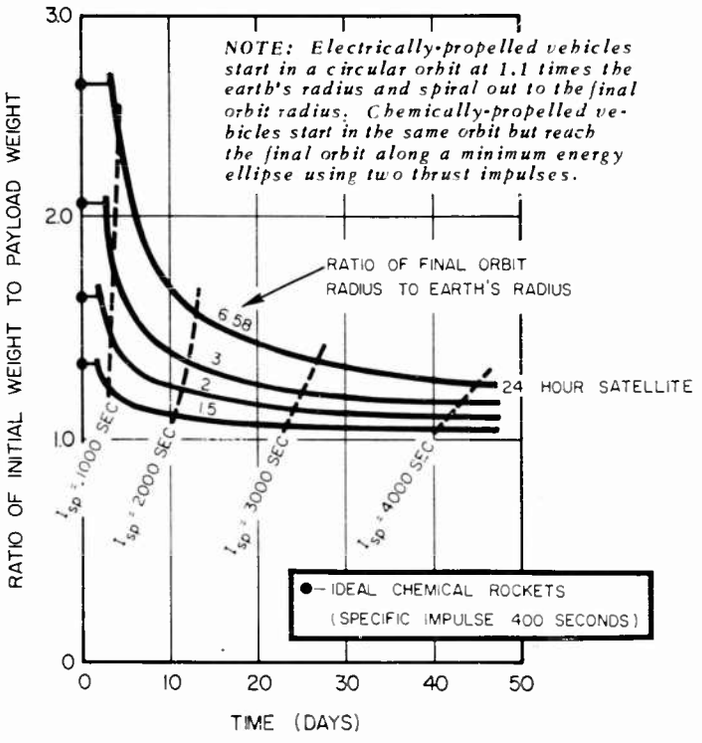

Fig. 1 Performance of Optimum Electrical Propulsion Systems for Changing Satellite Orbit Radius

Figure 2 shows the performance of a series of vehicles designed to make a one-way trip to the Moon. Each vehicle starts in a circular orbit at 1.1 times the earth's radius and spirals out until it has sufficient energy to reach the Moon along a minimum energy ellipse. As the vehicle approaches the Moon, the propulsion system is again put in operation and it spirals in to a circular orbit at 1.1 times the Moon's radius. Such a vehicle could be used either as a Moon probe or as a one-way cargo carrier. The ratio of initial weight to payload weight is again plotted as a function of the time required to complete the mission. In this case, the arc jet is superior if the mission must be completed within 21 days while higher specific impulses would be desirable if a longer duration for the trip is acceptable. The actual operating time for the 21-day Moon trip is about 14 days.

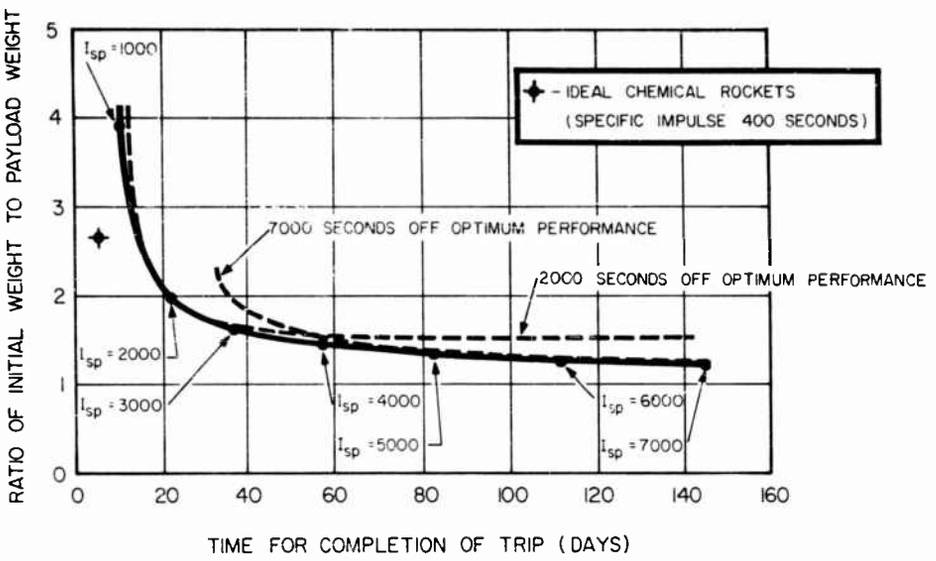

Fig. 2 Performance of Optimum Electrical Propulsion Systems for a One Way Trip to The Moon

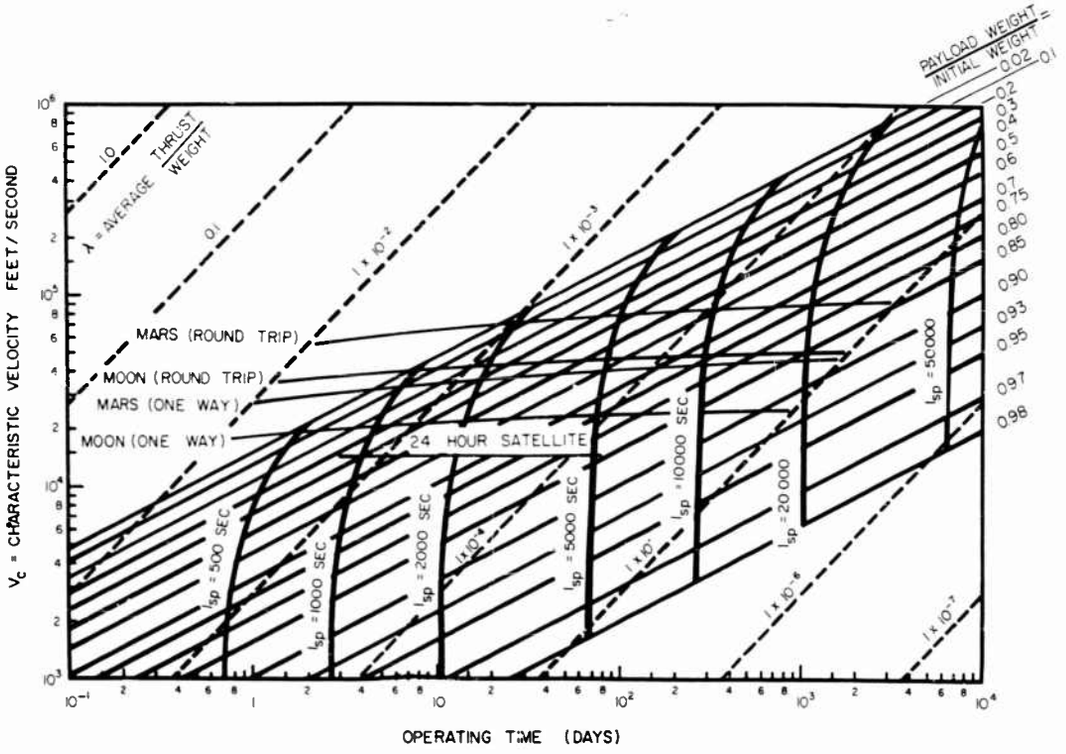

Fig. 3 Optimum Performance of Electrical Propulsion Systems (With αj = 10LBS / KW)

A similar analysis can be made for any desired mission and it can be shown that the arc jet fits whenever the operating time must be limited to a time period which varies from 10 to 20 days. This is better shown in Figure 3 which presents the results of a general analysis which gives the performance of a family of vehicles all using the specific impulse necessary to minimize the initial vehicle weight. Notice that the operating time required for optimum performance increases rapidly with increasing specific impulse. For example, a 7000-second ion rocket with an optimum ratio of power plant weight-to-propellant weight would require about 153 days to produce the same velocity change obtainable with a 2000-second arc jet in 20 days. These long operating times may be acceptable for interplanetary missions where the total mission time is necessarily long in any case. As an example of this, Figure 4 shows initial weight versus mission time for a family of vehicles making a one-way trip to Mars along a minimum energy path. The resulting saving in total time using the arc jet is not justified when its weight is compared to the weight of the higher specific impulse systems for this mission.

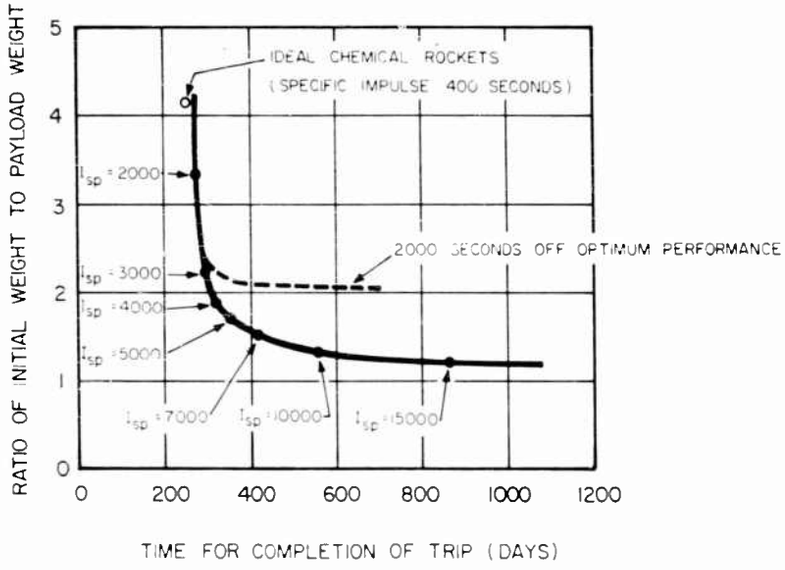

Fig. 4 Performance of Optimum Electrical Propulsion Systems for a One Way Trip to Mars

We can now conclude that the arc jet best fits missions to the Moon and missions requiring a change in satellite orbit whenever it is important to complete the mission in a relatively short time (operating times of 10 to 20 days, or less). If the power plant weight differs from 10 lb/jet kw, the operating time which characterizes arc jet applications will increase or decrease in proportion. For example, if a power plant is used which weighs 20 lb/jet kw, the arc jet will fit best when the operating time must be 20 to 40 days, or less. If competing electrical propulsion systems are found to be slow to develop or to require heavier power plants to produce a unit of jet kinetic energy, the field of application for the arc jet will undoubtedly broaden. More specifically, as can be seen in Figure 2, the arc jet propulsion sys-

tem, operating off-optimum, can be used for long trips without a severe weight penalty as compared to the propulsion system optimum for that mission duration. Further, the arc jet is less dependent than the higher specific impulse system on the availability of large power sources. If difficulties appear in the development of large power sources, the arc jet may be an attractive solution for the longer duration missions.

PLASMA JET DEVELOPMENT

From the results of the mission studies described so far, the following two general conclusions can be drawn:

1. For practically all space missions, a plasma-propelled rocket requires less mass than a chemical rocket.

2. Although ion rockets in general can complete a given mission with considerably less total mass than a plasma rocket, the operating time to obtain a given velocity increment with a plasma rocket is many times shorter than the ion rocket if the same power plant is used. This, coupled with the much simpler design and working system of the plasma propulsion unit, gives it a much higher reliability and more flexibility in its application than an ion rocket.

On the basis of these conclusions, for the last two and one-half years an extensive analytical and experimental program has been conducted at Plasmadyne to evaluate and develop plasma propulsion systems. This program was initiated with a preliminary evaluation of the propulsion principle followed by preliminary experiments having the objective of establishing its feasibility and to outline the relevant areas of interest requiring detailed study. The beginning of the activity was characterized by results portraying a rather poor performance. In fact, 58 seconds was the initial value obtained for specific impulse, experimenting with argon, with 34.5 kw input electrical power and a weight flow of 0.00655 lb/sec; but the work went on and consistent progress was made. Today, after almost three years of work, a specific impulse of 1500 seconds has been obtained with hydrogen exhausting into a low pressure chamber.

One phase of the over-all plasma propulsion development program still being conducted, is the analytical and experimental study of different substances to be used as propellants for a plasma propulsion unit. The criteria being considered in choosing a propellant are the following:

a. Obtainable specific impulse.

b. Storage of the propellant in the rocket and the effect of the propellant tank mass on the rocket performance.

c. Ability of propellant to efficiently convert electric power into effective jet power.

d. Availability and handling properties of the propellant.

e. The flexibility with which the propellant can be incorporated into propulsion units with widely different mission capabilities.

In conducting this study, it has been found desirable to define a parameter that can be used to compare the propellant effectiveness when incorporated in a propulsion system. Using a rocket analysis that has been carried out, it has been found possible to incorporate the four factors of

1. Propellant specific impulse.
2. Propellant tank storage mass.
3. Propellant-to-power plant mass ratio.
4. Number of times the rocket is refueled.

in one factor termed "modified specific impulse". In order to define this quantity, the double criteria of completing a given mission with minimum rocket mass and the shortest motor operating time was used. These criteria also define a relation between the propellant tank structure constant and the ratio of the mission characteristic velocity to the gas exhaust velocity. This relation is shown in Figure 5. Figure 6 shows

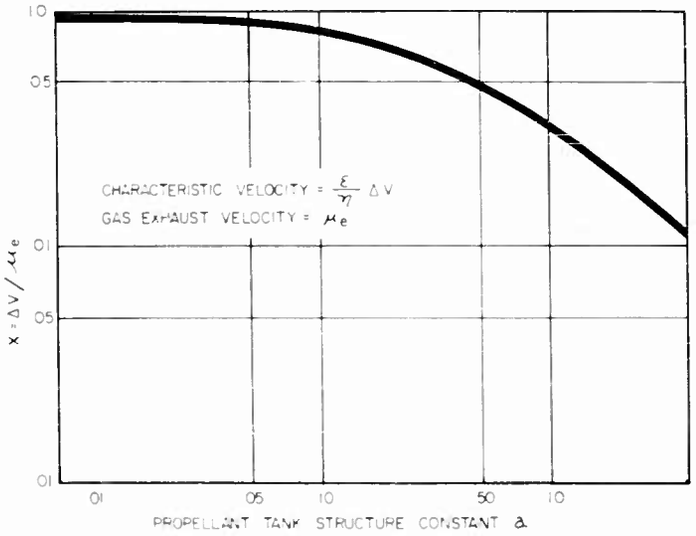

Fig. 5 Effect of Propellant Tank Structure Constant on The Ratio $\Delta V/\mu_e$

the factor by which it is necessary to multiply the propellant specific impulse to obtain the quantity defined as the modified specific impulse. The significance of this parameter is illustrated in the next two figures, where the exhaust velocities obtainable from a number of substances is computed for various methods of storing the propel-

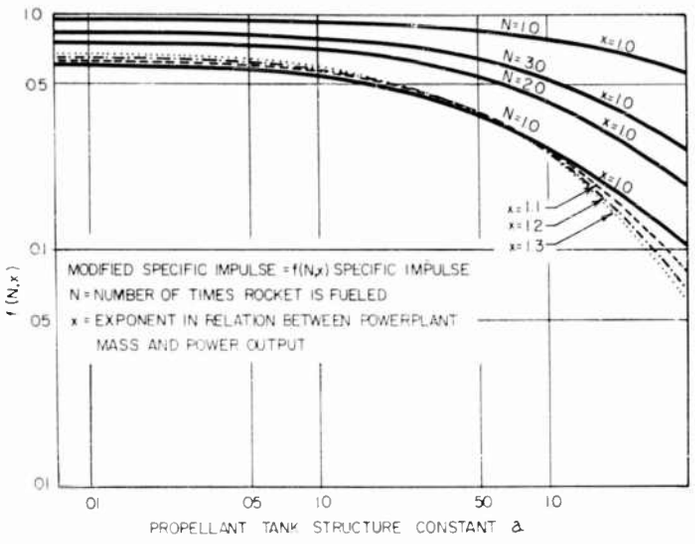

Fig. 6 Modified Specific Impulse

lants (Figures 7 and 8).' These graphs clearly indicate that the propellant exhaust velocity alone is not a useful parameter in evaluating its performance in a plasma propulsion unit. The next Figure 9 verifies this conclusion by actually computing out the rocket and propulsion system parameters for a hypothetical mission.

As already stated, the propellant study is being conducted on two parallel fronts: analytical and experimental. During the former one, the thermo-dynamic

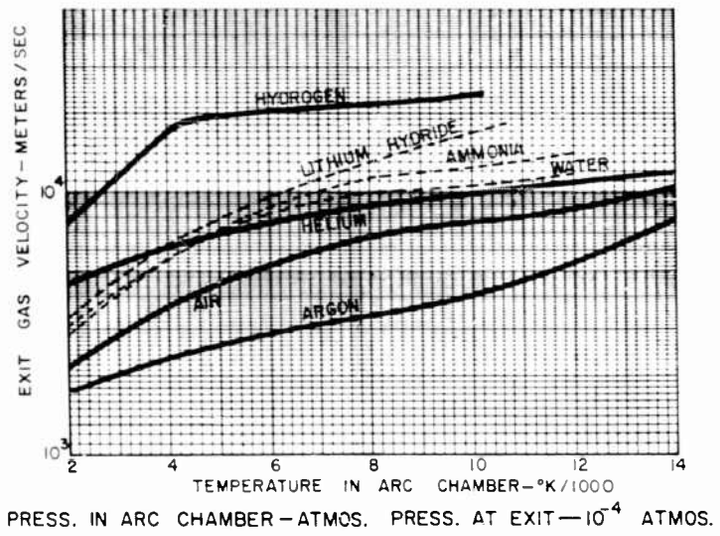

Fig. 7 Modified Specific Impulse

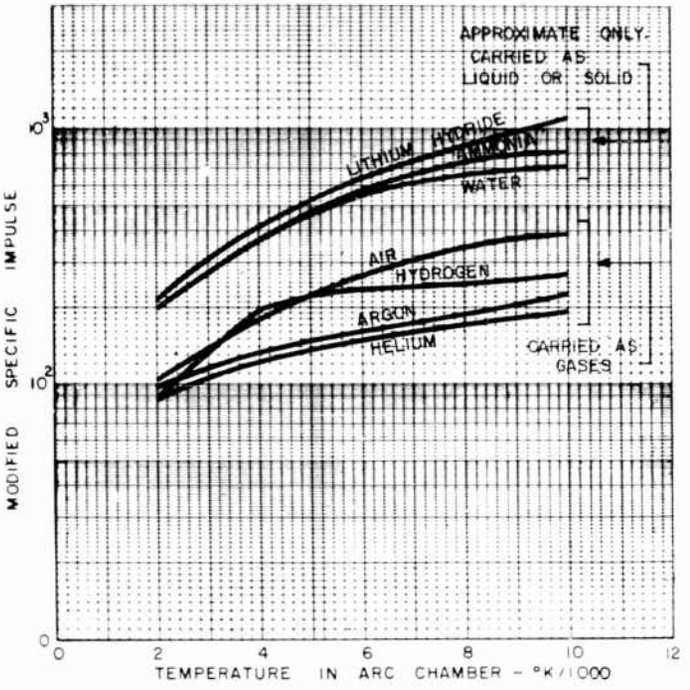

Fig. 8 Modified Specific Impulse for Various Propellants in Electric Rockets

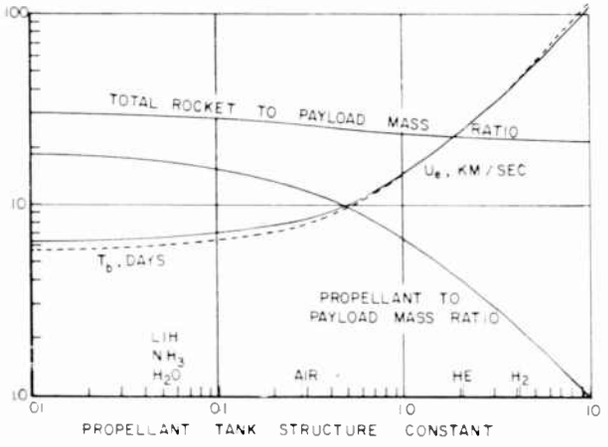

PAYLOAD	10^3 KGM
POWER	10^3 KGM
POWERPLANT	10^4 KGM
CHARACTERISTIC VELOCITY	5.0 KM/SEC
EFFICIENCY	50

Fig. 9 Rocket Design Parameters

properties of the propellant substances have been computed and plotted on Mollier Charts. Typical charts for helium and lithium are shown in Figures 10 and 11. From

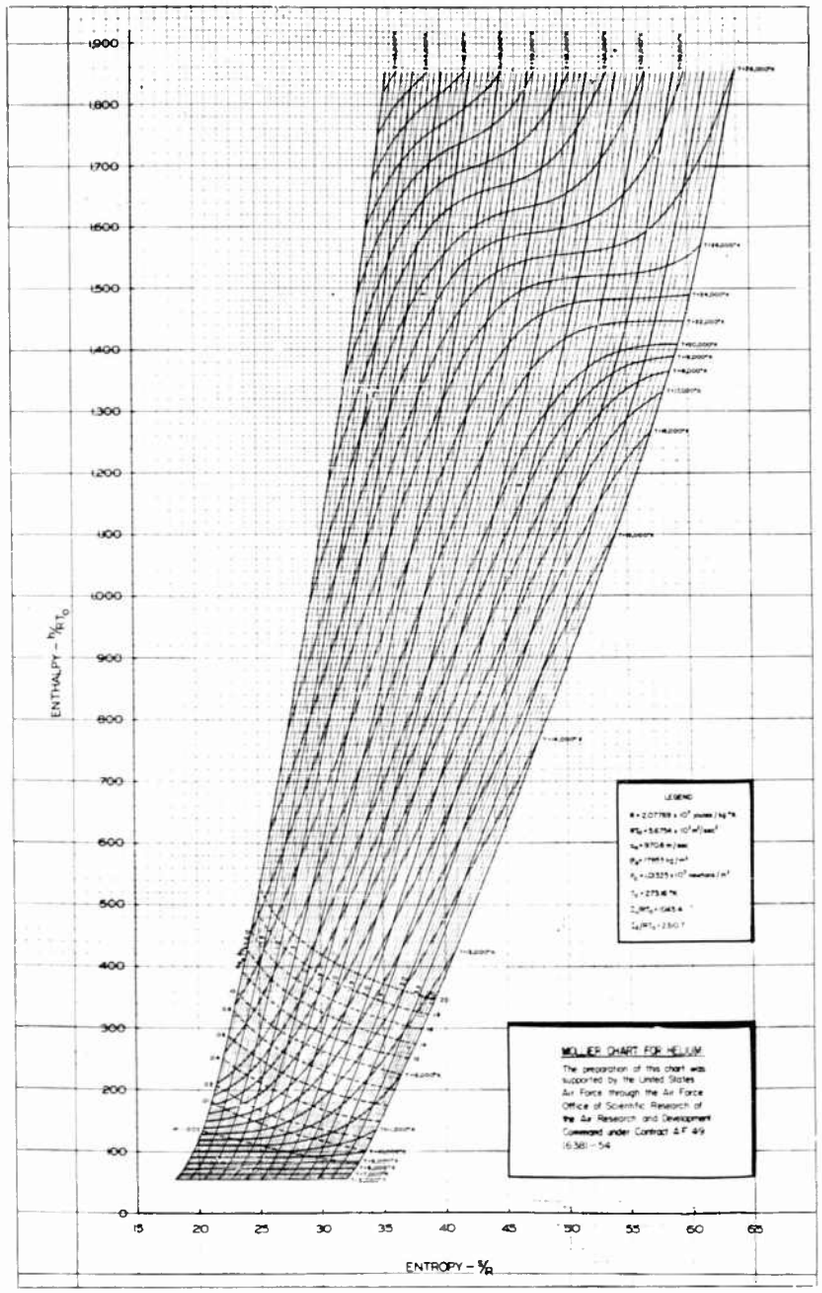

Fig. 10 Mollier Chart for Helium

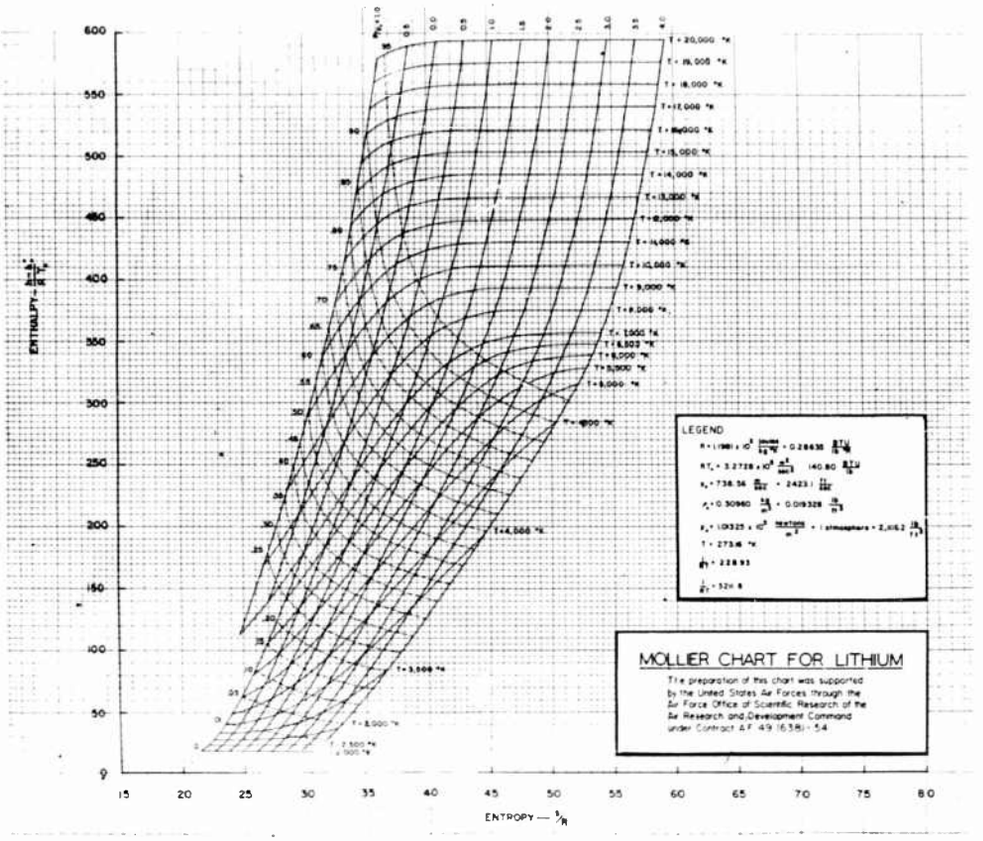

Fig. 11 Mollier Chart for Lithium

these charts isentropic and frozen flow expansions are calculated and the specific impulses and efficiencies determined. These quantities are plotted in Figures 12, 13, 14 and 15 for lithium and helium. To date argon, helium, lithium and lithium

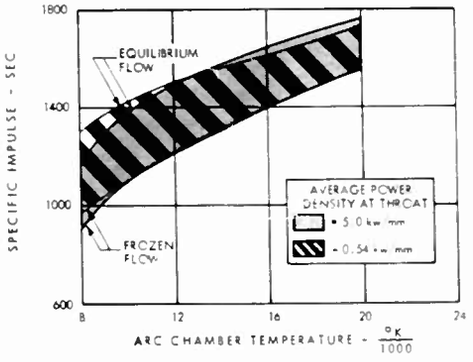

Fig. 12 Specific Impulse—Lithium

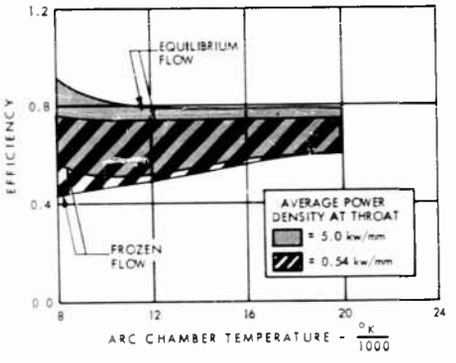

Fig. 13 Gas Dynamic Energy Conversion Efficiency —Lithium—

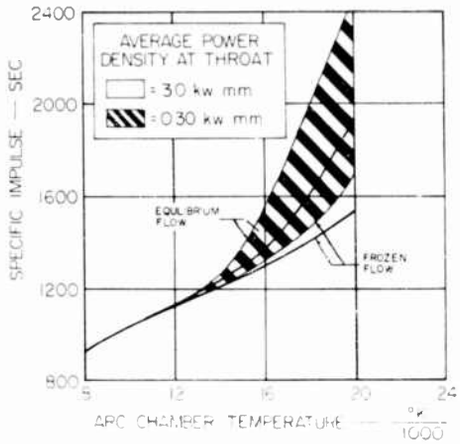

Fig. 14 Specific Impulse – Helium

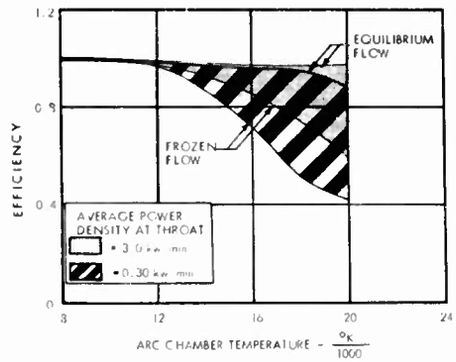

Fig. 15 Gas Dynamic Energy Conversion Efficiency – Helium–

hydride have been completed. Hydrogen, water and ammonia are being worked on at present.

In order to conduct the experimental phase, a thrust stand was constructed in which it is possible to make all of the measurements for an accurate determination of the gas specific impulse and energy conversion efficiency when the motor is exhausting into a low pressure region (as low as one mm of mercury). This equipment is shown in the next two pictures, Figures 16 and 17. Results of some tests on helium in this installation are shown in Figure 18a. Figure 18b shows the latest test results obtained with hydrogen.

A specific impulse in the range of 1500 seconds was obtained. During testing it was found difficult to raise the average gas temperature above 5000° K. The

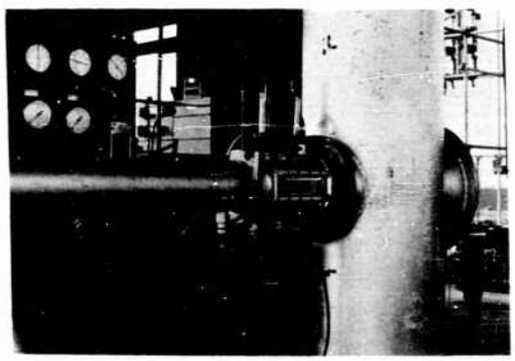

Fig. 16 Equipment Thrust Stand

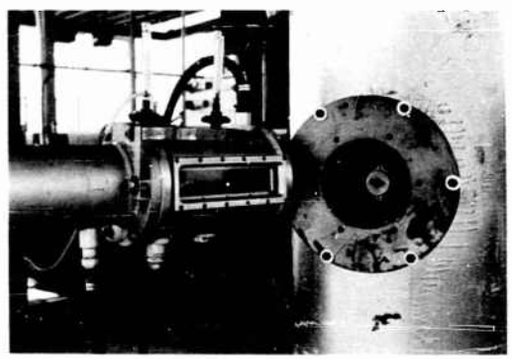

Fig. 17 Equipment Thrust Stand

expansion nozzle configuration has been found to be an important factor to obtain better results. To better determine the jet characteristics, a total pressure probe has been designed and pressure profiles of the jet have been taken. Figure 19 shows

Date	V	I	P	T_2	T_1	P_w	P_g	$\dot{m}$	p_{bottle}	$p_{t.s.}$
	volts	amps.	kw.	°C	C	kw	kw	gm/sec	p.s.i.	cm.
5-24-59	70	1850	130	40	27.5	34.7	95.3	0.78±.01	33.7	.5
5-24-59	85	2100	178.5	-	27.5	50	128.5	1.35±.01	44.7	.5
5-24-59	80	2200	176	47	28.0	56.5	119.5	1.35±.01	44.7	.5
5-24-59	78	2230	174	50	28.5	61.3	113	1.35±.01	44.7	.5
5-24-59	70	2500	175	54	28.5	71	104	1.35±.01	44.7	.5

Defl.	Thrust	S I	$\sqrt{2\dot{P}m}$	ϵ	ϵ^2	$\sqrt{2P_g\dot{m}}$	ϵ^1	h	h
in.	newtons	sec	newtons			newtons		m^2/sec^2	btu/lb
.082	6.47±.24	845	14.2	.456	.208	12.2	.530	1.21^8	51,600
.162	14.7±.27	1110	22.0	.669	.447	18.6	.791	9.65^7	41,500
.175	15.7±.27	1180	21.8	.720	.519	18.0	.873	9.00^7	38,700
.173	15.5±.27	1170	21.7	.715	.511	17.5	.887	8.51^7	36,600
.180	14.8±.27	1120	21.7	.682	.466	16.8	.882	7.85^7	33,800

Fig. 18a Thrust Stand Test Results With Helium

Date	V	A	P	P_w	ΔP_c	$\dot{m}$	Cant. Defl.	Thrust	S.I.
	volts	amps	kw	kw	kw	gm/sec	in	Newtons	sec
8-20-59	103	1000	103.0	63.0	40.0	.227	.0303	2.97	1330
8-20-59	90	900	81.0	57.4	23.6	.170	.0220	2.16	1300
8-20-59	114	1220	139.0	72.0	67.0	.363	.0465	4.56	1280
8-21-59	95	1450	109.0	94.3	44.3	.181	.0245	2.40	1350
8-21-59	85	1700	144.5	102.0	42.5	.157	.0250	2.45	1600

$\sqrt{2P\dot{m}}$	ϵ	$\sqrt{2P_g\dot{m}}$	ϵ^1	Nozzle Number	$p_{M.C.}$	$T_{M.C.}$	p_e	p_a	$p_{M.C.}$	ϵ^2
Newtons		Newtons			mm Hg	°K	mm Hg	mm Hg	p_e	
6.86	.432	4.27	.695	2	192	3500	14.2	3	13.5	.188
5.27	.410	2.83	.764	2	138	3300	10.5	3	13.2	.168
10.1	.452	6.98	.655	2	283	3650	19.6	3	14.4	.206
6.30	.381	4.05	.593	1	210	3920	14.0	3	15.0	.146
6.74	.371	3.68	.665	1	230	4250	13.6	3	16.9	.138

Fig. 18b Thrust Stand Test Results With Hydrogen

the probe in a helium jet. Some of the measured profiles are shown in Figure 20. The computed relation between the thrust and total pressure is shown in Figure 21. Correlations between the measured thrust and that computed from the pressure profiles are being made. Within the next few months we expect to have studied analytically and experimentally the properties of water, ammonia, hydrogen and lithium hydride.

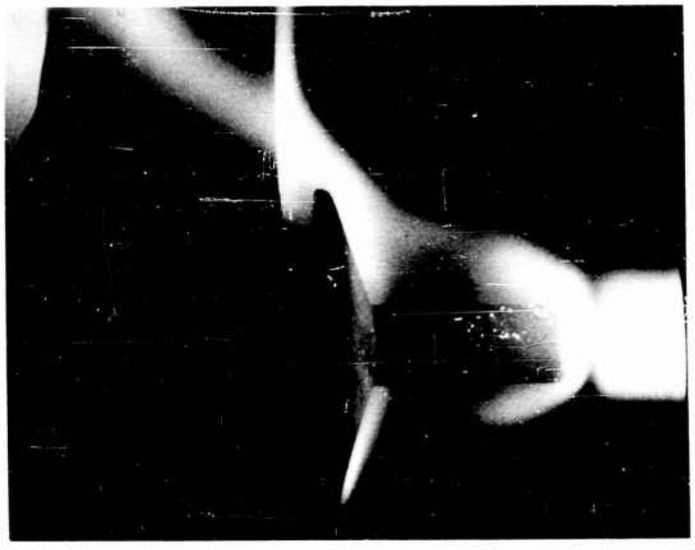

Fig. 19 Probe in a Helium Jet

We have just described some of the aspects of the detailed propellant studies being conducted at Plasmadyne and some of the results obtained clearly indicate the potential propulsive capabilities of these substances, based on the present technological status of producing, handling and storing them. In this connection a significant conclusion which can be drawn from this study is that if the substances hydrogen, helium, argon and air are carried as gases, a tank structure constant can be estimated. Using these estimated values and the information from Figures 2 and 3, the modified specific impulse for the various propellants can be computed. Figure 8 shows the results of this calculation when no refueling takes place. It becomes immediately evident that when a propellant must be carried in the rockets as a gas, its performance is degraded to such an extent that its usefulness becomes questionable, irrespective of the exhaust velocity that it is capable of delivering.

Following the completion of the work so far described, a program is contemplated to design, develop, construct and test the prototype of a flyable plasma jet motor to operate at 1000 kw input power and using a hydrogen compound as propellant. Thrust and specific impulse are in the range of 100 newtons (20 lbs) and 1500-2000 seconds, respectively.

To accomplish this task it is necessary to optimize the design technology of the present plasma jet units with the objective of minimizing the various power losses

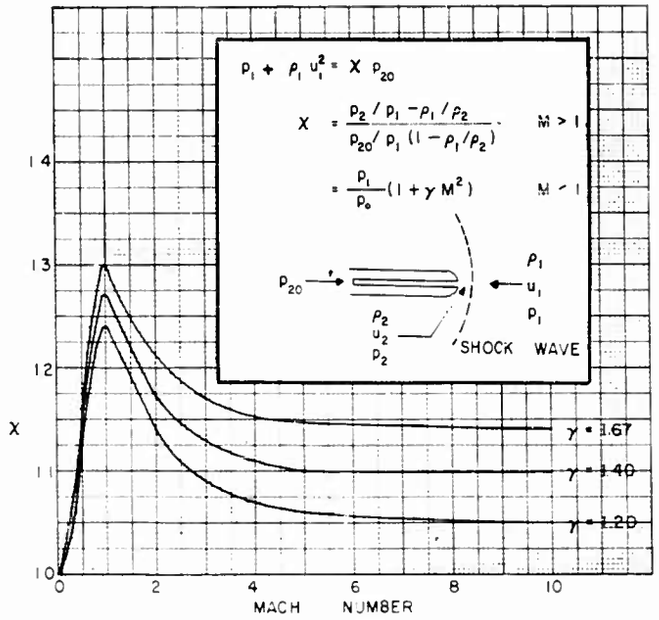

Fig. 20 Relation Between Pitot and Total Pressure

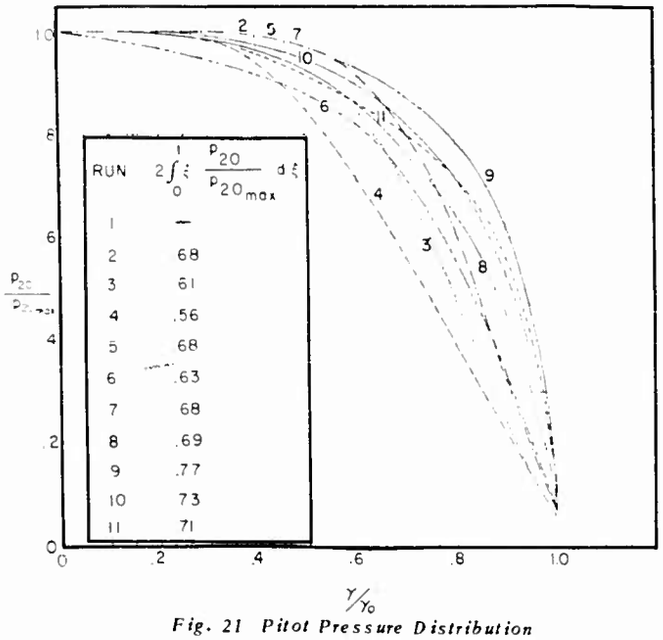

Fig. 21 Pitot Pressure Distribution

such as those associated with the positive and negative electrodes of electrical nature, radiation effects, the heat losses associated with the cooling of the electrodes, and in addition to these losses, those involving molecular dissociation. Of primary importance, of course, the optimum design must provide an efficient heat transfer process to the gas which is to be ejected downstream of the electrodes.

The mechanism of injecting the propellant through the electrodes seems to be particularly promising. It is possible with this regenerative method to partially solve the problem of cooling the electrodes. The function of the injected gas is primarily to provide electrode cooling. Since the mass flow rate involved will be relatively small, for appreciable heat transfer the specific enthalpy will be high. The cooling will then be accomplished while the inner wall temperature of the electrode and nozzle will be very high, but still well below the melting point of the materials used for the nozzle and the electrodes.

Another problem which must be solved by means of practical engineering principles is that of heating a large fraction of the gas to a uniformly high temperature while maintaining the power loss to the walls at a low level. Again, an optimization design study of methods originally employed at Plasmadyne must be conducted to increase the efficiency of the process. Field forces of magnetic nature are one of the principles considered.

Finally, we like to touch briefly the very general problem concerning the engineering of building such a plasma jet unit. The significant features of this plasma motor are its continuous, high temperature operation and the use of hydrogen compounds as a propellant which, regeneratively, cools the nozzle-electrode assembly. Evidently we are faced with the problem that, while it is necessary to keep the jet temperature very high (for efficiency purposes), it is also necessary to prevent the temperature from getting as high as the melting point of the material used. In other words, what would be highly desirable is an arc operation occurring at the highest available jet temperature which would decrease in the direction of the nozzle wall to a value safely below the melting point of the nozzle material. In this connection it is obvious that a first requirement of the material used for the nozzle is a high melting temperature. At the same time a high coefficient of heat conduction is necessary to prevent the formation of ''hot spots''. To avoid the generation of large thermal stresses, it is necessary to have a low thermal expansion coefficient. In addition to the insulation of thermic nature, electrical insulation between the electrodes must also be provided.

As can be seen a propulsion unit for space flight presents many problems of unusual nature which must be solved before one can develop a system with a high degree of reliability.

Specifically, a propulsion system for space flight must be able to perform under extremely adverse environmental conditions involving excessively high temperatures, pressures and perhaps cosmic radiation bombardment.

MAGNETOHYDRODYNAMIC ACCELERATION OF SLIGHTLY IONIZED, VISCOUSLY CONTAINED GASES

by

G. SARGENT JANES and JAMES A. FAY

AVCO-EVERETT RESEARCH LABORATORY
A DIVISION OF AVCO CORPORATION

ABSTRACT

The various physical and aerodynamic factors affecting the design of a steady flow MHD accelerator having viscous containment and crossed electric and magnetic fields are considered for the case of a slightly ionized gas. These include the effects of tensor electrical conductivity, ion slip, current diffusion, frozen flow and leaving losses, magnetic field and electrode losses, and viscous boundary layer losses. Some of these effects are also applicable to the case of a completely ionized gas. This may be the more interesting case, but it is not considered in detail. A particular example portraying most of these effects is presented for the case of a slightly ionized gas.

INTRODUCTION

Among the various kinds of electrical propulsion schemes, thermal acceleration (plasma jet) appears to be limited to specific impulses of 1500 seconds or less, while electrostatic accelerators appear most advantageous at impulses greater than 8×10^3 seconds. In the intermediate region of specific impulse, there are several possible magnetic acceleration schemes, only one of which we wish to consider herein; namely, a steady flow, viscously contained accelerator having an applied magnetic field and current mutually perpendicular to each other and to the flow (see Fig. 1). The principal acceleration is due to the $\bar{j} \times \bar{B}$ body force acting on the conducting gas, although thermal acceleration (conversion of thermal energy due to electrical heating to directed kinetic energy) may not necessarily be a negligible part of the total acceleration. Indeed, the optimum apportioning of the electrical power between heating and acceleration constitutes an important aspect of the design of such propulsion devices.

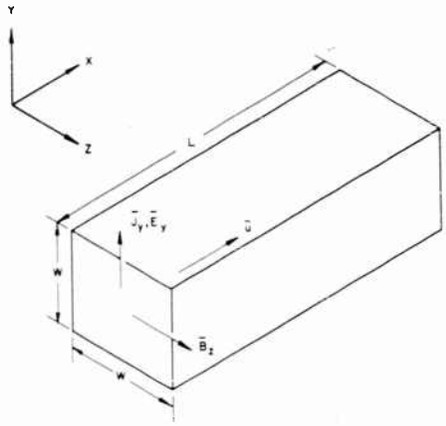

Fig. 1 Schematic diagram illustrating the geometry of a viscously contained magnetohydrodynamic plasma accelerator having an applied magnetic field and current mutually perpendicular to each other and to the flow.

The term "viscous containment" refers to the necessity of withstanding the gas pressure with cold, stationary walls, resulting in an inevitable thermal and momentum loss. This type of containment appears to be necessary for slightly ionized gases, the ions being formed from either the gas itself or from small amounts of seed material. Magnetic containment is obviously attractive for completely ionized gases, but will not be treated here. We shall also neglect the leaving losses associated with the flow of eddy currents at the exit of the accelerator. The relative importance of eddy current losses is to some extent a function of the "tailoring" of the exit section, and it is not clear at present what general limitations they impose on accelerator design.

The viscous boundary layers in this accelerator will be found to be of two types, the ordinary inertial type and the Hartmann type (Ref. 1) where

j x B forces are important. The latter gives rise to large electrical losses. Since the boundary layer losses are proportional to the perimeter of the accelerator, while the power is proportional to the cross sectional area, these losses set a minimum power for a given efficiency.

The purpose of this paper is to discuss the various losses involved in an accelerator of the type described above, and to show how the minimum power is determined if a given specific impulse and overall efficiency is specified. The possible modifications of this geometry, such as variable area, nozzle expansion, or annular cross section will not be considered.

PHYSICAL LIMITATIONS

With the exception of the viscous boundary layer, the continuum gas dynamics associated with the flow and current geometry under consideration is relatively simple. This is discussed in Section C below. However, there are many auxiliary effects which, taken together, define a possible range of operation not necessarily ascertainable from the gas dynamics alone. These auxiliary effects include the limitations of gas conductivity, Hall currents, ion slip, transverse current diffusion, frozen flow loss, leaving loss, boundary layer loss, applied magnetic field loss and electrode loss. It is our purpose to discuss some aspects of each of these below.

Before doing so, let us determine the order of magnitude of the gas dynamic effects alone. For a channel of constant area, the body force $\vec{j} \times \vec{B}$ integrated over the length L gives the momentum flux ρu^2 leaving the channel:

$$\vec{j} \times \vec{B} \, L = \rho u^2 \tag{1}$$

If f is defined by:

$$f \equiv j/\sigma uB \tag{2}$$

then L is given by:

$$L = \left(\frac{\rho u}{\sigma B^2}\right) \frac{1}{f} \tag{3}$$

In the absence of ion slip, the factor f is just the ratio of "heating" power input (j^2/σ) to the "acceleration" power input $(jB \times u)$. Large values of f correspond to predominantly thermal accelerations and low values to nearly isentropic magnetic accelerations. For a magnetic accelerator, it is to be expected that $f \ll 1$. Bearing in mind the general result (Eq. 3) for the size of the accelerator, we shall discuss the particular items enumerated above.

(1) Gas Conductivity: For reasonable values of B, L, and ρ, the scalar gas conductivity σ must be of the order of 10^2 mho/m. This can be achieved by about one tenth mole per cent ionization at standard density

or lower. To achieve this ionization by adding cesium or potassium, a temperature of 4,000°K is necessary. The corresponding temperatures for ionizing hydrogen, helium, and lithium to the same extent are 10,000°K, 14,000°K, and 5,000°K, respectively.

A typical curve of σ vs. temperature for a gas seeded with 1% potassium is shown in Fig. 2. It is not possible to achieve higher conductivities at the lower temperatures by adding more potassium, for the electron-ion collision cross section is about 100 times that for the electron-neutral collisions. At higher temperatures the conductivity approaches that

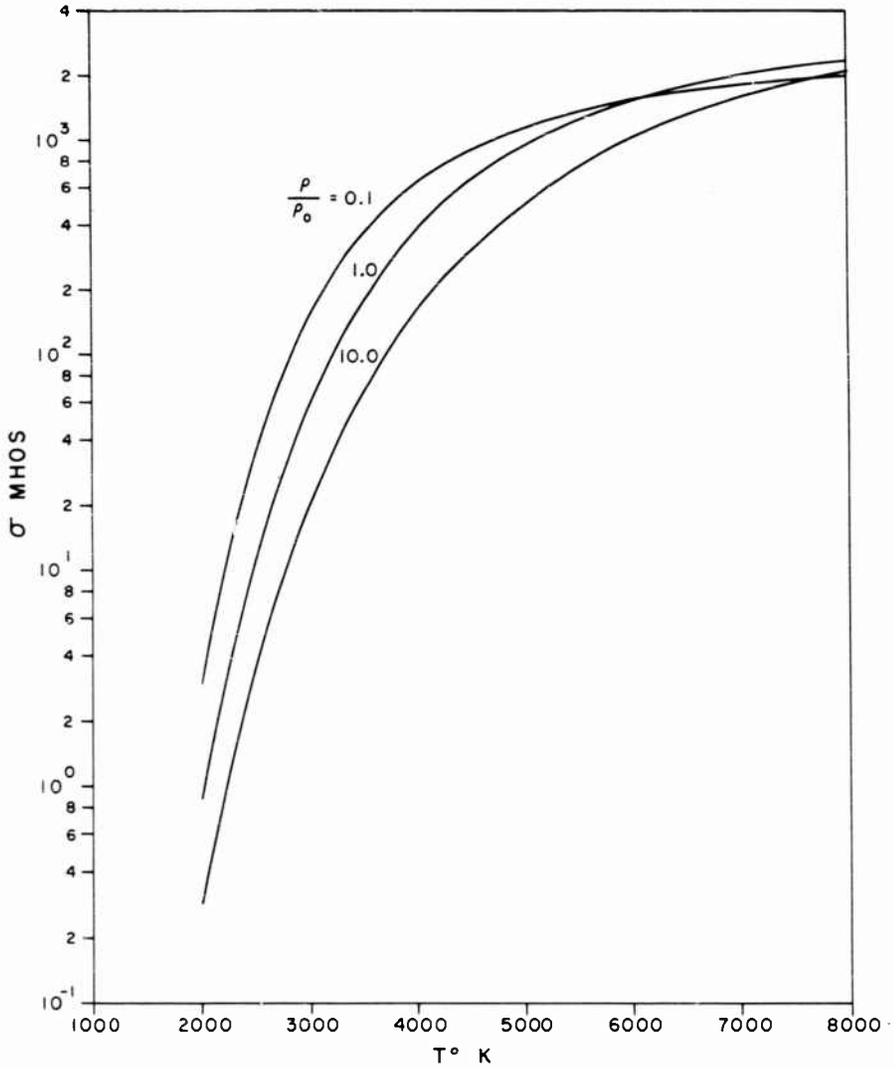

Fig. 2 Typical plot of electrical conductivity vs. temperature for a gas with 1% potassium which has a neutral atomic collision cross section, Q_a equal to 6×10^{-16} cm^2. The quantity ρ/ρ_0 refers to the density relative to the density existing at NTP.

of the completely ionized gas, (Ref 3), and is substantially independent of the density, since all the additive is completely ionized.

(2) Hall Currents: At high magnetic field strength, the electrons follow curved paths between collisions due to the $e(\bar{v} \times \bar{B})$ force. This results in a drift perpendicular to both the magnetic field and the net electric field (Hall current).

For the geometry of Fig. (1) in which the current is assumed to flow in the y-direction the electric field is related to the current density by the equations

$$E_y - u_i B = j_y/\sigma \tag{4}$$

$$E_x = (\omega_e \tau_e)\, j_y/\sigma \tag{5}$$

where σ is the ordinary scalar conductivity, ω_e is the electron cyclotron angular frequency, τ_e is the mean electron collision time, $\bar{E}$ is the net electrical field acting on the electrons and u_i is the velocity of the ions.

For large values of $(\omega_e \tau_e)$ the longitudinal field can be greater than the transverse field, so that great care must be taken to prevent the discharge of the Hall field E_x through the boundary layer. In any case, Hall effects become important for $(\omega_e \tau_e)$ of one or greater.

For a slightly ionized gas (1% ionization) in the temperature range of 4,000°K to 8,000°K, a simple empirical rule for determining $(\omega_e \tau_e)$ is:

$$(\omega_e \tau_e) = \frac{\sigma B}{n_i e} \simeq 10^{-1} B \frac{\rho_o}{\rho} \tag{6}$$

where n_i is the number density of ions, ρ_o is the density of the mixture at NTP and B is measured in webers/m^2. This relation is correct to within a factor of two for gases having electron-neutral collision cross sections of 10^{-15} cm^2. For completely singly ionized gases, $(\omega_e \tau_e)$ is approximately given by:

$$(\omega_e \tau_e) = 10^{-9} B \frac{\rho_o}{\rho} T^{3/2} \tag{7}$$

where T is measured in °K.

(3) Ion Slip: Since the current is due almost entirely to electrons, the $\bar{j} \times \bar{B}$ accelerating force is applied to the electrons. By virtue of a slight charge separation, electrostatic fields are generated which transmit this force to the ions. In order for the neutral particles to be accelerated, there must be sufficient collisions between ions and neutrals to transmit the momentum increase of the ions to the neutral gas. The relative velocity v_I of the ions, as compared to the velocity v of the neutrals, is a meas-

ure of the "ion slip." For the case of Fig. (1) where Hall currents do not flow, this ratio may be shown to be:

$$\frac{v_{neutral}}{v_{ion}} = \frac{1}{1+f\ (\omega_e\tau_e)\ (\omega_I\tau_{In})} \tag{8}$$

where $(\omega_I\tau_{In})$ is the product of ion cyclotron frequency and ion mean free time for neutral collisions. Thus, for $f\ (\omega_e\tau_e)\ (\omega_I\tau_{In}) \geq 1$, the slip velocity becomes appreciable compared with the gas velocity.

(4) Transverse Current Propagation: The accelerator geometry of Fig. (1) portrays a "quasi one-dimensional" flow; i. e., one in which conditions are uniform throughout a plane normal to the flow, although changing in the direction of flow*. For this to be so, any change in B or E with x must be felt by the gas within the time it takes to move less than one duct width (h/u).

In the absence of a magnetic field, currents diffuse a distance h in a time τ_o given by:

$$\tau_o = \mu_o \sigma\ h^2 \tag{9}$$

where μ_o is the magnetic permittivity. For this time to be short compared with the flow time,

$$\mu_o \sigma\ h\ u < 1 \tag{10}$$

Thus the magnetic Reynolds number $(\mu_o\ \sigma\ hu)$ based on channel height should not exceed unity if the flow is not to become two dimensional.

(5) Frozen Flow Loss: If the static temperature of the gas is sufficiently high, the gas will dissociate and ionize. The dissociation and ionization energy is not recoverable in the form of kinetic energy if the rates of recombination are too low. For small devices operating at low densities, this latter is the general rule. For efficient accelerators the maximum temperature should be low enough for the energy invested in dissociation and ionization to be a small portion of the exhaust kinetic energy.

The frozen flow loss may be computed from the following equation.

$$\epsilon_{ff} = \frac{e \Sigma_i \alpha_i I_i}{1/2\ m\ u^2} \tag{11}$$

where α_i represents the i^{th} degree of ionization and I_i represents the

* This weight includes the electrical propulsion system required for space flight or satellite maneuvers.
** This obviously neglects the cost of development.

corresponding ionization potential. This places certain limitations on the permissible degree of ionization consistent with reasonable efficiency. In a 2,000 second device with less than a 10% frozen flow loss, the maximum permissible degrees of ionization in sodium, lithium, helium, and hydrogen are 100%, 30%, $3\frac{1}{2}$ %, and $1\frac{1}{2}$ %, respectively.

(6) Leaving Loss: For reasonable efficiency, it is necessary that the static enthalpy of the exhaust gases be a small fraction of the total (stagnation) enthalpy. This "leaving" loss may be conveniently expressed as the ratio of static enthalpy (C_pT) to kinetic energy:

$$\epsilon_L \equiv \frac{C_pT}{u^2/2} = \frac{2}{M_e^2(\gamma - 1)} \tag{12}$$

where γ is the specific heat ratio and M_e is the exit Mach number. Thus a 10% leaving loss in a monatomic gas requires an exit Mach number of 5.5. For a given specific impulse in a given gas, the leaving loss therefore fixes the exhaust temperature.

(7) Boundary Layer Losses: There are two types of boundary layers in the viscous accelerator, each of markedly different characteristics. Along the electrode surfaces (y = 0, h in Fig. (1) , the current j is normal to the wall and equal to that in the free stream. The accelerating body force jB is equal to that in the free stream, and is comparable to the viscous and inertia forces in the boundary layer, having the same effect as a favorable pressure gradient. Thus a normal aerodynamic boundary layer develops on the electrodes, with its consequent momentum loss. On the side walls (z = 0, w in Fig. (1) ; however, the applied field E_y parallel to the wall is fixed. The counter field uB becomes small near the wall, so that currents as large as σE_y may flow parallel to the wall. Since these currents are generally much greater than those in the free stream, large electrical power losses will result. The motion of the boundary layer will be changed, since the jB body force will be large, compared with the inertia force:

$$\frac{\text{Body force}}{\text{Inertia force}} = \frac{jB}{\rho u^2/L} = \frac{\sigma u B^2 L}{\rho u^2} = \frac{1}{f} \tag{13}$$

since $f << 1$ generally. Thus the body force is balanced by the viscous forces. (This type of boundary layer was first discussed by Hartmann Ref. 1)

(8) Viscous Boundary Layer: We begin by finding the heat loss in a normal boundary layer on a surface of revolution. This can later be applied to the electrode boundary layer loss for any ratio of width w to height h.

For laminar flow in a channel of revolution, the local heat transfer q_L to a cold wall is given (for Prandtl number equal to one) by:

$$q_L = \frac{0.35\,\rho_{\mu r} h_s}{\left\{\int_o^x \rho\,\mu\,ur^2 ds\right\}^{1/2}} \tag{14}$$

where ρ, μ, h_s, and u are the free-stream density, viscosity, stagnation enthalpy, and velocity, respectively, r is the local radius of revolution and s the distance along the surface. This result is strictly applicable only where h_s is constant along the surface, which is not the case of the MHD accelerator. However, it appears reasonable to expect the local heat loss to be proportional to the local stagnation enthalpy, so that Eq. (14) expresses a local equilibrium hypothesis.

The viscous boundary layer loss E_{BV} will then be the ratio of integrated heat transfer to energy flux in the exhaust:

$$\epsilon_{BV} = \frac{\int_0^L (2\pi r q_L) ds}{\pi r_e^2 \rho_e \mu_e h_{se}} = \frac{1.24}{\sqrt{\rho_e u_e \pi r_e^2}} \int_{s_i}^{s_e} \frac{\mu \left(\frac{h_s}{h_{se}}\right) ds}{\sqrt{s - s_i}} \qquad (15)$$

where use has been made of the fact that $\pi r^2 \rho u$ is a constant. Replacing s by x and integrating from 0 to L with μ approximately constant, we obtain

$$\epsilon_{BV} = 2.48 \left(\frac{L}{\sqrt{\pi r_e^2}}\right)\left(\frac{\mu_e}{\rho_e u_e L}\right)^{1/2} \int_0^1 \left(\frac{h_s}{h_{se}}\right) d\left(\frac{x}{L}\right)^{1/2} \qquad (16)$$

The loss in a rectangular channel, which varies in proportion to the electrode perimeter divided by the area; i.e., 2w/hw or 2/h, may be proportioned to that in the circular channel having a perimeter to area ratio of 2/r. Thus the above equation gives the electrode boundary layer losses if r_e is replaced by h:

$$\epsilon_{BV} = 1.4 \left(\frac{L}{h}\right)\left(\frac{\mu_e}{\rho_e u_e L}\right)^{1/2} \int_0^1 \left(\frac{h_s}{h_{se}}\right) d\left(\frac{x}{L}\right)^{1/2} \qquad (17)$$

The boundary layer loss in turbulent flow can be estimated by multiplying the above equation by the ratio of turbulent to laminar average skin friction coefficients, giving:

$$\epsilon_{BV} = 0.076 \left(\frac{L}{h}\right)\left(\frac{\mu_e}{\rho_e u_e L}\right)^{1/5} \int_0^1 \left(\frac{h_s}{h_{se}}\right) d\left(\frac{x}{L}\right)^{4/5} \qquad (18)$$

The dimensionless integrals in Eqs (17) and (18) are never greater than 1, but must be evaluated after the relation between h_s and x has been determined (see Section C)

(9) Hartmann Boundary Layer: The electrical losses per unit area of side wall are computed (Ref. 2) for a gas with constant transport properties, and for any value of $(\omega_e \tau_e)$:

$$\text{Power/Area} = \sigma u^2 B^2 (1 + f) \left(\frac{\mu}{\sigma B^2}\right)^{1/2} H(\omega_e \tau_e) \qquad (19)$$

For $f \ll 1$ and $(\omega_e \tau_e) \leq 10$, H is approximately one. Thus the side wall boundary layer loss will be:

$$\epsilon_{BH} = 4\left(\frac{L}{w}\right)\left(\frac{\sigma B_e^2 L}{\rho_e u_e}\right)\left(\frac{\mu_e}{\rho_e u_e L}\right)^{1/2} \int_0^1 \left(\frac{u}{u_e}\right)^2 \left(\frac{B}{B_e}\right) \, d\left(\frac{x}{L}\right) \tag{20}$$

which may be compared with Eq. (17). The factor $\sigma B_e^2 L/\rho_e u_e$ is about $1/f$ from Eq. (2), and hence the Hartmann layer loss is considerably greater than the viscous boundary layer loss since $f < 1$.

(10) Field Loss: The power to maintain the field B is to some extent determined by the geometry of the field coil. For strong fields an air core field coil would be used having a winding cross section about equal to wh. If the coil with conductivity σ_F carries a current I, the field B would be about:

$$B \simeq \frac{\mu_o I}{w + 2h} \tag{21}$$

The field power per unit length of duct would thus be:

$$\text{Field power/length} = \frac{2I^2}{\sigma_F wh} = \frac{2B^2}{\mu_o^2 \sigma_F} \frac{(w + 2h)^2}{wh} \tag{22}$$

The input power to the gas, per unit volume is:

$$\text{Input power/volume} = E_y j = (f + 1) f \sigma u^2 B^2$$

The field loss ϵ_F is thus the ratio of field power to input power per unit length:

$$\epsilon_F = \frac{2}{\mu_o^2 \sigma_F \sigma u^2 f(f + 1)} \left\{\frac{1}{h} + \frac{2}{w}\right\}^2 \tag{23}$$

and is thus independent of B. If B were sufficiently small so that an iron core were profitable, then the factor 2h in Eq. (22) should be omitted.

It can be seen that the field loss essentially determines the cross-sectional area of the channel, as it will be seen later that f is determined by the leaving loss. Of course, ϵ_F must be averaged along the length of the channel, but it will be seen later that $u^2 f$ is nearly constant for the case studied, so that the local and average values are substantially equal.

(11) Electrode Loss: There will be electrode losses in which electrical power will be converted into heat at the electrodes without substantially affecting the gas motion. Assuming an electrode voltage drop ΔV, the electrode loss would be:

$$\epsilon_E = \frac{\Delta V}{Eh} = \frac{\Delta V}{(f + 1) u B h} \tag{24}$$

With respect to the losses, it can be seen from the expressions derived for each, that the frozen flow and leaving losses are determined by the thermodynamics of the fluid, while the boundary layer, field and electrode losses can be made small by having a short length and large cross-sectional area. The limits imposed on length and area will be discussed more fully below.

With respect to the boundary layer and field losses, no mention has been made of the limitation of cooling rates for the channel wall and field coil. This may be an important factor in small scale accelerators. For some specific cases which have been studied, however, it appears that the losses, rather than rates, determine the minimum size limit of the accelerator.

THE CONSTANT TEMPERATURE, CONSTANT AREA ACCELERATOR

The duct length required to accelerate the fluid to the desired specific impulse will depend upon the variation of magnetic field strength B, current j, and area A along the duct axis x. It is not immediately clear how these should be scheduled, but it appears desirable to have as high a conductivity, current, and field strength as is possible in order to make the length (and hence boundary layer loss) small. Similarly, a large current will heat the gas more than it accelerates it, since the heating varies as the square of the current while the acceleration as the first power. Too much heating, rather than acceleration, will give rise to a frozen flow loss. Finally, large values of B increase $(\omega_e \tau_e)$ and lead to ion slip and Hall current difficulties. It would thus appear desirable to operate with as high a temperature (and hence a high conductivity) as is consistent with the acceptable losses and to maintain the maximum magnetic field consistent with maximum acceptable Hall voltage.

In order to obtain a more refined estimate of the accelerator length than that given by Eq. (3), it will be assumed that the temperature, channel area and $(\omega_e \tau_e)$ are all constant along the channel axis. If this constant temperature is higher than the permissible exhaust temperature, then an adiabatic expansion nozzle must follow the accelerator section. Moderate area changes would be permissible in the accelerator, but for the sake of simplicity these will not be considered here.

The differential equations of conservation of mass, momentum and energy for channel flow of the type indicated in Fig. (1) with constant temperature and area are:

$$d(\rho u) = 0 \tag{25}$$

$$\rho u\, du + dp = j\, B\, dx \tag{26}$$

$$\rho u^2\, du = j\, E_y\, dx \tag{27}$$

The current in the y direction only will be:

$$j = \sigma\, (E_y - uB) \tag{28}$$

where it is assumed that j_x is zero. Finally, assume a perfect gas with constant specific heats:

$$p = \frac{\rho a^2}{\gamma} \tag{29}$$

where a is the ordinary sound speed. By combining equations (25) through (29), it is easily shown that:

$$f = \frac{1}{\gamma M^2 - 1} \tag{30}$$

and

$$\frac{(\gamma M^2 - 1)^2 dM}{\gamma M} = \sigma \left(\frac{u B^2}{\rho a^2} \right) dx \tag{31}$$

For $(\omega_e \tau_e)$ constant along the axis, B/ρ and hence also Bu are constant*. Assuming that σ is also constant, which will be true if the temperature is sufficiently high to ionize all the seed, then Eq. (31) may be integrated to give:

$$L = \frac{\rho_e u_e}{\sigma B_e^2} \frac{1}{M_e^2} \left\{ \frac{\gamma}{4} (M_e^4 - M_i^4) - (M_e^2 - M_i^2) + \frac{1}{\gamma} \ln \left(\frac{M_e}{M_i} \right) \right\} \tag{32}$$

where M_e and M_i are respectively the exit and inlet Mach numbers. For $M_e >> M_i$, this reduces to:

$$L = \frac{\rho_e u_e}{\sigma B^2} \frac{1}{4 f_e} \tag{33}$$

which may be compared with Eq. (3).

A useful approximation to the definite integrals in the viscous boundary layer loss, Eqs. (17) and (18), may be found from Eq. (31) by noting that for $M^2 >> 1$,

$$u^3 \, du \propto dx \tag{34}$$

or

$$u^4 \propto x \tag{35}$$

Thus

$$\frac{h_s}{h_{se}} \simeq \left(\frac{u}{u_e} \right)^2 \propto \left(\frac{x}{L} \right)^{1/2} \tag{36}$$

Hence the definite integrals for the laminar and turbulent flows are respectively one half and 8/13. Similarly, the definite integral in Eq. (20) for the Hartmann layer loss is 4/5.

The viscous Reynolds' number based on the length L may be determined from Eq. (33).

* This is true even for the completely ionized gas, since the temperature is constant.

$$R_{e_L} \equiv \frac{\rho_e u_e L}{\mu_e} \simeq \frac{\gamma (\rho_e u_e)^2 M_e^2}{4 \sigma B_e^2} \qquad (37)$$

Since B is inversely proportional to ρ for a constant $(\omega_e \tau_e)$, it can be seen that the viscous Reynolds' number is independent of the size of the accelerator and is determined entirely by the initial choice of specific impulse, $(\omega_e \tau_e)$, and the accelerator temperature. High specific impulses and low temperatures lead to high viscous Reynolds' numbers and hence turbulent boundary layers with their attendant higher losses.

The total boundary layer loss for an accelerator having constant temperature, area, and $(\omega_e \tau_e)$ may now be determined by adding the viscous and Hartmann layer losses (Eqs. (17) and (20)) to give:

$$\epsilon_B = \left\{ 0.70 \sqrt{\frac{w}{h}} + \frac{0.8}{f_e} \sqrt{\frac{h}{w}} \right\} \left(\frac{L}{\sqrt{wh}} \right) \left(\frac{\mu_e}{\rho_e u_e L} \right)^{1/2} \qquad (38)$$

ACCELERATOR SIZE AND POWER

The field, boundary layer and electrode losses will all decrease with increasing cross sectional area (and hence power). The leaving and frozen flow losses are essentially thermodynamic in character, and will not vary with accelerator size. Thus there is a minimum power below which the total losses are comparable with the ideal power and operation is marginal.

If a leaving loss is specified for a given specific impulse, the exit Mach number is thereby determined. For any given propellant, this also fixes the exit temperature and conductivity. By choosing a maximum $(\omega_e \tau_e)$ which is believed to be practical, then only the density may be chosen at will, provided that restrictions on magnetic Reynolds' number are not exceeded, that extreme aspect ratios (e.g., $w >> L$) do not result, and that required cooling rates are not too high.

To portray these effects simultaneously, Fig. (3) has been constructed for the particular case of a lithium accelerator having a 2,000 second specific impulse at an exit temperature of 6800°K, thereby giving a 20% leaving loss. $(\omega_e \tau_e)$ is taken to be 10. The vertical scale is the ideal power ($\rho_e u_e^3 hw/2$) and the horizontal scale is the exhaust density ρ_e. By virtue of Eqs. (6) and (33), additional scales of B and L were constructed, which depend only upon ρ_e. Lines of constant field loss, boundary layer loss, and electrode loss are plotted using Eqs. (23), (38), and (24). Also shown are the regions of large and small magnetic Reynolds' number.

In the case where the electrode and frozen flow losses are negligible compared with the others, the minimum power for a given total loss may be easily determined. By use of Eqs. (23), (38), and (33), the power P is found to be:

$$P = 1/2 \, \rho_e u_e^3 \, wh$$

$$P = \left(0.70 + \frac{0.8}{f_e} \cdot \frac{h}{w}\right)\left(\frac{w}{h} + 2\right) \left[\frac{\rho_e u_e^2}{2 B_e \sigma \mu_o} \sqrt{\frac{\mu_e}{2 \sigma_F}} \right] \left(\frac{1}{\epsilon_B \epsilon_F^{1/2} f_e} \right) \qquad (39)$$

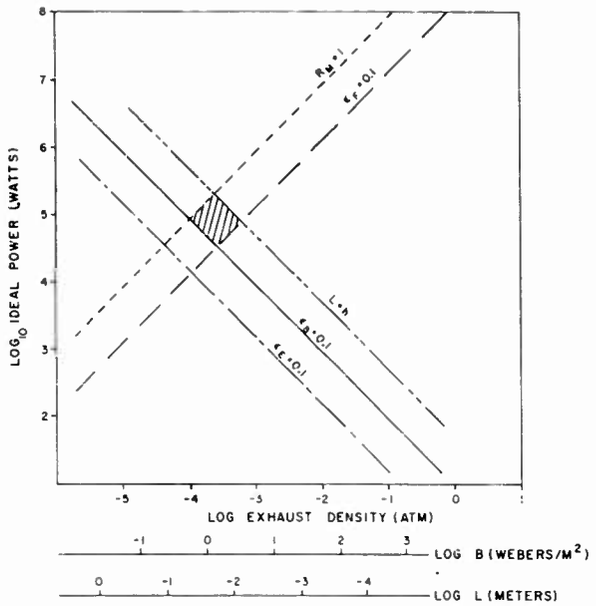

Fig. 3 A map showing the relation between power and exhaust density for fixed losses of the type discussed in the text. The shaded area shows the possible design conditions for boundary layer and field losses less than 10%, for magnetic Reynolds' number less than one, and for $L \leq b$. The chart is drawn for lithium as propellant having 30% combined frozen flow and leaving loss, $\omega\tau = 10$, a specific impulse of 2,000 sec., a 10 volt electrode drop, and $w = 2b$.

It is easily found that P is a minimum for $w = h\sqrt{2/f_e}$
Noting that f_e equals $(\gamma - 1)\, \epsilon_L / 2\gamma$, and that the third factor in Eq. (39) is a constant, one can minimize P for a fixed total loss ϵ, giving:

$$\min P = 32 \left(\frac{\gamma}{\gamma - 1}\right)^2 \left[\frac{\rho_e u_e^2}{B_e \sigma \mu_o} \sqrt{\frac{\mu_e}{\sigma_F}}\right] \epsilon^{-7/2} \tag{40}$$

if $\epsilon_L = 4\epsilon/7$, $\epsilon_B = 2\epsilon/7$, $\epsilon_F = \epsilon/7$ and $f_e \ll 1$

If the electrode and/or frozen flow losses are not negligible, a more elaborate variational process may be used to find the minimum power.

For a gas which is appreciably ionized, the relation of Eq. (7) may be used to replace ρ_e/B_e in the above equation. Using coulomb cross sections to determine the variation of σ and μ_e with temperature, one finds that

$$P_{min} \propto \frac{u_e^2}{\propto (\omega_e \tau_e)\, T_e^{1/4}\, \epsilon^{7/2}} \tag{41}$$

This places a clear minimum on the power of an accelerator of the type discussed.

REFERENCES

1 Hartmann, J. and Lazarus, F., Kgl. Danske Videnskab. Selskab, Mat.-fys. Medd. 15, Nos. 6 and 7 (1937).

2 Fay, J. A., "Hall Effects in a Laminar Boundary Layer of the Hartmann Type", Avco-Everett Research Report 81, (to be published).

3 Spitzer, L., "The Physics of Fully Ionized Gases," Interscience (1956).

A CRITICAL EVALUATION OF THE ION ROCKET

by

T. M. LITTMAN

ROCKETDYNE
A DIVISION OF NORTH AMERICAN AVIATION, INC.

ABSTRACT

A critical evaluation of the current status and future potentialities of the ion rocket is presented. Comparison is made, insofar as possible, with both conventional rockets and other electrical propulsion schemes. It is concluded that the ion rocket is unique among the advanced systems in its relative simplicity, high efficiency, wide range of applicability and early availability of a low power flight model.

574071 O - 60 - 4

CONCLUSIONS AND RECOMMENDATIONS

The conclusions reached in regard to the future of electrical propulsion in general and ionic propulsion in particular, and the recommendations based thereon, are presented in this section. The author has made a careful study of available information, but wishes to point out nevertheless, that what follows represents entirely his own opinion at the present time. Future developments, or even current results not known to him at the time of this writing, could alter many of the statements to follow. It is recognized that research on the fringe of knowledge frequently leads down novel and unexpected paths. If mankind is to reap the maximum benefit from our endeavors, we must be willing to accept and profit by these advances even at the expense of pet ideas or devices.

Conclusions

1.1 Sufficient information has been generated by laboratory experiments to indicate the scientific feasibility of obtaining thrust from ionic, plasma jet and (several) MHD devices. However, engineering practicality has not been demonstrated by any of these systems.

1.2 The most advanced electrical propulsion concept, in state-of-the-art development to date, is the ion rocket, followed closely by the plasma (arc) jet.

1.3 Of all of the advanced low thrust schemes currently under consideration, only ionic propulsion appears to offer relative simplicity in principle and design, combined with high efficiency, an extremely wide range of applicability and early availability of a low power flight engine.

1.4 It is estimated that the first generation ion engine will be available for flight test in 2 - 3 years.

1.5 The achievement of economically competitive (with chemical and nuclear rockets) electrical propulsion systems will only become a reality after low specific weight, reliable power plants have been developed.

1.6 For the widest range of anticipated missions, power demands will be such as to require the usage of power plants operating with nuclear reactor heat sources. It is expected that power requirements will range from several kilowatts up to tens of megawatts.

1.7 For missions requiring large amounts of auxiliary power for communications or human sustenance, electrical propulsion devices will exhibit an enhanced payload capability in comparison to chemical rockets.

1.8 The practical ranges of exhaust velocities (in terms of equivalent specific impulse) for electrical drives in the foreseeable future (say 5-10 years) appears to be roughly: plasma jet, 1000-3000 sec.; MHD devices, 2000-10,000 sec.; ion (using alkali metal propellants), 5000-20,000 sec.; and ion (using colloids, dust particles or heavy ions), 2000-10,000 sec.

1.9 Electrical propulsion systems using magnetic fields for acceleration or

containment will require a major decrease to be made in the specific weight of high field strength magnets, before these systems can become competitive with the ion rocket.

2. Recommendations

2.1 Greater emphasis should be placed on the solution of problems and the development of components common to all electrical propulsion systems. The nuclear reactor heat source is a prime example.

2.2 The greatest single problem confronting us in all areas of advanced research is materials compatibility. Activity in this area should be expanded. Greater emphasis is particularly recommended for fundamental work in such fields as solid state physics.

2.3 It is time to initiate the construction and operation of a prototype ion rocket engine with the objective of experimentally defining engineering problem areas.

INTRODUCTION

New types of propulsive devices, requiring large amounts of electrical power for their operation, are expected to compete with or become superior to conventional rocket engines for many future space missions. One such concept is the ion rocket engine. Although the low thrust ion rocket was considered as early as 1930 for interplanetary flight, it is only within the last half-decade that it has received serious attention. Other electrical propulsion schemes, such as the plasma jet and the various MHD devices, are also vying for the R&D dollar. This recent interest is due to (1) the anticipated near-future availability of large chemical booster rockets, and (2) advances in reactor technology which indicate the eventual development of a lightweight power source. This latter item is an absolute necessity if electrical propulsion is to become practical.

It is a well-known physical axiom that a very small thrust exerted on a body can achieve the same velocity as a very large thrust if the former is maintained for a proportionately longer period of time. Since the flight time of a feasible chemical rocket vehicle to the nearer planets would be approximately one year (due to a long coasting trajectory), the low-thrust technique becomes competitive. This is because the low-thrust would be maintained throughout most if not all of the flight time, thus producing the required increment of velocity. Even missions of shorter distance can be considered, especially if a short flight time is not of prime importance. Using a large specific impulse, a low-thrust vehicle with the same initial weight as its chemical rocket counterpart should be capable of delivering larger payloads for most space applications.

Rocketdyne has been engaged in a formal research program on ionic propulsion under Air Force cognizance since February 1957, although preliminary analyses and evaluations of electrical propulsion systems were initiated prior to that date.

The objective of our program is to develop complete ion rocket engines which

will be capable of operating economically and reliably in the regimes indicated by mission analyses. To accomplish this end, Rocketdyne is currently conducting application and systems evaluation studies on electrical rockets as well as analytical and experimental research on virtually all components and subsystems of the ion engine.

The mission analyses performed at Rocketdyne and elsewhere have shown the applicability of electrical rocket engines to various satellite maneuvers as well as to the aforementioned interplanetary flights. Some of these include (1) low altitude flight, (2) changing altitude, (3) precession control, (4) changing orbit inclination, (5) changing orbit ellipticity, and (6) vehicle altitude control. However, it must be pointed out that all of the proposed electrical propulsion devices are not competitive for all of the missions of interest, particularly when thrusting time is of importance.

Experimental ion work at Rocketdyne has consisted of the construction of test equipment and the testing of complete thrust chambers including (1) contact sources, (2) propellant feed systems, (3) electrode configurations, and (4) instrumentation. A valuable adjunct to our analytical effort is the current operation of an analog thrust chamber simulator, designed to study problems in electrode design and ion-electron beam dynamics. In addition, contractual work has been completed on the design of an experimental thrust device having 0.2-lb of thrust, and its supporting experimental equipment.

As part of its long range plan to develop advanced propulsion engines, Rocketdyne has constructed and is currently operating a small Rankine-type power loop using sodium as the working fluid. Future plans call for the testing of the system with rubidium metal also.

DISCUSSION

Mission Capability

In the development of any new rocket engine, it is axiomatic to inquire about its anticipated capability prior even to the establishment of technical feasibility. The justification for the undertaking of a costly R&D program lies ultimately in the economics of operation. If an analytical evaluation indicates that a new propulsion system should be capable of delivering payloads on a wide range of missions in acceptable flight times and at costs "reasonably" below those of available systems, sufficient justification exists for its development.

Numerous studies have been made to ascertain the potential applications of ionic and other electrical propulsion systems and compare them with high thrust chemical and nuclear rockets (Ref. 1, 2, 3, 4, 5, 6, 7, 8, 9). For many missions of interest too many unknowns still exist to determine the best system. In general, however, the trend of our mission analyses indicates that the use of ionic propulsion becomes increasingly advantageous as the assigned task becomes more ambitious.

Two distinct regimes of application may be considered for electrical propulsion: (1) satellite maneuvers and (2) interplanetary flight. The major satellite maneuvers of interest are shown in Table 1.

Table 1

Electrical Engine Applications for Satellites

1.	Low altitude flight
2.	Changing altitude
3.	Precession control
4.	Changing orbit inclination
5.	Changing orbit ellipticity
6.	Vehicle attitude control

The engine requirements for the maneuvers indicated in Table 1 are discussed in detail in a forthcoming Air Force Technical Note (Ref. 10).

Flight time has two distinct connotations. For certain missions such as changing orbital altitude, the term refers to the time required to perform the mission, that is, to go from one region in space to another. For other missions such as low altitude satellite flight, flight time more properly refers to the thrusting period required to maintain the vehicle in the prescribed orbit. In the former example, it may be desirable to minimize travel time at the expense of payload carrying capability or at least to keep it within reasonable limits, particularly for manned flight. In the latter case, it may be desirable to keep the satellite in orbit for an extended period, thus requiring a rocket engine capable of long operating times.

Figure 1 shows the competitive operating regimes for several low thrust systems based on a comparison of propulsion system weight (including propellant) versus required burning time for thrust levels covering the range 0.1 - 5.0 lbf. For

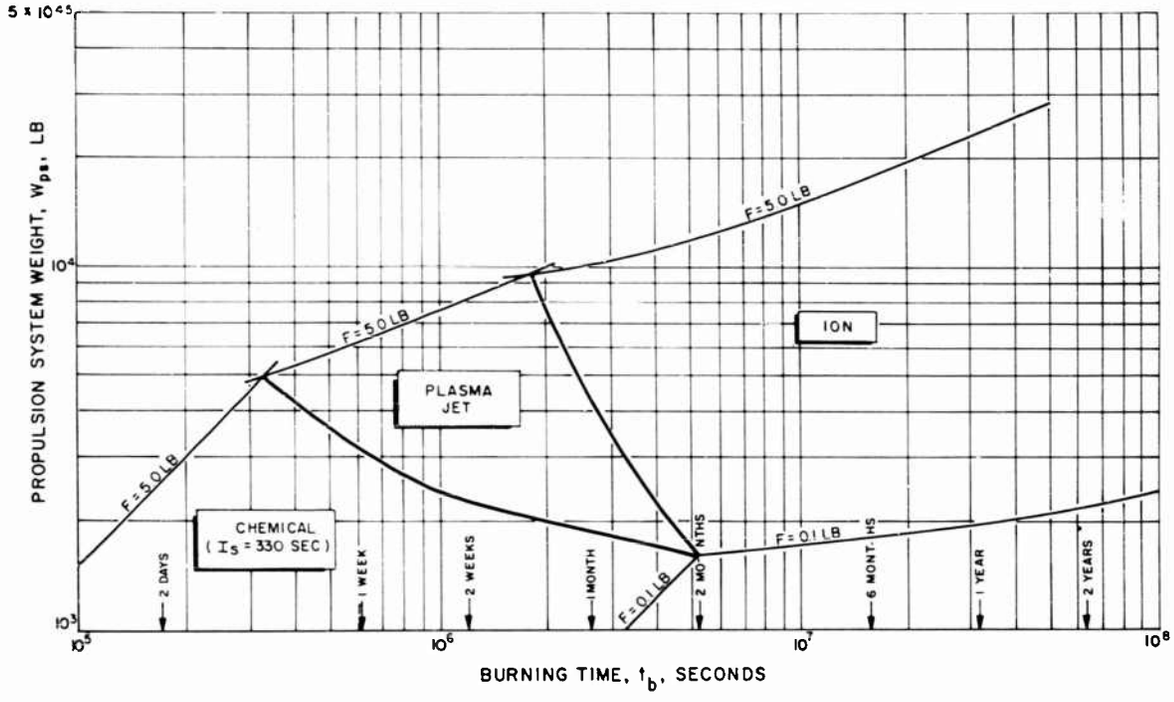

Fig.1 Competitive Operating Regimes for Low-Trust Space Rockets

example, to obtain the minimum powerplant weight for a thrust requirement of 5-lbf (corresponding to the atmospheric drag on a seven-foot diameter cylinder in a circular orbit at about 82 miles), an advanced chemical engine (I_s = 330 sec.) should be used for maintenance of orbit up to four days, with a plasma jet or colloid rocket for periods up to three weeks and an ion rocket for times in excess of three weeks.

The data from Figure 1 are based on a determination of the optimum specific impulse as a function of burning time and thrust level. Figure 2 is a more comprehensive version of Figure 1 and its derivation is given as follows.

The electrical power required for propulsion can be shown to be

$$P = (1/2) g I_s F \eta^{-1} \qquad (2)$$

where η is the efficiency of conversion of electrical energy into directed thrust.

If the thrust chamber, feed system and propellant tank weights are neglected (a reasonable assumption for electrical propulsion systems which do not use heavy magnets for propellant acceleration), the propulsion system weight is

$$W_{ps} = W_f + W_{pp} \qquad (3)$$

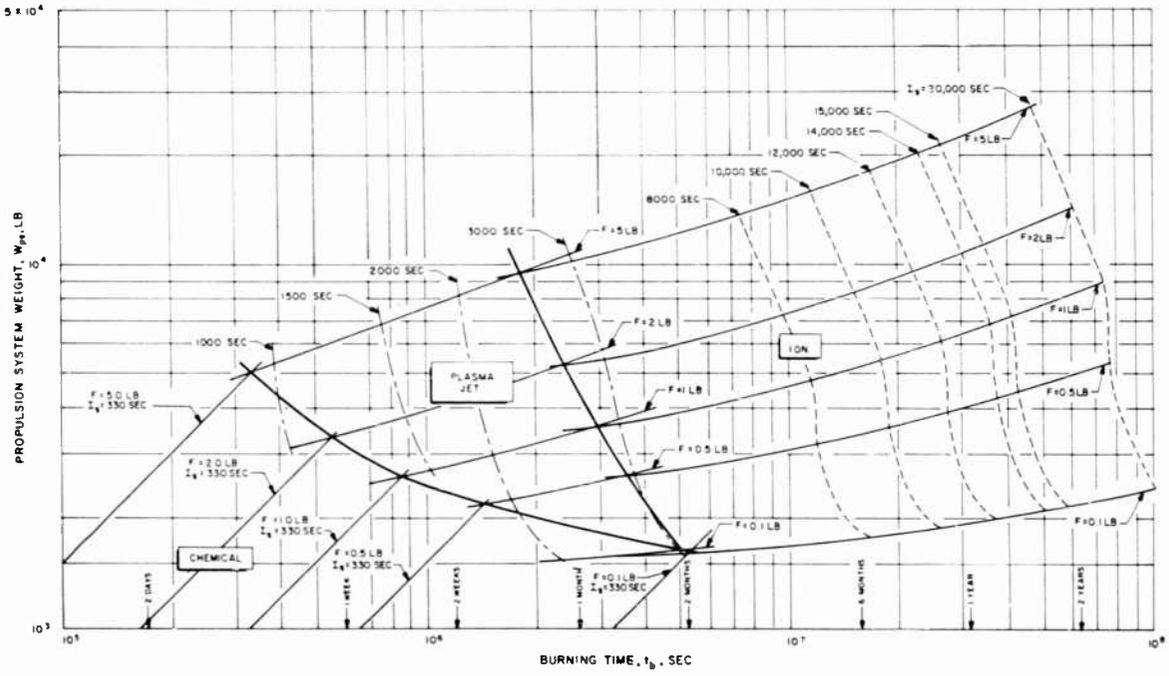

Fig.2 Propulsion System Weight vs Burning Time for Optimum Specific Impulse

or

$$W_{ps} = F t_b I_s^{-1} + W_{pp} \qquad (3A)$$

where W_{pp} is the powerplant weight (heat source, radiator and power conversion equipment), W_f the required propellant weight, and t_b the burning (thrusting) time.

In order to minimize propulsion system weight, eq. (3A) is differentiated at constant thrust and burning time and the derivative set equal to zero. The resulting equation is:

$$(I_s)_{opt} = \left\{ F\, t_b \Big/ \left(\frac{\delta W_{pp}}{\delta I_s} \right)_F \right\} \frac{1}{2} \qquad (4)$$

For calculational purposes, eq. (4) can be solved most simply by assuming values of F and I_s and calculating t_b. This avoids a trial and error solution since the partial derivative (slope of the W_{pp} vs I_s curve) is a function of I_s.

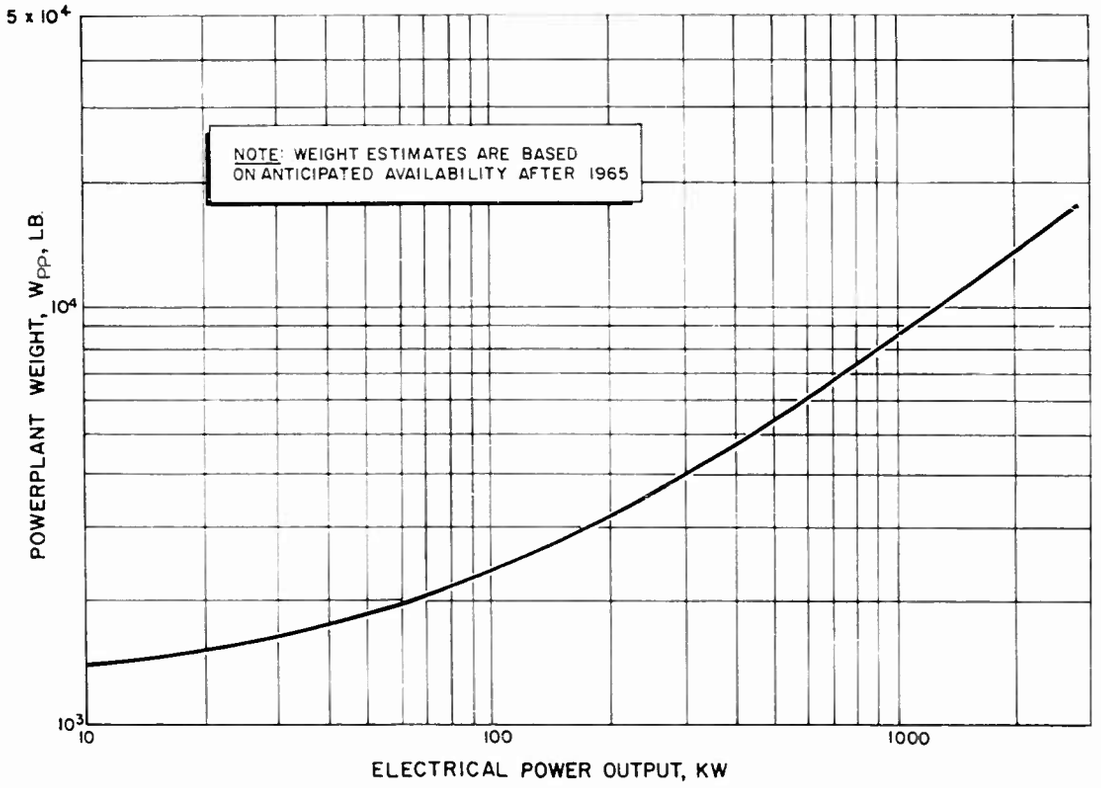

Fig.3 Nuclear Turboelectric Powerplant Weight Including 1000 lb. Shield

The relationship of powerplant weight to electrical power output is shown in Figure 3 for a nuclear turboelectric system (Ref. 8). By combining this data with eq. (2) and the assumed efficiency curves for ion and plasma jet thrust chambers, as shown in Figure 4*, a plot was made of W_{pp} vs I_s and the slopes measured for use in eq. (4). Figure 2 was then obtained by combining equations (3A) and (4).

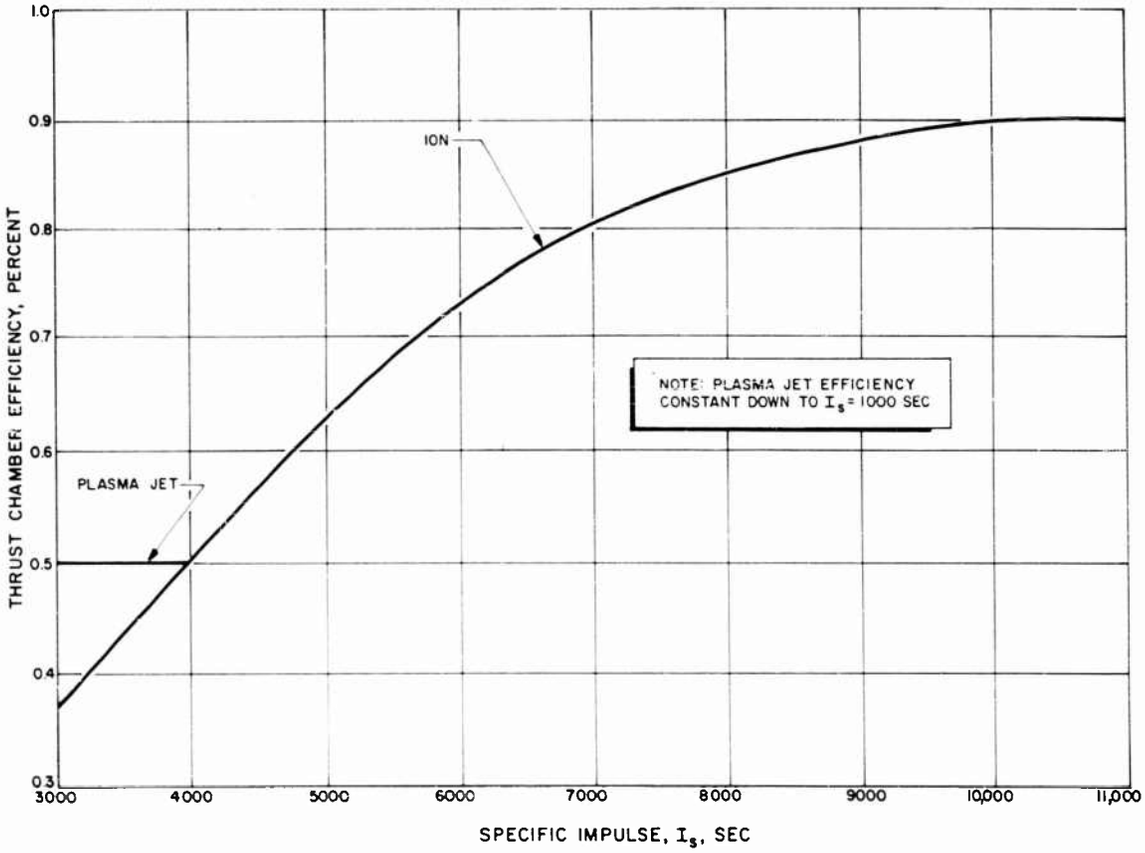

Fig.4 Assumed Thrust Chamber Efficiencies for Electrical Propulsion Systems

Figures 1 and 2 are quantitatively useful for obtaining the competitive operating regimes of the systems compared for certain missions such as low altitude flight and attitude control. For a fixed orbital stay time, the prime criterion usually is minimum powerplant weight since the major cost factor depends on the weight required to initially boost into orbit.

From a qualitative point of view, much can also be learned from the first two figures. For example, it is known that flight times to Mars (or Venus) will range up to about a year for low thrust systems (Ref. 2, 8, 9, 14). From Fig. 2 it can be seen that a high specific impulse ion rocket appears to be indicated. On the

* The efficiency curves shown in Fig. 4 are believed to be reasonable values for the first generation or two of electrical devices. These are based on experimental and analytical data obtained at Rocketdyne and elsewhere (Ref. 11, 12, 13).

other hand, lunar mission requirements tell a different story. Table 2 shows the required travel times for the one-way lunar trip as a function of initial-thrust-to-weight ratio (Ref. 9). Since ion rockets are expected to operate in the range of $F/W_o \leq 10^{-4}$ for many years to come, travel times of more than 40 days would be required for lunar flights. This is believed to be excessive for such a short space trip and either a plasma jet ($F/W_o > 10^{-4}$) or chemical rocket is indicated. However, for a lunar cargo shuttle, flight time might be of secondary importance to payload capability and the propellant weight advantage of a high I_s ion system would make this system more attractive.

Table 2
Flight Time for Earth-Moon Missions

F/W_o	Time to Moon Days
10^{-1}	2.1
10^{-2}	2.4
10^{-3}	5.6
5×10^{-3}	9.5
10^{-4}	42

For trips beyond Mars, the superiority of the ion rocket is definitely indicated as shown in Table 3 (Ref. 2).

Table 3
Comparison of Ion and Nuclear Rockets

Mission	Mars		Jupiter	
Rocket	Nuclear	Ion	Nuclear	Ion
Transfer Orbit	Elliptic	Elliptic	Elliptic	Parabolic
Characteristic Velocity, Km/Sec	7.5	35	17.5	74
Payload Fraction	0.36	0.36	0.10	0.20
Total Roundtrip Time, Days	970	1100	2200	1100
Waiting Time at Target Planet, Days	450	450	210	10

1.2 Payload

The problem of matching a propulsion system to a mission ultimately reduces to either maximizing the payload or minimizing the system weight (including propellant) for any specific mission (Ref. 15). Although extensive calculations have been made to determine the thrust requirements for various missions, few attempts have been made to match a complete propulsion system to a proposed space mission and determine the optimum operating conditions (Ref. 17). Mission analyses have indicated that for almost all satellite and space flights of interest, electrical propulsion systems are superior to chemical systems, payload-wise, particularly if flight time

is not of prime consideration (Ref. 1, 2, 7, 8, 9, 15, 16). Unfortunately, quantitative comparisons between different electrical propulsion systems are quite scarce, even though the anticipated capability of individual devices has been indicated for certain missions (Ref. 14, 18, 19, 20).

It has been stated (Ref. 12) that, with electrical rockets, payload can be maximized for operation within the gravitational field of the Earth and to the Moon if specific impulses of 1000 - 5000 seconds are used. However, as is discussed in Section 1.1, certain missions (e.g. low altitude flight) optimize out to higher values of I_s if long flight times are required.

For interplanetary trips to Mars, it has been concluded (Ref. 17) that specific impulses in the range 4,000 - 10,000 sec. yield the largest payloads. The results of one particular calculation performed at Rocketdyne are presented in Table 4. The values indicated were not optimized.

Table 4
Comparative Performance* of Typical Vehicles
for an Earth-Mars Mission

System	Payload Weight lb.	Travel Time Days	F/W_o	I_s sec.
Chemical	23,500	260	0.5	425
Nuclear	30,000	260	0.5	750
Ion	47,000	300	10^{-4}	10^4

*Launch from 300 mile Earth orbit with W_o = 64,000 lb; one-way flight; Hohmann transfer ellipse for chemical and nuclear.

1.3 Economics

As in most fields of endeavor, maximum economy is the ultimate controlling factor, within of course, the limitations of reliability. For low thrust electrical propulsion systems, two major cost items must be considered: (1) cost to boost the propulsion system plus its payload into Earth orbit, and (2) cost of the electrical propulsion system itself (including propellant). Although first generation ion (and probably plasma jet) engines should be available within the next three years, improved systems (from the standpoint of utility, reliability and economy) will probably not reach operational status until 1965. Therefore a discussion of economic considerations will be limited to the time period beyond about 1965.

Large chemical boosters, having thrust levels in excess of one million pounds, should be available in the period beyond 1965. These boosters (when combined with second stage chemical rockets) are expected to be capable of delivering multi-ton payloads into a low altitude Earth orbit at costs of $200 - $300 per pound of payload**. As an example consider a 50,000-lb satellite to be maintained in orbit

at an altitude of about 82 miles for one year (see Section 1.1). The cost of boosting this system into orbit (at $200/lb) is 10 million dollars.

For the above example an ion motor is required (F = 5-lb) to overcome drag. This system has a payload fraction of 0.50. As is shown in Fig. 2, the optimum specific impulse is about 16,000 seconds, thus requiring a total propellant weight of about 10,000 lb. Now, the current price of cesium is approximately $500 per pound, although the American Potash Co. estimates that this price will ultimately drop to $25-100 per pound in ton lots. Therefore, if cesium is used as the propellant, it will add one quarter to one million dollars to the propulsion system cost. The other major cost item is the nuclear powerplant, of which the reactor cost predominates. Although information is completely inadequate in order to accurately estimate powerplant cost, it is believed to be somewhere between one and ten million dollars**. For the first few systems built, costs will probably be close to the latter figure. Neither the chemical nor the plasma system is capable of supporting this low altitude mission.

Cost reductions may ultimately be achieved through the exploitation of several avenues of approach. Nuclear rocket development should eventually lead to a reduction in booster costs. Similarly, reactors for auxiliary power usage may someday reach a high enough rate of production to drop powerplant costs to one million dollars or less. Propellant cost can be reduced by switching to low cost colloids, dust particles or heavy ions (when large propellant weights are required).

1.4 Versatility

Low thrust electrical propulsion systems are characterized by a versatility of operation unmatched by chemical or nuclear rockets. Electrical systems should be capable of varying such parameters as thrust level and specific impulse in order to obtain the optimum performance for any given mission. In addition, the long burning times associated with these systems for interplanetary flights will permit continuous steering adjustments to be made (Ref. 14). Deviations in vehicle flight path due to such factors as engine thrust variations, launch timing errors, mismeasurement of applicable solar system data, etc., can cause a ballistic interplanetary vehicle to fail. In the case of a continuously powered vehicle, however, continuous correction for those factors can be accomplished by vectoring the thrust by means of a proper closed loop guidance system.

A second factor to be considered is the availability of the electrical powerplant for communications and other APU usage. Thus, part or all of the electrical generating system normally used for propulsion can be classified as payload. For high power APU requirements, particularly on extended flights, chemical rockets will require heavy electrical powerplants which do not contribute to propulsion. With nuclear rockets, it is uncertain whether the reactor system can be converted to closed cycle operation and operated at the required low power levels compared to its normal operating level.

* This weight includes the elcetrical propulsion system required for space flight or satellite maneuvers.
** This obviously neglects the cost of development.

A third factor to consider under versatility is the potential utility of the electrical propulsion system for cargo shuttling. If many trips are carried out prior to major overhauling of the engine (an excellent possibility for the lunar voyage), the weight of the powerplant becomes relatively unimportant. In addition, since propellant weight requirements are small in comparison to chemical systems, fuel replacement weight is minimized and payload weight can be maximized.

1.5 Reliability

Without a doubt the most critical factor influencing rocket flight today is reliability. Chemical systems are composed of many thousands of components with the malfunction of any one likely to lead to complete flight failure. It is almost redundant to state that manned flight cannot precede the achievement of a major increase in overall system reliability.

Now reliability is directly related to both system complexity and number of test firings. Unfortunately, electrical propulsion devices will be considerably more complex than their chemical counterparts since power must be supplied by an auxiliary electrical system rather than the propellant itself. One relative advantage of the ion rocket (compared to plasma types) is that it appears to be inherently the simplest device. However, the utmost simplicity in design must be combined with the minimum number of components if reliability is to approach a reasonable figure.

Since reliability can also be increased by increasing the number of static and flight tests, the need for an accelerated ion engine development program is indicated if sufficient tests are to be performed leading to a highly reliable system within the next 3-5 years.

Technical Feasibility

Prior to the First Advanced Propulsion Symposium held in December 1957, a number of paper studies were carried out on ionic propulsion. Although mission analysis indicated that this concept showed great promise for low thrust space flight, particularly where interplanetary distances are involved, technical feasibility was yet to be demonstrated.

2.1 Progress since First Advanced Propulsion Systems Symposium

During 1958, experimental programs were initiated by Rocketdyne and other organizations in order to establish the feasibility of the ion rocket concept as well as to investigate the problem areas and to develop a satisfactory propulsion system. In a remarkably short period of time and with modest dollar expenditures, great strides have been made toward the realization of an operational ion engine. The operation of small, research thrust chambers has demonstrated without a doubt that it is technically feasible to accelerate charged particles by an electrostatic field gradient for the development of thrust under the vacuum conditions of space. In addition, it has been shown that technical break-throughs are not required, but rather straight-forward research and development programs in such areas as materials and ion-electron optics.

2.2 Ion Engine Subsystems and Components Status

The major problem area hindering the development of the ion rocket engine is one of materials compatibility. Alkali metals such as cesium (propellant), rubidium and sodium (power loop) are highly corrosive, particularly at elevated temperatures. Although some encouraging results have been obtained with the refractory metals (eg. W and M_o), much work remains to be done in this area before suitable construction materials are available.

The ion rocket engine is composed of four major subsystems: (1) Ion thrust chamber; (2) Power source; (3) Power converter; (4) Thermal radiator. The status of each of these will be discussed briefly in turn.

2.2.1 Ion Thrust Chamber

The major direct effort in support of ion rocket development is in the area of the thrust chamber. This subsystem is composed primarily of an ionizer, accelerating (and decelerating) electrodes, and an electron gun. The purpose of the electrostatic thrust chamber is to produce a dense, parallel beam of ions which are accelerated through a high potential drop.

A surface contact ionizer has received the most attention to date because of its simplicity and high ionization efficiency. In this source, an atom is ionized by contact with the surface of a heated metal, the work function of which exceeds the ionization potential of the atom. Cesium is easily ionized by this method and was chosen as the initial propellant for experimentation at Rocketdyne after an analysis indicated its favorable characteristics in this regard. Power is wasted if lightweight ions are used to develop thrust (Ref. 21). This is shown by the relationship

$$P/F = 30.89\ (V/A)^{1/2},\ \text{kw/lb} \qquad (1)$$

Where V is the potential gradient, A the effective ion mass per unit of charge, P the electrical power requirement and F the thrust level. Specific sources have been designed, fabricated and operated with porous graphite, nickel and tungsten disks as ionizers with the latter material proving quite successful. The data obtained agrees well with the theory (Ref. 22). This work has provided information about ionic and neutral efflux as a function of ionizer temperature, mass supply rate and ionizer porosity and thickness. Similar efforts are known to be underway at Electro-Optical Systems, Inc. (Ref.13) using potassium as the propellant and a tungsten ribbon ionizing surface; the General Electric Flight Propulsion Laboratory (Ref. 23) using cesium propellant and both porous plate and wire screen ionizers; Thompson-Ramo-Wooldridge Corp. (Ref.24) using cesium, potassium and rubidium as propellants and porous tungsten plugs for ionizers; and NASA Lewis Research Center using cesium and other propellants and a variety of ionizer materials and types.

Ionizer current densities of 30 ma/cm^2 have been obtained by Rocketdyne at 1500 K with cesium and porous tungsten (Ref. 31). This is the value anticipated at this temperature and is well in excess of requirements for efficient ion motor operation.

After the cesium (or other propellant) ions leave the ionizer surface, they are accelerated to high energy. The accelerating electrodes may then be subject to severe sputtering (erosion). The high specific impulse of the ion engine exhaust implies a high particle energy. Such a particle striking a surface can eject several surface atoms per incident ion. The ejection rate is dependent upon particle energy, mass, angle of incidence, surface structure, surface temperature, etc. It is possible for a poorly collimated beam to sputter away on the order of the total propellant weight in electrode material. Thus it can be seen that the design of the electrodes for the ion accelerating system is critical if long operating lifetime is to be achieved. Experiments at the Oak Ridge National Laboratory indicate, however, that by properly shielding the electrodes, it is possible to limit impingement to less than 1 ion in 10^4 (Ref. 33).

Various accelerator geometries have been examined experimentally as well as analytically (Ref. 25). However, accelerator designs in existence today may not be adequate to meet the requirements imposed by ion thrust chambers if extended lifetime is to be achieved. Because the fields formed by the presence of charged electrodes are complex when a high degree of geometric simplicity is not maintained, and because the presence of a charged beam affects the shape of the field, a closed analytical solution is seldom obtained for a given electrode design. Either approximation or analog methods must be employed to predict the behavior of the ion beam resulting within a given electrode configuration. The more satisfactory method is an analog device such as an electrolytic tank which can be used to plot the field and the ion beam distribution. From the information derived, it is possible to specify electrode geometries which will produce a well-collimated, high current ion beam. Rocketdyne has therefore designed and constructed an ion thrust chamber simulator as shown in Fig. 5, based on the electrolytic tank principle. When results are available from this equipment, it is anticipated that the problem of electrode design will be largely eliminated.

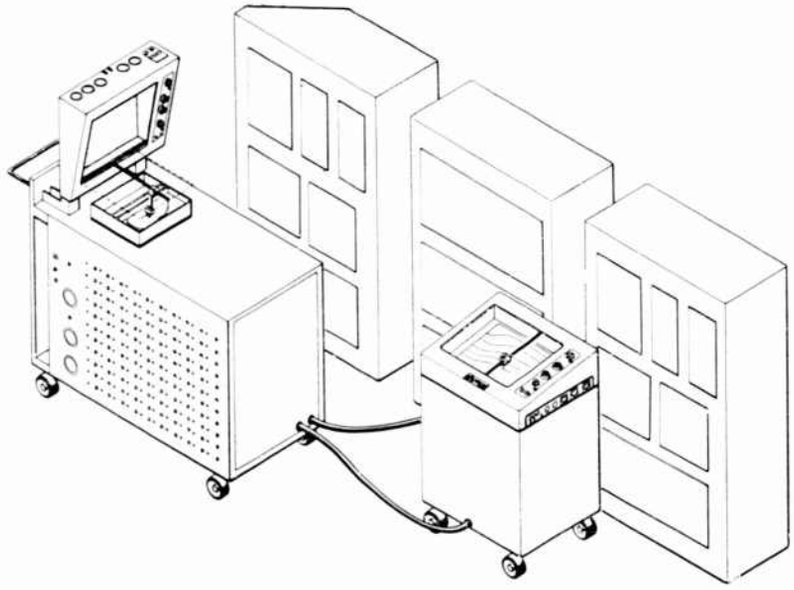

Fig. 5 Ion Thrust Chamber Simulator

The accelerator-decelerator system first accelerates the ions to a high velocity and then decelerates them to their required final value. This arrangement permits somewhat higher space charge limited current densities in the acceleration gap and prevents the beam neutralizing electrons from getting back to the ionizer.

The ion engine cannot operate unless there is a simultaneous emission of electrons from the vehicle at a rate equal to the ion current. Perhaps the simplest technique for the emission of electrons is by direct injection into the ion beam. The process of neutralization through the use of a thermionic emitter in close proximity to the beam appears to give satisfactory results. However, it has not yet been determined how close the filament must be to the ion beam for effective neutralization. In addition, it has been pointed out (Ref. 24) that neutralization of high currect density beams may not be just a matter of adding enough electrons to make the gross propellant current neutral with respect to the vehicle. An intimate mixing of electrons and ions may also be required at their point of exit in order to prevent deceleration of the ions and their subsequent return to the ship due to space charge forces. This problem could arise due to wide differences in mass between the ions and electrons.

2.2.2 Power Source

The major problem of an electrical propelled space vehicle is the continuous development of high specific power for long periods of time. Numerous papers have been written on the subject of power for space vehicles (eg., see Ref. 26, 27, 28). On the basis of anticipated availability in the period 5-10 years hence, the nuclear reactor heat source coupled either with (more-or-less) conventional turbomachinery or with a direct-conversion-to-electricity device such as the thermionic emitter, appears to be the most advantageous system for power requirements exceeding a few kilowatts. A reactor concept to be considered for this use must offer high temperature operation, light weight and be capable of long duration. High temperatures are required for increased thermodynamic cycle efficiencies and, for what is probably more important, reduced weight of the heat rejection system. The light weight requirement leads to high power density cores (minimum size) and the long endurance requirement to large fuel burnups and high system reliability. Several orders of magnitude improvement in reliability and endurance of reactor hardware will be required for competitive electrical propulsion systems.

In the next 3-5 years, low power reactors (less than 50 Kwe) should be available from the A.E.C. Snap program for Auxiliary Space Power. Prior to that time reliance will have to be placed primarily on chemical systems, possibly supplemented by solar cells.

2.2.3 Power Converter

Turboelectric power converters based on the mercury cycle for operation in the range up to tens of kilowatts appear to be in an advanced engineering state of development (Ref. 15, 16, 17). Rankine cycles, using Rb or Na, at temperatures in the neighborhood of 2000 F appear to be much lighter than Hg, especially for high power levels (Ref. 5, 6, 34). However, work on the alkali metal systems is in an early state of development. Rocketdyne is currently operating a test loop with boiling sodium as is shown in Fig. 6.

The most promising electrical generator for ionic propulsion is the electrostatic type (Ref. 17, 32) which produces a voltage from the change of capacitance of a variable condenser. The electrostatic generator is inherently a high voltage, low current, high efficiency device. However, the present statc-of-the-art is in its infancy. Much basic R & D is needed including studies on voltage breakdown in vacuum, mechanical stability due to electrostatic forces, commutators, brushes, sliprings, bearings and seals.

Other electrical generators which will probably precede the electrostatic type in terms of early availability arc based on the electromagnetic principle. Howevcr, numerous problems require solution before a practical device is available for use in space. These include reliability and lifetime at high temperatures in a radiation and possibly corrosive atmosphere, high speed operation, cooling, seals, bearings and lubrication.

2.2.4 Thermal Radiator

In space, all excess energy which is not carried off in the rocket jet can be dissipated to the rocket's surroundings only by radiation. A great many design problems arise from consideration of this excess energy disposal problem. For instance, radiation of a large amount of energy requires a large radiation surface area, the provision of which increases vehicle weight. With power levels in excess of 100 Kwe, the radiator becomes the heaviest component of the powerplant (Ref. 34). In addition, large radiator areas increase the danger of meteorite penetration, thus requiring either increased radiator wall thickness or some kind of shield, both of which increase radiator weight still further. Numerous configurations have been proposed for space radiators. However, knowledge of meteorite density and penetrability is inadequate at the present time for minimum weight design.

2.3 Efficiency

The overall efficiencies of electrical propulsion systems are unlikely to approach those of the chemical or nuclear rockets due primarily to system complexity. As was pointed out in Section 2.2, system efficiency is highly important since

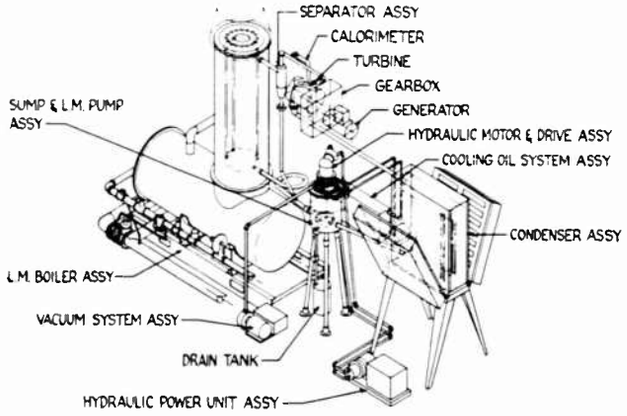

Fig. 6 Liquid Metal Boiling Loop Experiment

wasted heat not only requires larger and heavier power units but also excessively large and heavy radiators. With electrical rocket engines, the two major efficiency terms stem from the powerplant and the thrust chamber. Nuclear powerplants will probably have overall efficiencies of 20-40%, depending on choice of cycle, operating temperatures and efficiencies of the turbomachinery components. Thrust chamber efficiencies are measured by the conversion of electrical energy into directed thrust in the propellant exhaust, and varies both with type of electrical system as well as specific impulse.

At the present time, the ion rocket thrust chamber appears to have a significant advantage in efficiency compared to the plasma systems (Ref. 11). The cesium ion device is expected to have an efficiency of 90% or greater for specific impulses in excess of 10,000 sec., which decreases to about 50% at 4-5000 sec. Below this value, the efficiency is too low to be practical since the energy required to heat the ion emitter plus energy losses due to interception of the ions on the accelerator are too large a fraction of the input electrical energy.

Plasma jet thrust chamber efficiencies of 50% have been measured at specific impulses of about 1100 sec. (Ref. 12, 29). Although some increases can be expected as research progresses, it is unlikely that values will be achieved approaching that of the ion rocket at high specific impulses in the near future.

An inadequate amount of information appears to be available in order to estimate thrust chamber efficiencies for MHD devices. One source (Ref. 17) quotes values of 39% for a continuous MHD accelerator, 16% for an intermittent button-type and 40% for an intermittent shock tube device.

No information could be found on colloid systems.

2.4 Status of Competitive Systems

Development of the arc or plasma jet appears to be progressing rapidly. Efforts have been directed toward the use of the fixed gases as propellants (Ref. 12, 29). Major problem areas are electrode consumption, electrode and nozzle cooling, arc stability at low pressures, and energy losses.

Most of the MHD devices proposed are in the basic research or pre-engineering development phase (Ref. 12, 17, 18, 20). One major problem area is the need for light weight, high field strength magnets. The early development state of the various plasma accelerators eliminates them for serious consideration as competitors of the ion and arc jet engines during the next few years.

The status of the colloid rocket is not too clear based on available information (Ref. 30) although it probably can be considered to be in the pre-engineering development phase.

From a physical development point of view, the only electrical system which appears to be competitive with the ion engine today is the plasma jet and the latter system is restricted to a much smaller specific impulse range as has been discussed in Section 1 of this paper.

REFERENCES

1. Irving, J. and Blum, E.: Comparative Performance of Ballistic and Low Thrust Vehicles for Flight to Mars, Space Technology Lab. (1958).

2. Fox, R.: Preliminary Studies on Electrical Propulsion Systems for Space Travel, ARS 708-58.

3. Stuhlinger, E.: Possibilities of Electrical Space Ship Propulsion, Fifth International Astronautical Congress, Innsbruck, Austria (1954).

4. Dillaway, R. B.: Propulsion Systems for Space Flight, Aeronautical Engineering Review (April 1952) 42.

5. Ion Rocket Study Program at Rocketdyne, Final Report, AFOSR TR-58-81 (28 February 1958).

6. Ion Rocket Study Program at Rocketdyne, Final Report, AFOSR, R-1584 (1959)

7. Ehricke, K. A.: Comparison of Propulsion Systems; Solar Heating, Arc Thermodynamics and Arc Magnetohydrodynamics, First Advanced Propulsion Systems Symposium (Dec. 1957) 71.

8. Moeckel, W. C. and etal: Satellite and Space Propulsion Systems, NACA Flight Propulsion Conference, Vol. II (1957) 27.

9. Craig, R. T. and etal: Advanced Space Propulsion Systems, Vol. I, Mission Analysis, ER-3622

10. Denniston, J. B. and Moser, W. A.: Flight Mechanics of Low Thrust Vehicles in a Strong Gravitational Field, to be published as an AFOSR Technical Note (1959).

11. Fisher, E.: Advanced Propulsion Concepts, ARS 847-59.

12. Camac, M. and Janes, G. S.: Applied Magnetohydrodynamics at Avco - Everett Research Laboratory, ARS 902-59.

13. Naiditch, S.: Experimental Ion Sources for Propulsion, ARS 883-59.

14. Ferebee, F. M.: Flight Mechanics of Low Thrust, High Energy Space Vehicles, ARS 605-58.

15. Craig, R. T. and etal: Interim Technical Progress Report on Advanced Reaction Propulsion Systems for Period Ending December 31, 1958, ER-3673.

16. Craig, R. T. and etal: Interim Technical Progress Report on Advanced Reaction Propulsion Systems for Period Ending March 31, 1959, ER-4169.

17. Fairweather, S. H.: Advanced Space Propulsion Systems, Vol. 2, Propulsion Systems, ER-3623.

18. Kunen, A. E.: The Magnetic Pinch Engine for Space Flight, AAS 59-13 (August 1959).

19. Edwards, R. N. and Brown, H.: Ion Rockets for Small Satellites, ARS789-59.

20. Camac, M., Kantowitz, A., and Petschek, H. E.: Plasma Propulsion Devices for Space Flight, Avco Research Laboratory Research Report 45 (February 1959).

21. Boden, R.H.: The Ion Rocket Engine, Presented at the SAE National Aeronautical Meeting, New York (April 1958).

22. Langmuir, I. and Taylor, J.: Physical Review 40 (1932) 463.

23. Edwards, R. N. and Kuskevics, G.: Ion Rocket Propulsion Characteristics, Presented at the Second AFOSR Contractors Meeting on Ion and Plasma Propulsion (July 1959).

24. Shelton, H. and etal: Generation and Neutralization of Ions for Electrostatic Propulsion, ARS 882-59.

25. Eilenberg, S. L.: Accelerator Design Techniques for Ion Thrust Devices, AFOSR-TN-59-194 (February 1959).

26. Means, P.: Search for Space Vehicle Power; Missiles and Rockets (July 27, 1959) 22.

27. Hamilton, R. C.: Interplanetary Space Probe Auxiliary Power Systems, ARS 864-59.

28. Zwick, E. B.: Space Vehicle Power Systems, ARS 867-59.

29. Cann, G. L. and Ducati, A.C.: Research on High Intensity Ionic Jets, Presented at the Second AFOSR Contractors Meeting on Ion and Plasma Propulsion (July 1959).

30. Shultz, R. D.: Investigation of a Charged Colloid Propulsion System, Presented at the Second AFOSR Contractors Meeting on Ion and Plasma Propulsion (July 1959).

31. Forrester, A. T.: Cesium Ion Motor Development Presented at the Second AFOSR Contractors Meeting on Ion and Plasma Propulsion (July 1959).

32. Eilenberg, S. L. and Huebner, A. L. C.: Engineering and Scientific Problems of Ion Propulsion, ARS 880-59.

33. Luce, J. S.: Private Communication to R. H. Boden on July 24, 1959 from Oak Ridge National Laboratory.

34. Aircraft Nuclear Propulsion Project Semiannual Progress Report for Period ending March 31, 1959, ORNL-2711, p. 94.

THE COLLOID ROCKET: PROGRESS TOWARD A CHARGED - LIQUID - COLLOID PROPULSION SYSTEM

by

ROBERT D. SCHULTZ and LANE K. BRANSON

SPACE TECHNOLOGY DIVISION
AEROJET-GENERAL CORPORATION

SUMMARY

Theoretical and experimental research is described leading toward a space propulsion system in which microscopic oil droplets are produced with a high positive charge and accelerated electrostatically to exhaust velocities of over 50,000 miles per hour with a specific impulse of over 2200 seconds. This type of rocket system may prove to be of considerable value for controlling the orbit of an earth satellite, for earth-moon missions, and possibly for deep-space exploration such as a Mars or Venus probe.

INTRODUCTION: THE HISTORY OF CHARGED-LIQUID-COLLOID PROPULSION

A colloid may be defined as any substance in a certain state of fine division, the colloidal state, in which the particles range in diameter from about 0.5 to about 0.005 micron. The electrostatic acceleration of electrically charged, colloidal particles was discussed as a possible means of space propulsion by H. Preston-Thomas in 1952.[1] J. J. Barré, at the VIIIth International Astronautical Congress in Barcelona, October 1957,[2] presented a theoretical paper on ion propulsion which contained calculations of the performance characteristics of both liquid and solid charged-colloid particles. K. A. Ehricke, at the First Symposium on Advanced Propulsion Concepts, Los Angeles, December 1957,[3] estimated the theoretical performance of an "electric-dust" propulsion system to be as high as 7000 lb force/lb mass/sec. In June 1958, an experimental and theoretical investigation of charged-colloid propulsion was initiated in the Astronautics Laboratory of the Aerojet-General Corporation under Corporate sponsorship. Encouragement to this project was given by Dr. Morton Alperin, then Director of the Office of Advanced Studies, U.S. Air Force Office of Scientific Research; Mr. Y. C. Lee, present Manager of the Space Technology Division of the Aerojet-General Corporation; and Dr. George Moe, present Head of the Aerojet-General Corporation Astronautics Laboratory.

In the original concept of the project, it was hoped to charge solid particles—for example, graphite or silica of about 0.6-micron diameter—to a positive potential of 10 kv in high vacuum and accelerate them through a high negative potential of 200 to 1000 kv, thereby attaining velocities of 24 to 54 km/sec and specific impulses of 2500 to 5800 sec for a vehicle acceleration of 10^{-2} to 10^{-4} g. Unfortunately, there seemed to be no method, then available, for obtaining a steady, controllable stream of solid, colloidal particles with the requisite high initial positive charge. It was thought possible, however, to develop such techniques by bouncing particles off grids or surfaces maintained at high potentials. One method which was considered consisted of injecting solid colloidal particles under the surface of a liquid metal maintained at 10- to 20-kv positive potential in vacuum. It was reasoned that, when these colloidal particles emerged from the liquid-metal surface, they might pick up sufficient electrostatic charge to be repelled from the surface into vacuum. This idea was discussed in June 1958 by one of the authors, R. D. Schultz, with Mr. Robert Chaiken of the Chemical Division of Aerojet-General Corporation. Mr. Chaiken noted that a roughly similar method had been used in the past to obtain aerosol dispersion of liquids (see Figures 1, 2 and 3). A subsequent literature search revealed several papers[4-10] on the production of monodispersed liquid-colloid particles by electrical atomization of liquids, in some cases from large droplets and in other cases from capillary tubes filled with liquid, from needle tips, or from sharp edges wetted with liquid and subjected to high electrical fields. It was also found that this technique was the basis of a commercial paint-spraying process.[11] However, all these investigations had been conducted in air, and it was not known if liquids of low vapor pressure could be dispersed in high vacuum by this method. By October 1958, it had been established experimentally in our laboratory that such atomization in moderate vacuum, with liquids of moderately low vapor pressure, was possible, and an approximate value of 4×10^8 esu/g was estimated for the initial, positive, charge-to-mass ratio of the resultant colloidal droplets. (The word "initial" is used advisedly because the possible loss of charge from these droplets prior to acceleration is still a subject of investigation.) These results were deemed sufficiently encouraging to shift the emphasis of our project to the electrostatic acceleration of liquid rather than solid-colloid particles.

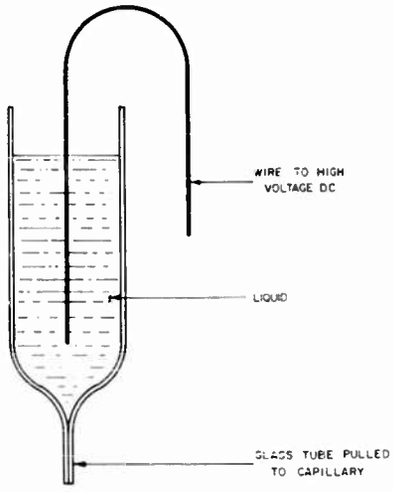

Fig. 1 Apparatus for Electrical Atomization

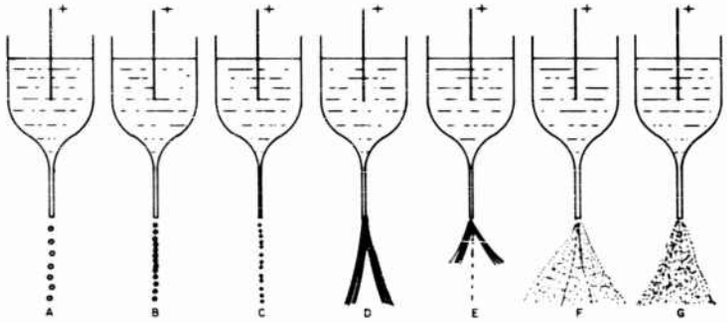

Fig. 2 Stages of Dispersion Observed by Increasing The Applied Potential From 1KV to 12 KV

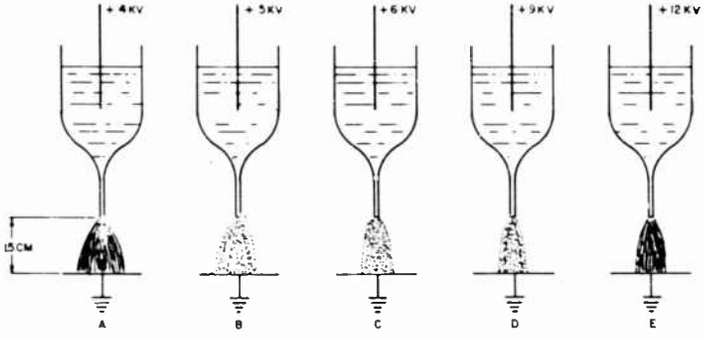

Fig. 3 Stages of Dispersion Observed When a Grounded Plate was Placed 1.5 CM From a Capillary Tip

This report is a summary of the theoretical and experimental progress on charged-colloid propulsion at the Aerojet-General Astronautics Laboratory through August 1959. Some months earlier, in May 1959, funding for the continuation of the project was obtained from the Advanced Research Projects Agency of the U. S. Department of Defense under Contract AF 49(638)-656, monitored by the Propulsion Research Division of the U. S. Air Force Office of Scientific Research. The writers are indebted to Col. Paul Atkinson and Dr. Milton Slawsky of that division and to Dr. Robert Youngquist of ARPA for their interest and encouragement.

THEORY OF THE FORMATION OF CHARGED-LIQUID-COLLOID DROPLETS

The Atomization of Liquids by Electrostatic Pressure

The phenomenon associated with electrical atomization of liquids into charged, colloidal-size particles has been named "dielectrophoresis" by Pohl[10] who defined it as the motion of matter caused by polarization effects in a non-uniform electric field. An electric dipole (induced or permanent) well inside the body of a liquid dielectric tends to be aligned with its axis parallel to the lines of electrical force. If the field is non-uniform, one end of the dipole will be in a weaker field than the other end. Thus, a net force results which pushes or tends to push the dipole in the direction of greatest field intensity. The same situation exists for the dipoles extending into the transition layer at the surface of a liquid droplet carrying a net charge. An exact solution for the electrostatic forces at the surface of the droplet is not possible because of the rapid manner by which the electrostatic field changes in the transition layer from a value E in the interior of the liquid dielectric to a value E_o outside. However, an approximate solution is possible, based on the following assumptions:

1. The liquid is an insulator with a specific electrical conductivity less than 10^{-5} mho/cm. (Note that Neubauer and Vonnegut have found that electrical atomization of liquids is possible if the conductivity is not greater than about 10^{-5} mho/cm.[8]

2. The dielectric constant of the liquid in the transition-surface layer changes continuously from the value ϵ in the interior of the liquid to the value 1 at the interface with air or vacuum.

3. The transition-layer thickness is about equal to the liquid-dipole length.

4. The surface of the droplet is ideally spherical.

On this basis, the electrostatic pressure which tends to expand the droplet can be shown[12,13] to correspond to the equation

$$p_\epsilon = \frac{E^2}{8\pi}\left[(\epsilon - 1)^2 + (\epsilon - 1) - \rho\frac{d\epsilon}{d\rho}\right] \qquad (1)$$

where p_ϵ is the electrostatic pressure, normal to droplet surface, in dynes/cm^2; E is the field strength in the interior of the droplet, just below the transition layer, in esu/cm; ρ is the density of the liquid in gm/cm^3; and ϵ is the dielectric constant of the liquid. Since $\epsilon = E_o/E$, where E_o is the field intensity in air or

vacuum just outside the droplet, it is possible to rewrite equation (1) as

$$p_\epsilon = \frac{E_o^2}{8\pi}\left[\frac{\epsilon - 1}{\epsilon} - \frac{p}{\epsilon^2}\frac{d\epsilon}{dp}\right] \tag{2}$$

or simply

$$p_\epsilon = \frac{E_o^2}{8\pi} f(\epsilon, p) \tag{3}$$

where $f(\epsilon, \rho)$ represents the term in brackets of equation (2), which term can be evaluated for many liquids by the method of Henriquez.[14]

If the charge on the droplet is sufficiently large, the field strength ($E_o \propto \frac{1}{r}$) can become very high at places where local fluctuations of surface curvature occur (i.e., where the radius of curvature r becomes small). This local increase in field strength raises the local electrostatic pressure ($p_\epsilon \propto E_o^2 \propto 1/r^2$), causing a filament of liquid to be drawn out of the droplet at high velocity. The end of the filament is unstable and disintegrates into charged colloidal particles a few tenths of a micron in diameter. For example, Vonnegut and Neubauer[7] have performed several experiments in which a drop of water is placed on a wire and the voltage steadily increased. At approximately +6000 volts, the water drop develops a tiny, sharp bump or filament, from which colloidal droplets are ejected. Judging from the earlier observations of this phenomenon by Zeleny[4], the radius of the filament would be about 2 microns and the velocity of ejection of the filament would be about 8 meters/sec. Let us assume that the tip of the filament is perfectly hemispherical ($r = 2 \times 10^{-4}$ cm) and that the full 6000-volt potential on the drop is transmitted in some manner to the exterior of the filament tip. As an approximation, the field strength of the exterior of the filament tip may be related to the voltage applied to the liquid drop and to the radius of the filament tip by the expression

$$E_o = V/300\ r \tag{4}$$

where E_o is expressed in esu/cm, V is the potential in volts, and r is the radius in cm. For V = +6000 volts and $r = 2 \times 10^{-4}$ cm, $E_o = 1 \times 10^5$ esu/cm. For water the function $f(\epsilon, \rho)$ in equation (3) is nearly unity, so that the electrostatic pressure at the end of the filament is simply $E_o^2/8\pi = 4 \times 10^8$ dynes/cm^2.

In the next section arguments will be presented to demonstrate that a liquid forms charged colloidal particles only when the electrostatic pressure exceeds the macroscopic tensile strength of the liquid at some point in the surface.

Role of Tensile Strength in the Electrical Atomization of Liquids

The value calculated above for the electrostatic pressure developed by the positive electric charges at the liquid filament tip is surprisingly large— so large, in fact, that an explanation is required of these forces that keep the charges attached to the liquid long enough to develop this high electrostatic pressure. Barre[2] and Vonnegut and Neubauer[7] have assumed that the forces that keep the charges attached to the liquid are surface-tension forces. However, these

investigators fail to distinguish between the negative pressure that opposes the breakup of a large drop of liquid into smaller drops and the negative pressure that keeps the charge attached to the liquid surface. A clarification of this point is of considerable importance in estimating the charge-to-mass ratio which may be attained by liquid-colloid droplets. For example, during the electrical atomization of the water droplet described earlier, the surface-tension-induced pressure which opposes the escape of the filament is given by

$$p = \frac{2\gamma}{r} \tag{5}$$

where p is the opposing pressure in dynes/cm^2, γ is the surface tension in dynes/cm, and r is the appropriate radius in centimeters. For a water filament 4 microns in diameter, $p = 2\gamma/r$ or $(2 \times 73)/(2 \times 10^{-4}) = 7.3 \times 10^5$ dynes/cm^2 Notice that this opposing pressure is orders of magnitude lower than the 4×10^8 dynes/cm^2 electrostatic pressure developed at the filament tip. Moreover, this pressure arises from forces which act parallel to the filament surface and so cannot oppose the escape of a molecule or an ion from that surface. (In fact, to some extent the opposite is true, so that the pressure of vapor from small liquid droplets is actually greater than that from large drops.[15]) In order to estimate the magnitude of the pressure normal to the surface which opposes the escape of a molecule or ion from a liquid, a rough approximation discussed by Frenkel[16] is useful. This approximation consists of assuming that the molecule or ion is itself a filament of radius r_m, which is being pulled out of the liquid surface. The negative pressure which opposes the withdrawal of a molecule or ion from the liquid surface is then given by equation (5) with r set equal to r_m. By identifying this negative pressure with the tensile strength τ of the liquid, it is possible to write

$$\tau \approx \frac{2\gamma}{r_m} \tag{6}$$

For water $r_m \approx 3 \times 10^{-8}$ cm and $\gamma \approx 73$ dyne/cm, so that $\tau \approx 5 \times 10^9$ dynes/cm^2.

It is also possible to identify the tensile strength of a liquid with its internal pressure $P_i = T\,(\partial P/\partial T)_v$ as discussed in reference (15) so that

$$\tau \approx P_i = T\,\alpha/\beta \tag{7}$$

where T is the absolute temperature, α is the coefficient of thermal expansion, β is the coefficient of cubical expansion. For water, $P_i = 17 \times 10^9$ dynes/cm^2. The average value of P_i for most other liquids is about 4×10^9 dynes/cm^2.

As noted in reference 17, experimental values of liquid tensile strengths are quite inconsistent among themselves and are, in general, much lower than the theoretical estimates given above. The tensile strength of a liquid, as measured in a device known as a tonometer, is taken as that stress (negative pressure) under which the liquid ruptures. There is a possibility that the limit to the observed maximum tension attainable in any particular tonometer does not correspond to the cohesive forces in the liquid but rather the chance release of the tension resulting from bubble formation during the passage of a cosmic-ray particle. Another concern is the possibility that rupture occurs at the wall of the container rather

than in the body of the liquid and that, therefore, the observed negative pressure is a measure of adhesive strength rather than that of the assumed cohesive strength. However, the highest direct measurements of the negative pressures of liquids have been obtained by Briggs[18], who developed the tensile stress by rotation of a capillary tube containing the liquid. The speed of rotation was increased gradually until the liquid in the capillary ruptured. The following macroscopic tensile strengths of liquids were reported by Briggs:

Liquid	Tensile Strength (dynes/cm^2)
Water	2.81×10^8
Acetic Acid	2.92×10^8
Benzene	1.52×10^8
Aniline	3.04×10^8
Carbon Tetrachloride	2.80×10^8
Chloroform	3.21×10^8
Mercury	4.31×10^8

In the previous section, a value of 4×10^8 dynes/cm^2 was estimated for the electrostatic pressure developed at the tip of a water filament from which colloidal droplets are ejected. It is of interest to note that this value of the electrostatic pressure is about equal to the experimental tensile strength of water listed above. On this basis it is suggested that, in general, formation of charged-liquid-colloid droplets will begin only when the electrostatic pressure at some point on a liquid surface just exceeds the macroscopic tensile strength of the liquid.

The Possible Charge-to-Mass Ratio of Liquid-Colloid Droplets

In order to estimate an upper limit to the charge-to-mass ratio which may be attained by a liquid-colloid droplet, the tensile strength of the liquid can be equated to the electrostatic pressure as given by equation (3), so that

$$\tau \approx \frac{E_o^2}{8\pi} f(\epsilon, \rho) \text{ dynes/cm}^2 \tag{8}$$

If polarization of the droplet is neglected, $E_o \approx q/r^2$, where q is the charge on the droplet in esu and r is the radius in cm. Since the mass of the droplet is $4\pi r^3 \rho/3$, the maximum charge-to-mass ratio for a stable droplet is given by

$$\left(\frac{q}{m}\right)_{max} \approx \frac{3}{rp} \left(\frac{\tau}{2\pi f(\epsilon, p)}\right)^{1/2} \text{ esu/gm} \tag{9}$$

If the average experimental values $\tau = 3 \times 10^8$ dynes/cm^2, $\rho \approx 1$, and $f(\epsilon, \rho) \approx 0.6$ are substituted in (9), the following table may be constructed.

Radius of Droplet (cm)	Charge-to-Mass Ratio (Upper limit) (esu/gm)
1×10^{-4}	4.3×10^8
1×10^{-5}	4.3×10^9
1×10^{-6}	4.3×10^{10}

A lower limit for the charge-to-mass ratio of liquid-colloid droplets is more difficult to estimate. For example, suppose that a radius of curvature of about 1×10^{-4} cm forms to the liquid meniscus at the positively charged capillary tip, needle point, or knife edge at which electrical dispersion is occurring. It is possible for the electrostatic pressure at this site to attain a value of about 3×10^{8} dynes/cm^2, at which value the liquid "explodes" into colloidal droplets. Each of these droplets could then have a charge-to-mass ratio of about 4.3×10^{8} esu/g but a radius considerably smaller than 1×10^{-4} cm. It is believed that the above process is actually occurring since, as noted earlier, preliminary values of initial charge-to-mass ratio (assumed equal to the rate of current* to liquid mass-flow rate) are about 3 to 5×10^{8} esu/g for a number of liquids.

The Role of Conductivity and Electric Strength of a Liquid Dielectric in the Electrical Atomization of Liquids

In Section B, arguments were presented to show that, in general, formation of charged-liquid-colloid droplets will occur only when the electrostatic pressure at some point in the liquid surface exceeds the macroscopic tensile strength of the liquid. It was tacitly assumed that the liquid dielectric possessed sufficient electrical conductivity to permit electrical charges to reach the liquid surface. Apropos of this assumption, the results of Neubauer and Vonnegut[8] and of Drozin[9] indicate that the conductivity of the liquid dielectric is of considerable importance in the production of monodispersed, charged-colloid droplets in air from a glass capillary tube in contiguity with a liquid reservoir containing a metal electrode at a high positive potential with respect to a metal plate several centimeters away from the capillary tip.

Drozin attempted to set up a criterion for the ease of electrical dispersibility (i.e., atomization) of various liquids in air by a comparison of the electrostatic pressure at an assumed constant value of the field strength E just inside the liquid dielectric. Drozin's dispersibility coefficient C $f(\epsilon)$ is equal to the term in brackets in equation (1) divided by 8π. By adopting this means of comparison, Drozin has overemphasized the influence of the dielectric constant on the ease of electrical atomization of liquids. It seems more logical to compare the electrostatic pressure developed in various liquids at an assumed constant value of the applied field strength E_o at the exterior of the liquid dielectric. Accordingly, the values of the parameter $f(\epsilon, \rho)$ of equations (2) and (3) have been calculated for the various liquids studied by Drozin and are listed, along with other properties, in Table 1. The derivative $d\epsilon/d\rho$ of equation (2) was evaluated for each liquid by use of the Henriquez equation[14] for the molar polarization

$$P_M = \frac{(\epsilon - 1)(\epsilon + 4)}{(8\epsilon + 7)} \cdot \frac{M}{\rho} = \frac{4\pi N\mu^2}{9kT} + \frac{M}{\rho} \frac{(n^2 - 1)(n^2 + 4)}{(8n^2 + 7)} \qquad (10)$$

where M is the molecular weight of the liquid, gm/gm-mole; ρ is the density, gm/cm^3; N is the Avogadro number, molecules/gm-mole; k is the Boltzmann constant, erg/^{o}K; T is the absolute temperature, ^{o}K; n is the refractive index

* Corrected for corona loss by a blank run in the system without oil.

of the liquid for light of long wavelength. For liquids with dielectric constant greater than 20, a term $1.7 \times 10^{-3} (\epsilon - 1)^3$ must be added to the term $(8\epsilon + 7)$ in Equation (10). It may be seen from Table 1 that the most important criterion

Table 1

PROPERTIES AND ELECTRICAL ATOMIZATION OF VARIOUS LIQUIDS FROM GLASS CAPILLARY TIPS

	σ	γ	$\epsilon_o = n^2$	ϵ	$\mu \cdot 10^{18}$	ρ	$f(\epsilon, \rho)$	Atomization
1. Water	1×10^{-6}	73	1.76	81	1.84	1.00	1.04	Fine atomization obtained at high potentials
2. Glycerin	6×10^{-8}	65	2.17	56.2	2.66	2.26	0.94	
3. Methyl alcohol	2×10^{-7}	22	1.77	31.2	1.68	0.80	0.95	
4. Acetone	6×10^{-8}	24	1.85	21.5	2.80	0.79	0.91	
5. Ethyl nitrate	5×10^{-7}	-	1.92	19.7	2.91	1.10	0.90	
6. Acetic acid	1×10^{-7}	24	1.88	6.3	1.73	1.05	0.64	
7. Chloroform	2×10^{-8}	27	2.09	5.1	1.10	1.50	0.72	Fine threads of liquid appear after high potential is applied
8. Ether	4×10^{-13}	16	1.82	4.4	1.15	0.71	0.68	
9. Xylol	1×10^{-15}	27	2.27	2.4	0.36	0.87	0.56	It was not possible to atomize these liquids even at high potentials up to 30 kv
10. Toluene	1×10^{-14}	27	2.25	2.34	0.37	0.87	0.55	
11. Benzene	1×10^{-18}	29	2.25	2.24	0.08	0.88	0.55	
12. Carbon tetrachloride	4×10^{-18}	26	2.13	2.25	0.00	1.60	0.56	

Specific conductivity σ in mho/cm, surface tension γ in dynes/cm, square of refractive index $n^2 = \epsilon_o$ dielectric constant ϵ, dipole moment $\mu \times 10^{18}$ in dynes$^{1/2}$cm^2, coefficient $f(\epsilon, \rho)$ from equations (2) and (3) for the electrostatic pressure, density ρ in g/cm^3. (Most of the data for σ, γ, n, ϵ, and μ are taken from I. C. T.) Note that the above data are not directly applicable to the electrical atomization of liquids from sharp metal points or knife edges (see discussion, Section II-D of text).

for the ease of electrical atomization of liquids from glass capillary tips in air is the electrical conductivity σ. If the conductivity σ of a liquid is greater than about 10^{-5} mho/cm, the structure of the surface transition layer is probably seriously altered so that the electrostatic-pressure equations (1), (2), and (3) are invalid, and the electrostatic pressure at the capillary tip drops to a value insufficient to cause atomization. On the other hand, if the conductivity σ is below about 4×10^{-13} mho/cm, it is difficult to atomize these liquids from a capillary tip in air even when high positive potentials up to 30 kv are supplied to the electrode in the reservoir contiguous with the capillary tube. Apparently, with this low electrical conductivity, it is not possible to transfer sufficient charge through the liquid in the capillary tube to build up sufficient electrostatic pressure in the liquid surface at the capillary tip. During the present investigation, however, it was found possible to obtain charged liquid droplets of colloidal dimensions by the electrical atomization in air of organic liquids of very low conductivity (i. e., approaching 10^{-12} mho/cm) at positive potentials as low as 20 kv from sharp, metal, needle tips or metal knife edges continuously covered with a microscopically thin layer of the liquid. In this case, it is probable that actual electrical breakdown of the liquid dielectric is occurring as a result of,

in part, the high electric field at the needle tips of knife edges. It is, therefore, pertinent to summarize some recent information on the electric strength of liquids.

The "intrinsic electric strength" of a liquid dielectric may be defined according to Bragg, Sharbaugh and Crowe[19] in terms of "the magnitude of the homogeneous electric field, existing in a region of the dielectric, necessary to disrupt this region or establish a conducting path across it, initiating processes from outside the region being excluded. The region considered must be large enough so that the property defined is independent of the size of the region." The preceding definition is phrased in terms of properties of the dielectric alone. However, measured electric strengths of liquids depend on external factors such as the nature of the electrodes and also upon the presence of microscopic particles. Consequently there have been no actual measurements of the "intrinsic electric strength" of a liquid dielectric. Results in the literature[19-23], are the "apparent electric strengths" characteristic of the method of measurement as well as of the dielectric. The apparent electric strengths of many liquids are about 1.2 to 2.8 x 10^6 v/cm at room temperature and are somewhat dependent on temperature. It is of interest to compare these apparent electric strengths with the voltage gradient that exists at a needle point at which the electrical atomization of an organic liquid, such as di-octyl phthalate, just begins to occur. In this case the radius r_p of the needle point is about 2 x 10^{-3} cm and the tip attains a positive potential V = 20 kv with respect to a metal accelerating grid (perpendicular to the needle) at a distance x = 5 cm from the point. If the shape of the needle point is assumed to be hyperboloidal, the field intensity E_p at the point is given[24] by the equation

$$E_p = \frac{2V}{r_p \log (4x/r_p)} \tag{11}$$

and the field varies with the distance x from the point according to the expression

$$E = \frac{r_p}{r_p + x} E_p \tag{12}$$

For the present example, the field intensity at the needle point is E_p = 2 x 10^6 volts/cm, which is approximately the same as the apparent electric strength of organic liquids. It is suggested, therefore, that electrical breakdown of the liquid dielectric at the needle point is occurring during the electrical atomization process. This electrical breakdown process is, of course, closely associated with the accumulation of high positive charge on the liquid surface. The resultant electrostatic pressure thereby rises to a value sufficient to overcome the tensile strength of the liquid and to permit electrical atomization into charged-colloid particles.

The Electrical Atomization of Liquids in High Vacuum

In our preliminary experiments on the electrical atomization of liquids, commercially supplied di-octyl phthalate and polypropylene glycol oils were employed. No attempt was made to purify these liquids and it was found that they atomized moderately well in a chamber connected to a high-speed, vacuum pumping system. It was suspected, however, that some corona discharge was occurring which would produce undesirable, extraneous ions in the colloid beam. The net effect of these extraneous ions is to waste power of the beam while con-

tributing little to the thrust. In order to eliminate corona discharge, special efforts were made to remove volatile constituents from the oils by lengthy periods of refluxing under vacuum, until the vapor pressure of the residual material was reduced to 5×10^{-6} mm Hg as measured by an ionization gauge. Whereas it had been possible to atomize electrically the unpurified oils from needle tips in vacuum at about 30 kv, it proved to be impossible to spray the purified material at 5×10^{-6} mm Hg even at 70 kv. No corona discharge was present but also no colloidal spray. As soon as air was introduced into the system, excellent atomization of the liquid into positively charged colloidal particles occurred. Clearly the explanation for this is the following.

In the presence of air, appreciable corona discharge occurs in the vicinity of each sharp needle tip at a positive potential of 20 kv. The positive ions formed in the corona discharge are, of course, repelled from the positively charged tip. The negative electrons, however, are accelerated toward the tip, where they collide with the oil molecules with sufficient energy to ionize them. The process may be described in equation form as follows:

$$(e^-)^* + RH \rightarrow RH^+ + 2e_c^-$$

Where RH represents an oil molecule, $(e^-)^*$ represents an energetic electron which has been accelerated in the anode-fall region surrounding the needle point, e_c^- represents an electron in the condensed phase in the oil covering the needle point, and RH^+ represents a singly ionized oil molecule. If the shape of the needle point is hyperboloidal and the point is situated 5 cm away from a plane conducting surface, it is known that the field intensity at the needle point is $E_p = 2 \times 10^6$ v/cm. This voltage gradient is the same as the apparent electric strength of organic liquids. In agreement with the oil-breakdown mechanism described by T. J. Lewis, J. Applied Phys. 27, 645 (1956), the electrons e_c^- condensed in the surface of the oil are capable, at a field intensity of 2×10^6v, of rapidly migrating through the oil to the metal of the needle point, where they disappear into the conduction band. This permits the heavy ions RH^+ to accumulate in the external surface of the oil covering the needle point until their mutual electrostatic repulsion (i.e., the electrostatic pressure) rises to a value sufficient to overcome the tensile strength of the oil and the liquid ruptures into fairly uniform sized colloidal droplets of oil whose surfaces contain appreciable numbers of RH^+ ions. When the ambient gas pressure is reduced to a value of 5×10^{-6} mm Hg the mean free paths of electrons and positive ions moving in the residual gas become large compared to the gap between electrodes. Under these high-vacuum conditions a self-sustained corona discharge is impossible, no energetic $(e^-)^*$ electrons are available to ionize the oil molecules into RH^+ ions, and the electrical atomization process ceases.

It follows that, in order to obtain charged liquid colloids by electrical atomization under the vacuum conditions simulating outer space, it will be necessary to provide substitutes for either the $(e^-)^*$ electrons of the corona discharge in air or for the RH^+ ions which are produced in the liquid surface. Possibly the simplest way of providing in high vacuum a substitute for the $(e^-)^*$ ions is to place an electron source (either a hot filament or cold cathode emitter) in the vicinity of the needle tips or knife edges which are covered with the liquid to be atomized. A bias of up to several hundred volts (possibly greater in the case of the cold cathode emitter) will be necessary to accelerate the electrons from the electron source to the dispersing tips or edges in order to ionize the

* Corrected for corona loss by a blank run in the system without oil.

oil molecules. The rate of formation of RH^+ ions can now be controlled by adjusting this bias voltage, by adjusting the heater current to the filament, or by varying the area of the electron emitter. The rate of formation of RH^+ ions will probably influence the size of the resulting charged liquid colloidal particles and their charge-to-mass ratio. It may, therefore, be possible to produce positively charged colloidal particles in vacuum with a charge-to-mass ratio as high as 10^9 to 10^{10} esu/g which are roughly 10 to 100 times greater than the apparent initial charge-to-mass ratios estimated from experiments in the presence of corona discharge. Such high charge-to-mass ratios would greatly simplify the overall charged-colloid propulsion system by reducing the magnitude of the accelerating voltage required to attain a given specific impulse. Such high charge-to-mass ratios could also extend the specific impulse range of the charged-colloid propulsion system to a value perhaps as high as 20,000 seconds, heretofore considered possible only with an ion propulsion system.

As an alternative to the electron-source techniques described above for creating positively charged liquid colloids in vacuum, it may be possible to find or synthesize liquid compositions with a sufficiently high number of charge carriers (i.e., positive and negative ions) in solution to permit automatic charging of the liquid surface. This approach will, however, require a great deal of research.

THE PROBLEM OF EXTRANEOUS ION IN THE CHARGED-COLLOID BEAM

General Considerations

Extraneous ions can arise in a charged-liquid-colloid beam by desorption of positive charge from the liquid surface during electrical atomization or from the resultant colloidal droplets during acceleration. Corona discharge during electrical atomization or acceleration is another source of extraneous positive and negative ions. Still another source is ionization of the liquid by secondary negative ions or field-emitted electrons which travel countercurrent to the colloid beam toward the spray bank.

It is evident that these negative ions or electrons would consume large quantities of electrical energy without contributing anything to the thrust. Extraneous positive ions, whose masses are orders of magnitude lower per unit charge than charged colloids, would attain undesirable, extremely high velocities in the acceleration system. The kinetic energy of each extraneous ion would be proportional to the square of its velocity but the thrust contributed by each would be proportional only to the first power of its velocity. It follows that these ions would soak up large amounts of electrical energy from the space-vehicle power plant and contribute comparatively little to thrust. To make matters worse, if charge leaked from the colloid droplets during their acceleration, the charged-colloid beam would not attain its optimum velocity or specific impulse. Thus the overall effect of extraneous ions or electrons in the charged-colloid beam would be a net loss of thrust for a given mass of power plant. The elimination of extraneous ions or electrons from the charged-colloid beam is, therefore, an important part of our present laboratory investigation.

Prevention of Corona Discharge

In order to minimize corona discharge, we have been obliged to work with vacua at 10^{-6} to 10^{-7} mm Hg residual gas pressure, in which the mean free paths of electrons and positive ions are large compared to either the radii of the needle points or knife edges used for atomization or to the gaps between acceler-

ating electrodes. Fortunately, the desired vacuum exists in space at altitudes greater than 190 km above earth. However, in our experimental chamber, very fast pumping during electrical atomization is required to maintain a high vacuum. Out-gassing from the chamber walls and from the liquid being atomized has proved to be a nuisance. For example, pure di-octyl phthalate has a vapor pressure of 10^{-6} to 10^{-7} mm Hg, which is compatible with the vacuum required to minimize corona discharge. However, di-octyle phthalate, as supplied to us commercially, contained a light volatile fraction which raised the overall vapor pressure to 10^{-4} mm Hg. Lengthy periods of reflux boiling under conditions of rapid, continuous evacuation are required to drive off these light fractions.

Prevention of Field Desorption

The extent of severity of the problem of field desorption of positive ions from the liquid surface during electrical atomization or acceleration is presently unknown. If field desorption should prove to be a problem, it might be advisable to investigate the use of liquids with high internal pressures. Judging from the information in Section II-B, the microscopic tensile strength of the liquid which holds the charges in the liquid surface may be equal to its internal pressure, which, in turn, is usually about three times larger than the apparent macroscopic tensile strength of the liquid. Hydrogen-bonded liquids, however, appear to possess internal pressures which are up to 57 times larger than the macroscopic tensile strength. A partially hydrogen-bonded liquid such as glycerol has an internal pressure of 7.7×10^9 dynes/cm^2 compared to the 3×10^9 dynes/cm^2 value for a typical liquid. Thus a glycerol derivative of low vapor pressure might be worth investigating as an alternative to di-octyl phthalate. The glycerol derivative might hold a positive charge much better than di-octyl phthalate.

Another possibility to minimize field desorption of positive charge is the use of dipolar substances, either pure or in solution with structures such as

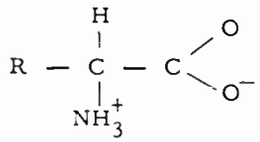

or

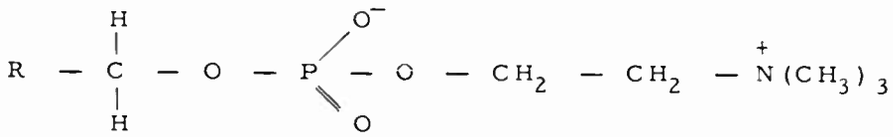

During electrical atomization, as positive ions accumulate in the liquid surface, the negative ends of these dipolar ions might be attracted to the positive ions and thereby anchor them to the surface by electrostatic means.

Eliminotion of Cold-Cathode Electrons

The elimination of cold-cathode electrons in the charged-colloid beam is regarded as a matter of proper accelerating-electrode design. Sharp edges on the accelerating electrodes (which would result in high negative field strengths) must be avoided. Cold-cathode electrons, in addition to wasting power, have the undesirable property of generating X-rays, which represent a hazard to laboratory personnel. Moreover, these X-rays might increase the shielding problems in a space vehicle.

ELECTROSTATIC ACCELERATION OF CHARGED LIQUID COLLOIDS

The maximum current density of electrons in a parallel-plane diode is given by Child's law as

$$J_e = \frac{4\epsilon}{9}\left(\frac{2q_e}{m}\right)^{1/2}\frac{V^{3/2}}{d^2} = 2.33 \times 10^{-6}\frac{V^{3/2}}{d^2} \qquad (13)$$

where J_e is the electron current density (amp/meter^2)

ϵ is the permittivity of free space (rationalized mks system)

(q_e/m) is the charge-to-mass ratio of the electron

V is the voltage across the diode (v)

d is the diode spacing (meters)

To calculate the maximum current density of charged liquid colloids in a parallel-plane-diode configuration, it is necessary to multiply equation (13) by the square root of the charge-to-mass ratio of the colloid droplet and to divide by the square root of the corresponding ratio for the electron. If the charge-to-mass ratio of a typical charged-liquid-colloid droplet is taken to be about 1.34×10^2 coulombs/kg ($\approx 4 \times 10^8$ esu/g), we obtain

$$J_{cc} = 6.43 \times 10^{-11}\frac{V_a^{3/2}}{d^2} \text{ amp/meter}^2 \qquad (14)$$

where J_{cc} = maximum current densit, of charged-liquid-colloid beam (amp/meter^2)

V_a = accelerating voltage (v)

d = acceleration gap distance (meters)

To illustrate the application of equation (14), consider our present experimental charged-colloid acceleration apparatus (Figures 4 and 5), in which electrically positive needle tips ($r_p = 2.5 \times 10^{-3}$ cm), continuously wetted with Octoil, are situated a distance of 4.0 cm from an accelerating grid. The maximum voltage that can be impressed without breakdown across the gap between the needle tips and the grid is about 1×10^5 volts. The maximum current density in the charged-liquid-colloid beam traversing this gap is calculated from equation (14) to be about 1.3 amp/meter^2 or 130 micro-amp/cm^2. The maximum field strength at the needle tip is found, by equation (11) to be about 9.1×10^6 volts/cm, which value should be sufficient to make the oil at the tip electrically conducting. The translation of the above geometry of the spray bank to a 100-kw 2 lb thrust unit operating at 0.1 amp and 1×10^6 volts would require a total beam cross-sectional area of about 800 cm^2, which corresponds to be the circle whose radius is about 16 cm. Post acceleration (through 1×10^6 volts) of the charged-colloid beam after passage through the first grid would be necessary to achieve velocities approaching 20 km/sec and specific impulses of 2000 sec. This post

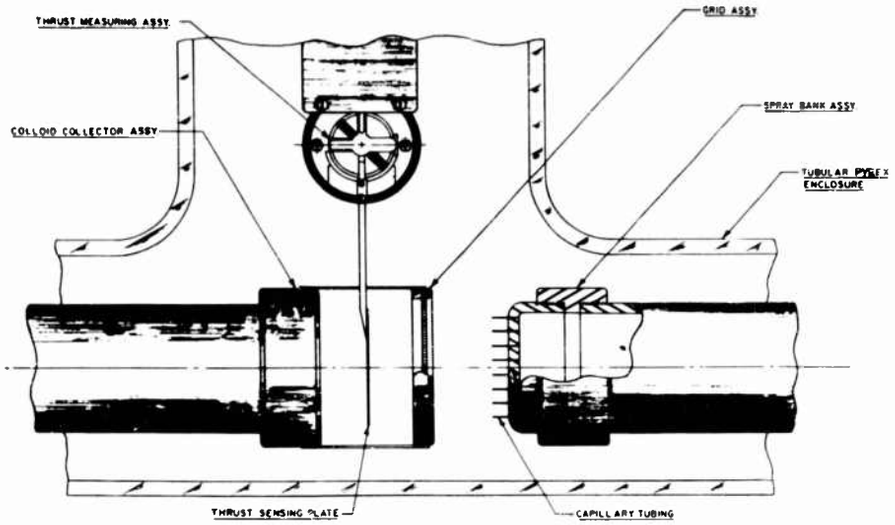

Fig. 4 Charged-Colloid Test Apparatus

acceleration could be achieved, for example, with six grids spaced about 5 cm apart with a potential difference of 200 kv between successive grids, the last of which is deceleratory in order to prevent negative electrons or ions required for charge neutralization from flying backward through the acceleration system. The extent of beam spreading and grid erosion must, of course, be a subject of further investigation.

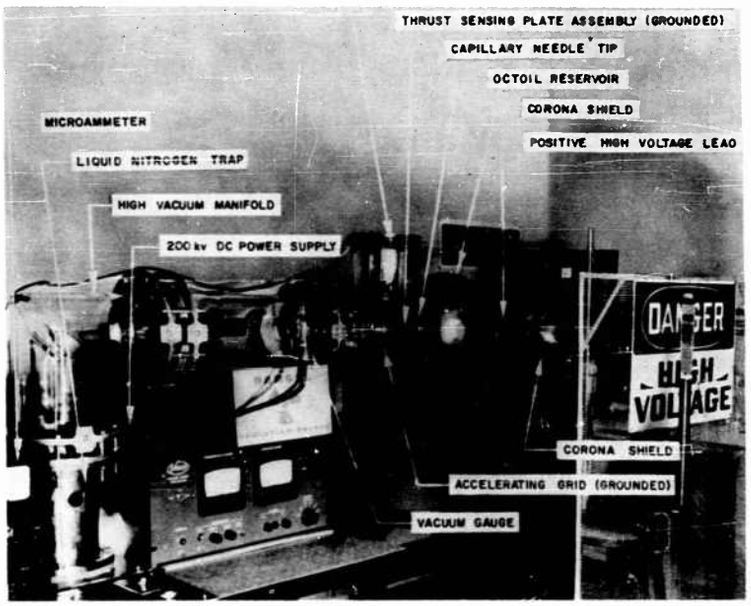

Fig. 5 Charged Liquid Colloid Acceleration Apparatus
Note: Radiation Shielding is not Shown

PERFORMANCE CHARACTERISTICS

An analysis of the performance characteristics of any electrostatic propulsion system must necessarily be a series of variations on three themes, which are Child's law (equation 13 or 14), the law of the equivalence of electrical and kinetic energy ($qV = mv^2/2$) and Newton's law ($F = d(mv)/dt$). For details of such calculations the reader is, therefore, referred to the system-analysis literature which is, by now, becoming voluminous. To amplify the present discussion, however, it is assumed that it will be feasible to produce a continuous beam of liquid-colloid droplets, each of 0.15-micron radius, 1.8×10^{-14} gm mass, and 1.2×10^{-5} esu charge. The charge-to-mass ratio would, in this case, be 6.7×10^{8} esu/gm. A preliminary estimate of the performance of a 100-kw electrostatic propulsion system using these particles is given in Table 2. A preliminary estimate of the system mass, based on the use of a direct thermionic conversion system in the nuclear reactor, is given in Table 3. If a conventional power system, such as the one depicted schematically in Figure 6, were employed, the system weight would increase by about 500 to 1,000 lb. In either case a system acceleration of 10^{-3} to 10^{-4} g appears possible, for a 2 lb thrust level and 2170-sec specific impulse. A comparison of the charged-colloid propulsion system with other systems is given in Figure 7.

Table 2

PRELIMINARY ESTIMATE OF PERFORMANCE OF A 100-KW CHARGED-LIQUID-COLLOID ROCKET	
Power delivered to Colloid jet	100 kw
Colloid charging current	0.1 amp
Colloid charging voltage	+100 kv
Accelerating voltage	1000 kv
Exhaust velocity	13 miles /sec
Specific impulse	2170 lb-sec/lb
Thrust	2.1 lb
Motor mass (including instrument shielding)	2000 lb
Acceleration	1×10^{-3} g
Propulsive liquid, exhaust rate	0.018 oz/sec 86 lb/day

Table 3

PRELIMINARY ESTIMATE OF MASS OF A 100-KW CHARGED-LIQUID-COLLOID ROCKET	
Item	Mass (lb)
Radiator Mass (+ headers)	175
Reactor-Converter Mass	250
Electrostatic Motor-Generator	220
Instrument Shadow Shield	1100
Thrust Unit and Miscellaneous	255
Total Propulsion System Mass	2000

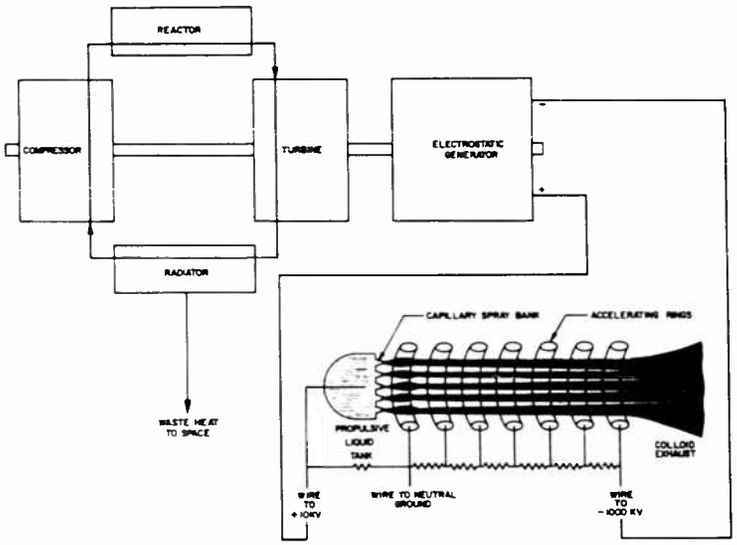

Fig. 6 Charged Liquid Colloid Propulsion System

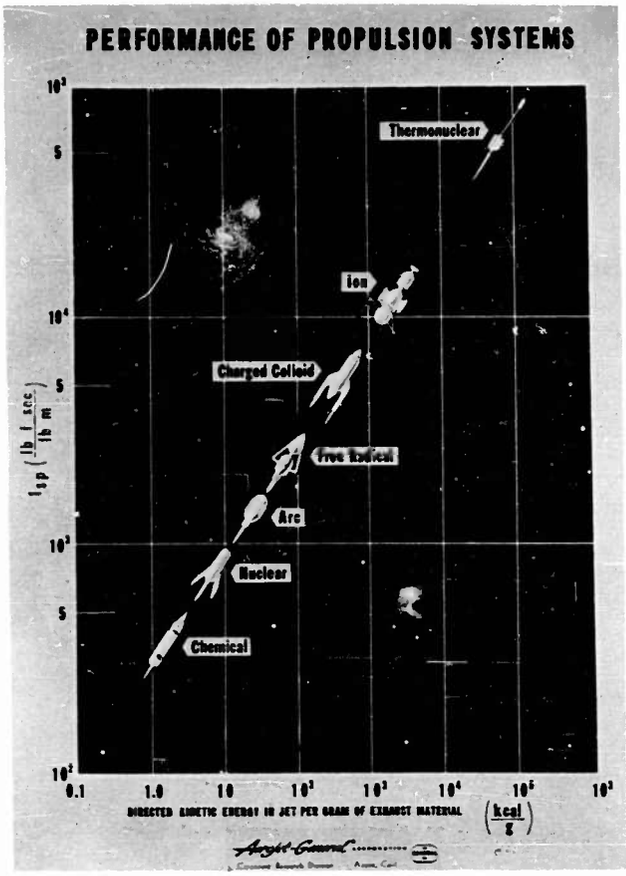

Fig. 7 Performance of Propulsion Systems

REFERENCES

1. H. Preston-Thomas, J. British Interplanetary Soc. 11, 173-192 (1952).

2. J. J. Barre, VIIIth International Astronautical Congress, Barcelona (1957), Proceedings, Springer-Verlag, Vienna (1958), pp 15-36.

3. K. A. Ehricke, Advanced Propulsion Systems Symposium of the U. S. Office of Scientific Research, Los Angeles, December 11-13 (1957), pp. 71-104.

4. J. Zeleny, Phys. Rev. 3, 69 (1914); ibid 10 (2), 1 (1917); ibid 16 (2), 102 (1920); Proc. Cambridge Phil. Soc. 18, 71 (1915).

5. E. F. Burton and W. B. Wiegand, Phil. Mag., 1912, published by the University of Toronto.

6. W. A. Macky, Proc. Roy. Soc. (London) 133, 565-587 (1931).

7. B. Vonnegut and R. L. Neubauer, J. Colloid Science 7, 616-622 (1952).

8. R. L. Neubauer and B. Vonnegut, J. Colloid Science 8, 551-552 (1953).

9. V. Drozin, J. Colloid Science 10, 158-164 (1955).

10. H. A. Pohl, J. Applied Physics 29, 1182-1188 (1958).

11. W. A. Starkey et al, U. S. Patent No. 2, 794, 417, June 4, 1957.

12. M. Abraham and R. Becker, Classical Theory of Electricity and Magnetism, 2nd Edition, Hafner Publishing Co., Inc., New York (1959) pp 100-101.

13. W. R. Smythe, Static and Dynamic Electricity, 1st Edition, McGraw-Hill Book Co., Inc., New York (1939) pp 32-33.

14. P. C. Henriquez, Rec. Trav. Chim. 54, 574 (1935).

15. S. Glasstone, Textbook of Physical Chemistry, 2nd Ed., D. Van Nostrand Co., Inc., New York (1946), pp 481-486.

16. J. Frenkel, Kinetic Theory of Liquids, Dover Publications, Inc. New York (1955).

17. A. F. Scott, F. D. Ayres, W. L. Nyborg, Am. Inst. Physics Handbook, 2-169 to 2-170, 1957.

18. L. J. Briggs, J. Appl. Phys. 21, 721 (1950); J. Chem. Phys. 19, 970 (1951); J. Appl. Phys. 24, 488 (1953).

19. J. K, Bragg, A. H. Sharbaugh, and R. W. Crowe, J. Appl. Phys. 25, 382-391 (1954).

20. R. W. Crowe, J. K. Bragg, and A. H. Sharbaugh, J. Appl. Phys. 25, 392-394 (1954).

21. R. W. Crowe, A. H. Sharbaugh, and J. K. Bragg, J. Appl. Phys. 25, 1480-1484 (1954).

22. A. H. Sharbaugh, R. W. Crowe, and E. B. Cox, J. Appl. Phys. 27, 806-808 (1956).

23. T. J. Lewis, J. Applied Phys. 27, 645 (1956): ibid 28, 503-505 (1957); Proc. Inst. Elec. Engrs. (London) 100, Pt II A, 141 (1953).

24. L. B. Loeb, A. F. Kip, G. G. Hudson, and W. H. Bennett, Phys. Rev. 60, 714 (1941).

PULSED PLASMA ACCELERATOR

by

THOMAS L. THOURSON

RESEARCH CENTER
BORG-WARNER CORPORATION

INTRODUCTION

It is well known that a conducting plasma formed by a spark discharge, exploded wire or high frequency discharge can be accelerated to rather high velocities (10^7 cm/sec) by electric and magnetic fields. These velocities correspond to specific impulses as high as 10^4 seconds. In some of these devices the acceleration is produced by the Lorentz force which results from the interaction between a current in the plasma and a magnetic field. Very often the device is designed so that the current feeding the plasma also produces the accelerating magnetic field.

As propulsive devices, pulsed plasma accelerators are competitive with the ion drive and the arc jet accelerator. However, the pulsed plasma accelerator differs from the above mentioned accelerators in that it must be pulsed to provide continuous thrust. While it is estimated that pulse rates of 10^3 and 10^4 are desirable to keep the weight of energy storage capacitors low, the highest pulse rate achieved in the laboratory to date is 20 pps. (9). Hence, the repetitive firing of the devices remains a major problem area.

DISCUSSION

Various types of plasma accelerators utilizing a Lorentz force for acceleration of plasma have been proposed. These include

1. The Bostick source (1, 2);
2. The rail type gun (3, 4, 5);
3. The AVCO coaxial shock tube (6);
4. The Kolb shock tube (7, 8).

Although the operation of these devices has been described in detail in the literature, we include here short qualitative descriptions for the sake of completeness.

The Bostick Source

Figure 1 is schematic drawing illustrating the principle of the Bostick source. A discharge is initiated across the electrodes by applying the high voltage of a high energy storage capacitor across them. While the current is flowing in the loop formed by the two electrodes and the plasma, the magnetic pressure on the inside of the loop is greater than that on the outside and the plasma experiences a force in the direction shown. Eventually, the plasma will break away from the electrodes and will continue to move at high speeds. Bostick claims that when the plasma breaks away, the two ends join to form a loop. He calls this globule of plasma a "plasmoid". The mass of the plasmoid is estimated to be of the order of 10^7 cm/sec. The energy for the formation and acceleration of the plasmoid comes from the charged capacitor. Bostick used a 0.12 μfd capacitor charged to 7 kilovolts. The total available energy was 3 joules. From Bostick's estimate of mass and velocity, the kinetic energy of the plasmoid is of this order of magnitude.

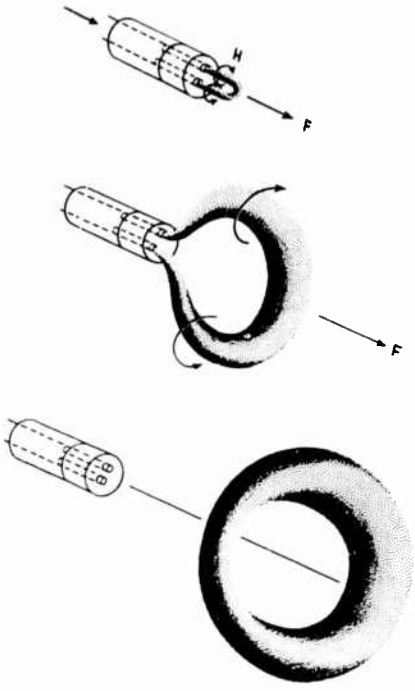

Fig.1 Schematic diagram showing plasmoid formation and acceleration by means of a Bostick source

Rail Type Accelerator

The operation of the rail type accelerator can be described with the aid of Figure 2. Figure 2-A is a schematic diagram of a simple rail gun and Figure 2-B is the equivalent circuit. The plasma is considered to be produced at position x_o. We do not specify at this time how the plasma is produced. The plasma is caused to conduct a current by imposing a voltage across the rails. This is most often done by connecting the device to a charged capacitor. The plasma is accelerated down the rails by the interaction of the current in the rails and a magnetic field which, in the case of the rail accelerator shown in Figure 2-A, must have a component perpendicular to the plane of the paper. The magnetic field produced by the current in the rails is properly oriented to produce acceleration although an external field might also be applied. If we consider only the field due to the current in the rails then the plasma will be accelerated away from the breech, or power input end of the accelerator, regardless of the direction of the current.

The rail type gun is described by Artsimovitch, et. al. (5). In their work they develop the differential equations describing the motion of the plasma assuming it remains a compact entity resembling a thin wire connecting the two rails. These equations turn out to be non-linear and they obtain solutions by numerical integration. These equations are discussed further in a later section.

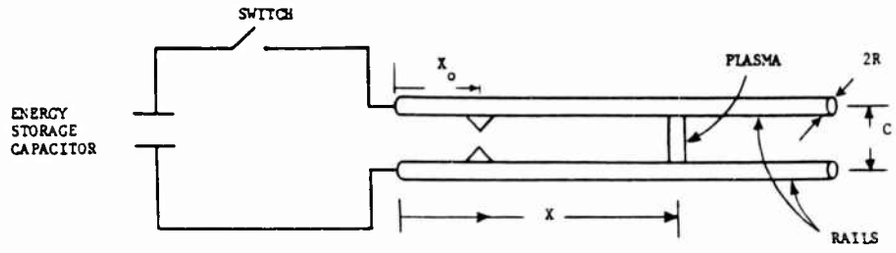

Fig. 2a Schematic diagram illustrating quantities used in Bostick's analysis of plasma acceleration by rails

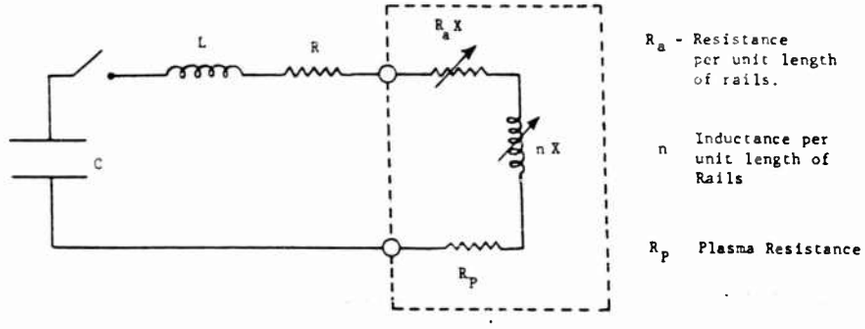

Fig.2b Equivalent circuit of plasma accelerator

In their experimental work a plasma is created by exploding a fine wire connected across the rails. The energy for exploding the wire and accelerating the plasma was obtained from a 75 microfarad capacitor charged to 30 kilovolts. The velocity of the plasma was measured by photographic and magnetic pick-up means. Velocities of the order of 10^7 cm/second were achieved. The fact that there was a discrepancy between the experimental and analytical results is attributed to the fact that the mass of the plasma does not remain constant during the acceleration and that the plasma does not remain compact but is subject to some spreading.

Experiments on rail type guns are also described by Korneff, Nadig and Bohn (4). In their experiments they mounted a thin wire across the rails. When a charged capacitor was connected across the rails, the wire exploded due to the large currents and a plasma was formed. The plasma was accelerated down the rails as is described above. In these experiments both cylindrical rods and flat plates were used for rails. They found that the flat plates provided more focusing resulting in a more unidirectional flow of the plasma. Velocities as high as 10^7 cm/sec were measured. It is estimated that the momentary thrust produced was 40 lbs.

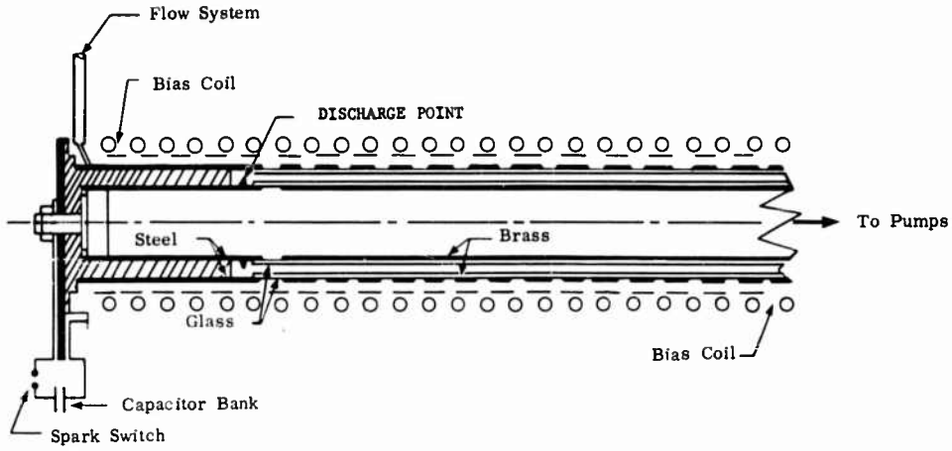

Fig.3 Schematic diagram of Avco coaxial shock tube

AVCO Coaxial Shock Tube

A schematic diagram of the AVCO shock tube is shown in Figure 3. In this device the current carrying electrodes are arranged coaxially. A gas is allowed to fill the region between the electrodes. A plasma is created by applying the voltage from an energy storage capacitor across the electrodes resulting in a gaseous discharge. An axial magnetic field is applied producing an azimuthal force on the plasma so that the plasma will be distributed uniformly around the tube. The Lorentz force produced by the interaction of the radial currents in the plasma and the azimuthal magnetic field due to the axial currents in the electrodes drives the plasma down the tube. The plasma acts as a piston driving the non-ionized gas ahead of it and a shock wave results. Patrick (6) has measured plasma velocities of 24×10^6 cm/sec in initial pressures of 10^{-3} mm Hg using Hydrogen as a working fluid. Based on this work, Patrick estimates that 85% of the electrical energy introduced in the motor will appear as energy in the exhaust. This figure compares favorably with estimated ion rocket performance.

Kolb Shock Tube

The work of Kolb at the Naval Research Laboratories in Washington (8) on magnetically driven shock waves offers promise of an alternate means of pulsed plasma propulsion. Kolb's apparatus can be described with the aid of Figure 4. The device consists of a glass T-tube with electrodes coming in as shown. The side arm is connected to a vacuum system. A plasma is generated by discharging a capacitor across the electrodes. The magnetic field produced by the current in the backstrap interacts with the current in the plasma to drive the plasma down the side arm. With no auxiliary driving coils, velocities of the order of 10^6 cm/sec can be obtained. Auxiliary coils can be added in the region of the discharge electrodes to increase the acceleration of plasma. In addition, a number of coils can be added to the side arm of the T-tube to produce axial fields of mirror geometry. If the coils are fired successfully from left to right so that the mirror geometry field appears

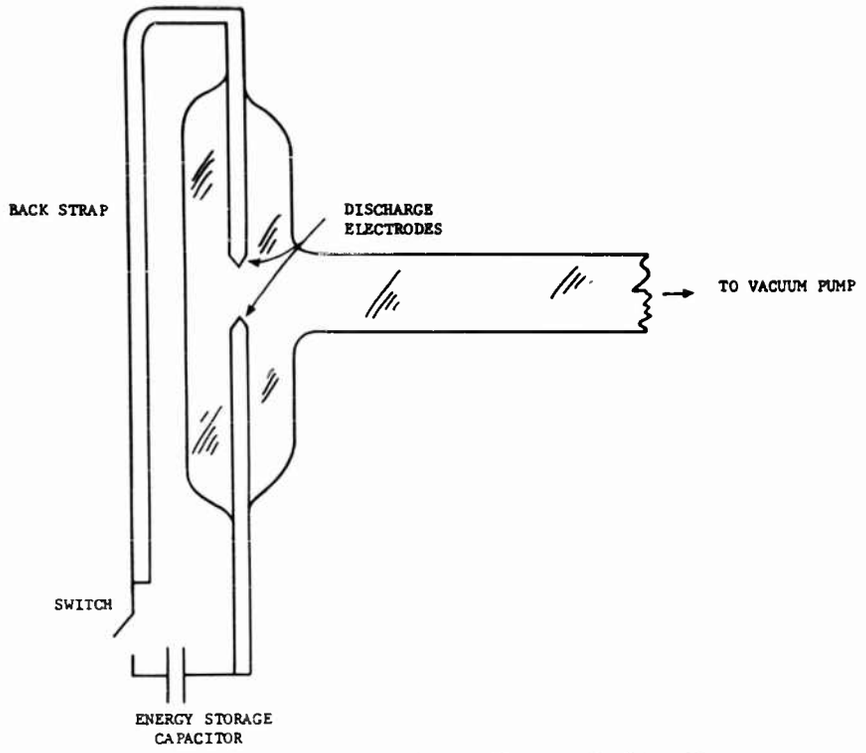

Fig.4 Schematic drawing of Kolb's tube

to move in that direction, the plasma will receive additional acceleration. This technique has been used in connection with some thermonuclear research where it is desired to inject plasma into confined regions.

Research on the application of the Kolb T-tube to pulsed plasma motors is described by Kovits (9). This unit was pulsed at a 20 pps and produced about 0.05 ounces of usable thrust. This required a power input of 3 KW. It was estimated that the mass per pulse was 60 micrograms and that the plasma velocity was 10^6 cm/sec. This yields an efficiency of about 2%.

ANALYSIS OF OPERATION OF PLASMA ACCELERATORS

The operation of some of these devices has been investigated analytically by Bostick (3,10), and Morozov (11), and by Artsimovitch, et. al. (5). The differential equations describing the operation are generally non-linear and do not lend themselves to analytic solutions. Both Bostick and Morozov make certain assumptions permitting analytic solutions to the equations and their results are valuable as a guide to the general behavior of these devices and in design of experiments.

In our investigation of the operation of plasma accelerators (12) Bostick's equation for the acceleration of plasma by parallel rails is taken as a starting point.

In this analysis the plasma is assumed to remain in a fairly compact form. That is, any spreading of the plasma, either in the direction of motion or transverse to it, is ignored. The voltage drop across the input to an accelerator is given by

$$V(t) = R_a(x)I(t) + \frac{d}{dt}\phi(x,t) \tag{1}$$

where $R_a(x)$ is the resistance of the accelerator as a function of the plasma position, x, ϕ is the total flux linking the accelerator circuit, and I(t) is the current in the circuit. The flux $\phi(x,t)$ is conveniently separated into two terms

$$\phi(x,t) = L(x)I(t) + \phi_e(x,t) \tag{2}$$

where the first term is the flux due to the current in the accelerator circuit and $\phi_e(x,t)$ is the flux due to externally excited magnetic fields. L(x) is the self inductance of the circuit as a function of plasma position. For the remainder of this discussion we will consider $\phi_e(x,t) = 0$. Taking the time derivative of (2) we get

$$\frac{d}{dt}\phi(x,t) = L'(x)I(t)\dot{x}(t) + L(x)\dot{I}(t) \tag{3}$$

where the prime indicates differentiation with respect to x and the dot refers to a time derivative. The total force acting on the plasma is

$$F = KI^2(t) - \left[\frac{m_e}{e}\right] I(t)\dot{x}(t) \tag{4}$$

where K is a constant dependent upon the geometry of the accelerator, m_e is the electron mass and e is the charge on the electron. The first term represents the acceleration of the plasma due to the Lorentz force as described above. The second term is a drag force which results from the transfer of electrons between the plasma and the electrodes. This term can be understood as follows: Assume that all of the current is carried by the electrons in the plasma. Then, as an electron traveling with the plasma velocity is transferred from the plasma to the rail, the momentum of the electron is lost. The electron from the opposite rail which replaces it is probably emitted by thermionic emission or field emission. There is no reason to assign any particular velocity in the acceleration direction to the emitted electrons. Rather it can be assumed that the average velocity is zero. Thus, for each exchange of electrons between the rails and the plasma a momentum $m_e\dot{x}(t)$ is lost. The total momentum lost per unit time is the drag force due to this process and is given by $\left[\frac{m_e}{e}\right]I(t)\dot{x}(t)$ as in equation (4). However, if representative numbers are put in for I, K and $\dot{x}$ it is found that this term is several orders of magnitude smaller than the acceleration term. Therefore, we will ignore this drag force in any further discussions in this paper.

It must be pointed out that there are probably other processes of greater importance which will, in effect, produce considerable drag. However, we do not know as yet how to describe them.

Neglecting all drag forces, equation (4) can be written

$$F = KI^2(t) \tag{5}$$

where m is the mass of the plasma.

The energy fed into the accelerator is given by

$$W(t) = \int_0^t I(t')V(t')dt'$$
$$= \int_0^t R_a(x)I^2(t')dt' + \int_0^t L'(x)I^2(t')\dot{x}(t')dt'$$
$$+ \int_0^t L(x)I(t')\dot{I}(t')dt' \qquad (6)$$

where t' is a dummy time variable of integration. Equations (1), (5) and (6) form a system equation describing the operations of the accelerator. Actually these three equations are not independent and a relationship between K, L' and m is required so that the three equations will be consistent.

In order to simplify equation (6) we now make the assumption that

$$L'(x) = n \text{ (constant)} \qquad (7)$$

that is that L'(x) is the inductance per unit length of the accelerator. The second term on the right hand side of equation (6) becomes

$$n \int_0^t I^2(t')\dot{x}(t')dt' = \frac{mn}{K} \int_0^t \ddot{x}(t')\dot{x}(t')dt'$$
$$= \frac{mn}{2K} \left[\dot{x}(t)\right]^2 \qquad (8)$$

where we have substituted from equation (5) for I^2, integrated by parts, and assumed that $\dot{x}(0) = 0$. The third term in equation (6) becomes

$$\int_0^t L(x)I(t')\dot{I}(t')dt' = n \int_0^t x(t') \, 1/2 \frac{d}{dt'} \left[I(t')\right]^2 dt'$$
$$= \frac{mn}{2K} \int_0^t x(t')\ddot{x}(t')dt'$$
$$= \frac{mn}{2K} \left[\dot{x}\, x - 1/2\, \dot{x}^2\right] \qquad (9)$$

where we have once again substituted from equation (5) for I^2 and integrated by parts. It was also assumed that $\dot{x}(0) = 0$. Substituting these results into equation (6) we get

$$W(t) = \int_0^t R_a(x)I^2(t')d(dt') + \frac{mn}{2K}\dot{x}(t)x(t) + 1/4 \frac{mn}{K}\dot{x}^2(t) \qquad (10)$$

If we substitute from equation (5) for $\ddot{x}(t)$, equation (10) becomes

$$W(t) = \int_0^t R_a(x) \left[I(t')\right]^2 dt' + 1/2nx(t) \left[I(t)\right]^2 + 1/4 \frac{mn}{K} \left[\dot{x}(t)\right]^2 \quad (11)$$

The first term represents the energy dissipated in joule heat and the second term is the energy stored in the magnetic field of the accelerator. In order to identify the last term with the kinetic energy of the plasma so that we can account for the total energy of the system we must have

$$n = 2K \quad (12)$$

Equation (12) specified a relation between the inductance per unit length of the accelerator and the total force per unit current on the plasma. It is reasonable to expect that such a relation might exist since both quantities are functions of the geometry of the accelerator. Thus, equation (11) can be written

$$W(t) = \int_0^t R_a(x) I^2(t') dt' + 1/2nx(t) I^2(t) + 1/2\, m\dot{x}^2(t) \quad (13)$$

Since the acceleration of the plasma constitutes a process by which energy is absorbed from the power source we can consider this as analogous to a resistive type load. To determine the effective impedance of this process we write

$$\int_0^t Z_L I^2 dt' = 1/2\, m\dot{x}^2 \quad (14)$$

Using the equation (5) we can write

$$\dot{x}\ddot{x} = \frac{K}{m} I^2 \dot{x} \quad (15)$$

Integrating this with respect to time, we get

$$1/2\, \dot{x}^2 = \frac{K}{m} \int_0^t \dot{x} I^2 dt'$$

or

$$1/2\, m\dot{x}^2 = K \int_0^t \dot{x} I^2 dt' \quad (16)$$

comparing with equation (14) above we can write

$$Z_L = K\dot{x} \quad (17)$$

The only other process by which energy is absorbed in this system is the joule heating of the circuit elements of the accelerator. Thus, to obtain the highest efficiency one would like to have Z_L as large as possible compared with the resistive impedance of the circuit. According to equation (17) this can be accomplished by making K, the average force on the plasma per unit current, large or by increasing the velocity $\dot{x}$. This might imply a reduction in plasma mass or an increase in total

energy of the system so as to increase $\dot{x}$ as rapidly as possible. This argument also suggests that some shaping of the input current pulse might improve the efficiency.

ANALOG COMPUTER RESULTS

Bostick's equation for the acceleration of plasma by parallel rails was programmed for solution by analog computer methods for the case where the electrical energy source is a charged capacitor (K). The equivalent circuit for this case is shown in Figure B-b. The voltage V(t) across the input to the gun is given by

$$V(t) = V_o - \frac{1}{C}\int_0^t I(t')dt' - L_o\dot{I}(t) - R_oI(t) \qquad (18)$$

where V_o is the voltage on the capacitor when the switch is closed, C is the capacitance of the capacitor, and L_o and R_o are the inductance and resistance of the external circuit. Combining this expression with equation (1) we get

$$\begin{aligned} V_o = {} & \frac{1}{C}\int_0^t I(t')dt' + (R_o + R_a)I(t) \\ & + \left[L_o + nx(t)\right]\dot{I}(t) + n\dot{x}(t)I(t) \end{aligned} \qquad (19)$$

This equation along with equation (5) was programmed for solution on the analog computer using the initial conditions:

$$\begin{aligned} I(0) &= 0 \\ x(0) &= 0.05 \\ \dot{x}(0) &= 0 \end{aligned}$$

The remaining parameters for the problem are given in Table 1.

The results of this study are given in Table 2. X-Y recorder plots for cases 1-3 and 5-3 are shown in Figures 5 and 6. In case 1-3 the major part of the total energy is dissipated in joule heating and only a small kinetic energy is imparted to the plasma. The current decay curve resembles that in a typical RLC circuit. This result is to be expected. In case 5-3, on the other hand, where about 68% of the energy is converted to kinetic energy of the plasma the form of the current cannot be described by simple functions. In this case the non-linearity of the differential equations is important. This result occurs because the small mass and subsequent large acceleration results in a large velocity, and, therefore, a large Z_L (see equation 17).

In Table 2 is a summary of results for the computer runs made to date. The frequency, f_0, is determined by measuring the time to the first peak of the current curve. I_{max} is the value of the current at the first peak. The remaining quantities were measured from the curves at times t = 100 microseconds.

From these results the improvement obtained by lowering the plasma mass is apparent. It is also apparent that, for the first nine cases listed, the kinetic energy imparted to the plasma is a direct function of the total energy of the system

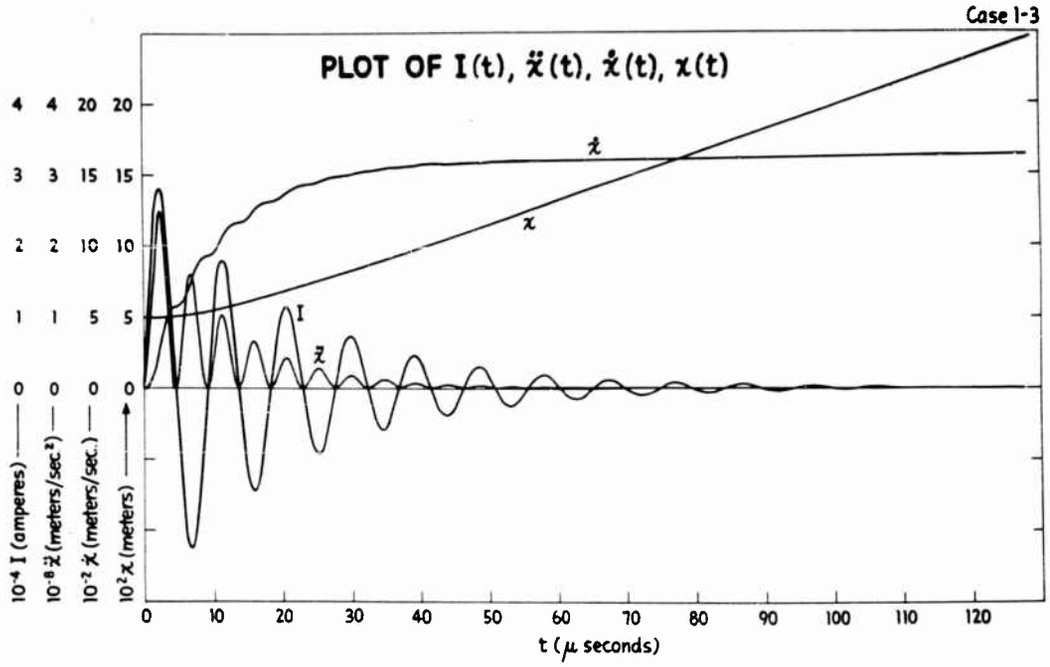

Fig.5 Plot of I(t), $\ddot{x}(t)$, $\dot{x}(t)$, x(t)

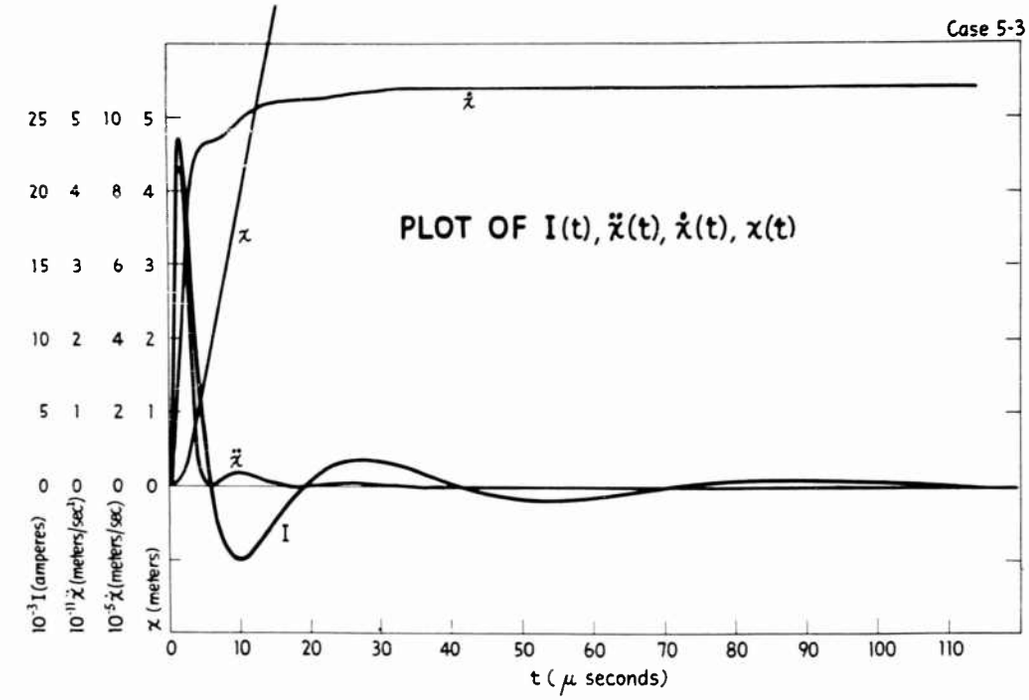

Fig.6 Plot of I(t), $\ddot{x}(t)$, $\dot{x}(t)$, x(t)

TABLE 1

Parameters used in analog computer solution of equations describing acceleration of plasma by parallel, flat plate rails.

Rail dimensions

Distance between rails	$a = 6.5 \times 10^{-3}$ meters
Rail width	$b = 2 \times 10^{-2}$ meters
Initial displacement of plasma	$x_o = 5 \times 10^{-2}$ meters
Total energy of system	$W_T = 202.5$ joules
Magnetic field strength per unit current acting on plasma	$K = 1.64 \times 10^{-3}$ newtons/ampere^2
Fixed resistance of circuit	$R_o = 4 \times 10^{-2}$ ohms
Resistance per unit length of gun	$R_a = 5.4 \times 10^{-4}$ ohms/meter
Fixed inductance of circuit	$L_o = 4 \times 10^{-7}$ henries
Inductance per unit length of gun	$n(=2K) = 3.28 \times 10^{-7}$ $\frac{\text{henries}}{\text{meter}}$

Quantity / Case No.	C (farads)	V_0 (Volts)	Q_0 (coulombs)	m (Kgm)
1-1	0.05×10^{-6}	9×10^4	4.5×10^{-3}	5.20×10^{-7}
1-3	5×10^{-6}	9×10^3	4.5×10^{-2}	5.20×10^{-7}
1-5	500×10^{-6}	9×10^2	4.5×10^{-1}	5.20×10^{-7}
2-1	0.05×10^{-6}	9×10^4	4.5×10^{-3}	1.90×10^{-7}
2-3	5×10^{-6}	9×10^3	4.5×10^{-2}	1.90×10^{-7}
2-5	500×10^{-6}	9×10^2	4.5×10^{-1}	1.90×10^{-7}
3-1	0.05×10^{-6}	9×10^4	4.5×10^{-3}	0.210×10^{-7}
3-3	5×10^{-6}	9×10^3	4.5×10^{-2}	0.210×10^{-7}
3-5	500×10^{-6}	9×10^2	4.5×10^{-1}	0.210×10^{-7}
4-3	5×10^{-6}	9×10^3	4.5×10^{-2}	0.210×10^{-8}
5-3	5×10^{-6}	9×10^3	4.5×10^{-2}	0.210×10^{-9}
6-3	5×10^{-6}	9×10^3	4.5×10^{-2}	0.210×10^{-10}

TABLE 2

Summary of Analog Computer Results

Case	f_0 (mc)	I_{max} (amperes)	x (meters)	as measured at t + 100 μ seconds						
				$\dot{x}$ (m/sec)	$m\dot{x}$ (Kgm m/sec)	W_R (joules)	W_K	$W_Q + W_L$	W_T (ΣW)	W_K/W_T
1-1	1.1	3.1×10^4	0.22	1.56×10^3	7.8×10^{-4}	202	0.6	0	202.6	0.0030
1-3	0.11	2.8×10^4	0.20	1.63×10^3	8.2×10^{-4}	202	0.7	0	202.7	0.0035
1-5	0.08	1.45×10^4	0.18	1.63×10^3	8.2×10^{-4}	205	0.7	0	205.7	0.0035
2-1	1.1	3.1×10^4	0.49	4.3×10^3	8.1×10^{-4}	201	1.7	0	202.7	0.0084
2-3	0.11	2.8×10^4	0.45	4.4×10^3	8.3×10^{-4}	201	1.7	0	202.7	0.0084
2-5	0.08	1.45×10^4	0.40	4.4×10^3	8.3×10^{-4}	204	1.8	0	205.2	0.0089
3-1	1.1	3.1×10^4	3.4	3.8×10^4	8.0×10^{-4}	199	15.2	0	214.2	0.075
3-3	0.11	2.8×10^4	3.4	3.7×10^4	7.8×10^{-4}	188	14.0	0	202	0.069
3-5	0.06	1.4×10^4	3.1	3.7×10^4	7.8×10^{-4}	192	14.4	0	206.4	0.071
4-3	0.10	2.8×10^4	23.2	25.4×10^4	5.3×10^{-4}	132	68	5	205	0.332
5-3	0.13	2.5×10^4	110	11.6×10^5	2.4×10^{-4}	62	140	8	210	0.666
6-3	0.25	1.65×10^4	400	4.1×10^6	8.6×10^{-5}	23	178	6	207	0.860

and does not depend on the frequency of the system. This effect was observed experimentally by Harris, Theus and Bostick (13).

EXPERIMENTAL INVESTIGATION

Some of the recent experimental results for various devices were described in previous sections. We wish to describe here some of the experimental difficulties presently being encountered.

Probably the most interesting experimental number is the efficiency, given as the ratio of the kinetic energy imparted to the plasma and the initial energy in the capacitor. Unfortunately, experimental data on this quantity is practically nonexistent. In the Borg-Warner work (12) with exploded wires, and a parallel rail accelerator, the estimated efficiency was less than 1%. Part of the difficulty appears to be in confining the plasma until the magnetic field can begin to act upon it. It appears that particles from the exploding wire receive radial velocities due to the explosion and that these particles rapidly leave the region of influence of the magnetic field. It is also suspected that the percentage of ionization is small and that much of the wire merely melts without vaporizing. It is suggested that the use of much finer wires will improve results. This will result in a much higher magnetic field density due to the current in the wire which may tend to contain the particles of the wire until it can become more fully ionized.

The same difficulty of transverse spread of the plasma occurs when the plasma is formed by gas discharge techniques. To overcome this, Bostick suggests using two convex rails. The accelerating field due to the current in the rails will be of a pseudo-mirror geometry tending to contain the plasma in the center of the rails.

This is not the only difficulty, of course, but it is one of the major ones. Other problems arise in understanding the mechanism by which the current is transferred from the rails to the plasma. This could conceivably result in energy loss.

ADVANTAGES AND LIMITATIONS

Probably the chief advantage of the pulsed plasma accelerator for space propulsion is its simplicity of operation. Discounting some of the experimental difficulties which are being encountered, it appears that a device based on these principles will be of simple construction and fairly reliable. The possibility of generating plasma by means of exploded wires offers the attractive possibility of carrying the propellant in a very convenient solid form. While this may present the difficulties of providing mechanical means to feed the wire to the accelerator, they should be no more severe than those encountered in storing and feeding a gaseous propellant. Even so, the pulsed plasma accelerator is also adaptable to use with a gaseous propellant.

REFERENCES

1. Bostick, W. H. "Experimental Study of Ionized Matter Projected Across a Magnetic Field" Physical Review Vol. 103, N.2, P. 292, 15 October 1956

2. Bostick, W. H. "Experimental Study of Plasmoids" Physical Review Vol. 106, N.3, pp. 404-412, 1 May 1957

3. Bostick, W. H. "Plasma Motors" Conference on Extremely High Temperatures pp. 169-178, John Wiley and Sons, Inc., New York 1958

4. Korneff, Nadig and Bohn "Plasma Acceleration Experiments" Conference on Extremely High Temperatures pp. 197-208, John Wiley and Sons, Inc., New York 1958

5. Artsimovitch, La.; Luk'ianov, S. Iu.; Podgornyi, I. M.; Chuvatin, S. A. "Electrodynamic Acceleration of Plasma Bunches" Soviet Physics - JETP Vol. 6, N.1, pp. 1-5, January 1958

6. Patrick, R. M. "A Description of a Propulsion Device Employing a Magnetic Field as the Driving Force" ASTIA No. A.D.-159 614, May 1958

7. Kolb, A. C. "Production of High Energy Plasmas by Magnetically Driven Shock Waves" Physical Review Vol. 107, N.2, pp. 345-350, 15 July 1957

8. Kolb, A. C. 'Magnetically Confined Plasmas" Physical Review Vol. 112, N.2, p. 291, 15 October 1958

9. Kovits, B. "Plasma Accelerator for Spacecraft Control" Space Aeronautics Vol. 31, N.3, p. 57, March 1959

10. Bostick, W. H. "Plasma Motors: The Propulsion of Plasma by Magnetic Means" IXth International Astronautical Congress, Amsterdam 1958 p. 794ff, Springer-Verlag, Wein. 1959

11. Morozov, A. I. "On the Acceleration of a Plasma by a Magnetic Field" Zh. eksper. teor. Fiz. Vol. 32, N.2, pp. 305-310 (1952)

12. "Pulsed Plasma Propulsion - An Advanced Reaction Propulsion System" WADC Contract AF 33(616) 6036, Final Report, WADC TR 59-321, Borg-Warner Corporation, June 1959 (Secret Restricted Data)

13. Harris, E. G.; Theus, R. B.; and Bostick, W. H. "Experimental Investigations of the Motion of Plasma Projected from a Button Source Across a Magnetic Field" Physical Review Vol. 105, N.1, p.46, 1 January 1957

THE PLASMA PINCH ENGINE

by

A. E. KUNEN, I. GRANET and W. J. GUMAN

PLASMA PROPULSION LABORATORY
REPUBLIC AVIATION CORPORATION

ABSTRACT

The phenomenon of the electromagnetic pinch effect is used to accelerate ionized gases for space propulsion. Electrical energy is discharged across two nozzle shaped electrodes wherein the radial pinch is converted to axial motion of the affected gases instead of confinement at the axis.

Pertinent parameters that can affect the mode of operation of a pinch engine are categorized.

Three analytical models are used for analyzing the radial pinch plasma engine and the results are compared with each other for two sets of system variables of interest.

A study has been made for application of an electrical propulsion system to two specific space missions; i.e., satellite control, and a one-way unmanned flight to a Mars orbit.

This paper is an unclassified version of AERL-05538 (classified "Confidential") presented at the Second Symposium on Advanced Propulsion Concepts, 7-8 October, 1959, Boston, Massachusetts.

INTRODUCTION

The use of the electromagnetic pinch effect for propulsion has been described in several references [1], [2]. Capacitors are discharged across two nozzle-shaped electrodes wherein a radial pinch is converted to axial motion of the ionized gas between the electrodes (see Fig. 1). The sketches on the right of Fig. 1 indicate how a "magnetic piston," caused by the interaction of a thin cylindrical current sheet (discharge) with its own induced magnetic field, sweeps the gas between the electrodes out of the nozzle. A forward shock wave is formed ahead of which the gas is stationary. The high temperature gas or plasma between the shock wave and the piston is driven out of the nozzle with the speed of the piston. Velocities of 48,000 meters per second have been obtained and it is anticipated that velocities up to 100,000 meters per second can be achieved if desired.

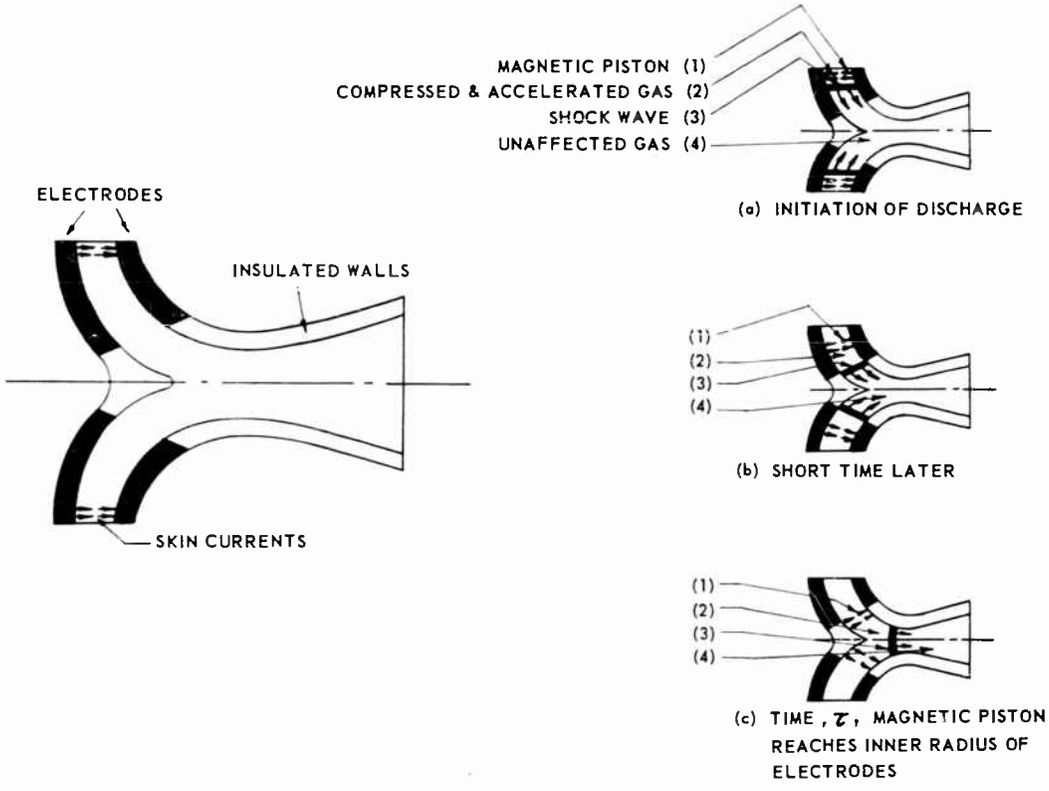

Fig. 1 Curved Nozzle-Electrodes

Three types of electrodes have been used for experimentation and they are illustrated in Fig. 2. The cylindrically symmetrical electrodes (Fig. 2a) are similar to the linear discharge electrodes which have been the subject of much experimentation for controlled thermonuclear fusion. The "one Dimensional" nozzle electrodes (Fig. 2b) are designed with a constant cross-sectional flow area throughout the annular path. The width of the annular path is considered small enough compared to the average radius of curvature of the path so that

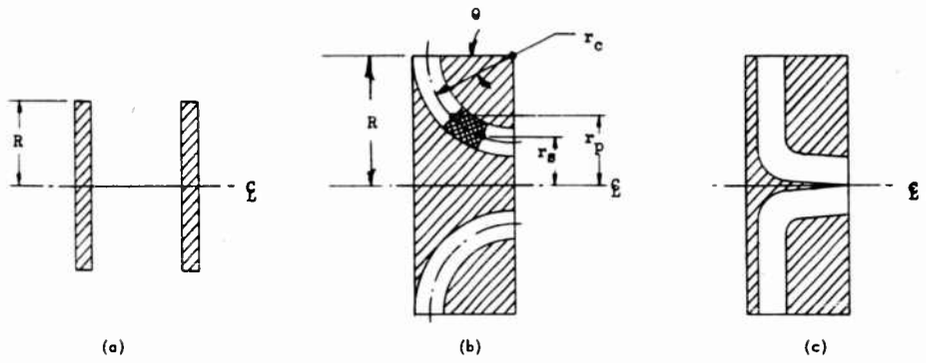

Fig. 2 Three Types of Pinch Experiments

one dimensional, time dependent, flow analysis can be applied. The nozzle electrodes of Fig. 2c were designed to permit the maximum length of radial travel before turning the driven gas in an axial direction.

The results obtained with each of these electrodes indicate the following:

1. A cylindrically symmetrical pinch can be easily obtained with many shapes of electrodes and the phenomenon can be repeated many times with the same quantitative results.

2. The formation of the initial skin current, herein called the magnetic piston, is fully determined by the initial circuit and gas conditions. The location of the initial current is always at the outer radius of the electrodes and the current is apparently axisymmetric.

3. The familiar Lorentz force created by the interaction of the skin current and its associated magnetic field (no externally applied magnetic field is required) is acting uniformly on a surface normal to the desired flow lines between the electrodes. This latter statement is true at least prior to any sharp curvature of the electrodes.

4. Essentially all of the initial bulk motion produced in the radial pinch appears in a directed, readily usable thrust producing sense. This leads to a highly efficient method of energy utilization for propulsion.

Based upon the foregoing and other pertinent considerations, it is reasonable to conclude that the radial pinch effect is a practical and simple principle for the realization of space propulsion systems.

To date, all of the experimental work on pinches for propulsion has been confined to a single discharge. The initial conditions of capacitor charge and gas pressure in the electrodes have been brought to steady values and a single

discharge has been initiated by closing an open circuit with the use of a mechanically operated switch. The gas in the electrodes was swept out within the first half cycle of the current and the circuit was allowed to ring.

A brief discussion and comparison of three analytical models of the radial pinch and their application to a specific geometry and set of system parameters is also presented.

GENERAL CONSIDERATIONS

To design a system for application to a cyclic space propulsion device, the following two fundamental objectives are of principal importance:

a. The conversion of available energy to directed kinetic energy of the propellant must be as efficient as possible.

b. As high a proportion of the gas in the chamber at the beginning of discharge should be ejected; as little as possible should leak out.

It is desirable to classify the many possible ways of operation. Table 1 presents such a classification:

Table 1[3]

I.	Type of Propellant
	a. Metal or Liquid
	b. Gas
II.	Means of Triggering Discharge
	a. Mechanical or Electrical Switch in Circuit
	b. Propellant Completion of Circuit
III.	Number of Current Pulses Utilized per Electrical Discharge
	a. One
	b. Many
IV.	Number of Slugs of Gas Ejected per Electrical Discharge
	a. Many
	b. One
V.	Method of Introducing Propellant
	a. Intermittent Feed
	b. Steady Flow Feed
VI.	Mass of Gas Being Affected During Discharge
	a. Constant
	b. Varying

Methods of Anolysis

In principle it is possible to derive relations which will account for all of the complex interactions that occur in the nozzle electrode geometry utilizing the pinch effect. Such a procedure would be extremely complex and not necessarily capable of solution. An alternate approach that has been successfully used in many problems is to postulate a physical model which gives a reasonable approximation to the gross properties while it may actually be in error in detail.

For the present system three models have been selected to represent the plasma propulsion system. These are:

1. The quasi-static (hydrodynamic) model[1]
2. The slug model[5]
3. The snow-plow model[6]

Each model is limited by the assumptions (explicit or implicit) that enter from the basic concept of the model. In order to recognize these limitations the following brief descriptions are given and Table 2 has been prepared for a direct comparison of the three methods. These models will subsequently be applied to an axisymmetric nozzle electrode assembly for purposes of comparison.

Table 2

CHARACTERISTICS OF ANALYTICAL MODELS USED

Slug	Snow-Plow	Gas Dynamic
Mass:*		
Fixed quantity accelerated from zero time and located at the advancing "piston"	Mass continuously picked up while accelerating. Mass picked up assumed accumulated in a thin layer at the advancing "piston."	Mass continuously overtaken by the advancing shock wave and situated in the space between the "piston" and the shock.
Fluid:		
Incompressible	Incompressible	Compressible** (Strong shock Rankine-Hugoniot Relations valid)
Inviscid	Inviscid	Inviscid
Adiabatic, infinite conducting thermally	Adiabatic, infinite conducting thermally	Adiabatic, infinite conducting thermally
Infinite conductor electrically	Infinite conductor electrically	Infinite conductor electrically at the thin "piston" only
Continuum	Continuum	Continuum
Negligible energy to ionize	Negligible energy to ionize	Negligible energy to ionize
Electrical:***		
Small constant resistance	Small constant resistance	Small constant resistance
Variable inductance	Variable inductance	Constant total inductance (de-coupled case)
Neglects displacement current	Neglects displacement current	Neglects displacement current
Governing Equations:		
Non-linear	Non-linear	Linear (Electrodynamic and gas-dynamic equations de-coupled for numerical evaluation of experiments.)

* Total amount of mass accelerated is the same for each case in the numerical evaluation.
** Gasdynamic parameters adjusting instantaneously to uniform conditions in the space between the "piston" and shock.
*** Circuit parameters used are the same for each case (whenever applicable).

The quasi-static or hydrodynamic model assumes that the rapid discharge of the electric circuit occurs through a thin current sheet behaving as a "magnetic piston" which drives a shock wave ahead of it. The magnetic pressure exerted by the piston is assumed to be instantaneously in equilibrium with the pressure behind the shock. As a consequence of the foregoing, the thermal conductivity of the fluid between the piston and shock is taken as infinite and the electrical conductivity at the piston is taken to be infinite.

Since the equations governing this model represent a set of non-linear coupled electrical and hydrodynamic differential equations, a further assumption can be made that the inductance of the external circuit is large compared to the plasma inductance or that the total inductance of the system is essentially constant. This latter condition is true for the present experimental equipment. The gas mass is assumed to be uniformly distributed and at rest until over-

taken by the shock.

The slug model presumes that all of the mass is initially concentrated at the outer periphery of the electrodes and the acceleration of the mass is equated to the force exerted by the electrical discharge. Gas dynamic effects are assumed to be negligible and the gas slug is taken to have infinite thermal and electrical conductivity. The inductance of the system is taken to be variable and a set of non-linear differential equations result. The slug treatment may be considered as equivalent to a movable conductor of constant mass.

The third model has appropriately been called the "snow-plow" model. The mass involved at any instant is the accumulated mass from the outer electrode periphery to the pinch radius and the equation of motion is based upon the time rate of change of momentum equaling the force exerted by the electrical circuit. All of the accumulated mass up to the pinch radius is assumed to be concentrated at the pinch radius. This fluid at the pinch radius is assumed to be a perfect electrical and thermal conductor and the circuit resistance is taken to be constant. The coupled differential equations including the variable inductance plasma are similar to those for the coupled hydrodynamic and slug models. As has been previously noted, it is possible to uncouple these equations if the circuit parameters warrant it.

The non-linear coupled equations of the slug and snow-plow models have been programmed for an IBM 704 calculator. A specific case has been computed for the axisymmetric nozzle electrodes shown in Fig. 2c for the following parameters:

1.	Initial circuit inductance	0.025 microhenrys
2.	Capacitance	600 microfarads
3.	Resistance of circuit	0.0002 ohms
4.	Total mass accelerated	10^{-6} kg.
5.	Initial voltage	2,000 and 4,000 volts

These parameters were chosen to yield values of specific impulse corresponding closely to optimum for satellite control and several missions to Mars.

The results of the calculation are shown in Fig. 3. It will be noted that the hydrodynamic analysis appears to yield consistently higher velocities than either the slug or snow-plow methods, and the voltage for the hydrodynamic method appears consistently higher than for the other two methods.

The relatively good agreement between these several methods of analysis indicates that a reasonable estimate of system parameters is possible regardless of the mode of propellant introduction for the cases considered.

System Concepts

In the preceding section two values of specific impulse are considered. These values have been chosen because the lower value, approximately 2,000 sec., is optimum for immediate application to satellite control, whereas the upper value, approximately 5,000 sec., is optimum to certain future interplanetary missions and satellite control.

An important parameter for considering the performance of a propulsion system for satellite control is the ratio - total initial weight (engine plus propellant, $W_E + W_p$) per pound of average thrust developed by the engine. This parameter is plotted versus specific impulse in Fig. 4. The time of operation is 200 days and the following definitions apply:

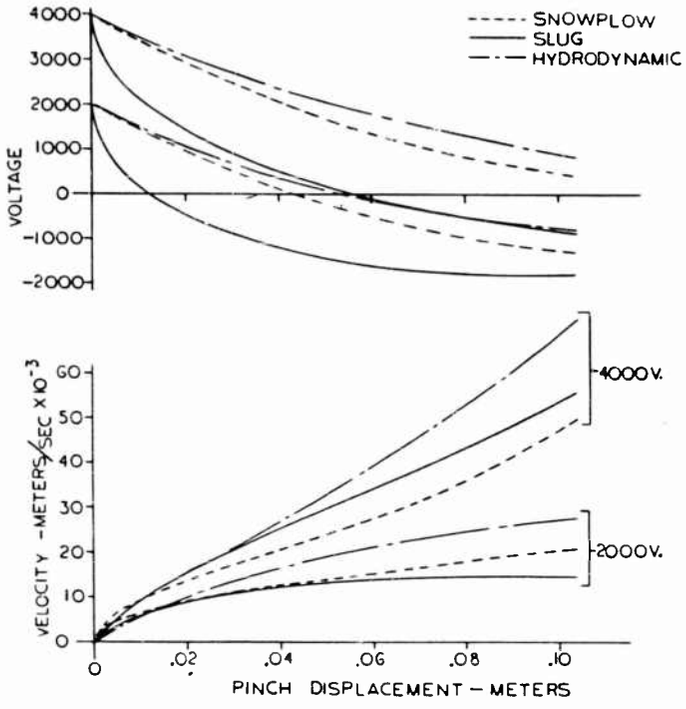

Fig. 3 Parametric System Study

η_c - Fraction of condenser energy converted into directed kinetic energy of propellant, assumed to be 0.6.

η_g - Fraction of generated electrical energy converted into condenser-energy, assumed to be 0.6.

n - Number of capacitor discharges per second.

j - Weight of all equipment (nuclear or solar plus generator) required to produce electrical energy per unit of electrical energy, lbs./kw.

K - Capacitor unit weight, lbs./joule

In the case of a continuous electrical propulsion system, such as the ion or plasma arc, the value of n is infinity. To consider a chemical rocket on the same chart, the value of j can be thought of as the weight of the rocket per kw of enthalpy increase resulting from combustion and the efficiency, $\eta_c + \eta_g$ is the ratio of the jet kinetic energy to the increase in enthalpy due to the energy released in combustion.

Referring to Fig. 4, the optimum specific impulse can be chosen. For a realistic present day value of j = 100 lbs/kw, the optimum specific impulse is of the order of 2,000 sec. For a value of j = 20 lbs./kw, which is considered to be reasonable for near future development, the optimum specific impulse is

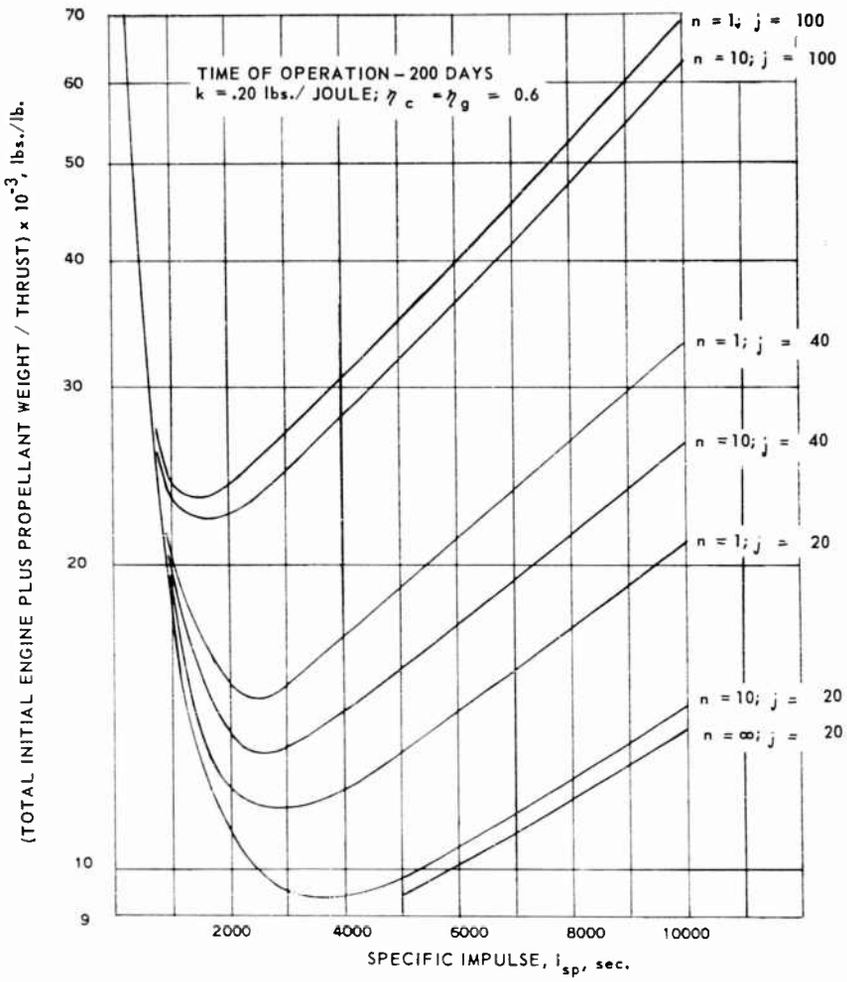

Fig. 4 Engine and Propellant Weight to Thrust Ratio vs. Specific Impulse

of the order of 5,000 sec. The chemical rocket with a specific impulse of 250 sec., with n = ∞ and j of the order of 1 lb/kw is still not a desirable system when compared with an electrical system which can achieve a specific impulse of 1000 or more, despite the weight of electrical equipment expressed by $100 < j < 200$.

For a satellite control mission it is instructive to consider a particular set of operating conditions. Thrusts of the order of 1/100 to 1/10 of a pound have been considered for stabilization. For a mission time of 200 days and for the following conditions:

j = 100 lbs/kw
$\eta_c = \eta_g = 0.6$
K = 0.03 lbs/joule
n = 1 discharge per second

the table below indicates the system parameters:

Electrical Power	= 1.21 kw	Electrical Power	= 12.1 kw
Capacitor Storage	= 740 joules	Capacitor Storage	= 7400 joules
Capacitor Weight	= 22.2 lbs	Capacitor Weight	= 222 lbs
Electric Generation Weight	= 121.0 lbs	Electric Generation Weight	= 1210 lbs
Propellant Weight	= 86.4 lbs	Propellant Weight	= 864 lbs
Total Initial Weight	= 229.6 lbs	Total Initial Weight	= 2296 lbs

Obviously, the optimization of specific impulse becomes more important as the required thrust increases.

Studies have been made of missions starting from an orbit around Earth and culminating in an orbit around Mars[7]. Round trips have also been considered wherein the mission culminates in the same orbit around Earth that it began. In all cases the optimum specific impulse is of the order of 5,000 sec. or less. (It was assumed in these calculations that $j = 20$ lbs/kw and that $\eta_c = \eta_g = 0.6$.)

For much longer journeys to more distant planets, higher specific impulse values may be required, but for the next 10 years a specific impulse of the order of 5,000 appears to be sufficient.

REFERENCES

1. Kunen, A. E., "The Electromagnetic Pinch Effect Applied to a Space Propulsion System," PPL Report No. 108, Republic Aviation Corporation, August, 1958. Presented at A.A.S. West Coast Meeting, Stanford University, August, 1958.

2. Kunen, A. E. and McIlroy, W., "The Electromagnetic Pinch Effect for Space Propulsion," PPL Report No. 116, Republic Aviation Corporation, August, 1959. Presented at A.R.S. Gas Dynamics Symposium, Northwestern University, August, 1959.

3. Hughes, J. Victor, "Plasma Propulsion - The Problem of Repeated Pinches," Technical Note No. 41, Republic Aviation Corporation, Scientific Research Staff, March 20, 1959.

4. Wyld, H. W. and Watson, K. M., TID 7520 (unclassified 1958).

5. Schock, A., "Electromagnetic Acceleration of Plasma for Space Propulsion," PPL Report #118, Republic Aviation Corporation, August, 1959. Presented at Ballistic Missiles Symposium, Los Angeles, California, August, 1959.

6. Rosenbluth, M., "Infinite Conductivity Theory of the Pinch," Los Alamos Scientific Laboratory, March 24, 1955.

7. Hughes, J. Victor, "Low Thrust Engines for Interplanetary Missions," Technical Note No. 42, Republic Aviation Corporation, Scientific Research Staff, April, 1959.

A COMPARISON OF THE SPECIFIC THRUST OF ION AND PLASMA DRIVE ACCELERATORS

by

S. W. KASH

LOCKHEED AIRCRAFT CORPORATION
MISSILES AND SPACE DIVISION

ABSTRACT

The parameter specific thrust T_{sp} is introduced and estimates are given for the maximum T_{sp} for ion drive and plasma drive accelerators. The maximum T_{sp} for plasma drive is at least one hundred times as great as that for ion drive. The limitation on ion drive T_{sp} cannot be overcome with a double-grid accelerate-decelerate system. Charged colloidal particle accelerators will provide a T_{sp} even lower than that of the heavy ion accelerator. The relationships between T_{sp} and the efficiency and mass flow rate are shown. Because of the unfavorable dependence of the specific thrust on the applied voltage, the efficiency of an ion engine is drastically reduced at both high and low I_{sp}. Measurements obtained on the specific thrust for a collinear electrode plasma accelerator confirm the estimated value. The practicality of deriving the plasma by electrode erosion is demonstrated.

INTRODUCTION

Several ways have been suggested for the acceleration of propellant material to very high velocities. In one way electrostatic forces are used to accelerate charged particles of one sign, such as heavy positive ions or charged colloidal or dust particles. In another way, rapidly varying magnetic fields are used to accelerate plasma consisting of ionized material, but containing an equal amount of positive and negative charges. In yet a third the acceleration is provided by a combination of electric and magnetic fields. The first two have been most often mentioned and appear most promising. For convenience they will be designated by simply ion drive and plasma drive, respectively.

A question of interest is how do ion drive and plasma drive compare? Now there are many factors to consider, such as reliability, efficiency, specific impulse, weight, and so on. Since the theme of this symposium and this session in particular is concepts, and since the discussion time is quite limited, the comparison will be in the main restricted to a single parameter, the specific thrust. This parameter is important in that it influences the efficiency, mass flow rate, accelerator weight and even the specific impulse. The parameter has the virtue of permitting a comparison without too detailed a consideration of the ion drive or plasma drive accelerators.

DEFINITION OF SPECIFIC THRUST

The specific thrust T_{sp} will be defined as the thrust per unit area produced by the accelerator. Obviously T_{sp} should not be so little that an enormously large accelerator area will be required for an adequate thrust. Quite obviously also is the fact that a low specific thrust will entail a weight penalty in the form of additional structural material, propellant feed lines, radiating surface and so forth.

With respect to specific thrust, plasma drive is considerably superior to ion drive. The maximum T_{sp} of plasma drive is at least 100 times as great as that of ion drive. Devices have actually been built which provide a T_{sp} many times that of the practical limit of ion drive devices.[1,2]

SPECIFIC THRUST FOR ION DRIVE ACCELERATORS

The smallness of T_{sp} for an ion drive device is a basic limitation inherent in the use of electrostatic fields for the acceleration of charged particles. This can be seen by the following analysis of the ion accelerating mechanism in terms of Maxwell stresses, that is, in terms of the electric field lines. In the ion accelerator positive ions are produced at an anode and accelerated by an electric field toward a negatively biased grid or cathode. Figuratively, we may imagine electric field lines emanating from the accelerating grid and terminating on the ions. The tension along the field lines accelerates the ion backward; simultaneously the grid (and attached rocket) is accelerated forward. The forward thrust on the rocket is obtained from the forces between the grid and the ions through the electric field tension. Per unit area of accelerator this tension is $4.42 \times 10^{-7} E_g^2$ dynes/cm^2, where the field at the grid E_g is expressed in volts/cm. Only field lines ending on ions contribute to the thrust. If the ion current is less than the maximum or saturated value, some of the field lines from the grid will end on the anode and the thrust will be reduced.

If E_a represents the field at the anode, T_{sp} will be proportional to $E_g^2 - E_a^2$.

Let us for simplicity assume the usual idealized one-dimensional model, with a separation d between the anode and grid and a voltage drop V_g from the anode to the grid. In the absence of any ion current the field between the anode and grid will be uniform (equal to V_g/d) and the potential will vary linearly. In this case $E_a = E_g$ and $T_{sp} = 0$. As the ion current density j is increased, some of the field lines will no longer terminate on the anode, but instead on the intervening ions. The potential will vary more slowly near the anode, and hence more rapidly near the grid; the field at the grid will be increased and the field at the anode decreased. As j increases further, a value will be reached for which all field lines emanating from the grid terminate on ions and no lines terminate on the anode. The field at the anode would then be zero and no more ions can be accelerated. This, of course, corresponds to the space charge limited case $j = j_s$. Analysis* readily shows that in this case the potential varies as the distance to the 4/3 power. Accordingly, the field at the grid, which is now at a maximum, is 4/3 the zero current value and the maximum tension or maximum T_{sp} is 7.85×10^{-7} $(V_g/d)^2$ dynes/cm^2 or 16.4×10^{-10} $(V_g/d)^2$ lbs/ft^2.

It should be emphasized that this result is entirely independent of the type of charged particles used, be they ions, charged dust or colloidal particles. For an applied voltage of 10,000 volts and an anode to grid spacing of one centimeter the specific thrust is at most only 0.16 lbs/ft^2.

LIMITATION OF ION DRIVE Tsp

As shown the maximum specific thrust T_{sp} for an ion accelerator depends only upon the voltage gradient at the accelerating cathode, which is determined by the voltage and interelectrode spacing. The voltage itself is determined by the specific impulse and the mass of the ions, for example, for single ionized cesium ions and an I_{sp} of 10^4 seconds, a voltage of about 7000 volts is required.

Ion optics considerations set a lower limit on the interelectrode spacing. It is presumed that to reduce erosion, the cathode aperture does not contain grid wires. Thus, if the interelectrode spacing is made less than the diameter of the beam, the average current density over the beam cross section will be less than the space-charge limited value based upon parallel plane electrode theory. There will also be increased divergence of the beam. If a low divergence, high intensity beam is to be obtained from the whole anode area, the interelectrode spacing should be larger than the beam diameter. Thus, for example, for a one centimeter diameter beam and an accelerating voltage of 10 kv, the field at the cathode will be of the order of 10^4 volts/cm.

If the grid to anode spacing cannot be substantially reduced, a larger gradient is still possible providing a larger voltage can be used, which means heavier ions. Heavier ions are of course also advantageous from the standpoint of efficiency, since the energy required to produce the heavy ions is a smaller fraction of the kinetic energy imparted to the ion than is the case for a lighter ion.

* Equate $E^2/8$ (in esu) and the momentum flux nmv. Express E and v in terms of V and integrate. The saturated current density j_s is given by n/e.

For the cesium ion example mentioned above, an energy less than one percent of the kinetic energy is required to produce the ion, neglecting of course the thermal radiation of the anode.

If efficient means were available to provide heavier particles, such as dust or colloidal particles, with an adequate charge, it might be supposed that the specific thrust could be substantially increased. Actually this is not so. Even with the maximum charge to mass ratio obtainable, such heavy particles would require potentials of the order of a million volts or more for a satisfactory specific impulse. Now experiments have shown[3,4] that for vacuum insulation the maximum voltage and maximum voltage gradient are inter-related. Over a fairly wide range of voltage breakdown, the product of the voltage and voltage gradient is approximately constant. The large voltage required for the acceleration of the heavier particle would entail a large reduction in the voltage gradient. Accordingly, a colloidal accelerator should yield a smaller specific thrust than the heavy ion accelerator.

The electrical breakdown limitations on voltage and voltage gradient also apply to the cesium ion accelerator. With heated irregular surfaces, such as a porous tungsten anode and a partially eroded cathode, plus of course the deliberate presence of ions, maximum voltage gradients averaged over the plane of the cathode will be of the order of 10^4 volts/cm for an applied voltage of 10 kv. This implies a maximum T_{sp} about 100 dynes/cm^2. For currents less than the saturated value T_{sp} will be correspondingly decreased.

It has been suggested that higher specific thrusts might be obtained by a two-grid accelerate-decelerate system, in which the ion is first accelerated to a much higher voltage and then decelerated to the appropriate exit voltage. Since the specific thrust depends only upon the voltage gradient, an accelerate-decelerate system would require both a higher voltage gradient and higher voltage to increase T_{sp}. However, as indicated, a higher gradient is not compatible with a higher voltage. Accordingly, it is not likely that an accelerate-decelerate system can be used to appreciably increase the T_{sp} of an ion accelerator.

SPECIFIC THRUST FOR PLASMA DRIVE ACCELERATORS

In comparison with ion accelerators, a greater complexity of devices is available for plasma acceleration. In many of the plasma accelerators a plasma formed in a discharge is accelerated by the interaction of the currents in the plasma and the current in the fixed parts of the discharge circuit. Generally, the current elements in the nearest portion of the circuit to the plasma contribute the most to the acceleration. The acceleration of the plasma arises of course directly through the interaction of the plasma currents with the magnetic fields in their vicinity. If during the acceleration there is little penetration of the plasma by the magnetic field, the field will in effect act as a magnetic piston. In this case, if the magnetic field behind the plasma discharge is H gauss, the maximum magnetic pressure or maximum T_{sp} is 0.04 H^2 dynes/cm^2.

Fields of 10^4 gauss or greater can be obtained in plasma drive devices, so that the maximum T_{sp} is of the order of 10^7 dynes/cm^2 or greater. As noted earlier the maximum T_{sp} for an ion drive device is about 100 dynes/cm^2. Thus, the ratio of the obtainable specific thrust with plasma drive is 10^5 or more times as great as that with ion drive.

In practice this ratio cannot be achieved. The magnetic fields in a plasma drive device act only intermittently, whereas the electric field in an ion drive device

acts continuously. Nevertheless, if the magnetic fields were effective 0.1 percent of the time, for example, one microsecond out of each millisecond, the maximum specific thrust of a plasma drive device would be at least one hundred times that of an ion drive device.

RELATION OF SPECIFIC THRUST TO EFFICIENY AND SPECIFIC IMPULSE

The kinetic power and mass flow rate per unit area are readily expressed in terms of the specific impulse and specific thrust. With I_{sp} in seconds and T_{sp} in dynes/cm^2, these are respectively

$$P_{sp} = 5 \times 10^{-8}\, g I_{sp} T_{sp} \quad \text{watts/cm}^2$$

$$M_{sp} = T_{sp}/g I_{sp} \quad \text{gms/cm}^2 \text{ sec.}$$

For a cesium ion accelerator with an accelerating voltage of 10 kv and an anode to grid spacing of only one centimeter, $I_{sp} = 1.2 \times 10^4$ sec, a maximum T_{sp} = 78 dynes/cm^2, a maximum P_{sp} = 47 watts/cm^2 and a maximum M_{sp} = 6.5 μgms/cm^2 sec. For a plasma accelerator with a comparable I_{sp} and a magnetic field of only 10^4 gauss, and operating only 0.1 percent of the time, the maximum T_{sp} = 4000 dynes/cm^2, the maximum P_{sp} = 2350 watts/cm^2 and the maximum M_{sp} = 340 μgms/cm^2 sec.

P_{sp} represents the power usefully converted. To obtain the efficiency one must take into account all other power required or lost. For the ion drive this includes power radiated by the anode and surrounding structure, power for neutralizing electrons, power to vaporize and ionize the ions, and power lost because of sputtering. For the plasma drive this includes the power to produce the plasma, power radiated by the plasma, power lost in the electrical circuits and so forth. Account must also be taken with each system for any loss of unaccelerated propellant material.

Now most of these losses are proportional to P_{sp}, or for a fixed I_{sp} proportional to T_{sp}. However, the loss due to anode thermal radiation in the ion drive is relatively constant. For an anode temperature of 1200°K and emissivity of 0.9, the radiated power is about 11 watts/cm^2. This is about one-fourth the maximum P_{sp} for ion drive. Any significant decrease in ion T_{sp}, such as would be introduced by an inability to maintain the saturation current density or by a reduced accelerating voltage, would seriously affect the ion drive efficiency.

A comparable situation for plasma drive would exist if, for example, power were required for a steady state magnetic field. This, however, can be avoided by a suitable choice of plasma accelerator. Thus, the efficiency of a plasma drive device need not fall with operation at lower specific thrust.

LIMITATION ON ION DRIVE SPECIFIC IMPULSE

It is often stated that an ion accelerator can produce particle velocities higher than those produced in a plasma accelerator. However, for very high I_{sp}, the efficiency of an ion accelerator decreases greatly with increasing I_{sp}. For a given mass of ion, the accelerating voltage required increases as the square of the ion velocity. But as pointed out previously, as the voltage is increased the voltage gradient must be decreased (roughly as the reciprocal

of the voltage) to prevent electrical breakdown. Since the specific thrust depends upon square of the voltage gradient, an increase in I_{sp} means a decrease in T_{sp}, roughly as the fourth power of I_{sp}. Now the kinetic power P_{sp} of the ion beam is proportional to the product of I_{sp} and T_{sp}, so that an increase in I_{sp} will necessitate a decrease in P_{sp}, roughly as the cube of I_{sp}. This results in a large reduction in the efficiency of the ion accelerator at very large I_{sp}.

At low I_{sp}, geometric limitations necessitate a proportionate reduction in both the voltage and the voltage gradient. In this case P_{sp} varies approximately as the fifth power of I_{sp}, so that the efficiency is also seriously reduced at low I_{sp}. Thus, the velocity range for efficient operation of an ion drive device is severely limited.

For plasma drive, analysis indicates that the efficiency will also be reduced at low I_{sp}. However, the efficiency should continue to increase with increasing I_{sp}.

MEASUREMENTS ON THE SPECIFIC THRUST OF A PLASMA ACCELERATOR

Experiments have been performed with a collinear electrode plasma accelerator and measurements of impulse, effective specific impulse and efficiency have been made. The specific thrusts obtained are in accord with the values indicated earlier. In essence the device (Figure 1) consists of a pair of collinear discharge electrodes connected to a low inductance, high energy capacitor. The leads between the condenser and the electrodes are arranged to keep the inductance of the discharge circuit as low as possible and also to provide the accelerating forces for the plasma.

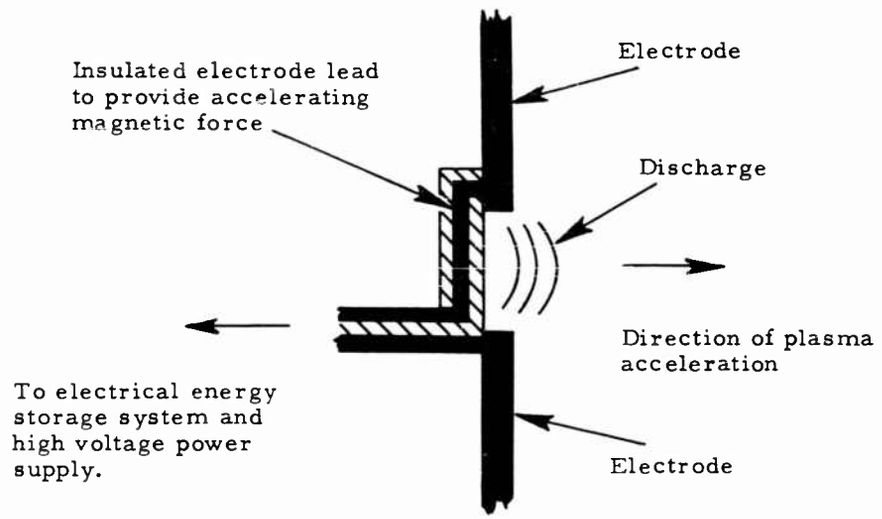

Fig. 1 Schematic Diagram of the Collinear Electrode Plasma Accelerator

In operation the region around the electrodes is evacuated and the condenser is charged to a high voltage. A discharge is initiated by the introduction of plasma between the electrodes. For one set of measurements the plasma for the discharge was produced by exploding a fine wire mounted between the electrodes at right angles to the plane of the discharge circuit. In a second set of measurements the discharge was initiated by the introduction of a tiny amount of gas between the electrodes, the major portion of the plasma being supplied by the electrodes themselves. To facilitate replacement of the wire, and admission of the gas, the electrode assembly was mounted outside an evacuated bell jar, directed to fire into a ballistic pendulum inside the bell jar. The pendulum for measuring the impulse was made out of sheet aluminum and to catch the propellant it was curved and tapered in the form of a light trap. It was supported by four long fine wires and provided a sensitivity of about 320 dyne·sec per cm of horizontal travel. The electrodes were connected to a 1.1 μf, 30 kv condenser located directly beneath. The electrodes were one-quarter inch in diameter and were spaced about 5 cm apart. The distance between the lead to the upper electrode and the electrode gap was about 1 cm. Additional details are given in References 1 and 2.

For the exploding wire system a number of firings were made with different material and different diameter wires. The vaporization of the fine wire was accomplished by discharging a 3 kv capacitor through it. Impulse measurements obtained are shown in the second column of Table I below. The

Table I

Results of Impulse Measurements

Wire size	Measured impulse* (dyne·sec)	Mass of wire (mg)	Effective Specific impulse (sec)	Efficiency (percent)
1 mil platinum	1380	0.90	1530	21
5 mil Nichrome	1620	6.4	260	4
1 mil tungsten	1800	0.83	2210	39
2 mil tungsten	1750	3.3	540	9
5 mil Nichrome	1750	6.4	279	5

* *For the first two measurements the electrodes were about 10 cm from the pendulum; for the latter three measurements the distance was reduced to about 4 cm.*

mass of the wire vaporized is shown in the third column and the effective specific impulse determined from the impulse and wire mass is shown in the next column. It is important to note the specific impulse values listed are not those determined by streak camera measurements, which usually give values a half order to an order of magnitude greater. The final column presents the efficiency obtained by comparing the computed kinetic energy of the ejected

plasma with the initial energy stored in the main condenser. As can be seen the smaller size wires yield the greater specific impulses and greater efficiency. Higher velocities and efficiencies than those presented should be possible by further improvement of the system.

The end-on area of the collinear electrode accelerator was of the order of 10 cm^2. Thus, for a firing rate of only once per second, T_{sp} is about 100 dynes/cm^2, which is of the order of the maximum of the ion drive accelerator.

For the expendable electrode system a small piston was used to admit a minute amount of triggering argon gas through a hole in the upper electrode. The impulses obtained were not sensitive to the amount of gas admitted, and as little as 6 μgms of argon was adequate to trigger the discharge. The major portion of the propellant was obtained by erosion of the electrodes. The impulse measurements for this system are shown in Table II. Note that at the higher

Table II

Variation of Impulse with Voltage and Energy of the Electrical Storage Condenser

Condenser Voltage V (kv)	Measured Impulse I (dyne·sec)	I/V^2 (arbitrary units)	CV^2/I (cm/sec)
15	160	.711	15.5×10^6
20	320	.800	13.8
25	416	.655	16.8
32	832	.812	13.5
35	960	.783	14.0

voltage the specific thrust for a firing rate of only once per second is again of the order of the maximum value for ion drive. If the firing rate can be increased to 100 times per second, the specific thrust of this plasma accelerator would be about two orders of magnitude larger than that obtainable by an ion drive accelerator.

Analysis for the expendable electrode system shows that both the impulse and the mass eroded from the electrodes should be proportional to the square of the initial voltage. The proportionality between the impulse and the square of the voltage is experimentally demonstrated by the results shown in the third column of Table II. A further consequence of the analysis is that both the specific impulse and the efficiency should be independent of the initial voltage.

The specific impulse can be changed by varying the composition and/or the spacing of the electrodes.

Column four presents the effective velocity if the efficiency were one hundred percent. With an assumed efficiency of 40 percent the effective velocity computed from this data is about 6×10^6 cm/sec. For this velocity the propellant mass ejected for a 35 kv firing is computed to be about 160 μgms. With less than 6μgms of gas needed to trigger the discharge, over 96 percent of the propellant is provided by the electrodes.

REFERENCES

1. W. L. Starr, "A Propulsive Device Using an Exploding Wire Plasma Accelerator," Exploding Wires, Plenum Press, Inc., 1959.

2. S. W. Kash and W. L. Starr, "Experimental Results with a Collinear Electrode Plasma Accelerator and a Comparison with Ion Accelerators," Paper 1008-59, American Rocket Society Meeting, November 1959.

3. J. G. Trump and R. J. Von de Graff, "The Insulation of High Voltages in Vacuum," Journal of Applied Physics, Vol. 18, p. 327, 1947.

4. J. G. Trump, "Insulation Strength of High-Pressure Gases and of Vacuum," pp. 147-156, Dielectric Materials and Applications, John Wiley and Sons, 1954.

DISCUSSION

DR. M. L. GHAI, Flight Propulsion Department, General Electric Co.: I would like to make a few comments on electrical propulsion with particular reference to papers by Kunen, Littman and Kash.

It is interesting to note that during the past two years the arc jet engine and the ion engine have moved from the stage of being considered initial concepts to a stage where efficient operation is most important.

At the General Electric Company, Flight Propulsion Laboratory Department, Evendale, Ohio, we are now operating ion and arc jet engines. In the ion engine, the generation and acceleration of ions has been achieved, and an engine has been in operation. We feel that 50% efficiency is possible within a year if a respectable amount of effort is put in the engine.

In the arc jet engine, high efficiency is made possible by operation at high pressures. The high pressures enable low ionization level which in turn reduces the losses which might be normally expected during expansion. I might also mention that we have a unit operating at as low a power level as 300 watts.

What is really needed in the electrical propulsion area now is a good size effort to develop workable engines so that we have them available for space propulsion.

Regarding comparison between different types of space engines, it is my personal belief that there will be three types of electrical space engines--the arc jet engine, the ion engine, and the plasma engine. It appears that they are not in competition, but instead are complimentary to each other. The arc jet engine can operate efficiently in the specific impulse ranges of 1000 to 2000 seconds, and is essentially a high thrust device. The ion engine can operate efficiently at specific impulses above 5000 seconds, and is capable of efficient operation in the specific impulse range of 2000 to 5000 seconds--the range in which neither the arc jet engine nor the ion engine may be capable of operating efficiently.

ION PLASMA RESEARCH

CHAIRMAN

MILTON M. SLAWSKY

AIR FORCE OFFICE OF SCIENTIFIC RESEARCH

AIR RESEARCH AND DEVELOPMENT COMMAND

GRID ELECTRODE ION ROCKETS FOR LOW SPECIFIC IMPULSE MISSIONS

by

J. HOWARD CHILDS and WILLIAM R. MICKELSEN

LEWIS RESEARCH CENTER
NATIONAL AERONAUTICS AND SPACE ADMINISTRATION

574071 O - 60 - 9

INTRODUCTION

The great potential of ion rockets as a propulsion system for long duration space missions requiring very high values of specific impulse has been well documented (e.g., refs. 1 to 3) This paper will deal with some of the analytical studies that have been conducted to determine the feasibility of using ion rockets for space missions requiring comparatively low values of specific impulse (below 4000 seconds). The primary purpose of the paper is to present the theoretical design and performance calculations that have been made for ion rocket configurations employing surface ionization and grid electrodes for ion acceleration.

The paper first considers the propulsion requirements for a single space mission; namely, the raising of an earth satellite from 300-nautical mile orbit to a 24-hour orbit using electric rockets. This mission represents one of the earliest likely uses for electric propulsion. The possibility of meeting the propulsion requirements for this mission through the use of simple ion rocket configurations employing grid electrodes is considered. Grid electrode configurations appear promising for several reasons, as follows: (1) Their simplicity. This may result in comparative ease of development and greater reliability. (2) Their high efficiency when employing surface ionization systems. The grid electrode permits a very close spacing between the ion emitting surface and the accelerating grid. This close spacing is essential for obtaining high current densities and high efficiencies with moderate accelerating voltages. In the early days of electric propulsion, generators for extremely high voltages may not be available. If the required generators are available, then the high voltages may still be undesirable because of the high energy losses associated with ion interception when using high-voltage accelerate-decelerate systems to obtain low specific impulse (ref. 4). (3) The possibility of replacing or replenishing grid wires if they erode. An extremely low level of ion impingement on the accelerating electrode may be very difficult to obtain with any ion rocket configuration. If this proves to be the case, then the simple grid electrode configuration shows great promise for early electric propulsion missions because grid wires can be more easily replaced than more complicated electrodes.

This paper is not comprehensive; it is restricted to the examination of a single space mission and to the analysis of a single basic type of ion rocket configuration. There is nothing in the paper that should be construed as a recommendation that ion rockets are the only means or even the best means for electric propulsion of satellites. It is the authors' opinion, however, that ion rockets for low specific impulse missions show sufficient promise to warrant their development concurrently with the development of other possible propulsion systems, such as the electric thermal rocket.

A POSSIBLE APPLICATION

One attractive application for electric rockets is for raising earth satellites from initial low-altitude orbits to the desired higher-altitude orbits in cases where the electric power generating plant is required as a part of the satellite payload. In such cases the weight of the electric rocket necessary to adjust the satellite orbit is

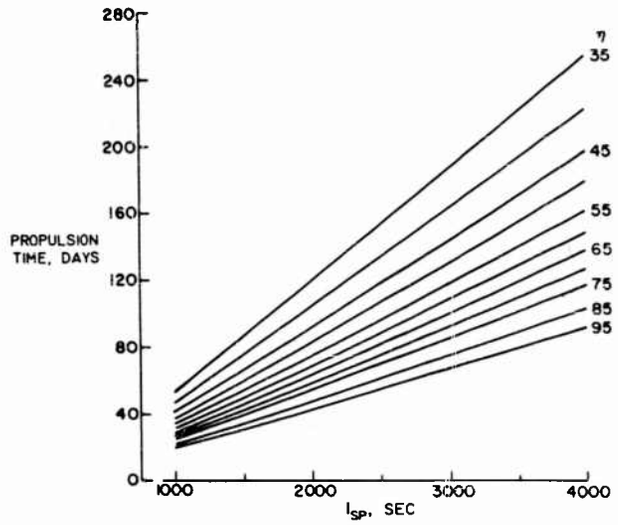

Fig.1 Satellite raising time to 24-hour orbit for 6000-pound satellite with 30 kw electric powerplant in initial 300 nautical mile orbit. Final orbit, 19,300 nautical miles and one degree off circular.

quite small in comparison with the weight of the chemical rocket plus propellant necessary to do the same job. Whether the ion rocket will ever be used for such missions depends, of course, on the efficiency and reliability of the ion rocket as compared with other types of electric rockets at the levels of specific impulse desired for these missions. Unfortunately for the ion rocket, the desired specific impulse is below the range where the ion rocket attains its highest efficiency; it may nevertheless be competitive with other types of electric rockets. Figure 1 compares the satellite raising time for different values of specific impulse and for the different energy efficiencies of the electric rocket used for raising the satellite. This figure was prepared by William R. Kerslake of the NASA Lewis Research Center using the charts of reference 5. Figure 1 is for a specific mission in which a 6000-pound satellite with a 30-kilowatt electric powerplant in an initial 300-mile circular orbit about earth is raised by electric propulsion to a 24-hour orbit. The actual values shown are for a final orbit at 19,300 nautical miles and 1° off circular. The figure shows that the satellite raising time becomes so long as to make the use of high values of specific impulse very questionable. Before we can determine the best specific impulse for this particular mission, we must first consider the effect of specific impulse on ion rocket efficiency and on propellant consumption. The remainder of this paper is devoted to just that consideration. The study is made for the case of ion rockets employing surface ionization and grid electrodes for ion acceleration.

GRID-ELECTRODE ENGINE CONFIGURATIONS

Several possible configurations for ion rockets employing grid type electrodes for accelerating the ions are shown in figure 2. The potential distribution through each configuration for zero ion current is indicated on the figure. Figure 2 (a) shows

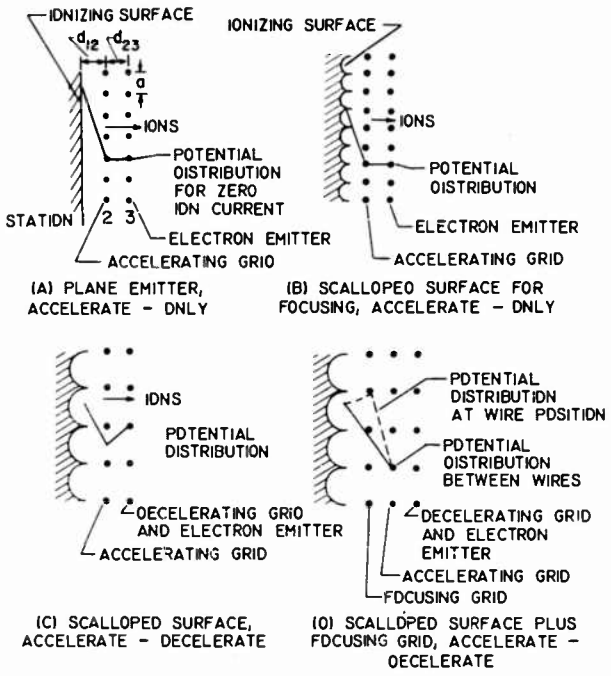

Fig.2 Some Simple Ion Rocket Configurations.

a case where the ions are emitted from a plane surface, accelerated through a grid electrode, and then passed through a second grid from which electrons are emitted to neutralize the beam. The method of introduction of propellant onto the ionizing surface is beyond the scope of this paper; the ionizing surface could conceivably consist of a slab of porous metal through which the propellant is supplied from the backside.

Figure 2 (b) indicates a similar configuration with the emitting surface scalloped to provide some electrostatic focusing of the ions between the grid wires. Figure 2 (c) shows this same configuration with the second grid operated at a positive potential relative to the first grid in order to decelerate the ions. The advantages of such an accelerate-decelerate system for ion rockets are well known; it permits higher current densities from the emitting surface and also provides a potential gradient at the back of the engine that will prevent electrons from flowing upstream to the ion source.

Figure 2 (d) shows still another configuration in which a focusing grid has been added just upstream of the accelerating grid. The focusing grid can be operated at a positive potential relative to the ion emitter and thus force practically all of the ions to miss the grid wires.

While other types of ion rockets are also worthy of consideration for operation at low specific impulse (ref. 4), the analysis presented herein is restricted to

the simple grid electrode configurations shown in figure 2. The analysis is also restricted to cesium propellant and a tungsten ionizing surface; the general conclusions arrived at from the analysis should however be applicable to other contact ionization ion rockets where different propellants and ionizing surfaces might be employed.

EFFICIENCY

Thermal Radiation Losses

As discussed in reference 4, the principal energy losses from this type of ion rocket at low specific impulse are due to thermal radiation from the heated tungsten ion source. Figure 3 (from ref. 4) shows how these radiation losses affect the ion source efficiency in cases where ideal current density is obtained.

The solid curve shows the efficiencies obtainable with an accelerator length of 1 millimeter. Such short accelerator lengths are probably attainable only with the type of engine configurations shown in figure 2. If the accelerator were longer than 1 millimeter, the efficiency would be lower than those indicated by the solid curve unless the accelerate-decelerate principle were employed. The two dashed curves indicate the efficiencies computed for two accelerate-decelerate ion rocket configurations. The upper dashed curve is for one of our engines that employs a Pierce electrode configuration for producing a rectilinear beam and accelerates the cesium ions through a potential difference of 40 kilovolts in a length of 1.31 centimeters. By using higher accelerator voltages or shorter lengths it would be possible to improve the efficiencies above those corresponding to this dashed curve. However, we have had sufficient difficulties with electrical breakdown near insulating surfaces in this particular engine to make us believe that even this level of performance will be difficult to obtain where engine reliability and long operating life are also important considerations.

The lower dashed curve shows performance of a simple configuration like that depicted in figure 2 (a), but with the grid potentials fixed to provide accelerate-decelerate operation. In this engine a simple screen of tightly-stretched parallel wires is used as the accelerator electrode in order to obtain very short lengths. An accelerating potential difference of only 1059 volts (corresponding to 4000 seconds with cesium ions) was assumed in computing the performance of this configuration, since it was desired to minimize the sputtering erosion and secondary electron emission that would result from impingement of higher voltage ions on the accelerating electrode. Even with this comparatively low accelerating voltage, the efficiency for this simple engine is almost as good as that indicated by the upper dashed curve for the engine employing more sophisticated electrodes.

If design techniques like those indicated in figures 2 (c) and (d) prove sufficient to insure that only a very small fraction of the ions impinge on the accelerating electrode, then higher accelerating voltages can be employed and the performance of the simple grid electrode configuration can be considerably improved over that noted in figure 3. In the analysis which follows, this possibility will be considered. Energy losses other than those resulting from thermal radiation from the ion source will also be considered; these include grid electrode effects, ion interception on the electrodes, and secondary electron emission. Consideration will also be given to

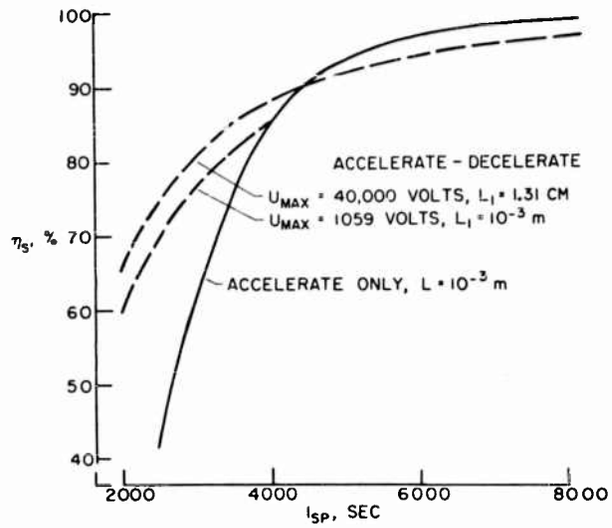

Fig. 3 Energy efficiency for ion rocket surface ionization system for cases where a high voltage is used to pull high current densities from the system. Tungsten surface. Cesium propellant. Data from Ref. 4.

the energy required for heating and ionizing the propellant and for emitting the electrons to neutralize the ion beam.

Grid Electrode Effects

The similarity between the grid electrodes considered herein and the screen grids employed in vacuum tubes makes it convenient for us to adopt the terminology and equations that have been developed for vacuum tubes (e.g., ref. 6). Thus the terms "screening fraction" S and "amplification factor" μ are used herein in the same context as in vacuum tube technology. The former refers to the fractional area blockage by a grid electrode and the latter is a measure of the effectiveness of the grid in determining the potential gradient at the ionizing surface. It is desirable to have high μ so that the current density will approach that of the ideal diode, but it is necessary to keep S to reasonably low values in order to reduce ion interception on the accelerating grid. These terms are related by the following equation from reference 6:

$$\mu = \frac{\left(\frac{2\pi d_{23}}{a}\right) - \ln \cosh \pi S}{\ln \coth \pi S} \qquad (1)$$

where

$$S = 2r_g/a \qquad (2)$$

A higher value of μ can be obtained for a given value of S by using finer wires and a closer spacing than by changing to larger wires and wider spacing. Thus r_g and a (see fig. 2) should be made as small as possible. To obtain a high current density, it is also desirable to have d_{12} as small as possible as discussed in ref. 4.

Hence the grid electrode geometry will be dictated by considerations of manufacturing tolerances and reliability. For the discussion that follows we will select the following values which are believed to be near the lower practical limits: a = 1 millimeter; d_{12} = 1 millimeter; $2r_g$ = 0.0029 inch. For this case μ = 4.2, and S = 0.0735.

The configuration of the accelerating grid determines the ion current density J that can be attained.

For an ideal diode with spacing d_{12};

$$J_{ideal} = \frac{C_1 (V_1 - V_2)^{3/2}}{d_{12}^2} \tag{3}$$

For a triode with grid spacing d_{12} and amplification factor μ, from reference 6;

$$J_{actual} = \frac{C_1 \left(V_1 - V_2 + \frac{V_1}{\mu}\right)^{3/2}}{d_{12}^2 \left[1 + \frac{1}{\mu}\left(\frac{d_{13}}{d_{12}}\right)^{4/3}\right]^{3/2}} \tag{4}$$

Then,

$$\frac{J_{act}}{J_{ideal}} = \left[\frac{1 + \frac{1}{\mu}\left(\frac{V_1}{V_1 - V_2}\right)}{1 + \frac{1}{\mu}\left(\frac{d_{13}}{d_{12}}\right)^{4/3}}\right]^{3/2} \tag{5}$$

This is a general equation relating the triode current density to the current density of the ideal diode having the same spacing between ion emitter and accelerating grid. Equation (5) is not exactly applicable to the configurations of figure 2; these configurations are not simple triodes, since a grid instead of a plate is used at station 3. However, for cases where the beam is neutralized very close to station 3, the value of J_{act} from equation (5) should approach the value to be expected from the engine configurations under consideration.

For the specific engine geometry to be considered throughout this discussion, $d_{13} = 2d_{12}$, and μ = 4.2. For this case;

$$\frac{J_{act}}{J_{ideal}} = \left[0.625 + 0.149\left(\frac{V_1}{V_1 - V_2}\right)\right]^{3/2} \tag{6}$$

Figure 4 shows a plot of J_{act}/J_{ideal} from equation (6) in terms of specific

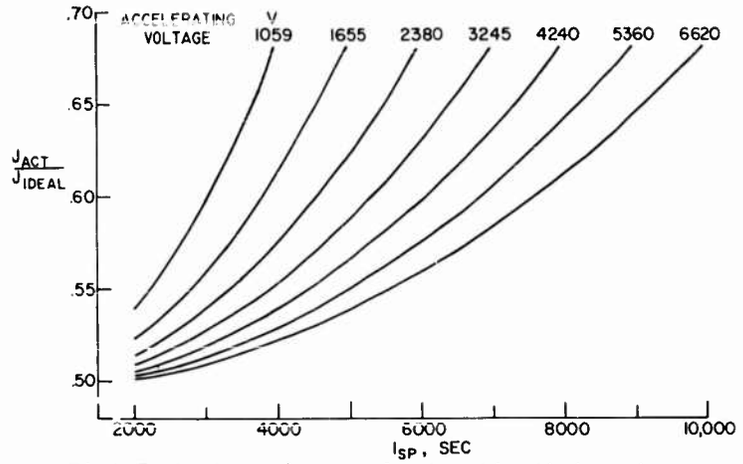

Fig.4 Ratio of actual current density with grid electrode to current density for ideal diode having same spacing. Screen amplification factor, 4.2. Spacing, 1 mm.

impulse and accelerating voltage ($V_1 - V_2$). Although the ratio of actual to ideal current density decreases with increase in accelerating voltage, the attainable current density for a given specific impulse increases with accelerating voltage as shown in figure 5.

Figure 6 shows a typical example of the effect of the grid electrode on ion source efficiency. The data were computed for an accelerate-decelerate ion rocket employing 1059 volts accelerating potential, an accelerator length of 1 millimeter, and a plane ion emitter. The upper curve in figure 6 shows the thermal radiation losses from the ion source that would be obtained if the accelerating electrode grid had a very large amplification factor so that the current density was equal to that of the ideal diode. This curve is identical with the lower dashed curve from figure 3. The lower curve in figure 6 indicates the increased thermal radiation losses that are obtained using the accelerating grid configuration previously noted. The additional energy loss that is produced by the grid electrode effect is due to the decreased current density obtainable in comparison with the ideal diode, which necessitates a larger engine frontal area and increased radiation losses for a given beam power.

Ion Interception

A rough indication of the amount of ion interception on the accelerating electrode can be obtained from experience with beam power tubes. If the emitting surface is planar as in figure 2 (a) and no attempt is made to focus the particles away from the accelerating grid wires, then the fraction of the particles intercepted by the wires is approximately equal to the fractional area blockage due to the wires. This relation between the intercepted current and the total current will be employed in some of the calculations which follow.

In cases where electrostatic focusing of the particles is employed as in figures 2 (c) and (d), references 6 and 7 indicate that the intercepted current can be re-

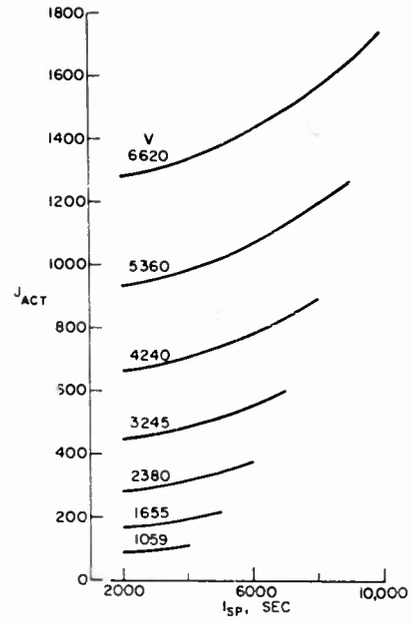

Fig.5 Current Density for Various Accelerating Voltages with Grid Electrode Having μ = 4.2 and Spacing of 1 mm.

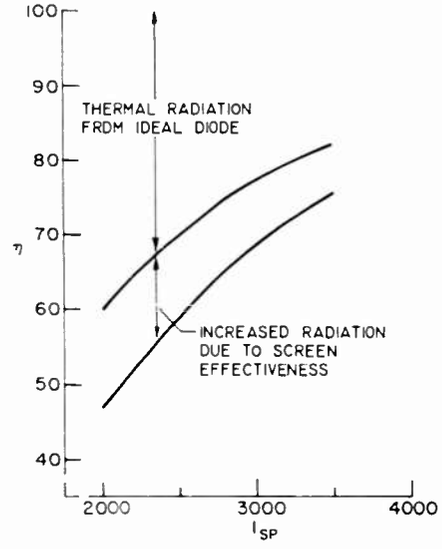

Fig.6 Some estimated efficiences for a low-specific-impulse ion rocket. Accelerate-decelerate with acceleration length and voltage of 1 mm and 1059 volts, respectively. Screen parameters: μ = 4.2 and S = 0.0735. Tungsten contact ion source. Cesium propellant.

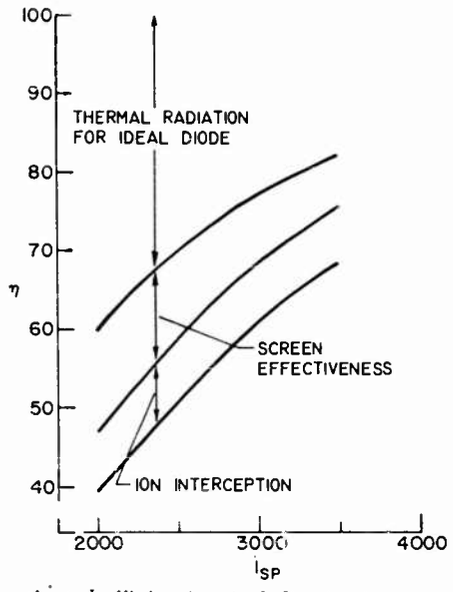

Fig. 7 Some estimated efficiencies, including ion interception, for a low-specific-impulse ion rocket. Accelerate-decelerate with acceleration length and voltage of 1 mm and 1059 volts, respectively. Screen parameters: μ = 4.2 and S = 0.0735. Tungsten contact ion Source. Cesium propellant.

duced to 1 percent or less of the total current. One percent interception will be assumed to be typical of the scalloped emitter configurations in the analysis which follows.

Figure 7 illustrates the effect of ion interception on ion rocket energy efficiency. The upper two curves in figure 7 are identical with the curves of figure 6. The lowest curve includes the additional energy losses obtained with ion interception proportional to the screen blockage; that is, 7.35 percent interception.

If we consider a scalloped ion-emitting surface such that $A_{ion} = 1.5\ A_{rad}$ and postulate 1 percent ion interception on the accelerating grid, then the efficiencies are within 1 percent of those shown by the intermediate curve in figure 7. A small decrease in radiation loss results from the change to a scalloped emitter, and this is largely cancelled when the interception loss is considered.

Secondary Electron Emission

Secondary electron emission due to ion bombardment of the accelerating grid is another consideration that dictates the use of a low accelerating potential in cases where some ion impingement is expected. Secondary electrons from the accelerating grid will fall back to the ion source and give a power loss. If we limit the engines of figure 2 to accelerating potentials of about 1 kilovolt, then the secondary emission coefficient is probably between 0.05 and 0.10 (ref. 8). Thus at 1 kilovolt accelerating potential the loss due to secondary electrons will be small compared to the loss of high-velocity ions; the efficiency values for ion interception proportional to grid

area blockage will be reduced by less than 1 percent, and efficiencies for 1 percent ion interception will be reduced less than 0.1 percent if allowance is made for secondary electrons falling back to the ion emitter.

As accelerating voltage is increased, the effect of the secondary electrons becomes greater. The secondary emission coefficient could conceivably approach unity at about 2 kilovolts. With a coefficient of unity, the energy loss in recycling the secondary electrons would exactly equal that due to loss of the ions. Because data are not available for the secondary emission coefficient at voltages above 1 kilovolt and any extrapolation of the low-voltage data involves uncertainties of at least one order of magnitude, no attempt was made herein to calculate the energy losses due to secondary electron emission.

The following rough estimates can be made of the magnitude of secondary electron effects on efficiency: For cases where ion impingement is proportional to area blockage (7.35 percent) secondary electron effects will be small for accelerating potentials up to 1 kilovolt; they may possibly be small up to about 2 kilovolts, although this is not certain; thereafter, they probably become very large. For the case of 1 percent ion impingement, secondary electron effects on efficiency are probably small up to 2 kilovolts; they may possibly be small up to about 3 kilovolts, although this is uncertain; thereafter, they are probably large.

Energy Required to Heat and Ionize Propellant and to Emit Electrons

These three energy requirements can conveniently be considered together since each is quite small and directly proportional to the ion current. They are given by the following approximate equation:

$$\sum\left(\frac{P}{A}\right) \approx 0.006J \qquad (7)$$

The exact magnitude of the constant in equation (7) will, of course, depend upon such factors as the work function of the electron-emitting surface. These energy losses have been computed for several representative cases herein and are usually less than 1 percent of the other energy losses. For this reason they have not been included in computing the values of efficiency indicated on the various figures.

Other Energy Losses

Other possible energy losses in the ion rocket which have not been included in this analysis are as follows: (1) Thermal radiation from electron emitter. These losses could become appreciable if high-work-function surfaces and high temperatures are employed for electron emission. The following analysis is therefore valid only if low-work-function surfaces are employed for electron emission. (2) Energy losses due to ion deceleration to voltages above those at the electron emitter grid. This is briefly discussed in reference 4. (3) Energy contained in electron oscillations in the exit beam. (4) Ohmic losses.

Effeciencies for Three Engine Configurations

Figures 8, 9, and 10 show the effect of specific impulse and accelerating voltage on the overall energy efficiency of the ion rocket for three configurations. Figure 8 is for the engine geometry shown in figure 2 (a) but with the engine operating on the accelerate-decelerate principle. It is assumed that the backside of the heated tungsten ion source is insulated so that the area radiating to outer space is equal to the ion beam area. It is further assumed for this configuration that the fraction of ions intercepted on the accelerating grid is equal to the fractional area blockage afforded by that grid. Figure 9 is for the engine shown in figure 2 (c) having a scalloped emitting surface and also operating on the accelerate-decelerate principle. For this configuration the effective area for ion emission was assumed to be 1.5 times the area for thermal radiation, and it was also assumed that 1 percent of the ions are intercepted by the accelerating grid. Power loss due to secondary electron emission is neglected in both figures 8 and 9. Figure 10 is for an engine such as shown in figure 2 (d) with negligible ion interception.

Figures 8, 9, and 10 show the efficiency to increase progressively with increase in specific impulse. This is due to the fact that the beam power increases while the thermal radiation remains fixed as specific impulse is increased for any fixed value of accelerating voltage. Figure 8 indicates a slight increase in efficiency with increase in accelerating voltage from 1059 up to 2380 volts. This occurs because the higher current densities obtainable with higher accelerating voltages permit a reduction in engine frontal area and a corresponding reduction in the thermal radiation loss. Further increases in accelerating voltage above 2380 volts in figure 8 produce a decrease in the overall efficiency. This is due to the large amount of energy being lost by ion interception on the accelerating grid; the higher the accelerating voltage, the higher the energy loss for a fixed ion interception rate.

Figure 9 shows trends that are identical with figure 8 but the general level of the efficiency is somewhat higher. For the particular values of accelerating voltage selected in the analysis, the efficiency increased up to 5360 volts and thereafter decreased at the lowest specific impulse considered. At higher values of specific impulse the efficiency began to decrease for accelerating voltages higher than 4240 volts. Actually the trends just noted were very slight and consequently the curves for the three highest accelerating voltages are shown as a single broad curve on figure 9. The differences in overall efficiency for these three highest accelerating voltages were in all cases less than 1 percent.

Figure 10 shows a continuing increase in efficiency with increasing accelerating voltages, since ion impingement is assumed negligible. For the higher specific impulses, only small gains in efficiency are realized by increasing the accelerating voltage.

DURABILITY AND STRUCTURAL CONSIDERATIONS

Grid Wire Temperature

Figure 11 shows the temperature that circular grid wires will assume for

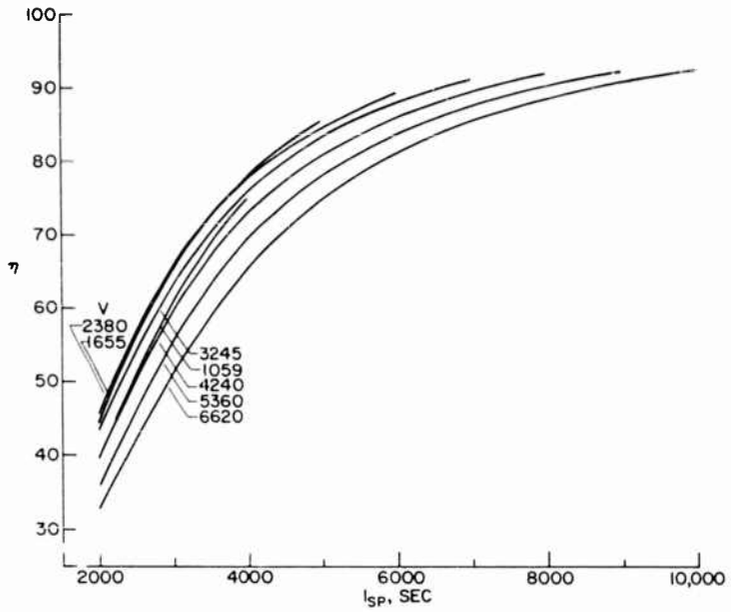

Fig. 8 Estimated overall ion rocket efficiencies for $A_{ion} = A_{rad}$ and 7.35 percent ion interception. Length, 1 mm. Screen parameters: $\mu = 4.2$ and $S = 0.0735$. Tungsten contact ion source. Cesium propellant. No allowance for secondary electron emission.

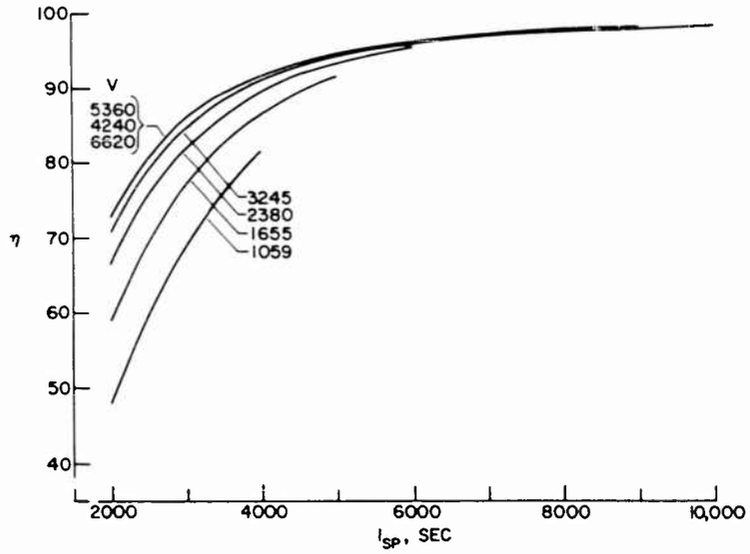

Fig. 9 Estimated overall ion rocket efficiencies for $A_{ion} = 1.5\ A_{rad}$ and one percent ion interception. Length, 1 mm. Screen parameters: $\mu = 4.2$ and $S = 0.0735$. Tungsten contact ion source Cesium propellant. No allowance for secondary electron emission.

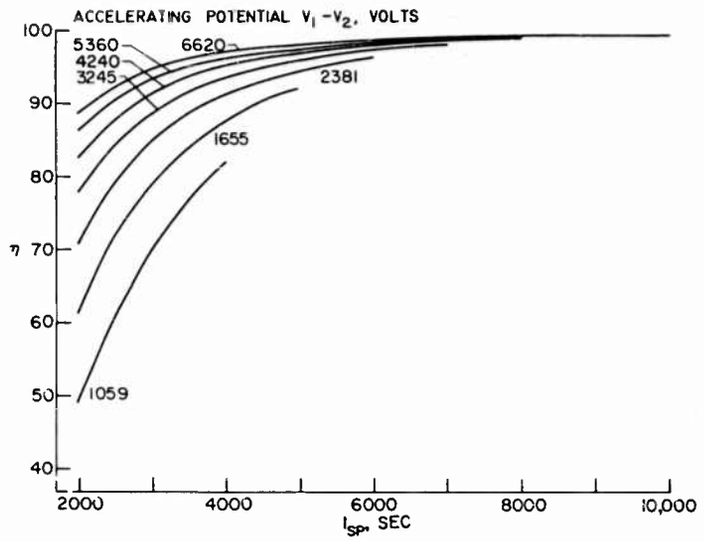

Fig.10 Estimated overall ion rocket efficiencies for A_{ion} 1.5 A_{rad} and negligible ion interception. Length, 1 mm. Screen parameters: 4.2 and S 0.0735. Tungsten contact ion source. Cesium propellant. No allowance for secondary electron emission.

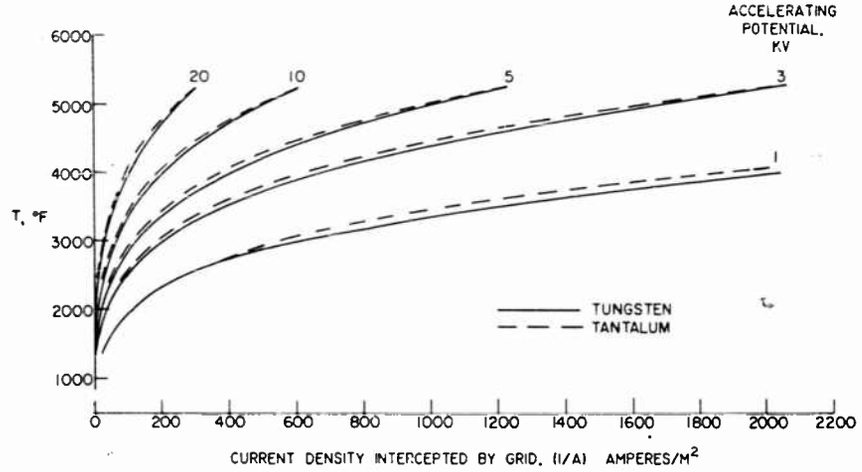

Fig.11 Temperature of Grid Wires of Circular Cross Section.

various current densities intercepted by the grid wires and for various accelerating voltages. With tantalum or tungsten wires moderately high current densities at the location of the grid wires can be tolerated even with accelerating voltages as high as 20 kilovolts. For the low accelerating voltages considered in this analysis, the grid wire temperatures will not be excessive.

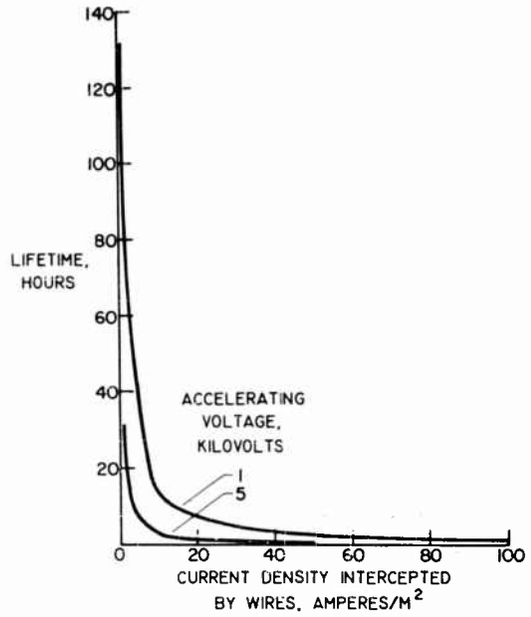

Fig. 12 . Approximate lifetime of 0.0029-inch diameter grid wires computed from data of Ref. 8 for sputtering of nickel by mercury ions.

For configurations wherein the ions are not diverted around the accelerating grid wires by electrostatic focusing, the grid wire temperatures may exceed the temperature of the tungsten ion source. In this case, thermal radiation from the grid wires will serve to reduce the radiation losses from the ion source. No correction for this effect has been made in the calculations presented herein. The thermal radiation losses from the grid wires themselves have been fully allowed for, however, by assuming that all of the energy in the intercepted ions is lost.

Lifetime of Grid Wires

Sputtering erosion of the wires will limit them to a very short lifetime unless extremely low current densities approaching the wires can be achieved through some means of electrostatic focusing of the ions away from the grid wires. This is indicated in figure 12. Even with accelerating voltages of the order of 1 kilovolt and with the low current densities corresponding to 1 percent ion interception, the lifetime of the wires is very short. Therefore, unless ion interception can be reduced to levels far below 1 percent by techniques such as those indicated in figure 2 (c) and (d), we must consider some scheme for replacing the grid wires in order to obtain the required engine operating life.

In an actual engine, if all the wires are allowed to erode simultaneously the current density from the engine will decrease as the wires decrease in size. This will prolong the lifetime over the values indicated in this figure, but at a cost in engine thrust that cannot be tolerated. Figure 12 is presented herein in order to provide

rough estimates of the length of time that the wire can be allowed to remain in the beam without replacing them or restoring them to their original size to avoid the effects noted above. It appears that their allowable dwell time in the beam may range from a few minutes to a few hours for the various engines considered herein. For the case where I_{sp} = 2000 seconds, and $(V_1 - V_2)$ = 2380 volts, J_{act} = 280 amperes/m^2 (fig. 5). If 1 percent ion impingement is obtained, then the current intercepted by the grid wires is 280/7.35 = 38 amperes/m^2, and the lifetime is about 3 hours (fig. 12). For this particular case, a dwell time for the wires in the beam of about 1 hour would appear reasonable, after which the wires should be restored to their original size.

Figure 12 should be regarded as being very approximate since the data were computed using experimental sputtering rates for mercury ions impinging on nickel (ref. 8) and assuming that the sputtering rate for cesium on materials such as tantalum would be comparable. The data of figure 12 are therefore indicative only of the order of magnitude of the effects involved; they may be somewhat pessimistic, since sputtering rates increase with the atomic weight of the bombarding ions.

It should also be observed that the data for figure 12 were computed for a wire diameter of 0.0029 inch. For other wire diameters the lifetime will be different; the lifetime is directly proportional to the wire diameter.

Grid Sputtering Rate

The requirement for replacing the grid wires has been indicated. The wires could be forced to move continuously through the beam on a system of pulleys, passing through a molten metal bath where eroded material is restored to the wire surface, and then returning for another pass through the ion beam. While such a system would introduce a great deal of mechanical complexity, it should not be ruled out until such time as some other system has been proven to give ion rockets having the required performance and reliability. Figure 13 shows the rate at which material must be added to the grid wires expressed as a percentage of the cesium propellant flow rate. For the case previously considered where the accelerating grid intercepts 7.35 percent of the ion current the required rate of mass addition to the wires becomes an appreciable fraction of the cesium flow rate unless accelerating voltages are restricted to about 1 kilovolt.

If ion interception can be reduced to 1 percent, corresponding to another case considered in this analysis, then higher accelerating voltages appear feasible.

The sputtering rates for figure 13 were computed from the same data as figure 12, and the same restrictions apply to the figure as previously noted for figure 12.

Grid Wire Span

Supports must be provided along the length of the accelerating grid wires to prevent excessive bending arising from the engine thrust. The wire deflection can be easily calculated; the wires constitute beams that are uniformly loaded by the thrust force, and are fixed at the ends of their span. The length of the span can be

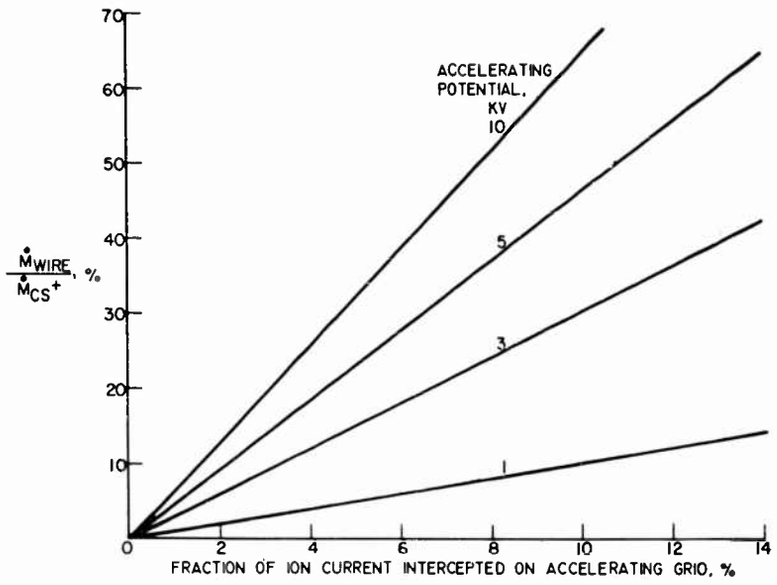

Fig. 13 Rate of mass erosion from accelerator grid. Gor cesium propellant, assuming sputtering rate same as for Hg^+ on Ni. Data from Ref. 8.

varied by suitable insulator supports between the emitter surface and the wires. For unstretched 0.0029 inch tantalum wires, the allowable span is given by:

$$\text{Span (cm)} = \left[\frac{7.65 \times 10^8}{JI_{sp}}\left(\frac{y}{a}\right)\right]^{1/4} \qquad (8)$$

For a deflection y of 0.05 millimeter, and a wire spacing a of 1.0 millimeter, allowable wire spans are shown in figure 14 as a function of specific impulse and current density.

As indicated by figure 14, spans are limited to a few centimeters for unstretched wires. By applying an axial tension to the wires, the allowable span may be greatly increased as shown by the following expression derived from an approximate equation in reference 9:

$$\text{Span (cm)} = \left\{\frac{1.065 \times 10^5 \left(\frac{y}{a}\right)_s}{JI_{sp}}\left[1 + \left(1 + 0.0677\frac{JI_{sp}}{(y/a)s^2}\right)^{1/2}\right]\right\}^{1/2} \qquad (9)$$

Allowable spans are shown in figure 15 for a stretched wire with an applied axial tensile stress of 5000 pounds per square inch, a deflection y of 0.05 millimeter, and a wire spacing of 1.0 millimeter. As indicated by the curves in figure 15, the allowable span is substantially increased by a moderate applied axial tension.

574071 O - 60 - 10

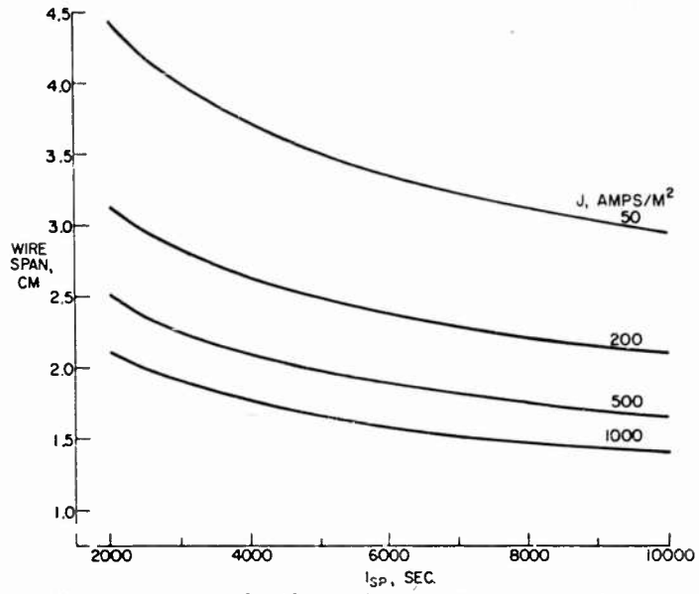

Fig.14 Unsupported grid span for a maximum wire deflection of 0.05 mm. For tantalum wires; diameter, 0.0029 in.; spacing, 1 mm.

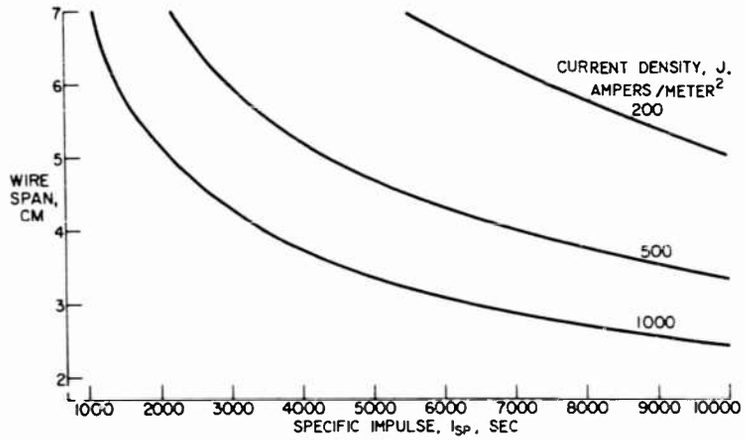

Fig.15 Unsupported grid wire span for a deflection of 0.05 mm. For tantalum grid wires, 0.0029 inch diameter, 1.0 mm spacing, with applied axial tension of 5000 lb/in².

OTHER CONSIDERATIONS

Electron Reversal

An additional consideration of possible importance in the ion rocket is the voltage on the decelerating grid relative to that on the accelerating grid necessary to prevent backward flow of electrons. In figure 16, the solid curve indicates the

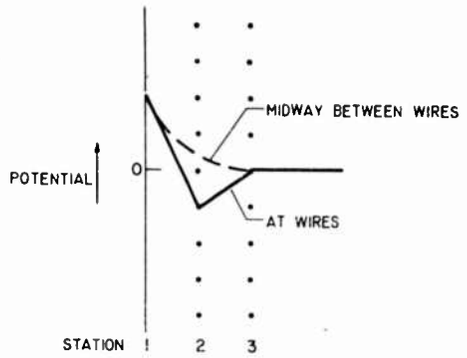

Fig.16 Potential Distributions Through Engine for Zero Electric Field at Station 3 Midway Between Grid Wires.

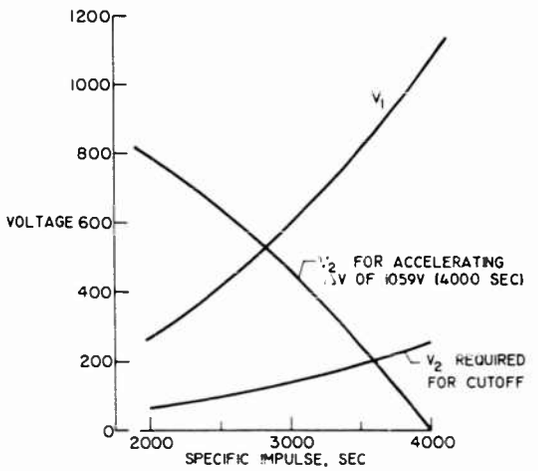

Fig.17 Comparison of voltages required in accelerate-decelerate system with voltages required to prevent electron reversal into ion accelerator. Screen amplification factor, 4.2 Decelerating grid at zero potential.

potential distribution through the engine at the location of the grid wires and the dotted curve shows the potential distribution midway between the grid wires for the case where the potential of the accelerating grid is negative with respect to the decelerating grid by an amount just sufficient to produce zero slope on the potential curve (zero electric field) midway between the grid wires. Lower voltages on the accelerating grid will produce a positive slope on the potential curve at the back of the engine which will insure against backward flow of electrons. By the same token, smaller voltage differences between the accelerating and decelerating grids will allow a negative slope between the wires which will permit electron flow back to the ion source.

The situation depicted in figure 16 is exactly analogous to the cutoff condition in vacuum tubes. At this condition the following relation holds:

$$\mu = V_1/-V_2 \qquad (10)$$

for V = 0 and dV/dL =0 at station 3.

Figure 17 compares the voltage necessary on the accelerating grid to produce various levels of specific impulse with those voltages necessary to produce zero electric field at the back of the engine where the electrons are injected. These computations were made for the case where the accelerating voltage difference is 1059 volts (4000 seconds with cesium ions) and the amplification factor of the accelerating grid is 4.2. For values of specific impulse below 3590 seconds the accelerating grid voltage is of a sufficiently low voltage to produce the desired electric field at the back of the engine. If this particular engine is operated at higher values of specific impulse, difficulties due to backward flow of electrons may be encountered.

It should be emphasized, however, that the foregoing considerations are only accurate in the absence of ion space charge effects. At high current densities, the potential distribution through the engine can be considerably different than indicated in figure 16 and the crossover point for the two curves can be shifted from that of figure 17. A quantitative consideration of space charge effects is beyond the scope of this paper. For the satellite raising mission being considered herein it appears that low specific impulse will be desirable to reduce the satellite raising time, as will be subsequently discussed. It also appears probable that moderately high accelerating voltages will be employed in order to take advantage of the high efficiencies previously indicated. This combination of low specific impulse and moderately high accelerating voltage will result in sizable potential differences between the accelerating and decelerating electrodes, thereby minimizing the likelihood of backward flow of electrons.

Contamination of Ion Emitter

Sputtered material from the grid wires may coat the tungsten ionization surface and reduce the ionization efficiency. One possible method of avoiding this is to use tungsten grid wires. This presents two difficult problems: (1) The brittleness of the wires, and (2) The difficulty of restoring eroded tungsten to their surface. If tungsten wires must be used it may prove necessary to discard the wires after some erosion. This will increase the mass of wire material consumed over the values indicated in this analysis.

If sputtering contamination does not prove to be a problem then it may be possible to use tantalum grid wires with an outer coating of some other metal having a lower melting point. This coating could be replenished as discussed previously.

Ion Rocket Exhaust Area

The ion beam area for a given powerplant output may be expressed in terms of ion rocket efficiency, specific impulse, accelerating voltage, charge to mass ratio, and accelerator length:

$$A = 0.373 \times 10^{10} \sqrt{\frac{e}{m}} \frac{\eta d_{12}^2 P}{I_{sp}^2 (V_1 - V_2)^{3/2}} \left(\frac{J_{ideal}}{J_{act}} \right) \qquad (11)$$

For an accelerator length of 1 mm, a power of 30 Kw, and cesium propellant, the equation for beam area becomes:

$$A = 0.955 \times 10^{11} \frac{\eta}{I_{sp}^2 (V_1 - V_2)^{3/2}} \left(\frac{J_{ideal}}{J_{act}} \right) \qquad (12)$$

The largest exhaust area for the range of design variables considered herein will be for a specific impulse of 2000 seconds and an accelerating voltage of 1059 volts. From figure 10, the efficiency for these conditions is 49 percent, so that allowing for the area blockage of the grid wires, the largest exhaust area would be roughly seven square feet, which is quite modest.

EFFECT OF ENGINE DESIGN ON SATELLITE RAISING MISSION

Raising Time

The effect of accelerating voltage and specific impulse on satellite raising time is shown in figure 18 for engines giving the efficiencies noted in figure 8; that is, engines having a plane emitter surface and intercepting 7.35 percent of the ions on the accelerating grid. At the lowest accelerating voltage considered, 1059 volts, the raising time is nearly constant for values of specific impulse below 3000 seconds. This is because of the rapid decrease in ion rocket efficiency with decrease in specific impulse in this range. Thus, despite the fact that the thrust per unit power increases with decrease in specific impulse, the decrease in efficiency produces such a reduction in beam power that the thrust remains essentially constant.

At low specific impulse the satellite raising time can be reduced by about 10 percent if somewhat higher accelerating voltages are used. The data for accelerating voltages of 1655 and 2380 fall almost on a common curve since the efficiencies for these two values of accelerating voltage are almost identical (see fig. 8). Accelerating voltages higher than 2380 would produce increases in raising time because of the lower efficiencies that would result.

With the assumptions made in computing the values of engine efficiency used in figure 18, it appears that about 92 days is the minimum possible satellite raising time.

Figure 19 shows similar data on satellite raising time for engines having efficiencies like those indicated in figure 9; that is, engines having scalloped ion emitter surfaces and intercepting only 1 percent of the ions on the accelerating grid. Here again, there is little advantage in going to values of specific impulse below a-

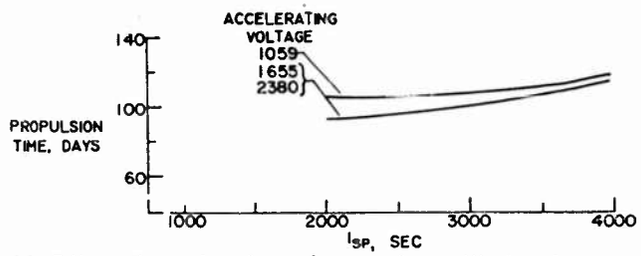

Fig.18 Effect of accelerating voltage and specific impulse on satellite raising time for configuration having $\mu = 4.2$ accelerating grid and ion interception proportional to grid area blockage (7.35 percent). $W_o = 6000$ lb; power, 30 kw; initial orbit - circular, 300 nautical miles; final orbit - 24-hour, 19,300 nautical miles, 1° off circular. No allowance for secondary electron emission.

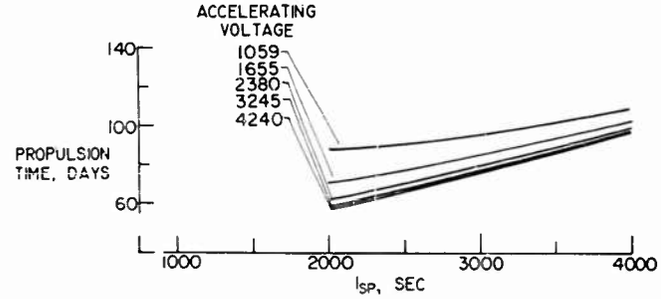

Fig.19 Effect of accelerating voltage and specific impulse on satellite raising time for configuration having $\mu = 4.2$ accelerating grid and 1 percent ion interception. $W_o = 6000$ lb; power, 30 kw; initial orbit - circular, 300 nautical miles; final orbit - 24 hour, 19,300 nautical miles, 1° off circular. No allowance for secondary electron emission.

bout 3000 seconds if very low accelerating voltages are utilized. However, for this case, sizable reductions in satellite raising time can be obtained by going to low specific impulse in conjunction with moderately high accelerating voltages. The reduction in satellite raising time is appreciable as the accelerating voltage is progressively increased up to 3245 volts. Further increases in accelerating voltage produce only very small reductions in raising time. If values of accelerating voltage much above 4240 volts are considered, then the raising time will begin to increase because of the trends in engine efficiency noted in figure 9. As previously noted, energy losses resulting from secondary electrons may make it necessary to keep the accelerating potential below 3000 volts.

If practical ion rockets can be built to perform in accord with the assumptions used in figures 9 and 19, then it appears that a satellite raising time of 61 days may be possible using 2380 volts accelerating potential and a specific impulse of 2000 seconds.

For ion rockets with negligible ion impingement on the accelerators the efficiency continuously improves with increasing accelerating voltage, as shown in figure 10. The satellite raising time therefore decreases as accelerating voltages

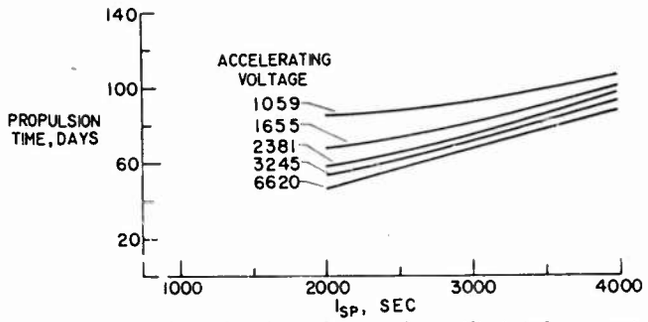

Fig.20 Effect of accelerating voltage and specific impulse on satellite raising time for configuration having $\mu = 4.2$ accelerating grid and negligible ion interception. $W_o = 6000$ lb, power, 30 kw; initial orbit - circular, 300 nautical miles; final orbit 24 - hour, 19,300 nautical miles 1° off circular. No allowance for secondary electron emission.

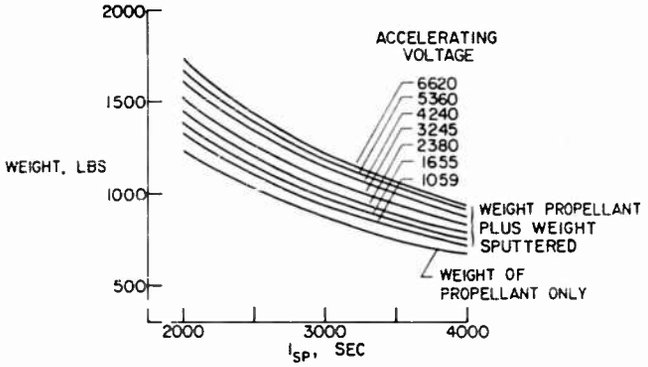

Fig.21 Propellant plus accelerating grid weight consumed in raising satellite to 24-hour orbit for case where ion interception is proportional to grid area blockage (7.35 percent).

is increased as shown in figure 20. At the higher specific impulses, the raising time for an accelerating voltage of 6620 is close to the minimum possible since the efficiency there is nearly 100 percent. At a specific impulse of 2000 and an accelerating voltage of 6620, the raising time is 46 days. The raising times at the lower specific impulses can be lowered somewhat by using higher accelerating voltages. This improvement will be limited by insulator breakdown and electron field emission at high accelerating voltages.

Weight of Propellant and Grid Material Consumed

The lowest curve in figure 21 shows the weight of propellant consumed in the satellite raising mission for various levels of specific impulse. The increments between this lowest curve and the other curves on the figure indicate the quantities of grid material that are sputtered away while raising the satellite with various accelerating voltages. The data of figure 21 were computed for the case where 7.35 percent of the ions are intercepted on the accelerating grid; this figure is therefore representative of the performance of the same engines considered in figures 8 and 18. Figure 13 was used in computing the weight of sputtered material; thus the data

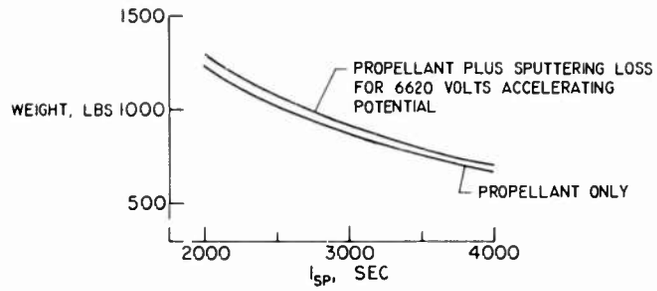

Fig.22 Propellant plus accelerating grid weight consumed in raising satellite to 24-hour orbit for case where one percent of ions are intercepted.

shown in figure 21 are only rough approximations of the actual sputtering to be expected, at best.

Examination of figure 21 in conjunction with figure 18 shows that for this type of ion rocket a likely selection of the design point for engine operation might be 1655 volts for acceleration and a specific impulse of about 3000 seconds. At this design point, the satellite raising time is only about 7.5 days greater than the minimum obtainable, and the weight transferred into 24-hour orbit is about 400 pounds greater than that for minimum raising time.

Figure 22 shows similar data on weight consumption for engines in which 1 percent of the ions are intercepted (assumptions consistent with those of figs. 9 and 19). The lowest curve in figure 22 is identical with that in figure 21 and shows the weight of propellant consumed. The upper curve shows the weight of propellant plus the sputtering loss for the highest accelerating voltage (6620 volts) considered in the analysis. If 1 percent ion interception can be attained in practice then there is little penalty in weight in going to high accelerating voltages.

A study of figures 19 and 22 indicates that for the engine performance characteristics assumed in computing these figures, accelerating voltages of at least 3245 volts are very worthwhile since they provide appreciable decrease in raising time with very little decrease in weight transferred into 24-hour orbit. However, the effects of secondary electrons previously discussed would probably make it necessary to restrict the accelerating potential to values below 3000 volts. For this case, then 2380 volts would be a likely choice for the accelerating potential. The selection of the specific impulse would depend on the relative importance of raising time and weight in 24-hour orbit. Decreasing the specific impulse from 3000 to 2000 seconds decreases the satellite raising time by about 17 days; at the same time, however, the weight transferred into 24-hour orbit is decreased by more than 350 pounds.

CONCLUDING REMARKS

The foregoing discussion has indicated the various factors that must be considered in designing grid-electrode ion rockets for use in satellite raising missions. If a negligible amount of ion impingement on the accelerating grid can be obtained through the use of the design techniques described herein, then ion rocket efficiencies

approaching 100 percent can be obtained by using high accelerating voltages. At 6620 volts accelerating potential, the efficiency is 89 percent at 2000 seconds and 95 percent at 3000 seconds specific impulse. With 2000 seconds specific impulse and 89 percent efficiency, only 46 days are required to raise a satellite having an initial weight of 6000 pounds into 24-hour orbit with a 30 kilowatt electric powerplant.

The analysis shows that even with 1 percent of the ions impinging on the accelerating grid this type ion rocket still looks quite promising for the satellite raising mission. The mass of wire material that will be eroded is not large compared to the propellant consumed during the mission. If contamination of the ion source by sputtered grid material proves damaging then tungsten wires could conceivably be used to eliminate this problem. Ion rocket efficiencies are still quite good with 1 percent ion impingement: efficiencies over 70 percent are attainable at 2000 seconds and over 85 percent at 3000 seconds specific impulse. However, these efficiencies are only obtained with moderately high accelerating voltages. Consideration of grid wire replenishment and energy losses associated with secondary electron emission make it probable that accelerating voltages will be restricted to about 2380 volts. With this accelerating voltage and 1 percent ion impingement the attainable efficiency is about 67 percent at 2000 seconds and 82 percent at 3000 seconds specific impulse. These efficiencies give a raising time of 61 days at 2000 seconds and about 78 days at 3000 seconds specific impulse. The weight transferred into high altitude orbit can be increased by more than 350 pounds by accepting the higher value of satellite raising time.

If ion impingement on the grid wires is approximately proportional to the grid area blockage, as is the case in some vacuum tubes, then the type of ion rocket proposed herein is of questionable feasibility. The weight of grid material that is eroded is appreciable, particularly if it proves impractical to continuously replenish the outer coating of the wires as they are eroded. It appears likely that ion source contamination will dictate the use of tungsten wires, thereby making it especially difficult to replenish the outside coating on the wires. This fact together with the low efficiency (about 45 percent at 2000 seconds specific impulse) makes it very doubtful that this amount of ion impingement could ever be tolerated in a practical system.

The limited data available from vacuum tube experience using some of the ion focusing techniques proposed herein makes it appear reasonable to expect that ion impingement of less than 1 percent can be attained with grid-electrode engines.

It is not clear that any other type of ion rocket configuration could yield efficiencies comparable to those indicated for the grid-electrode configurations at low specific impulse. If more sophisticated electrodes are employed they will probably require a greater spacing and greater accelerating voltage. This would result in excessive energy losses and sputtering erosion unless ion impingement of essentially zero can be obtained.

In view of the favorable results obtained in this analysis it appears desirable to continue the development of grid-electrode ion rockets for propulsion of earth satellites.

SYMBOLS

A	area, square meters
a	grid wire spacing, meters
C_1	constant
d	distance, meters
e	electronic charge, coulombs
I_{sp}	specific impulse, sec
J	current density, amperes per square meter
L	distance
m	ion mass, kilograms
$\dot{m}$	weight flow rate, kg/sec
P	electric generator output power, watts
r_g	grid wire radius, meters
S	grid area blockage, $S = 2r_g/a$
s	unit tensile stress, $lb/in.^2$
V	potential, volts
W_0	initial gross weight, lb
y	grid wire deflection, meters
η	overall ion rocket efficiency
η_s	energy efficiency of ion source
μ	grid electrode amplification factor

Subscripts:

1	ion emitter (see fig. 2)
2	accelerating grid (see fig. 2)
3	final grid (see fig. 2)

act actual

ideal pertaining to ideal diode having same configuration and spacing as engine under consideration

rad radiation

ion ionization

REFERENCES

1. Stuhlinger, Ernst: Possibilities of Electrical Space Ship Propulsion. Paper presented at Fifth Astronautics Congress (1954).

2. Moeckel, W. E.: Propulsion Methods in Astronautics. Paper presented at General Session of First International Congress of Aeronautical Sciences, Madrid (Sept. 13, 1958).

3. Moeckel, W. E.: Advances in Aeronautical Science (Proceedings of the First International Congress of the Aeronautical Sciences, Madrid, 1958). Pergamon Press (1959).

4. Childs, J. Howard: Design of Ion Rockets and Test Facilities. Paper No. 59-103, IAS (1959).

5. Moeckel, W. E.: Trajectories with constant tangential thrust in central gravitational fields. NASA TR R-53 (1959).

6. Spangenburg, K. R.: Vacuum Tubes. McGraw-Hill Book Co., Inc., (1948).

7. Knoll, M.: Verstärker und Senderöhren als elektronenoptisches Problem. Zeit. für Tech. Phys., Bd. 15, pp. 584-591 (1934).

8. Massey, H. S. W., and Burhop, E. H. S.: Electronic and Ionic Impact Phenomena. Clarendon Press (1956).

9. Timoshenko, S.: Strength of Materials, Part II, Second Edition. D. Van Nostrand Company (1941).

TRANSIENT MAGNETIC PROPULSION OF PLASMA

by

RALPH W. WANIEK

PLASMADYNE CORPORATION

ABSTRACT

Some of the basic approaches to intermittent magnetic plasma propulsion are summarized and reviewed in terms of the features deemed important for practical space applications. The class of inductively coupled devices is examined in detail and some of the requirements necessary for efficient magneto-kinetic energy transfer are outlined. Experimental results obtained with asymmetric high field collapse trustors are presented.

Transient plasma accelerators make use of a Lorentz force to impart a net momentum to a gaseous configuration. At times, such a JxB force is implemented by the expansive force induced by the joule heating of the conducting gas. The latter force can sometimes be comparable with the effects of the magnetic force applied. Since all the transient methods of plasma propulsion rely on the same basic principle, differences can be found only in the geometries used and in the plasma parameters which the specific geometry is able to induce. Almost all the methods of electromagnetic plasma propulsion shown feasible and reported until now can be divided into two broad categories.

The first class (References 1 through 10) includes all those devices where the electrodes are an integral part of the discharge circuit itself. In such cases, gas together with an abundant amount of electrode material is usually accelerated. Among the various types of "direct-coupling geometries", we can find one, two and three-dimensional schemes (see synoptical table, Figure 1). The increase in dimensionality makes containment more feasible which is quite essential for this type of operation. This category will operate more efficiently than the second one of the "induced-current geometries", at least for low plasma temperatures.

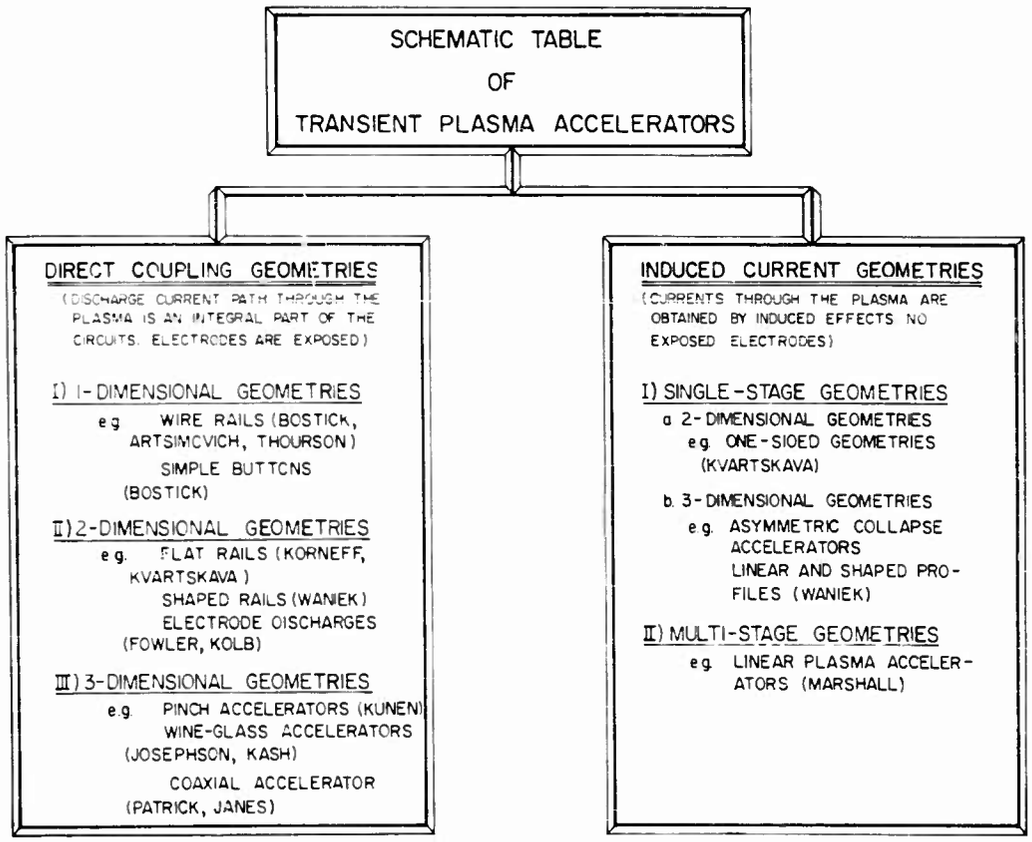

Fig. 1

The main drawback, however, resides in the amount of material sputtered during operation. A rough evaluation of the rate of erosion may be obtained from the knowledge of the energy of vaporization at the boiling point (4850 joules/gm for copper), from the electrode excess energy, and from the current density. A typical figure for such discharge devices might amount to 50 micrograms/coulomb or 0.6 gm/cm^2 sec for a current density of 10^4 amp/cm^2. For a one year mission, carried out at a duty cycle of 10 pps, this would require the evaporation of about 200 lb of copper. Other materials used for the electrodes will not alter this figure appreciably because of the increase in resistive losses. Propelling such a mass, which is conveniently stored at such high densities, would appear as a rather attractive possibility. In effect, one could envisage a series of expendable units with continuous electrode feeding, like in the case of the old-fashioned carbon arcs used in projectors. The difficulty, however, is that a good fraction of the material will deposit in the interelectrode space and cause premature breakdowns at unwanted places. Besides, the plasma is composed predominantly of metallic ions of high-Z giving rise to strong dissipative Bremstrahlung radiation.

The second class of devices (References 11 through 14) achieves propulsive effects by induced current patterns and avoids, therefore, exposed electrodes. In these cases, the magnetic field set up by the current through the conductor will interact with the currents induced in the conducting gaseous configuration. The resulting Lorentz force will act at the field-plasma boundary and will cause translational motion. A simple example is given in Figure 2 which shows a symmetric

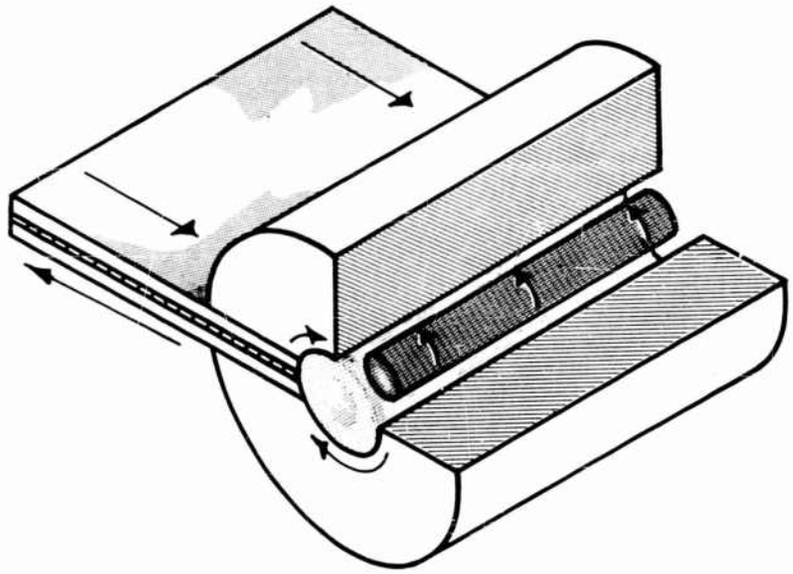

Fig. 2 Symmetrical Collapse Configuration

collapse geometry. In such an instance, the plasma is constricted radially inward by the Lorentz force, or in an equivalent expression, by the magnetic pressure. The sudden magnetic compression, however, does not yield any net momentum, since the gas will leave the configuration at both ends. The application of the field has merely decreased the modes of freedom transverse to the magnetic field by favoring the longitudinal mode. It is conceptually simple to unbalance such a geometry in order to obtain a net momentum in one direction. This is achievable

by increasing the magnetic field at one end of the coil which introduces a field gradient within the geometry and along the axis of the configuration. In a single turn coil, this can be done by shaping the conductor itself (Figure 3) to fit a linear

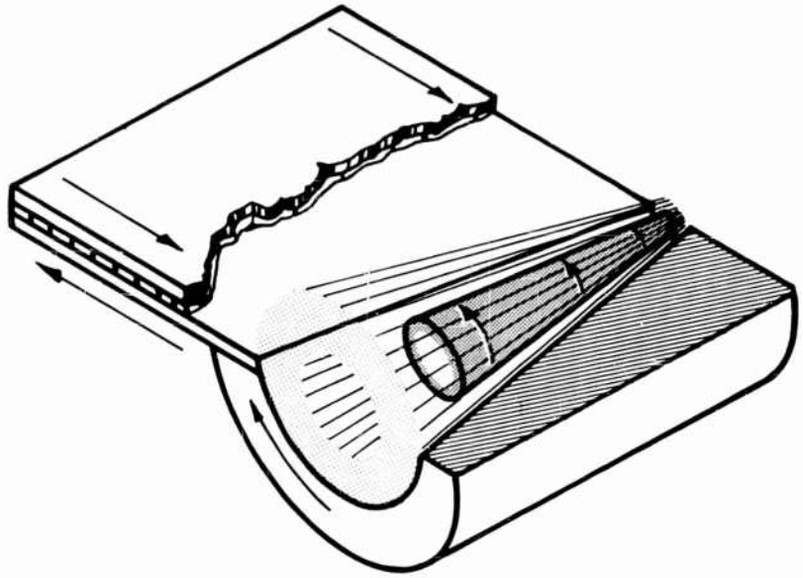

Fig. 3 Asymmetrical Collapse Configuration

(cone) or curved contour line (trumpet) according to the gradient which one intends to achieve. The resulting action can be understood by simply splitting the magnetic field vector into a transverse H_r and into a longitudinal component H_z. The H_z-component will drive the plasma radially inward, just like in the case of the linear collapse geometry (symmetric) and, hence, cause plasma heating (increased conductivity) and simultaneous containment (no wall contaminations). The H_r-component, on the other side, will act so as to impart to the configuration a net momentum in the z-direction.

The requirements for efficient propulsion in such induced current geometries are indicative for the high temperatures needed:

1. The magnetic skin depth in the plasma (fully ionized gas) (Reference 15)

$$\delta = \eta/2\pi\omega^{1/2}$$

should be small in comparison to the radius of the geometry. η is the plasma resistivity in e.m.u. and ω the angular frequency of the field applied. For system sizes of interest (one to ten cm) and for capacitor resonant frequencies available (100 kc to one Mc), a temperature of 10^6 ^{o}K is necessary for a skin depth of roughly one mm.

2. The containment fields must be appropriate to balance and overcome the

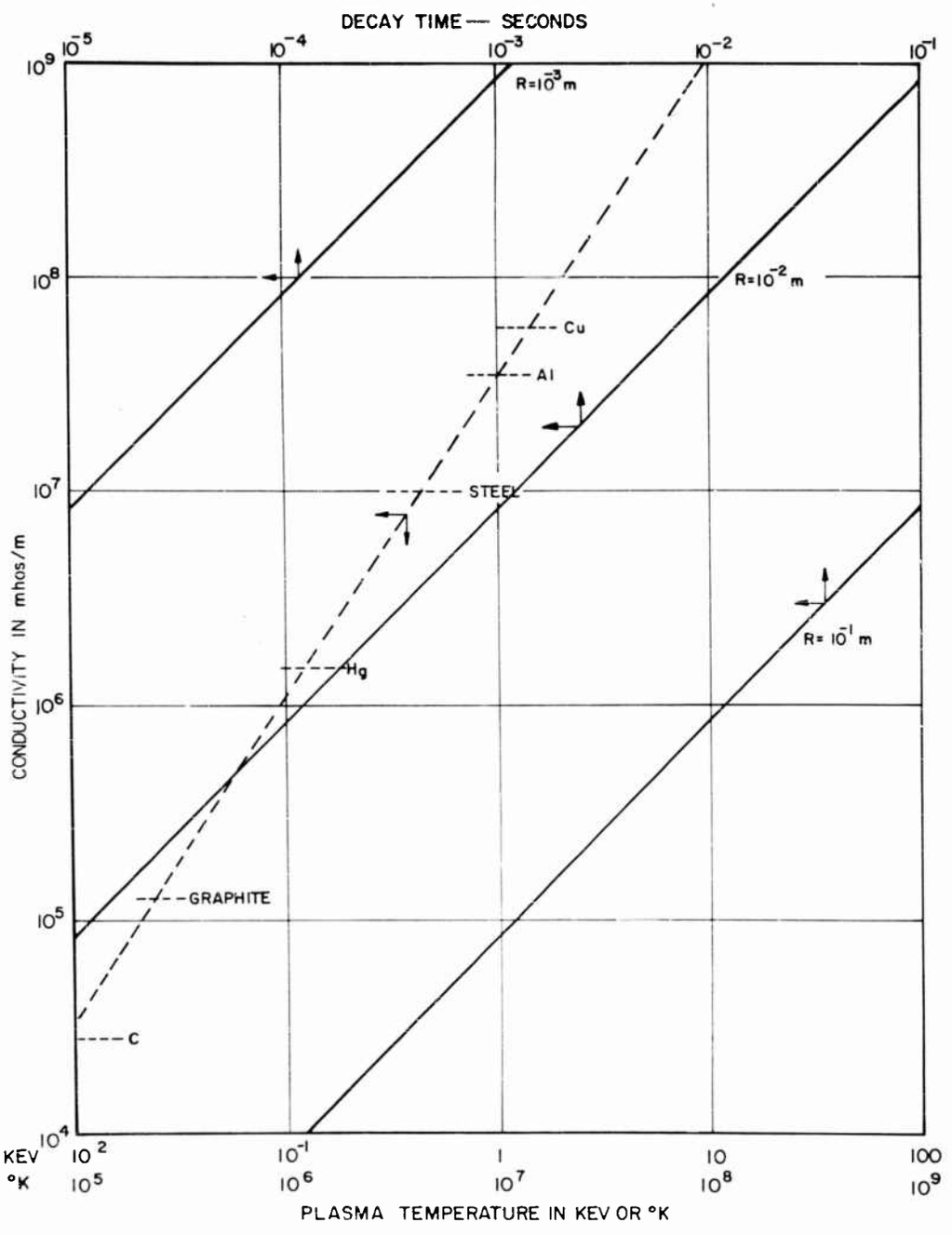
DECAY TIME — SECONDS
10^{-5}
10^{-4}
10^{-3}
10^{-2}
10^{-1}
10^{9}
10^{8}
10^{7}
10^{6}
10^{5}
10^{4}
$R=10^{-3}$m
$R=10^{-2}$m
$R=10^{-1}$m
Cu
Al
STEEL
Hg
GRAPHITE
C
CONDUCTIVITY IN mhos/m
KEV
°K
10^{2}
10^{5}
10^{-1}
10^{6}
1
10^{7}
10
10^{8}
100
10^{9}
PLASMA TEMPERATURE IN KEV OR °K

Fig. 4

kinetic pressures of the plasma in the configuration, according to

$$H^2/8\pi = 2NkT$$

At 10^6 °K for a particle density of several times $10^{17}/cm^3$, the pressure amounts to 10^2 atmospheres requiring a minimum magnetic field of 50,000 oersteds.

3. The acceleration time should be commensurate with field-plasma interpenetration times. The decay time of the field into the plasma,

$$\tau = \frac{4\pi L^2}{\eta}$$

indicates that at 10^6 °K for L = 1 cm geometry some 100 microseconds are available, which is ample time. On the other side, at 10^5 °K the time would be only a few times 10^{-6} seconds, which is clearly too short.

The above-mentioned asymmetric collapse geometries have been operated in strong field geometries (References 16 and 17). Typical figures for the magnetic gradient of 40 kilooersteds per inch have been used. The accelerators were operated at apex fields of 150 kilooersteds with exit fields of 12 kilooersteds giving energy density ratios of more than 150.

These geometries have produced thrusts of some 10^0 dyne (=10^4 newtons) per pulse with plasma velocities between a few times 10^6 cm/sec ($I_{sp} = 10^3$ sec) and to a maximum of 10^8 cm/sec ($I_{sp} = 10^5$ sec). Experiments were conducted in a variety of gases and high temperature diagnostic techniques were applied to understand the time-dependent behavior of the accelerated geometry. Figure 5 shows a Kerr cell picture of a plasma configuration "frozen in flight" with an

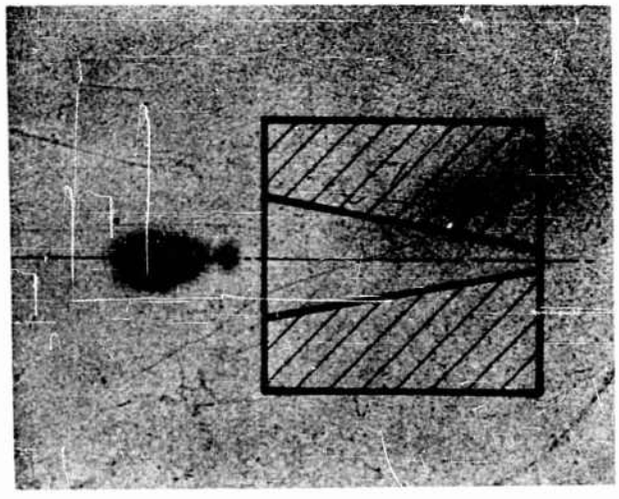

Fig. 5

effective time exposure of 30 millimicroseconds. A scaled magnet is superposed for reference. The combined measurement of velocity and momentum yields, at present, efficiency figures ranging from 0.5 per cent to a maximum of three per cent. The conversion efficiency from the electrostatically stored energy into mag-

netic energy of the "useful" field portion amounted to about 15 per cent. Of this energy 20 per cent at best was converted into kinetic energy of the plasma configuration. The rather low temperatures obtained so far are partly responsible for this low figure of transfer eificiency. Nevertheless, one should be cautious about expecting or accepting figures which are very much higher than these. Presently, the plasma heating phase is being separated from the acceleration stage in order to improve somewhat the magneto-kinetic transfer efficiency.

Unfortunately, both classes of devices rely for operation on techniques of energy storage and transfer (switching) which are very much in their infancies. In effect, the present specific weight of electrostatic energy storage of 25 joules/lb at a volume density of one joule/cu in. is scarcely attractive for space applications, and some intensive effort should be applied to improve this situation.

Eventually, however, and in spite of the several difficulties, the method of transient magnetic plasma acceleration should find a useful place in our propulsive schemes for space travel. A number of magnetic thrustors have been shown to cover the same velocity range as ionic drives but at much higher thrust levels, provided certain duty cycles of some 10 pps can be maintained continuously over prolonged periods (an assumption which has not been demonstrated to be valid as yet). Nevertheless, plasma and ionic drives can even be compatible.

Nobody would ever attempt to drive uphill in the third gear, unless he is a poor driver, and such an attempt would cost him plenty of time. It is precisely in the concept of gear shifting in space that we might find an efficient way to reach destination rapidly. Even a superficial look at plasma and ionic power systems would indicate that these would not have to be individual units but that they could be made to be interdependent.

In this world of ours where events can happen so fast, it might be reassuring to possess hybrid vehicles which can bring a crew to a certain point in a minimum time by judiciously shifting thrust and acceleration capabilities to fit in an optimized fashion the requirements of the gravitational potential rather than worrying only about minimizing fuel consumption.

REFERENCES

1. Bostick, W.H., Phys. Rev. 104, p. 292, 1956.

2. Artsimovich, L., Chuvatin, S., Lakijavov, S. and Podgorny, I., Jet Propulsion 33, p. 3, 1957.

3. Korneff, T., Nadig, F., and Bohn, J., "Conference on Extremely High Temperatures," edited by Fischer, H. and Mansur, L., J. Wiley, 1958.

4. Kash, A.W., Gauger, J., Starr, W. and Vali, V., "The Plasma in a Magnetic Field," Second Lockheed Symposium, edited by Landshoff, R., Stanford University Press, 1958.

5. Josephson, V., Journ. Appl. Physics 29, p. 30, 1958.

6. Janes, G.S. and Patrick, R. M., "Conference on Extremely High Temperatures," edited by Fischer, H. and Mansur, L., J. Wiley, 1958.

7. Kunen, A., OSR Plasma Meeting, Los Angeles, July 1959.

8. Khvartsava, J.F., Meladze, R.D., and Suladze, K.V., in print, private communication.

9. Fowler, R.G., Goldstein, J.S., and Clotfelder, B.E., Phys. Rev. 82, p. 879, 1951.

10. Kolb, A.C., Phys. Rev. 107, p. 345, 1957.

11. Thoneman, P.C., Cowlong, W.T., and Davenport, P.A., Nature 169, p. 34, 1952.

12. Marshall, J., Second U.N. Conference on Peaceful Uses of Atomic Energy, Paper 355, 1958.

13. Kvartskhava, I.F., Kervalidze, K.N. and Gvaladze, Y.S., in print, private communication.

14. Waniek, R.W., Proceedings Tenth Astronautical Congress of the I.A.F., London, 1959.

15. Spitzer, L., "Physics of Fully Ionized Gases," Interscience, 1956.

16. Furth, H.P. and Waniek, R.W., Rev. Scient. Instr. 27, p. 195, 1956.

17. Furth, H.P., Levine, M.A. and Waniek, R.W., Rev. Scient. Instr. 28, p. 949, 1957.

DISCUSSION

MR. S. P. ZIMMERMAN, Air Force Cambridge Research Center: Where did you get the calculation for slide No. 2? I remember the type of discharges we got in toroids, with skin depths of the order of one millimeter at 10,000 amperes, and only 100 kc. You show this as way off.

DR. RALPH W. WANIEK: This is quite straightforward. The skin depth shown is valid for a fully ionized hydrogen plasma with electron densities ranging between 10^{12} and 10^{15} electrons/cm^3. The basic formula applies to a Lorentz gas with the appropriate correction for electron-electron encounters. I believe the values shown are correct. On this scale, skin depths in metals would correspond to the ones obtainable in a 10^{7o} K plasma.

DR. G. SARGENT JANES, Avco-Everett Research Laboratory: I am tempted to accuse you of being a little pessimistic in quoting your efficiency figures. As I interpret your statements, the primary inefficiency to which you are referring arises because of energy stored in the magnetic field which pushes on the plasma. I agree that this is an important consideration, and that use of this as a basis for arriving at a net efficiency will in many cases lead you to come out with a very low figure. My objection is that you have left out the very fruitful possibility of inductively recovering this energy back into the capacitors. If this can be accomplished (and I believe it can), these efficiency figures will look much better.

DR. RALPH W. WANIEK: I agree that it would be expedient to try to recover the energy in all those devices where only the first pulse accelerates the gas. It would be also a difficult proposition because of the relatively long deionization times in the switching gaps.

However, in the specific case of the asymmetric geometries shown, every pulse (including the ones of reversed polarity) is used for the acceleration of the gas. Up to the third or fourth pulse there is still appreciable gas ejection; hence it is only the Q of the circuit which counts. I remain still rather skeptical about expecting large figures for the efficiency of magnetic thrustors.

HIGH SPEED SHOCK WAVES IN A MAGNETIC ANNULAR SHOCK TUBE

by

RICHARD M. PATRICK

AVCO-EVERETT RESEARCH LABORATORY
A DIVISION OF AVCO CORPORATION

ABSTRACT

A magnetic annular shock tube has been used to produce magnetically driven shock waves with very high velocities. Experiments were carried out with this device with two magnetic field configurations ahead of the shock front. The first configuration had a magnetic field ahead of the shock front in the direction of motion of the shock. In the second configuration the magnetic field ahead of the shock had its principal component in the plane of the shock front and a small component in the direction of motion of the shock. The continuum radiation emitted by the shock-heated plasma was measured with photomultipliers. The use of probes to measure the change in the local magnetic field in the shock front was investigated. With the second configuration shock velocities in excess of 4×10^7 cm/sec were measured in hydrogen. For these high speed shock waves, a shock thickness was obtained from measured rise times of the emitted visible radiation. These shock thicknesses are thinner than the mean free path in the shock-heated plasma, an observation which agrees with a theoretical prediction.

INTRODUCTION

This paper reports both the development of a magnetic annular shock tube (MAST) in which a magnetic field is used to produce the driving force for high speed shock waves with velocities over 4×10^7 cm/sec and a preliminary experimental investigation of the structure of these very high speed shock waves.

The use of shock tubes to produce a gas sample at temperatures of the order of 10^{4o} K in order to study the transport properties of the gas, and relaxation phenomena has been established.[1, 2, 3] One of the principle advantages of the shock tube over other methods of producing gas temperatures in this range is that the gas state can be accurately determined from a simple measurement of the shock velocity. If the shock wave propagates at a constant velocity in a uniform channel, there is a region of plasma behind the shock whose properties are uniform and can be determined by applying the conservation laws for mass, momentum, and energy across the shock. MAST, which is described in this paper, is a device for producing a high temperature plasma for study which retains the advantage of the lower temperature shock tube that the plasma properties can be determined from the shock velocities, and are reasonably uniform.

The objective of the experiments carried out with MAST is to use a high speed shock wave to furnish a fully ionized plasma where the thermal energy density is of the same order as the magnetic energy density, the mean free path for the ions is large compared to the ion cyclotron radius, and the ion cyclotron radius is small compared to the channel size.

It has been pointed out[4, 5] that the basic interaction between particles in such a plasma arises through the magnetic field rather than through interparticle collisions. The various regions of magnetohydrodynamics have been classified[4] and a chart showing them is reproduced in part in Fig. 1. It is assumed that the gas pressure equals the magnetic pressure and the chart is made for hydrogen. At high densities and temperatures corresponding to one electron volt per particle (S region) the mean free path is less than the cyclotron radius for both ions and electrons. At somewhat higher temperatures the electrons undergo a complete cyclotron orbit between collisions (T region) and the transport properties are functions of the magnetic field. At still higher temperatures the ion cyclotron radius becomes less than a mean free path (M region).

The objective of the experiments given above is to produce a plasma in the M region. It can be seen from Fig. 1 that a laboratory experiment that produces an M region plasma required a magnetic field strength of the order of 10 kilogauss, a particle density of the order of 10^{14} to 10^{15} particles per cm^3, and a temperature of the order of 10^{6o} K. Since a completely ionized gas is required with such high kinetic temperatures, hydrogen was chosen as the working fluid because the simple structure of this atom permits complete ionization at relatively low energies per particle.

A temperature of 10^{6o} K generated by a shock wave implies a very high shock velocity. Therefore, magnetic fields were used to furnish the driving force and containment of the shock-heated plasma. The requirements of magnetic containment and a constant driving force through a uniform channel led to the development of MAST.[6, 7]

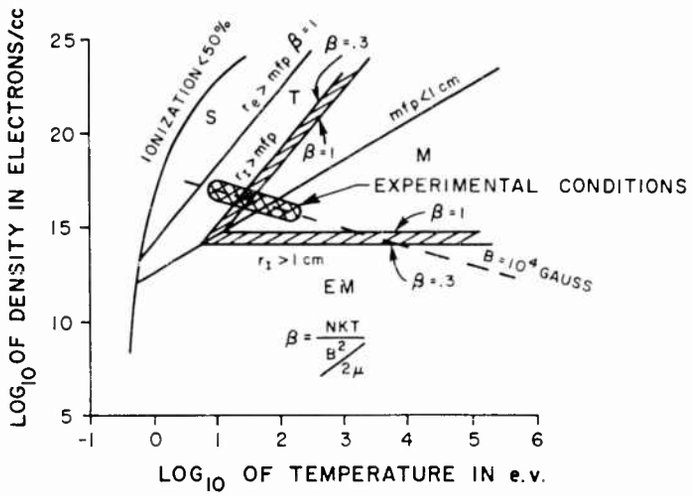

Fig. 1 The magnetohydrodynamic flow regions for fully ionized hydrogen are exhibited, where S, T, M, and EM denote the regions, r_e and r_i the cyclotron radius for electrons and ions, and mfp, the mean free path.

The experimental conditions in the shock-heated plasma are also shown on Fig. 1.

The driving magnetic field was furnished by the currents due to a discharge of a capacitor bank. The time for the currents to reach a maximum value (quarter cycle time of the discharge cycle) was approximately 2×10^{-6} sec. The time duration of the experiment was of the order of 10^{-6} sec, since for this period of time the shock conditions were nearly uniform. At the plasma temperatures shown on Fig. 1 for the experiments the skin depth based on the experimental times of 10^{-6} sec was less than 0.2 cm, which is small compared to the channel width, 2.4 cm.

The study of the structure of the shock wave had two basic motivations. One was a means of studying the basic dissipation mechanism in an M region plasma. It has been pointed out[5] that the basic interaction between particles in an M region plasma arises through the magnetic field rather than through interparticle collisions. On this basis it was anticipated that the behavior of an M region plasma would be fundamentally different from an ordinary collisional gas. As a particular example of this it was pointed out in reference 4 that a compression pulse in an M region plasma would steepen to form a shock wave which was thinner than the mean free path for interparticle collisions. The required dissipation in the shock wave must then be produced by a mechanism other than ordinary collisions. Several attempts to give a theoretical description of such a shock wave have been made;[8] thus far most of these attempts have been unsuccessful and none has been completely convincing. The experimental study of the structure of such a shock wave is therefore of fundamental interest in understanding the interactions of an M region plasma.

The second motivation for studying the structure of this shock wave is that in most of the M region which is accessible at moderate pressures the mean

free path is of the order of 1 cm or larger. If the thickness of the shock wave were of the order of the mean free path then, in many cases, the shock width would be larger than the size of the test gas sample which one would expect in laboratory apparatus of moderate size. In this case the shock tube would not operate as a source of a uniform sample of test gas. Therefore, the question of the shock structure is coupled to some extent to the development of a shock tube which operates in the M region.

EXPERIMENTAL TECHNIQUE

The container for the working gas in the magnetic shock tube experiments is formed by the annulus between two concentric glass cylinders (Fig. 2). The driving force which produces the shock wave is furnished by the azimuthal magnetic field due to radial currents in the annulus. These radial currents are created by discharging a capacitor bank (Fig. 2) connected to the electrodes. When the gas between the electrodes breaks down, the capacitors are discharged through the gas and this provides the radial drive currents.

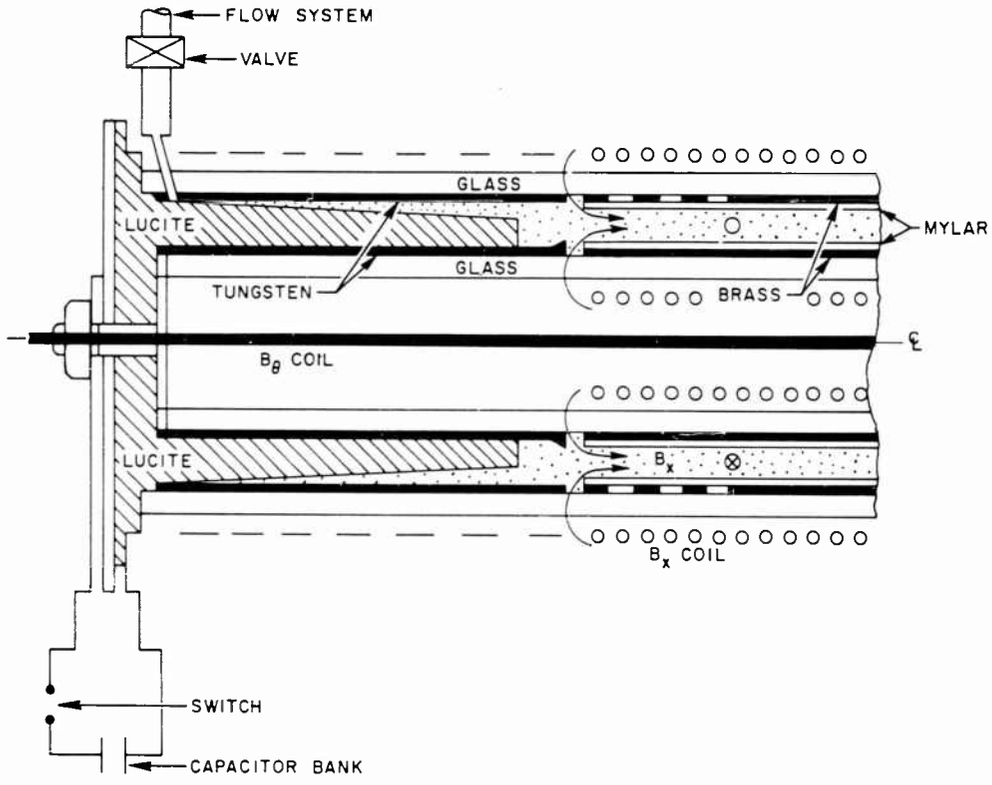

Fig.2 This is a schematic cross section drawing of the experimental apparatus. The solid line on the axis denotes the conductor producing the B_θ bias field, and the two concentric coils shown by rows of circles denote the axial bias field coils.

The working fluid for the experiments described in the paper is hydrogen. The space between the two cylinders was evacuated and during the experiments hydrogen was allowed to pass through an external valve, through an annular passage around an insulating spacer between the electrodes (Fig. 1) and through the annulus to the pumping system. This flow system provided a means of obtaining a small fraction of impurities (approximately 5×10^{-4}).

Two different magnetic field geometries have been used throughout the annulus to provide uniform gas breakdown at the electrodes and containment during the acceleration process. These magnetic fields were furnished by external coils connected to capacitor banks which were discharged at frequencies of the order of several kilocycles. During the acceleration process (times of the order of 2 μsec) these bias fields changed less than two per cent and can be considered as "steady" during the experiment.

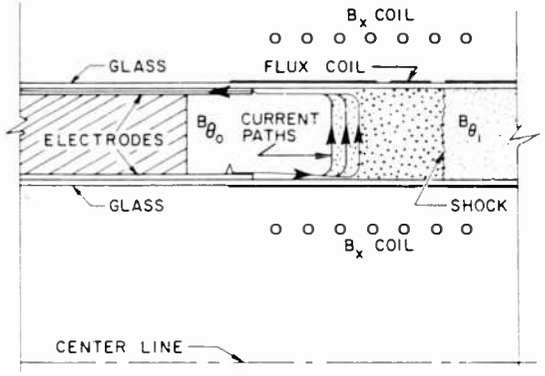

Fig.3 The breakdown region of the magnetic annular shock tube is shown with the drive current paths. The flux coil is indicated by a break in the outside brass shield.

The first bias field geometry that was used was an axial magnetic field, created by currents in a single solenoid placed around the electric shock tube (Fig. 2). In this case, the breakdown at the electrodes was made uniform by preionizing the gas in the vicinity of the electrodes approximately 1 μsec before the main discharge took place. The preionization process was carried out by creating a relatively weak discharge at high frequencies (1 megacycle and 10 amperes) between the two electrodes. The large electric field, E_r, caused charged particles to undergo an azimuthal motion in the $\bar{E}_r \times \bar{B}_x$ direction with a velocity equal to E_r/B_x. For the conditions of the experiments reported here, this velocity was approximately 10^9 cm/sec. The intensity of the axial bias magnetic field was sufficient to make the cyclotron radius of the electrons smaller than their mean free path. This led to a uniform breakdown in the vicinity of the electrodes.

After the initial breakdown the currents in the gas consist of two cylindrical sheets, one near the inside wall and one near the outside wall (Fig. 3), and a radial current sheet connecting these. The force in the axial direction was furnished by the interaction between the radial current in the gas and the azimuthal magnetic field, behind the radial currents.

In addition to the $\bar{j}_r \times \bar{B}_\theta$ accelerating force on the shock-heated plasma there is a $\bar{j}_r \times \bar{B}_x$ (shear) force at the current interface in the azimuthal direction. A theoretical investigation of a shear discontinuity in a perfectly conducting fluid with a magnetic field perpendicular to the direction of the shear motion has been outlined by Friedrichs.[10] This problem was solved in detail by Bazer,[11] and a detailed discussion of magnetohydrodynamic shock waves has been given by Ericson and Bazer.[12] Furthermore, an extension of Bazer's work to an arbitrary orientation of the magnetic field and calculations specifically for the magnetic shock tube problem have been carried out by Kemp and Petschek.[13] In these calculations the gas was assumed to be a perfect conductor throughout and the drive magnetic field was assumed to be constant, and the problem was assumed two dimensional in the x, θ directions.

Some of the results of these calculations are shown on Fig. 4. The top proportion of Fig. 4b is a time distance diagram of the shock phenomena for constant $B\theta_o$. The lower two portions show the qualitative variation of the θ component of the magnetic field and the gas density throughout the region of the shock front and the interface between the shock-heated gas and the drive field. Figure 4a shows the results of the computation of the plasma conditions behind the shock wave as a function

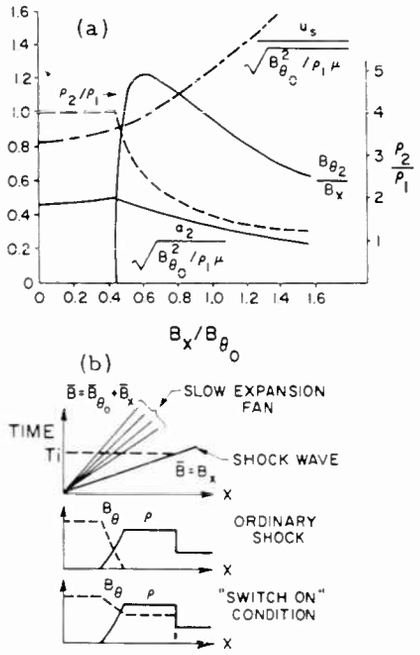

Fig.4 Figure 4a shows the dependence of the shock-heated plasma conditions on B_x/B_{θ_o} for the axial bias field case. Figure 4b shows a time distance diagram of the shock and expansion fan for constant drive field, the variation of the density ρ, and the azimuthal magnetic field B_θ, with x through the shock and expansion fan. Both the ordinary shock and "switch on" shock pictures are shown for the given time T_i.

of the ratio of the axial field ahead of the shock B_x to the drive magnetic field B_{θ_o}. When $B_x/B_{\theta_o} = 0.41$ which corresponds to the Alfven velocity $(B_x^2/\mu_o\rho_2)^{1/2}$ behind the shock equal to the gas velocity with respect to the shock front, the currents in the radial direction are distributed all the way up to the shock front. At this condition B_θ takes on a finite value immediately behind the shock. This type of shock has been called a "switch on" shock by Friedrichs[10] since the magnetic field in the plane of the shock is "switched on" at the shock front. For the still greater values of B_x/B_{θ_o} the density ratio across the shock ρ_2/ρ_1 and the speed of sound in the shock-heated plasma decrease, and B_θ takes on a finite value immediately behind the shock (Fig. 4). The variation of the gas density and B_θ throughout the shock-heated plasma and current interface are shown on the lower portion of Fig. 4b.

During the acceleration process the radial motion of the gas which has passed through the shock front is inhibited by the presence of the axial magnetic field. A radial motion in the presence of the axial field produces an electromotive force in the azimuthal direction which forms current loops around the annulus. These produce a force which interacting with the axial field opposes the radial motion of the gas. Moreover, there are two concentric cylinders of brass surrounding the gas in the annulus (Figs. 1 and 2) which keep the axial field from diffusing out of the annulus during the acceleration process (2 μsec). The gas in contact with the walls is cooled and becomes more dense, and the axial magnetic field associated with this gas is also compressed. This provides an insulating layer of compressed magnetic field surrounding the gas.

Azimuthal Bias Field

The second bias field geometry that was used was an azimuthal magnetic field combined with an axial field (Fig. 2). The azimuthal field (θ component) was produced by discharging a capacitor bank through a conductor through the center of the coaxial system (Fig. 2). The axial component of the bias field was produced by using two coaxial solenoids connected so that the current in the inside solenoid was in the opposite direction to the current in the outer one. The resulting field configuration is shown on Fig. 2. The bias magnetic field had only an azimuthal component in the vicinity of the electrodes. The axial field fringes in downstream from the electrodes with radial components emanating from inside and outside the annulus. The two solenoids were adjusted so that the two radial components of this field canceled in the center of the annulus (Fig. 2).

The preionization for the second bias field geometry was done by producing an azimuthal electric field in the vicinity of the electrodes. This was done by discharging a capacitor which was charged to 60×10^3 volts through a coil embedded in the insulating spacer between electrodes. This electric field was sufficiently high to break down the gas in the presence of a bias magnetic field in the same direction, and the discharge when the main driving currents occurred was uniform.

The containment of the gas during the acceleration process with the combined azimuthal and axial bias fields is essentially the same as for the axial bias field. The axial component of the bias field is compressed due to a radial motion of the gas and forms an insulating layer of magnetic field between the hot gas and the conducting walls.

The effect of B_x and B_θ ahead of the shock on the conditions behind the shock has also been theoretically investigated.[8] The results of the above-mentioned calculation for the case where the initial bias field has both x and θ components in the ratio such that $\tan^{-1}(B_{\theta_1}/B_x) = 75^\circ$, which corresponds very closely to the experimental condition, are given in Fig. 5. The effect of a magnetic field ahead of the shock wave in the plane of the shock front has the same qualitative effect on the shock-heated plasma as the large values of B_x alone (Figs. 4 and 5).

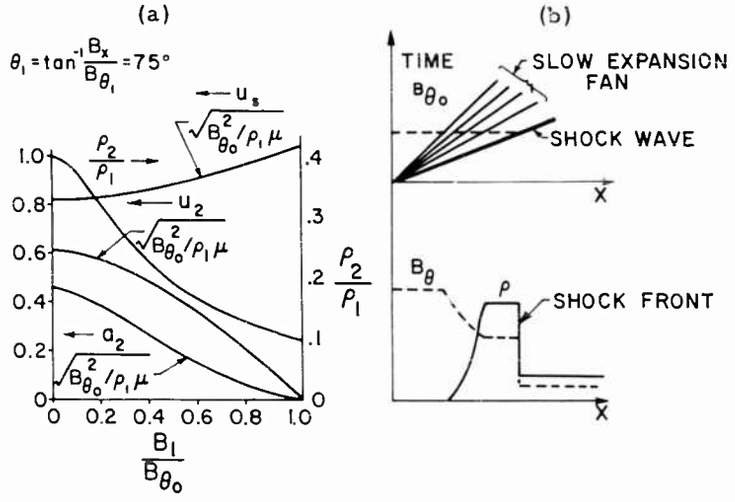

Fig.5 Figure 5a shows the dependence of the shock-heated plasma conditions on B_1/B_{θ_0} for the case where the bias field has both axial and azimuthal components such that $B_x/B_{\theta_1} = \tan 75^\circ$. Figure 5B is a time distance diagram for azimuthal bias field case with a constant drive field and the qualitative variation of the density and azimuthal field with x at a given time.

Diognostics

The shock velocities and the intensity of the visible radiation emitted by the shock-heated gas have been measured with photomultipliers. This was done by focusing a slit in front of a photomultiplier with a suitable lens system at a point on the annular shock tube where there was a hole in the brass and mylar liner (Fig. 2). The shock velocities were measured by measuring the time required for the shock front to traverse the distance between ports of the photomultiplier system. The radiation was measured on opposite sides of the assembly to check the uniformity of the shock front.

The absolute intensity of the visible radiation emitted by the shock-heated plasma was measured with photomultiplier-interference filter combinations which were calibrated to measure the continuum radiation over band widths of approximately 50 Å. The intensity of the continuum radiation emitted by ionized hydrogen is independent of the frequency in the visible region[7] and proportional to $N_e^2/T^{1/2}$,

where N_e is the electron density and T is the temperature. The magnitude of this intensity was calculated using the results obtained by Kirkpatrick,[14] and the results of these computations are shown in Figs. 8 and 12.

The second measurement that was made was an attempt to measure the increase in the axial bias field near the outside wall due to the presence of the shock-heated gas. This was done by placing the outside brass shield around the outside of the coaxial system. This shield was interrupted around the annulus and a coil placed in the open unshielded portion of the outside wall (Fig. 3). An increase in the intensity of the axial component of the bias field induces a voltage in the coil and this was calibrated to measure the absolute time rate of change of the axial magnetic field.

Another method was used to measure the change in the local magnetic field due to the passage of the shock wave. Small coils attached to the end of microdot cable were placed inside quartz tubing. The coils were oriented such that their axes were in line with the component of the magnetic field to be measured. The diameter of the coils was approximately one mm and the characteristic ringing frequency of the coil-cable combination was of the order of 10^8 cycles/sec. The quartz tubing was closed at the end inside the annulus (where the coils were located) and the other end was outside the vacuum system. These coils were calibrated so that the integrated voltage signal from the coil was proportional to the change of magnetic field in the vicinity of the coil.

EXPERIMENTAL RESULTS

Axial Bias Field System

The shock velocities due to the coaxial discharge in hydrogen were measured using the three methods described in the preceding section. Since the currents that furnished the drive magnetic field were obtained by discharging a capacitor bank, the intensity of this field was a function of time during the discharge cycle. The time, τ, between the initial breakdown and the maximum field (quarter cycle) varied from 1.4 to 2.5 microseconds, depending upon the storage capacitance. The measured values of the shock velocity as a function of the initial pressure are given in Fig. 6. These measurements correspond to the

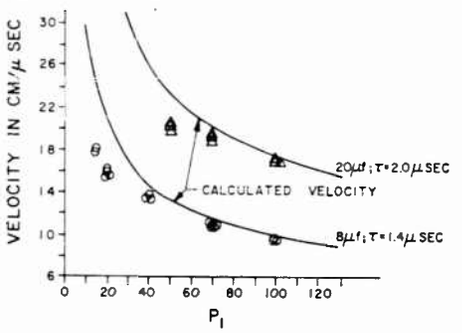

Fig. 6 This is a plot of the maximum shock velocities during the discharge cycle calculated using Eq. (1) and measured with the techniques described in this paper. The data is shown for two different capacitor banks that were used to furnish the driving current; τ is the time required to reach current maximum. The data is plotted as a function of the initial pressure in hydrogen.

maximum velocity the shock attained during the discharge cycle, that is, at drive field maximum. The results are shown for two different storage capacitances; the voltage on the capacitors before the discharge was 15 KV. The calculated velocities for the axial bias field case were obtained using the results given in Fig. 4 for small values of B_x/B_{θ_o}. For small B_x/B_{θ_o} the following relation can be written for the shock velocity.

$$B_\theta^2/2\mu_o = 3/4\,\rho_1 u_s^2 + \rho_1\, du_s/dt \int_o^t u_s dt \qquad (1)$$

where

u_s = shock velocity

B_{θ_o} = drive magnetic field intensity

ρ_1 = initial gas density

μ_o = permeability of free space

t = time from the initial breakdown

The calculated velocities given in Fig. 6 are for $t = \tau$, when the value of B_θ is maximum and $du_s/dt = 0$. By inspecting Eq. (1) it can be seen that the driving force for these experiments is the magnetic pressure $B_\theta^2/2\,\mu$. The pressure behind a strong shock is equal to $3/4\,\rho_1 u_s^2$. The last term in Eq. (1) is the force necessary to accelerate the gas between the shock and the magnetic field, and is negligible at $t = \tau$.

The shock velocities given in Fig. 6 were obtained by measuring the time required for the shock to traverse a measured distance along the shock tube with the photomultipliers. Two sample photomultiplier oscillograms are shown in Fig. 7. The onset of shock radiation is shown on these oscillograms. This was taken as the time of arrival of the shock at the point on the shock tube where the photomultiplier was focused.

The intensity of the continuum radiation was obtained from the photomultiplier voltage as shown in Fig. 7, and the results are given in Fig. 8 as a function of the initial pressure. The conditions for these light intensity measurements were such that $B_x/B_{\theta_o} < 0.41$, so that $\rho_2/\rho_1 = 4$ (Fig. 4). The calculated continuum radiation given in Fig. 8 was obtained using the results presented in Ref. 8.

The continuum radiation from the shock heated plasma for $B_x/B_{\theta_o} > 0.41$ was measured and the intensity of this radiation decreased below the value measured for $B_x/B_{\theta_o} < 0.41$. The quantitative variation of this radiation corresponding to the density ratio dependence on B_x/B_{θ_o} shown on Fig. 4 was not verified. The experimental results for $B_x/B_{\theta_o} > .41$ were not sufficiently consistent to establish the quantitative dependence of ρ_2/ρ_1 on B_x/B_{θ_o}.

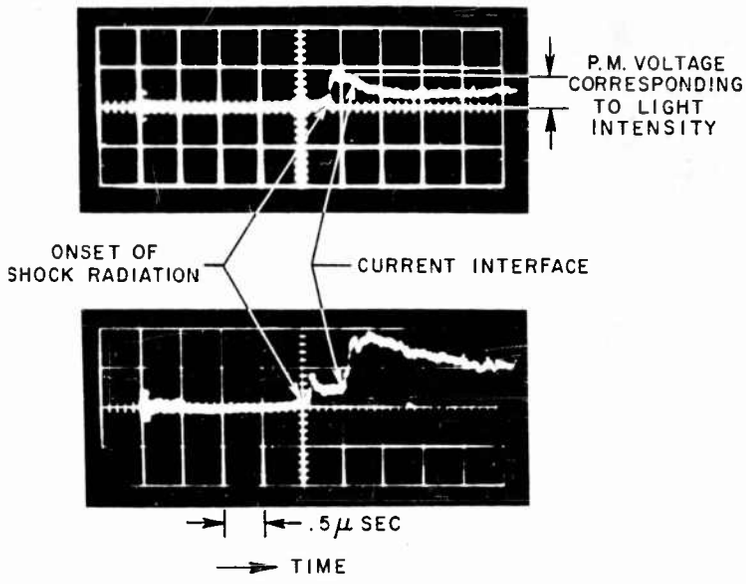

Fig.7 These two oscillograms show the variation of the photomuliplier voltage (ordinate) with time (abscissa). The photomultipliers were monitoring the light intensity at a position 15 cm downstream from the electrodes for the axial bias field experiments. The top oscillogram shows the P. M. voltage where there is a decrease in the visible radiation at the current interface; the lower picture shows an increase in the light emitted by the gas at the current interface which corresponds to a greater drive current density.

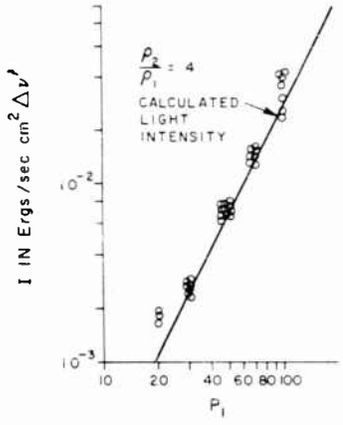

Fig.8 These measured light intensities for the axial bias field experiments were obtained from oscillograms such as those shown on Fig.7. The calculated light intensity curve was obtained using the results from Reference 14 and assuming the density ratio across the shock was equal to four.

The shock velocities for the axial bias field case were also measured using the flux coil (Fig. 3). The voltage on this coil was proportional to the amount of magnetic flux in the x direction that had diffused through the coil due to the passage of the shock. The shock velocities obtained using the flux coil agreed with those obtained from the light intensity measurements shown on Fig. 6. An attempt was made to use this flux coil to measure the increase of the axial bias field, which is proportional to total gas and magnetic pressure behind the shock. This was unsuccessful because the coil was electrically shielded from the gas by the insulation placed between this coil and the shock-heated plasma. The insulating materials which were used, that is, mylar and pyrex glass, became sufficiently good electrical conductors, in the presence of the shock-heated plasma, to shield the flux coil during the time that the shock-heated plasma was in the vicinity of the flux coil (3×10^{-7} sec).

The maximum shock velocities obtained with the axial bias field configuration are shown in Fig. 6. It is interesting to note that the maximum shock velocities obtained (18-20 cm/μ sec) with either capacitor bank furnishing the drive field are approximately equal (Fig. 6). For lower initial gas pressures than 15μ for the 8μ f

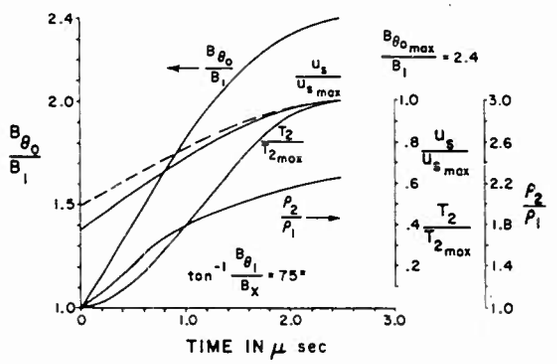

Fig. 9 The ratio $B_{\theta_0} / B_{\theta_1}$ as a function of time after breakdown was obtained by measuring the current from the capacitors during the acceleration cycle. The values of u_s (shock velocity). T_2 (temperature behind the shock), and ρ_2 (density behind shock) were calculated using the measured values of $B_{\theta_0} / B_{\theta_1}$. The subscript max denotes the maximum value the quantity attains during the acceleration; the calculations on this plot can be compared to all the experiments where $B_{\theta_{0\,max}}/B_1 = 2.4$ and $\tan^{-1}B_{\theta_1}/B_x = 75^o$.

bank and 50μ for the 20μ f bank no shock was observed at drive field maximum. The mean free path in the shock-heated plasma at the conditions of maximum shock velocity based on a measured gas density from the continuum intensity, and the coulomb cross section calculated from the temperature based on the shock velocity, is approximately 1cm. A higher shock velocity would correspond to a larger mean free path for ions and a collision shock thickness[15] which is larger than the experimental apparatus. The maximum shock thickness that could be observed is approximately 1 cm due to the apparatus size. This experimental fact is discussed in detail below (Fig. 15). Therefore, the observable shock velocity in the axial bias field experiment is limited by the mean free path in the shock-heated plasma.

Azimuthal Bias Field System

A central conductor was added to the electric shock tube geometry (Fig. 2) to produce a component of B in the azimuthal direction, that is, in the plane of the shock front. This was done in order to achieve higher shock velocities than were obtained with the axial bias field alone, with the hope that a shock wave thinner than a mean free path would be created.[5] With the azimuthal bias field higher shock velocities were obtained with the criterion that the ion cyclotron radius based on the intensity of B_θ in the shock front be small with respect to the annulus spacing (2.4 cm).

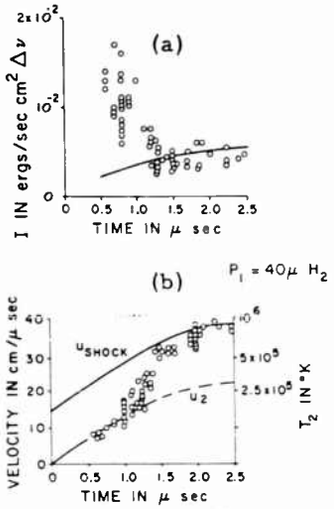

Fig.10 Figure 10a is a plot of the measured and calculated light intensities as a function of time for the azimuthal bias field experiments where the initial pressure on hydrogen was 40 microns. Figure 10b shows the measured shock velocities as a function of time, and the calculated shock velocity u_s and interface velocity u_2. The calculated temperature behind the shock corresponding to the shock velocities is given on the right hand ordinate, the value of $B_{\theta_{max}}$ was 9170 gauss.

The conditions in the shock-heated plasma as a function of time are given on Fig. 9. The variation of the ratio of the magnetic intensity behind the current interface to the intensity ahead of the shock, B_{θ_o}/B_1, was obtained from the characteristics of the capacitor discharge. The variation with time of the gas conditions behind the shock were then obtained from Fig. 5, where these quantities are shown as a function of B_{θ_o}/B_1. The two curves for $u_s/u_{s_{max}}$ are plotted to show the difference between the shock velocity calculated neglecting the acceleration term in Eq. (1) (the dashed curve) and the shock velocity taking the acceleration into account (solid $u_s/u_{s_{max}}$ curve).

The measured light intensity, I, behind the shock for an initial pressure of 40 H_2 is shown on Fig. 10a. The measured value of I at the beginning of the discharge $t < 1\,\mu$ sec was several times the calculated value. The measured shock velocities are presented on Fig. 10b. The measured shock velocities for $t < 1.0\,\mu$ sec are less than the calculated small disturbance speed ahead of the shock, $B_1^2/\rho_1 2\mu^{1/2}$. This

indicates that it was not the shock velocity but the interface velocity that was measured for $t < 1\mu$ sec. This is verified on Fig. 10b where the measured velocity agrees with the calculated velocity of the current interface, u_2. For $t < 1.0\ \mu$ sec the shock could not be distinguished from the interface because the distance between them was relatively small, and the intensity of visible radiation emitted by the gas in the interface was much greater than the radiation by shock-heated gas. For $t > 1.5\ \mu$ sec, the measured and calculated values for the continuum radiation and shock speed agreed within the experimental variation between different experiments (Fig. 10). The measured and calculated shock velocities for $P_1 = 30\ \mu\ H_2$ are given on Fig. 11. The agreement for $t > 1.5\ \mu$ sec is again within the experimental variation.

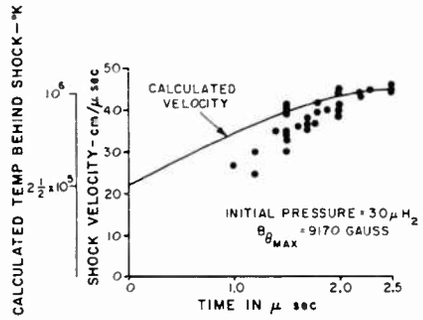

Fig.11 This is a plot of the measured and calculated shock velocity as a function of time measured from the start of the discharge for an initial pressure of 30 microns of hydrogen.

The measured visible continuum radiation for $1.5\ \mu$ sec $< t < 2.5\ \mu$ sec is given as a function of P_1 on Fig. 12. The calculated curves are for two density ratios across the shock, that is, for $\rho_2/\rho_1 = 4$ which is for a strong shock in hydrogen with no magnetic effect and for $\rho_2/\rho_1 = 2.2$ which takes into account the change in magnetic field across the shock. The measured values of light intensity verify that the magnetic field is increased through the shock wave as predicted by the calculation

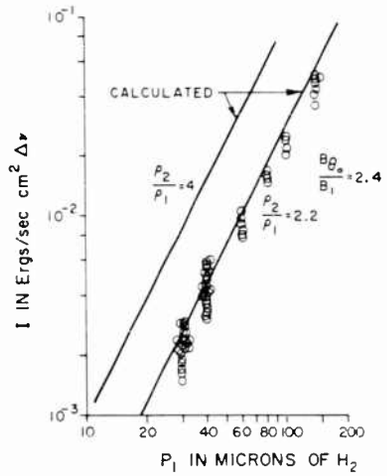

Fig.12 This is a plot of the measured light intensities obtained in the azimuthal bias field experiments as a function of the initial presure. The two calculated curves are for different density ratios across the shock.

of Reference 13, where the gas was assumed to have an infinite electrical conductivity.

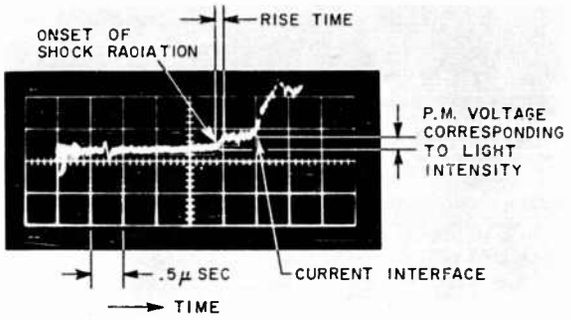

Fig.13 This is an oscillogram showing the P. M. voltage as a function of time for an experiment with the azimuthal bias field with an initial pressure of 30 microns. The photomultiplier was monitoring the light at a station 32 cm downstream from the electrodes.

The shock thickness was obtained by dividing the measured time on a photomultiplier oscillogram for the light intensity to reach a steady value behind the shock by the measured shock velocity. A sample oscillogram for $P_1 = 40\ \mu\ H_2$ is shown on Fig. 13 where the quantities described above are shown. The measured shock thicknesses for the azimuthal bias field geometry and for $2.0\ \mu$ sec $< t < 2.5\ \mu$ sec (Fig. 10) are given on Fig. 14. The mean free path behind the shock was calculated

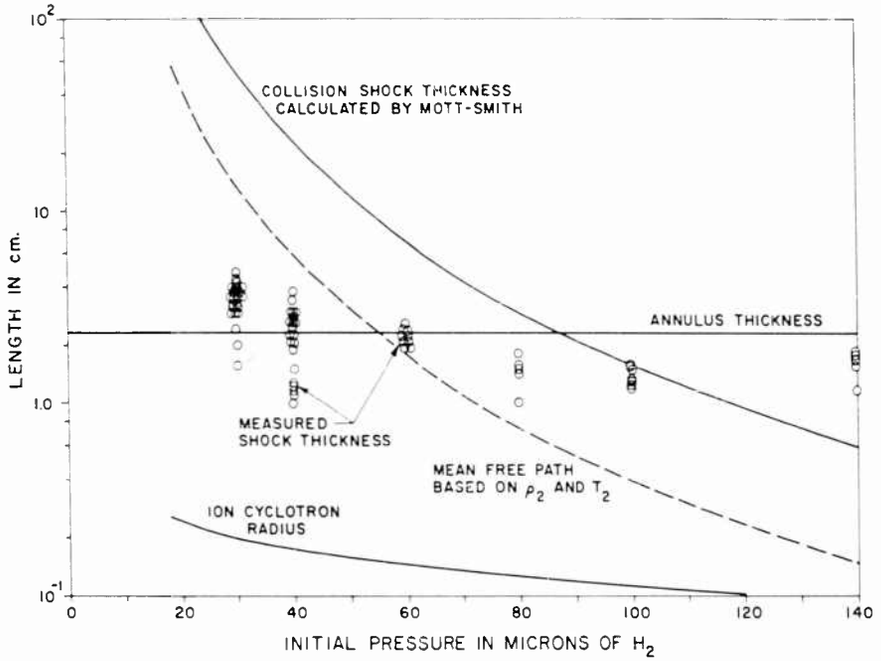

Fig.14 This is a plot of the measured shock thicknesses obtained by dividing the measured rise time (Fig.13) by the measured shock velocity (Figs.10 and 11). The calculated ion cyclotron radius in the shock-heated plasma is also shown along with the mean free path and a shock thickness according to Mott-Smith.

from the measured density behind the shock and the calculated temperature behind the shock based on the measured shock velocity. The ion cyclotron radius behind the shock was calculated assuming the magnetic field was increased through the shock and the energy of the ions corresponded to the temperature behind the shock, T_2. It can be seen on Fig. 14 that the measured shock thickness is much less than the calculated mean free path behind the shock for P_1 equal to 30 and 40 microns of hydrogen.

For all values of P_1 the measured shock thickness is relatively insensitive to the value of P_1. It can be seen by inspecting Fig. 14 that the shock thickness appears to be comparable to the annulus thickness. This is in part due to the radial variation of B_θ across the annulus, since B_θ is proportional to $1/r$. The annulus thickness is 2.0 cm; the mean radius of the annulus is equal to 6.3 cm. Hence, the magnitude of B_θ changes by 30 percent throughout the annulus and the magnetic pressure which is proportional to B_θ^2 changes by 60%. This could account for a non-uniform shock front and lead to the dependence of the annular spacing of the apparent shock thickness measured normal to the axis of the shock tube.

The experimental criterion for obtaining the high velocity shock waves (above 30 cm/μ sec for $P_1 < 80$ microns H_2) was that the ion cyclotron radius in the shock heated plasma be small compared to the annulus thickness. If the value of B_θ ahead of the shock was insufficient to fulfill this criterion no high speed shock was observed;

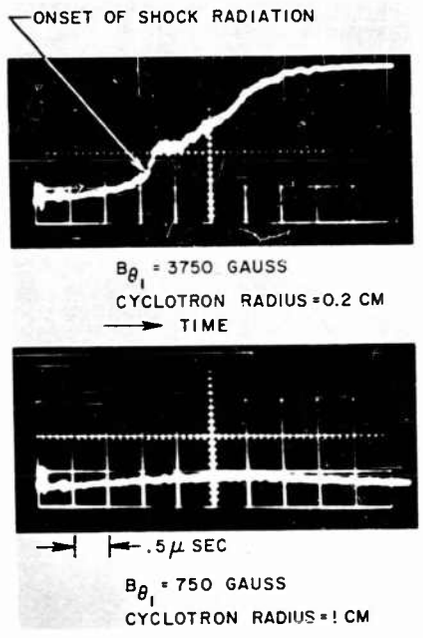

Fig. 15 These two P. M. oscillograms show the effect of decreasing the azimuthal component of the bias field, B_{θ_1}. The top oscillogram shows a typical experiment with the bias field intensity used for the data shown on Fig. 14. The lower oscillogram shows the effect of decreasing the value of B_{θ_1} so the ion cyclotron radius is of the order of the annulus.

in fact, for $P_1 < 60$ microns H_2 and with $B_{\theta_0} = 9170$ gauss no shock wave whatsoever was observed for $t > 1.5\,\mu$sec. This point is illustrated in Fig. 15 where the top oscillogram shows a shock wave with the strength of B_{θ_1} ahead of the shock used to obtain the data shown on Fig. 14. The lower oscillogram shows the photomultiplier voltage as a function of time for B_{θ_1} ahead of the shock equal to 750 gauss which corresponds to a calculated ion cyclotron radius behind the shock equal to 1 cm. It can be seen that with the lower value of B_θ no shock whatsoever was observed.

The variation of the measured shock thickness with B_{θ_1} could not be obtained since the scatter of this thickness at a constant value of B_{θ_1} (the maximum used) was sufficiently large to mask any variation with different values of B_{θ_1} large enough to produce an observable high velocity shock.

CONCLUSIONS

From the results of experiments reported in this paper one may make the following conclusions:

1. It is possible to accelerate and contain shock-heated plasmas with magnetic fields.

2. The use of a magnetic field in the direction of motion of the shock-heated plasma provides a means of containment and produces a current interface configuration between the driving magnetic field and plasma so as to provide a stable acceleration.

3. The production of high velocity shock waves in hydrogen with magnetic fields can be described by a theory which takes into account the effect of the magnetic field on the wave motion of the shock-heated plasma and assumes a perfectly conducting fluid.

4. The presence of a magnetic field in the plane of the shock front provides a means of achieving shock waves whose radiation thickness is smaller than a mean free path in the shock-heated plasma provided that the cyclotron radius of the ions is small compared to the channel width.

REFERENCES

1. Lin, Resler and Kantrowitz, J. Appl. Phys. 26, 95 (1955).

2. Petschek, Rose, Kane, Glick and Kantrowitz, J. Appl. Phys. 26, 83 (1955).

3. Petschek and Byron, Ann. Phys. 1, 270 (1927).

4. Kantrowitz, A. R. and Petschek, H. E., Magnetohydrodynamics, Ed. by Lansdshoff, Stanford University Press, 1957, p. 3.

5. Petschek, H. E., Rev. Mod. Phys., Vol. 30, No. 3, p. 966-974 (1958).

6. Janes, G. S. and Patrick, R. M., Conference on Extremely High Temperatures, Ed. by H. Fischer and L. Mansure, Wiley, (1958), Avco Research Laboratory Research Report 27.

7. Patrick, R. M., Vistas in Astronautics, Ed. by M. Alperin and H. F. Gregory, Vol. 2, p. 119, Avco Research Laboratory Research Report 28.

8. Davis, Lust and Schluter, Z. Naturforch, Vol. 13a, No. 11, 916 (Nov. 1958).

9. NYU Inst. of Math. Sci., Research Report No. NYO-2538 (Jan. 30, 1959).

10. Friedrichs, K. O. and Kranzer, H., NYU Inst. of Math. Sci., Research Report No. NYO-6486 (July 31, 1958).

11. Bazer, J., Astrophys. J, 128, 686 (1958).

12. Ericson, W. B. and Bazer, J., Astrophys. J., 129, 758 (1959).

13. Kemp, N. H. and Petschek, H. E., Avco-Everett Research Laboratory Research Report 60, July 1959.

14. Kirkpatrick and Wiedmann, Phys. Rev. 67, July 1945.

15. Mott-Smith, Phys. Rev. 82, 885-92 (June 15, 1951).

CHARGED DROPLET EXPERIMENTS

by

CHARLES D. HENDRICKS, JR.

RESEARCH LABORATORY
RAMO-WOOLDRIDGE
A DIVISION OF THOMPSON RAMO WOOLDRIDGE, INC.

CHARGED DROPLET EXPERIMENTS

The present interest in high efficiency, low-thrust propulsion units has indicated that some earlier physical research should be re-evaluated. In 1915[1] and again in 1917[2] Zelany reported theoretical and experimental results on the instability of electrified liquid surfaces. These experiments are very interesting from a contemporary viewpoint because they show the technique by which a liquid may be formed into charged droplets which could in turn be accelerated and possibly used as the working medium in a propulsion unit. In recent papers[3] results on charge to mass ratios of drops have been given for various experiments similar to those of Zelany. These results were computed from the currents and the total mass transferred. This paper will describe experimental techniques by which charge-to-mass ratios and drop size of individual droplets were measured.

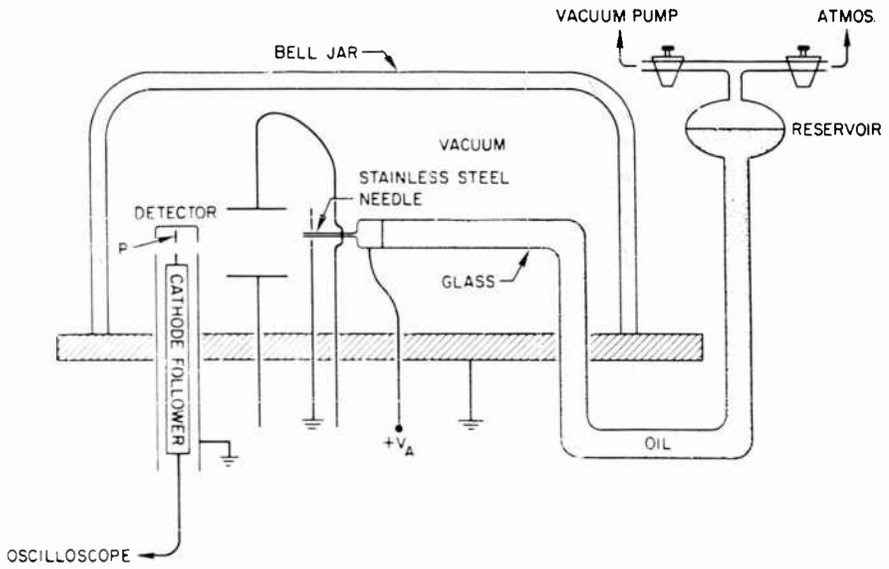

Fig.1 Experimental apparatus

Experimental Arrangement

Octoil at room temperature was used as the working fluid. The pressure in the evacuated chamber was 10^{-5} mm Hg. A high voltage, V_a, was applied to the hollow steel needle connected to an oil reservoir. A spray of charged oil droplets was produced in the space between the needle and the detector. Some of the drops in the spray travel through (or at least into) the detector. In principle the deflection plate potentials may be adjusted to deflect the desired portion of the spray into the detector. However, it has been observed visually that at reasonable potentials, the deflection plates have very little effect. At potentials high enough to be effective, oil which has been collected by the plates was pulled off by the high fields and gave spurious results. As a charged particle enters the detector the potential of the

plate P begins to rise. Since the plate is connected to a high input impedance ($\sim$100 meg) cathode follower circuit, it will rise to maximum potential $V_p = \frac{q}{C_{in}}$ volts where q is the droplet charge and C_{in} is the input capacity of the cathode follower plus the capacity of plate P with respect to the surrounding ground surfaces. The potential rise will take place in a time t determined by the distance d from the entrance hole in the detector to the plate and by the velocity v of the droplet. The output signal of the cathode follower is displayed on the oscilloscope. By making a photographic record of the pulses appearing on the oscilloscope it is possible to obtain, after analysis of the photographs, the size, velocity, mass, and q/m for each droplet entering the detector.

Elementary Detection Theory

From the oscilloscope observation, values of t and V_p may be obtained directly. Since d, C_{in}, and V_A (the total accelerating potential between the needle and the detector) are known, the droplet mass m, radius r, charge-to-mass ratio q/m, and surface field E_s may be computed. The droplet velocity is

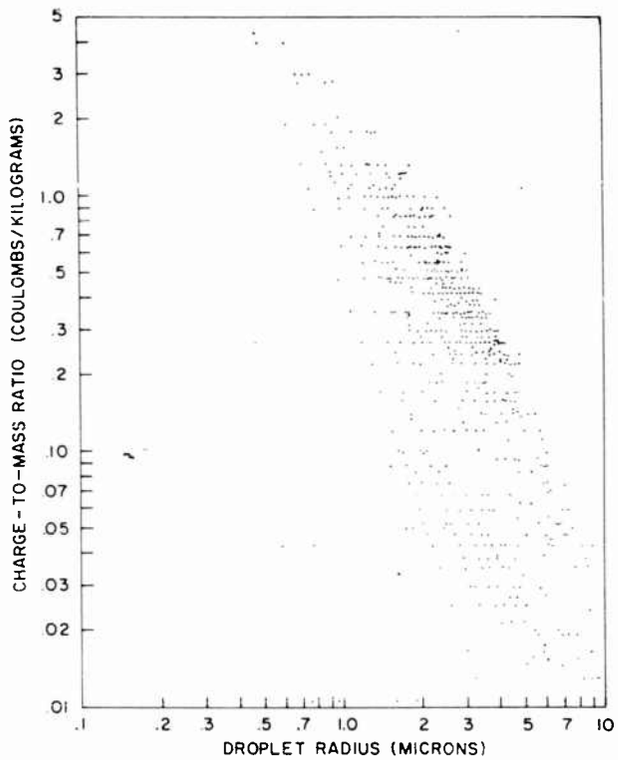

Fig.2 Charge-to-mass ratio as a function of droplet radius

$$v = \frac{d}{t} \quad \text{meters/sec} \tag{1}$$

The charge-to-mass ratio can be computed from simple conservation of energy

$$\frac{q}{m} = \frac{v^2}{2V_A} \quad \text{coulombs/kilogram} \tag{2}$$

where the velocity v is in meters per second and the accelerating potential V_A is in volts. By combining equations (1) and (2), the charge-to-mass ratio is found in terms of the quantities d, t, and V_A.

$$\frac{q}{m} = \frac{d^2}{2t^2 V_A} \quad \text{coulombs/kilogram} \tag{3}$$

The charge q can be found from the cathode follower output V_o, the input capacity C_{in}, and the cathode follower gain G

$$q = \frac{C_{in} V_o}{G} \quad \text{coulombs} \tag{4}$$

The mass of the individual droplets is found from equations (3) and (4)

$$m = \frac{2C_{in} V_o V_A t^2}{Gd^2} \quad \text{kilograms.} \tag{5}$$

Since the liquid density ρ is known the radius of the droplet can be found from equation (5)

$$r = \left(\frac{3C_{in} V_o t^2 V_A}{4\pi \rho G d^2} \right)^{1/3} \quad \text{meters} \tag{6}$$

It is of some interest to examine the potential V and the field E_s at the surface of the droplets. These two quantities are given by

$$V = \frac{q}{4\pi\epsilon_o r} \quad \text{volts} \tag{7}$$

and

$$E_s = \frac{q}{4\pi\epsilon_o r^2} \quad \text{volts/meter} \tag{8}$$

Results

By using the detector and techniques described in Section I preliminary data have been obtained on the significant parameters involved in the electrostatic acceleration of oil droplets. Figure 2 is a plot of observed values of charge-to-mass ratio q/m as a function of droplet radius r. The maximum values of q/m are about 4.5 coulombs/kg., and occur with particles of about 0.5 microns.

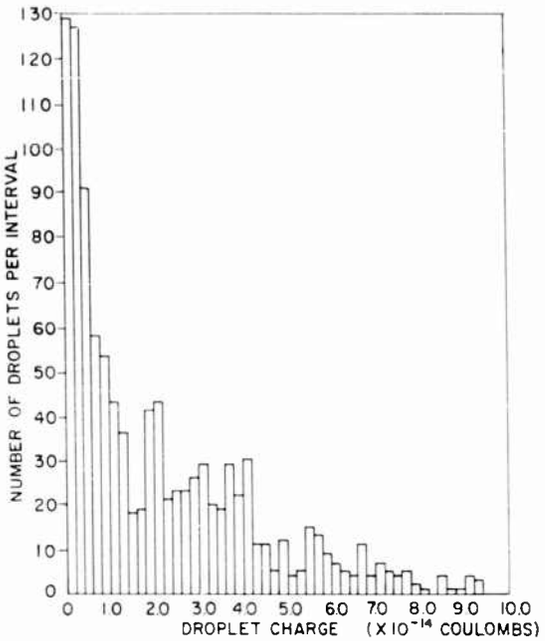

Fig.3 Droplet charge distribution

The plots in Figures 3, 4, 4a, and 5 are histograms of distributions of q, q/m, and r. All of these data were taken with accelerating potential of 13 kilovolts (needle positive). It is significant that the size distribution of the droplets has a maximum but that there is a very large range of droplet radii. The charge-to-mass distribution had a similar maximum and also a very broad spread in values. However, the maximum occured about 0.06 coulombs/kilogram and does not appear as a maximum on the histogram. It is also found that charge-to-mass ratios vary with needle potential. The histograms in Figures 4 and 4a were constructed from data taken at 12 and 13 kilovolts needle potential respectively. The maximum in the charge-to-mass ratio distribution shifts to higher values with an increase in needle potential, also with a decrease in needle diameter.

If the rate of flow of oil to the needle is restricted, the charge-to-mass ratio increases, but a broad distribution still occurs.

Summary

Using small hollow needles raised to a high potential, it has been possible to obtain sprays of charged oil droplets. These droplets had radii in the range of 0.2 to a few microns. Broad distributions were found for radii and charge-to-mass ratio. The spray of oil droplets from the needles spread through rather large solid angles (up to about $\frac{\pi}{2}$ steradians) and experiments are being carried out to investigate the angular distribution of droplet size and charge. The effects of needle size, oil flow rate, and needle potential are also being analyzed. The possibilities of using liquid metals is also being studied. At the present time molten Wood's metal (melting point 65° C) is being tried as the working fluid.

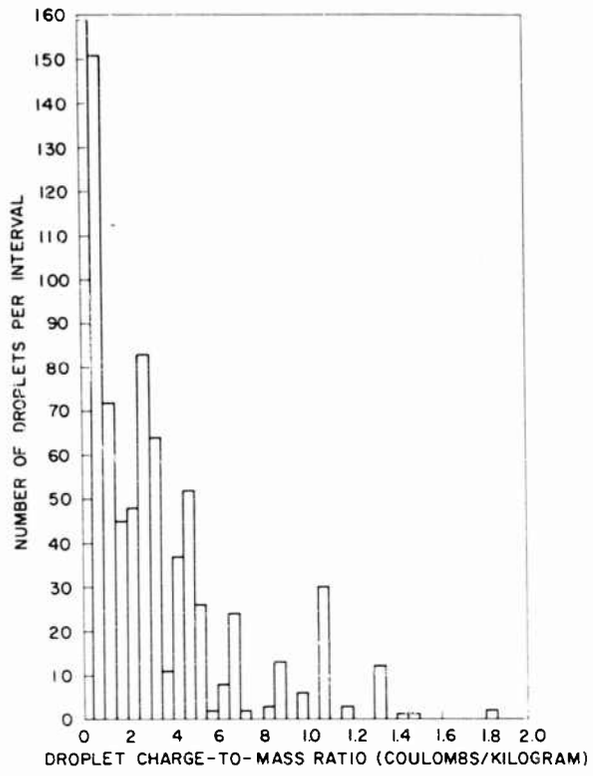

Fig.4 Droplet charge-to-mass distribution with accelerating potential of 12 kilovolts

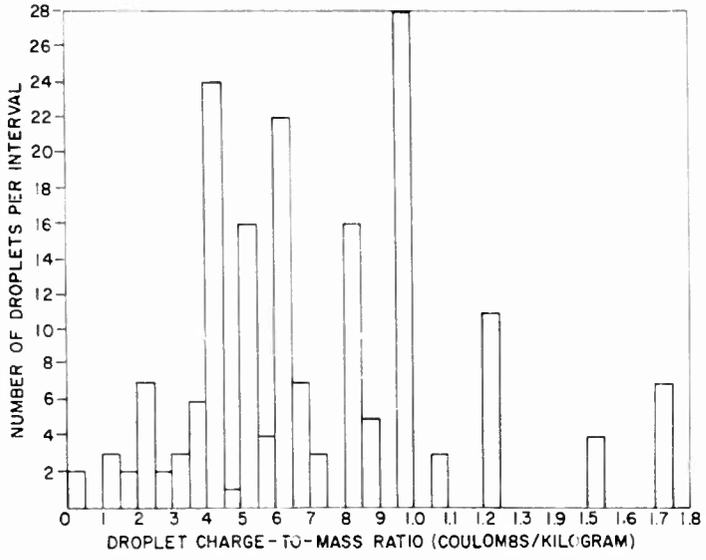

Fig.4a Droplet charge-to-mass distribution with accelerating potential of 13 kilovolts

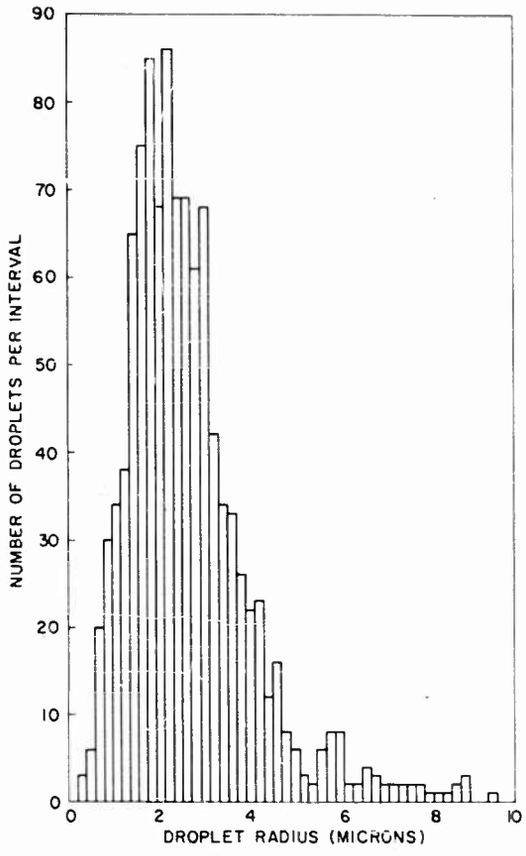

Fig.5 Droplet radius distribution

REFERENCES

1. John Zelany, "On the Conditions of Instability of Electrified Drops, with Applications to the Electrical Discharge from Liquid Points", Proc. Camb. Philos. Soc, 18, p. 71, 1915 (read 9 November, 1914).

2. John Zelany, "Instability of Electrified Liquid Surfaces", Phys. Rev., 10, 1-6, July 1917.

3. R. Schultz, "Colloidal Propulsion", American Rocket Society San Diego Meeting, June 11, 1959.

DISCUSSION

DR. RICHARD M. PATRICK, Avco-Everett Research Laboratory: Can you measure the size of the drop?

DR. C. C. HENDRICKS, Jr.: I should have gone into that a little bit more clearly. From the traces on the oscilloscope we find that until the oil drop goes through the shield around the detector plate, no potential appears at the input of the cathode follower. As soon as the droplet starts through the shield, the potential begins to rise on the plate; as soon as the drop hits the plate or goes through the plate, a break appears in the potential curve. If the drop goes through the plate, the potential immediately starts to drop. Thus, you know when the drop came into the shield and when it went through the flat plate in the middle. By knowing the time on the oscilloscope trace and by measuring the distance, physically, inside the detector, you can certainly calculate the velocity. As I mentioned, you just measure the voltage output from the cathode follower. This gives us an independent measurement on the velocity and the charge; and by knowing the total potential between the accelerating point and the detector, we know all that is necessary to get all the variables concerned. We know the energy the particle has gained; we know the particle radius; we know the velocity, charge, and mass. Of course, this assumes we also know the density of oil used and it makes one further assumption which may be argued with slightly, and that is that the droplet may or may not change charge along its trajectory. If the drop starts out with a high charge and loses it along the way, then we will measure a lower charge for the drop. The measured charge-to-mass ratio will be less and we would very much like to have high charge-to-mass ratio. The charges actually would start away from the point with a higher charge-to-mass ratio than we measure at the detector, if they are losing it along the way. The velocity will still be high, however, since most of the acceleration occurs very near the point.

DR. ROBERT D. SCHULTZ, Aerojet General Corporation: Was there a charge in the mechanism explained yesterday, or didn't you have an electron emitter?

DR. C. D. HENDRICKS, Jr.: There was no electron emitter. We were very careful to completely eliminate the corona. As far as we could possibly tell by all the means that we had at our disposal to detect any corona, it was not there.

DR. ROBERT D. SCHULTZ: The reason I raised the question is that I wonder if this spread in charge-to-mass ratio could be narrowed if you had a uniform source of electrons rather than depending on some other process.

DR. C. D. HENDRICKS, Jr.: I think I expressed that it was not due to corona. I think it is the fact that one particle comes off the point and, by being there, immediately shields the point. The droplets following will then be somewhat larger, since the point field will be less. We found that at low voltages we would get droplets out of the point that sometimes would come in three streams; the streams would rotate and move around a great deal and we would get non-reproducible results. The farther up in voltage we got, the more uniform this brush of droplets became. Now, one thing that I should mention, perhaps, is that we are quite certain there is an angular dependence of the charge-to-mass ratio and that our experiments were done at one angle out in front of the point. Now, we would very much like to examine the angular distribution for a given voltage, given geometrical configuration, and so on. We did find that by moving the point back and forth so that we had some angular shift, we could definitely shift the maximum of charge-to-mass ratio so that at one angle we would get one charge-to-mass ratio distribution and one droplet radius distribution, and at another angle an entirely different distribution of both charge-to-mass and radius. Incidentally, the velocity distribution also changes with angle for a given accelerating potential.

574071 O - 60 - 13

CESIUM ION MOTOR RESEARCH

by

R. C. SPEISER and C. R. DULGEROFF

ROCKETDYNE
A DIVISION OF NORTH AMERICAN AVIATION, INC.

INTRODUCTION

One of several methods of electrical propulsion involves the electrostatic acceleration of ions. Part of the ion motor research program at Rocketdyne has been devoted to experimental studies with cesium surface ionization devices operated as miniature ion motor configurations. Although the experiments reported in this paper were on a small scale they cover many of the phenomena of significance to the development of practical size ion motors.

APPARATUS

The test system (Fig. 1) consists of an 8 inch diameter, 2 foot long vacuum chamber with an ion device mounted on an insulator at one end and an ion beam collector mounted on the other end. Two types of collectors were used in the tests, a calorimetric beam power measuring system and a beam thrust measuring device.

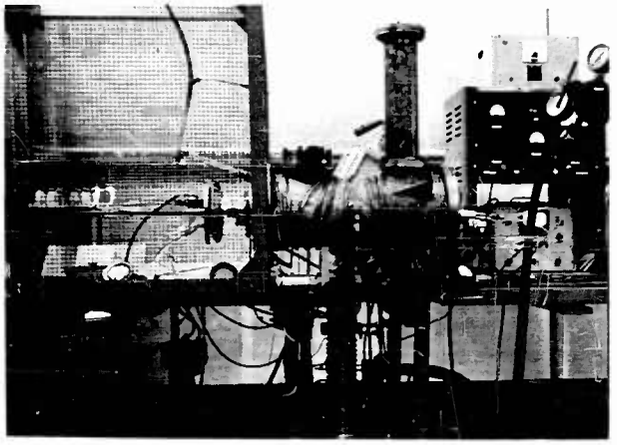

Fig. 1 Photograph of Test System

The calorimetric collector was a long narrow copper cone (to reduce sputtered material) wrapped with copper tubing. Platinum resistance thermometers on the inlet and outlet lines together with a regulator and a flowmeter in the lines provided power measurements accurate to 0.05 watts. A built in heater allowed calibration and test of this device.

The thrust measurement device had a radiatively cooled, deeply grooved graphite collector plate mounted on pendulum type supports. Coupled to this was a displacement transducer calibrated to give an output signal proportional to the thrust. The accuracy was limited by the noise level of this system to about 20 micropounds. Both collectors could be biased and biasable or grounded grids could be mounted directly in front of them to allow suppression or measurement of secondary electrons due to ion bombardment. Direct ion current measurements were made with both collectors.

A particular device is shown schematically in Fig. 2. The ionizer is a porous tungsten disk 3/16 inch in diameter mounted on the end of a molybdenum tube

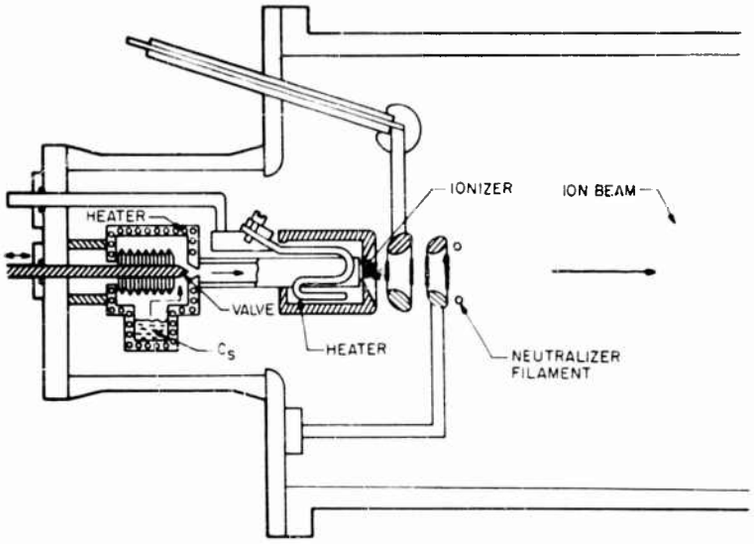

Fig. 2 Schematic of Ion Source

which serves as part of the cesium delivery system. Inside the field shaping electrode which bounds the ionizer is an electrical resistance heating element and appropriate radiation shielding. A needle valve at the reservoir end of the delivery tube allows more rapid control of the propellant flow than that afforded by temperature control of the reservoir.

The electrode system has a much smaller gap to aperture size ratio than a Pierce design and has a cesium ion perveance between 1 and 2 x 10^{-9} amp/volt$^{3/2}$ depending on electrode spacings. The source including the ionizer and its field shaping electrode was operated at a high positive potential. The accelerating electrode was run at a high negative potential and a third electrode was held near ground to provide accelerate-decelerate operation.

To provide for electrical neutralization of the beam, a thermionic electron emitter was placed around the periphery of the ion beam at the exit aperture of the electrode system.

EXPERIMENTAL RESULTS

Typical data taken with the device described above, using a porous ionizer of 70% theoretical tungsten density composed of 4 to 15 micron granules, is presented in Fig. 3. For a fixed potential of - 2.8 kv on the negative or accelerating electrode, the currents intercepted by various parts of the system are plotted against the net accelerating voltage. The current to the collector increased with increasing voltage but the current intercepted by the accelerating electrode passed through a minimum indicating optimum focusing properties near that point. Similar tests indicated that for the electrode geometry used, the magnitude of the potential applied to the negative electrode should be 1/4 to 1/2 the net accelerating potential.

The 1.9 milliamperes at 10 kilovolts corresponds to a current density of 10.6 ma/cm^2 at the ionizer surface. The temperature was about 1500° K. The temperature is higher than theoretical calculations would indicate necessary but the ionizer was never raised to a high enough temperature to completely clean it of adsorbed oxygen. •

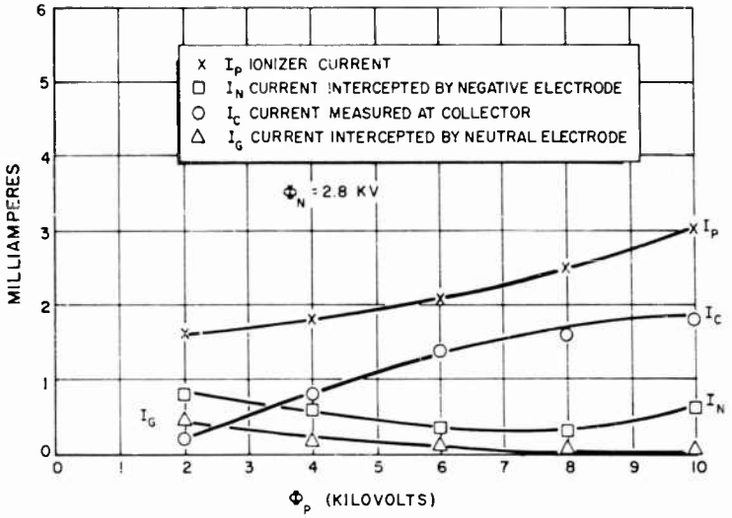

Fig. 3 Various Current-Voltage Characteristics

During operation without the grids in front of the collector, oscillations at frequencies around 100 kilocycles per second with amplitudes corresponding to 100% modulation of the collector current were observed. Some data is presented in Fig. 4. The frequency suggests two possible mechanisms. It is the correct magnitude for ion plasma oscillations corresponding to the average density of ions between the source and the collector. The half period of the oscillations also corresponds to the transit time of the fast ions. The variation of frequency with current suggests a 1/4 power dependence on the density rather than the 1/2 power dependence expected for

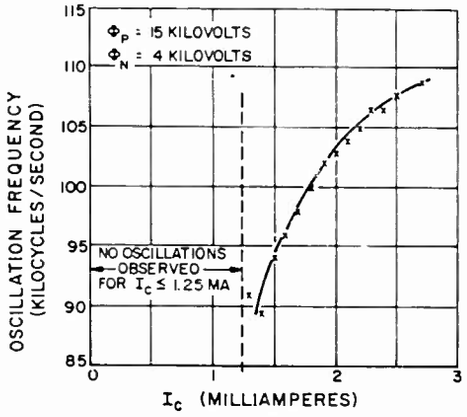

Fig. 4 Oscillation Data

• Shelton, Wuerker, and Sellen, Paper No. 882-59, ARS Meeting, San Diego, California, June 8-11, 1959

pure plasma oscillations. The oscillations could be readily quenched by raising the voltage on the accelerating electrode or by allowing the pressure in the chamber to rise. No oscillations were observed with the collector grids in place.

In an extended duration run with a 60% theoretical tungsten density ionizer, a beam of 1.2 ma at 9 kv net accelerating potential was sustained until the cesium in the reservoir was exhausted. The amount of cesium used was compared with the integrated current to the collector as calculated from the recorded calorimetric power measurement. In this run, 70% of the propellant consumed was delivered to the collector as high energy ions. Estimates based on the current drains of the various electrodes and secondary electron emission coefficients derived from the literature indicated that an appreciable number of ions were intercepted by the electrodes and that over 90% of the propellant was ionized at the ionizer.

Examination of the grids after such runs indicated a sputtering ratio of about 10 nickel atoms per incident 10 kv cesium ion. This value is in close agreement with the literature on sputtering by heavy ions. Measured coefficients of secondary electron emission are also in good agreement with reported values for other ions.

In beam neutralization tests, collector power measurements remained unchanged while the directly measured collector current could be decreased to zero or even made to go negative by increasing the temperature of the thermionic electron source. This is not surprising because although the electrons are drawn into the ion beam by small space charge potentials they have much higher velocities than the ions. Since the dimensions of the laboratory apparatus are small compared to the distance required for the electrons and ions to equilibrate, at equal currents there is still a net positive space charge.

Photographs of the device in operation have disclosed total beam spreading angles from 8° to 12° at the exit aperture of the accelerating system. At normal operating chamber pressures in the 10^{-6} to 10^{-5} mm Hg range the beam is not visible but by allowing the pressure to rise over 2 or 3 x 10^{-5} mm Hg the beam becomes clearly observable and diagnostic photographs can be taken. As expected, beam collimation improved when more electrons were introduced.

Thrust measurements are lower but in good agreement with calculated values being about 85% of the theoretical optimum.

CONCLUSIONS

The experimental results indicate that the cesium surface ionization system can provide adequate current densities for electro-static ion propulsion at moderate temperatures. Beam neutralization with electrons injected at the exit aperture also appears promising although in an operational device in space, electron injection in addition to those drawn into the beam by space charge forces may be required.

Finer structured porous ionizers are required to raise the mass utilization factor, and due to sputtering considerations, nearly perfect electrode geometries must be achieved. It is important to determine whether oscillations would occur under the boundary conditions of operation in space and what effect they would have on performance. However, experimental work to date has indicated that no major technological "break-through" is necessary for the development of a practical cesium surface ionization ion motor.

DISCUSSION

MR. DAVID B. LANGMUIR, Ramo-Wooldridge Division, Thompson Ramo Wooldridge, Inc.: I want to compliment the speaker on his paper and to disagree freely with his last remark.

It seems to me that his last statement and those made yesterday are involved in misconception, in our opinion, based on logic. I would like to present the problem that is absolutely unsolved and extremely difficult and which will constitute a breakthrough when it comes to pass. Now, the logic goes as follows: The crucial parameter here is the aspect ratio: the diameter of the beam as compared to acceleration distance. That, in this experiment, is small--less than one. It is easy to show that a narrow beam with aspect ratio less than one needs no neutralization. It will go out to kilometers into space with no electrons added; the paper makes quite clear that the additional electrons neutralize the current, not the charge. I would like to point out that to get thrust, you must operate many of these beams in parallel. I would like to state that force is equal to a universal constant, times the square of the voltage, times the square of the aspect ratio for all ions. Now, if you want a hundredth of a pount of thrust at about 2000 volts, the aspect ratio comes out fifty, which means that you must parallel 2000 of these beams. You cannot parallel these current neutralized beams, because when they overlap the narrow beams make a broad beam which will turn around and come back within two or three acceleration distances.

Now, until we neutralize a broad beam, we cannot say we have this problem solved. My final comments present reasons why we consider this to be very difficult. The electrons are inevitably going to be moving many times faster than the ions. You cannot have this beam so uniform in potential as to have less than a tenth of a volt potential difference through it. Therefore, the electrons must make many transals of the space before they leak out down the beam. You must have a very effective engine. When you have ions turning around and going back without electrons, you cannot make them go straight through merely by adding electrons. This experiment we have tried. We set up a configuration from which some of the ions returned. We added all the electrons we could pump in; the ions failed to notice them. We didn't have an engine with an effective enough trap. We do not think anybody has devised such a trap, and we do not think it is just a question of finding a suitable configuration. We think it is a very tough problem.

DR. C. R. DULGEROFF: If I understand you correctly, you say that neutralization of the beam becomes complicated as the number of ion sources are increased, and our experimental engine has only one source. I would like to point out that our analytical results do not indicate any greater difficulty other than location of electron emitters for an iteration of sources. Of course, these results will have to be verified experimentally for source iteration.

CHARGE EXCHANGE NEUTRALIZATION OF ION BEAMS

by

A. JOHN GALE

GOODRICH-HIGH VOLTAGE ASTRONAUTICS, INC.
and
HIGH VOLTAGE ENGINEERING CORPORATION

ABSTRACT

Beams from ion propulsion engines must be made electrically neutral at or before the vehicle exit. In principle this may be accomplished by the intimate injection of electrons in the right velocity range, or by capture processes occurring in atomic collisions. The latter method is of importance in accelerators. Some results of such analytical and experimental studies are given, together with the implications for ion propulsion.

ELECTRON NEUTRALIZATION

Ion beams for thrust purposes will generally have current densities on the order of 10 milliamp/cm^2 and energies on the order of 2 kev per ion. It can be shown that the potential depression from surface to axis of such a beam is in excess of 2000 volts and injected electrons will experience resulting accelerations and oscillations. With a diverging beam - the natural result of space charge - a net axial accelerating force exists that causes electron flow towards the ion source. Under some conditions highly collimated electron beams are formed and have been observed by the ionization of residual gas molecules in the vacuum tank. Electrons may even gain energy in a reverse field*. Neutralization by electrons therefore requires an intimate knowledge of the ion beam geometry and density.

CHARGE EXCHANGE NEUTRALIZATION IN THE MODERATE TO HIGH ENERGY RANGE

The passage of energetic atoms and ions through matter is accompanied by charge exchange processes of which the most familiar is ionization. The inverse process of neutralization is the one in which we have most interest - the capture of an electron in an atomic collision.

In the passage of the ion beam through a gas canal the competing processes of electron capture (neutralization) electron loss (ionization) and to some extent successive capture (negative ion formation) take place. To each of these events a probability or cross-section can be ascribed and the appropriate differential equations set up

$$\frac{dn_1}{dt} = -n_1\sigma_{10} + n_o\sigma_{01} \tag{1}$$

$$\frac{dn_0}{dt} = n_1\sigma_{10} - n_0\sigma_{01} - n_0\sigma_{0-1} + n_{-1}\sigma_{-10} \tag{2}$$

$$\frac{dn_{-1}}{dt} = n_0\sigma_{0-1} - n_{-1}\sigma_{-10} \tag{3}$$

t = target thickness atoms per square centimeter

nj = fraction of total beam in charge state j

σjk = cross-section for exchange charge state j to charge state k

From the above equations the solution for n are derived in the general form

$$nj = A_j e^{\left[\frac{a}{2} + \left\{\frac{a^2}{4} - b\right\}^{\frac{1}{2}}\right]t} + B_j e^{-\left[\frac{a}{2} - \left\{\frac{a^2}{4} - b\right\}^{\frac{1}{2}}\right]t} + C_j \tag{4}$$

* "Electron Acceleration against an Opposing Field in a Vacuum Electromagnetic Discharge" J. Slepian Phys of Fluids Vol. 1, No. 6 547-8 (Nov.-Dec. 1958).

$$a = \sigma_{10} + \sigma_{01} + \sigma_{-10} + \sigma_{0-1}$$

$$b = \sigma_{10}\sigma_{-10} + \sigma_{10}\sigma_{0-1} + \sigma_{01}\sigma_{-10}$$

The three sets of three arbitrary constants are determined in accordance with the boundary conditions.

Of particular interest to accelerator design is the percentage of neutral and negative ion beam obtained for certain gases, in particular, hydrogen.

Table I shows the cross-sections for hydrogen, nitrogen and argon at three different energies*, and Table II the fractional intensities for hydrogen ions traversing hydrogen gas. It will be noted that at 5 kev energy about 90% of the exit beam is neutral at exit and the net charge is about 8%.

For heavy element ion engines the negative ion beam is quite unimportant and we can concentrate on the single capture and loss process. The analysis simplifies to the two differential equations

$$\frac{dn_0}{dt} = n_0\sigma_{10} - n_0\sigma_{01} \tag{5}$$

$$\frac{dn_1}{dt} = -n_1\sigma_{10} + n_0\sigma_{01} \tag{6}$$

TABLE I

Cross-Section $\times 10^{-16} cm^2$	Element	Energy KV		
		4	12	40
0-1	H_2	.065	.12	.055
	N_2	.055	.16	.055
	A	.4	.17	.10
10	H_2	3.8	4	1.3
	N_2	5.80	5.50	2.0
	A	16.0	9.0	4.2
01	H_2	.42	.48	.82
	N_2	.85	1.8	2.4
	A	.9	2.6	4.3
-10	H_2	5.0	5.0	3.0
	N_2	9.0	7.5	6.7
	A	8.0	14	16.0

The cross-sections of interest shown above were obtained from Stier and Barnett+.

+ P. M. Stier and C. F. Barnett PR, 103, 896, 1956

* Derived from P. M. Stier & C. F. Barnett Phys. Rev. 103 p. 896 (1956)

TABLE II

Element	Energy kev	Charge State	Fractional Intensity							
			t = 0	.1	.2	.3	.4	.5	.6	∞
H_2	4	Pos. Neut. Neg.								.098 .890 .012
	12	Pos. Neut. C -1	1.0 0	.689 .342	.479 .538	.362 .661	.259 .738	.789	.169 .821	.105 .873 .021
	40	Pos. Neut. C -1	1.0 0	.881 .121	.789 .213	.714 .287	.652 .347	.597 .401	.559 .438	.383 .607 .011

with derived solutions including the boundary conditions

$$n_1 = \phi_1 + \phi_0 e^{-\left[\sigma_{01} + \sigma_{10}\right] t} \tag{7}$$

$$n_0 = \phi \left\{1 - e^{-\left[\sigma_{01} + \sigma_{10}\right] t}\right\} \tag{8}$$

$$\phi_1 = \frac{\sigma_{01}}{\sigma_{01} + \sigma_{10}} \qquad \phi_0 = \frac{\sigma_{10}}{\sigma_{01} + \sigma_{10}} \quad .$$

In order to determine the expected fraction of neutralized beam we need to know the capture and loss cross-sections. Approximate analytical treatments have been given by a number of authors. Bohr* derives an estimation for the capture cross-section given by

$$\sigma_c = 4\pi a_o^2 z^5 Z^{1/3} \left[\frac{v_o}{v}\right]^6$$

and for the loss cross-section

$$\sigma_l = \pi a_o^2 Z^{2/3} z^{-1} \left[\frac{v_o}{v}\right]$$

The ratio $\frac{\sigma_c}{\sigma_l} = 4z^6 Z^{1/3} \left[\frac{v_o}{v}\right]^5$ can only be used as a

* N. Bohr Kgl. Danske Videnskab Selskab Mat-fysk Medd. 18,8 (1958)

qualitative guide since the underlying analysis was developed with emphasis on relatively energetic particles ($H^+ > 25$ kev) and for low Z elements. It is interesting to note, however, the high dependence of this ratio on the atomic number of the incident particle, low dependence on the target nuclei and, in the valid range, a rapid decrease with increasing incident velocity. One would therefore expect heavy ion engine beams to show much higher than 90% neutralization by the charge exchange process.

CHARGE EXCHANGE FOR MODERATE AND LOW ENERGY BEAMS

The statistical arguments given by Bohr are valid only when the incident particle velocity is much higher than $2 Zv_o$ (v_o = Bohr velocity). As the incident beam energy is decreased the velocity approaches, or may even be less than the Bohr velocity. The analytical approach can no longer give an estimate of the cross-section. The best that can yet be done is an estimate of the energy at which the cross-section maximizes.

This maximum is estimated to occur when the adiabatic parameter

$$\frac{a\Delta E}{hV} = 1 \tag{9}$$

where a = atomic diameter

ΔE = internal energy exchange

h = Planck's constant

V = relative velocity

Equation (9) may be rearranged and $v = \left[\frac{2eV}{M}\right]^{\frac{1}{2}}$ substituted to give for the energy (eV_{max}) of maximum exchange cross-section the relationship

$$a = \frac{0.57 \times 10^{-8}}{\Delta E} \left[\frac{V_{max}}{M}\right]^{\frac{1}{2}} \tag{10}$$

Hasted* and co-workers determined $a = 7.2 \times 10^{-8}$ cms from many ion/gas combinations and F. J. de Heer* et al have added information concerning nitrogen and rare gas ions in hydrogen.

An important implication from the foregoing concept is that ions incident on their own monatomic gas

$$R^+ + R \rightarrow R + R^+$$

have $\Delta E = 0$ and the capture cross-section maximum essentially at zero energy. This condition exists, for example, for mercury ions into mercury vapor and the capture cross-section will be high in the energy range of interest to ion propulsion.

The maximum ionization cross-section on the other hand for

$$Hg + Hg \rightarrow Hg^+ + Hg + e^-$$

* Hasted J. B. Proc Roy Soc. A227 p. 476 (1955)
* F. J. deHeer W. Huizenza & J. Kistemaker Physica 23 p. 181 (1957)

theoretically occurs at about 300 kilovolts and the ionization cross-section is low in the ion propulsion range.

The extent to which the exchange

$$Hg + Hg^{+} \rightarrow Hg^{+} + Hg$$ proceeds

for which $\Delta E = 0$ and the low energy cross-section is high is dependent on the relative populations of slow ions and atoms in the target gas and therefore on the incident ion beam density.

The target thickness required for equilibrium in the exit beam is on the order of 10^{16} atoms/cm^2. Expected beam densities for ion engines are on the order of 10 ma/cm^2 or 6×10^{16} ions/cm^2.sec. The drift time of the slow ion formed in the charge exchange process, particularly in the presence of the incident beam space charge, will probably be much less than 1 millisecond so that the population ratio of neutral atoms to slow ions may well be 100:1 or more.

Current experimental work involves the measurement of neutralizing efficiency in mercury ion/mercury vapor systems and the effect of high beam density.

CONCLUSION

Charge exchange beam neutralization has a promising analytical basis and experiments so far performed indicate its probable high efficiency. The heavier elements and energy range useful in ion propulsion are specially suited to this method.

"PROGRESS IN PROPULSION"
PANEL DISCUSSION

PANEL

MODERATOR:	DR. ARTHUR KANTROWITZ, Director, Avco-Everett Research Laboratory
RESEARCH:	BRIGADIER GENERAL BENJAMIN G. HOLZMAN, USAF, Commander, Air Force Office of Scientific Research
SYSTEMS DEVELOPMENT:	BRIGADIER GENERAL HOMER A. BOUSHEY, USAF, Director of Advanced Technology, United States Air Force
OPERATIONAL COMMAND:	COLONEL ROBERT W. CHRISTY, USAF, Commander, 644th Strategic Missile Squadron, Vandenberg Air Force Base
ECONOMICS:	DR. HORACE N. GILBERT, Professor of Business Economics, California Institute of Technology
HISTORY:	DR. THOMAS M. SMITH, Assistant Professor of the History of Science, University of Oklahoma
JOURNALISM:	MR. F. CLARKE NEWLON, Executive Editor, "Missiles and Rockets"

DISCUSSION

DR. ARTHUR KANTROWITZ, Moderator: The members of this panel have had some preliminary discussion and found that one subject moves all of us greatly. We would like to talk to this point--namely, what stands in the way of this country's developing a really adventurous policy in space? What can be done? What is the situation? What are the limitations?

One aspect of the situation was covered most eloquently last night by Professor Thomas Gold. Today we will try to touch on other aspects closer to engineering and military considerations.

I would like to start the discussion by asking General Holzman to tell us something about the attitude that exists in basic research and how it effects our military stature.

BRIGADIER GENERAL BENJAMIN G. HOLZMAN: There seems to be an element of unreality in our attitude toward basic research. All day yesterday I was asked questions which seemed unrealistic to me. To cap it off, on a television program last night, the commentator announced that "General Holzman is going to talk on why we couldn't go to the moon."

Let me say at once that that is not true. I think we can go to the moon whenever someone with the required authority decides that we should and allocates the necessary funds and manpower. It was obvious that the commentator and the audience were thinking about why the Soviets are ahead of us. Well, they obviously are ahead of us in propulsion units, but this does not mean that they are ahead of us in over-all technology, nor that we could not build bigger rockets. It is a lot like building small cars or big cars--it's a question of engineering for a specific objective.

The accusing finger seems to be pointed at the military. Why are we not competing with the Soviets and beating them in every phase of astronautics? Actually, I think we have done a magnificent job. You may recall that it was not until late in 1954 that General Schriever was given the job of developing a missile capability for the defense of the country. He was not told to go into space; he was told to build a military capability to defend the country. I think he has been eminently successful in this. We have built a missile which last month was turned over to SAC and is now actually on the firing line. (You will probably hear more about this from Colonel Christy.)

But, do you remember the climate of the mid-50's, when the theme was "What business is it of the Air Force what's on the other side of the moon or why the grass grows green?"

If we had tried to say, at the time General Schriever was given the missile job to do, that we wanted to go to Mars or find out if the moon had a layer of dust or learn about its magnetic field, we would have been severely reprimanded. Furthermore, I recall that when General Powers was head of the Air Research & Development Command, we received urgent instructions to take out any titles referring to research. We are not supposed to be doing research; we only build articles of war.

While I am recalling the climate of the times, I have another rather interesting point to make. Not many months ago we held a symposium on basic research in the Air Force with an international flavor. At that time, I spoke of some work that was being done in the life sciences field. Among the items I mentioned was a report on work we were doing on octopuses. (By the way, it's octopuses and not octopi. I checked the dictionary on it.) A few days later, I was accosted by several of my superiors in the Pentagon. "Ben, what did you do to us?" they asked me. "Where are the report cards?"

"What's that, sir?"

"The report cards. You've been training octopuses and we'd like to see the report cards."

Actually, the octopus work is a very minor program in the biology area. We had been training the octopuses to accept food at a certain signal, so that then the physiologist, by probing the brains, could learn something about how brain mechanisms of animals worked. You know that the brain is probably the most marvelous computer that has ever been made. We are trying to understand the fundamental principles of the brain and we hope to learn eventually some techniques on how the human brain reacts under terrific stresses, as when a pilot has to make drastic decisions in fantastically short times.

Well, in time I was able to defend the project, but it reflected to me again the anti-basic research climate of the times. I will say, though, that since Sputnik was put into orbit, everyone--the Administration, the Department of Defense, the Air Force, and I am sure the same thing is true of our sister services, the Army and Navy--is wholeheartedly behind basic research. The climate has changed and basic research is important.

At the time when the Soviets must have made their decision to go into missilry, they had captured a number of German enthusiasts who wanted to explore the unknown. Some of our experts say that the Russians had to build a big propulsion unit because the technology of their warhead had not been worked out, whereas we knew what our warhead was. We designed merely to get the warhead to the military target, whereas they may have had to design for a large propulsion system because of their need to transport a less refined warhead. I am not inclined to accept that completely, however, because we know that the Russians have always had an enthusiastic respect for basic research.

At this crucial time I believe the most important thing for us to do is to get on with our basic research support. It is an integral part of our Air Force program. I will end my part of this presentation with something that Dr. Kantrowitz said to me yesterday, "If we fail to explore the unknown, we are incurring a dire danger to our nation."

I believe this very sincerely. I think we must explore the unknown. There is nothing we can do in basic research that won't apply to the Air Force in some unpredictable way. You cannot name a single thing that can be done in fundamental science that won't ultimately apply in the defense of our country.

DR. ARTHUR KANTROWITZ: Thank you very much. I would like to hear now from Colonel Robert W. Christy of the Strategic Air Command, who can tell us something about the effects of newly developed weapons on SAC doctrine, and something about our current situation as distinguished from many of the things of the future we discuss.

COLONEL ROBERT W. CHRISTY: The tremendous reduction in warning time of an airborne Russian missile attack is the most significant effect propulsion progress has had on Strategic Air Command. Intelligence estimates and war games have established that after 1960 to expect more than 15 minutes warning would be assumptious and tactically dangerous. More than three years ago, Strategic Air Command established two major objectives to preclude having its strike force destroyed on the ground. The objectives were to create an alert force of continuously manned and ready aircraft and widespread geographical dispersion of its aircraft resources.

Action to create and train the alert force started in the summer of 1957. The plan was to progressively create and train a force of approximately one-third of SAC's 2700 bombers and tankers to be on a constant 15-minute alert not later than 1960. Excellent progress has been made on this plan to date, and I can state to you it is on schedule. At this moment, there is a sizable force of bombers and tankers scattered around the world on constant alert, briefed and prepared to strike specific Russian targets.

Now, a word about the dispersion of SAC forces. In the past we based two medium bomb wings and their supporting tanker squadrons at each SAC medium bombardment base. This was a force of approximately 150 airplanes (about the same number of aircraft that is owned by American Airlines) which made a concentration of retaliatory atomic force that would certainly have a high priority on the target list of a Russian sneak attack. The SAC dispersion plan called out that each medium bomb base would support one B-47 wing (or 45 aircraft) and its supporting tanker squadron. Each B-52 base would support only one squadron (or 15 B-52 aircraft) and be supported by ten KC-135 tankers. The dispersion plan is on schedule.

For two days we have listened to you gentlemen who are primarily engaged in the field of research and development. With the advent of the missile, we in SAC also became engaged in research and development. In January of 1958, SAC became responsible for the initial operational capability of both the IRBM and ICBM missile programs. This was a unique assignment of responsibility in that never before had an operational command been charged with integrating a new family of major weapons while these weapons were still in the research and development stage. This was a definite break in tradition.

The action to put Strategic Air Command into the program of missile development during the initial operational stage of development was the application of the principle of concurrency. This principle of concurrency of weapons systems development was authored by General Powers's staff in 1955. At that time General Powers was Commander of Air Research and Development Command. It was a technique devised to compress the weapons systems development cycle from the former period of 8 to 12 years down to a period of 3 to 5 years.

An interesting side light is that Strategic Air Command at the moment is participating in the principle of concurrency in the development of the B-58 at Fort Worth. Concurrent with phasing the B-58 into the strike force, Phase II evaluation of the weapons system is being accomplished.

The principle of concurrency is based on the conviction that a safe margin of deterent force could not be maintained unless there was a drastic reduction in the time formerly used to transform a scientist's idea to a practical weapon. It was recognized that there is scant opportunity to reduce the time required in each of the evolutionary events in which you gentlemen participate. Therefore, the principle lays down the concept that individual progressive actions will be overlapped; hence, the principle of concurrency.

DR. ARTHUR KANTROWITZ: Thank you very much, Colonel Christy. I think that the action SAC has taken to insure the situation for the time being gives us a little break, but it need not create any complacency about the future.

One of the things that we often hear is the great effect that a more vigorous space program would have on this country. One often hears a statement that we must control the "hysteria" or in time be bankrupt. This is in sharp distinction to the usual, and the attitude I regard as more reasonable is that money expended on progress is production--not expense. You always get more back than you put in.

We are fortunate in having Professor Horace N. Gilbert of California Institute of Technology with us. I would like to hear his views on this business of driving America bankrupt and also on the economic contributions that are to be expected from space research.

DR. HORACE N. GILBERT: I have been listening to some of the papers presented at this Symposium, and have acquired a general idea of what is going on.

My first observation as the economist member of this panel is that tremendous dividends can be expected from the research, both basic and applied, and from the development of systems that are being described. In other words, the broad technological advances stimulated by the cold war correspond to the advances that attended or followed the hot war of 1939-45. To mention just a few, World War II gave us atomic energy, jet power for our air transports, several electronic breakthroughs, especially radar and computers, and has launched us into an aluminum age. I expect similar developments applicable to our civilian economy to follow from the efforts which those at this symposium represent. This thought may console some of us who feel guilty about the way money is being thrown around. Great sums are being spent, much of it unproductively, but I venture the opinion that the long range payoff may justify these outlays.

My second observation has to do with the ability of our national economy to carry the present defense load. This is a usual question addressed to economists. Let us look at the record. In 1939, pretty much of a business-as-usual year, the defense budget was about 1 1/2% of our gross national product. At the peak of the war, 1944, the ratio had risen to 42%. This was a big effort, an all-out effort, and an awful lot of hardware was thrown at the other side. With peace the ratio fell. The Korean War caused it to rise to 14%. Since then it has fallen to about 10%, and for 1960 it is estimated to be about 8%.

This is the total of our Defense Department budget in relation to the tremendous output of our national economy. We are a very rich country. It must be pointed out, however, that some two-thirds of our output is used to give us a high material standard of living. This is what it is for. The other third goes to capital investment and to the support of all our government activities. Only 8 - 10%, as I have noted, goes to support the total of our present defense outlays. A country as rich as ours can very readily carry this load when the question of national survival is involved. In my opinion it could carry a greater load.

When it comes to the question of how much we can afford to spend on research, I believe that my argument can be made much stronger. I should defer to General Holzman regarding the relative costs of basic research, applied research, and the development of systems. I believe I am correct that research is relatively the lesser part of these costs. In this category I feel some confidence in saying that our economy could afford several times what we are now spending. The problem is, we all very well know, that money may not be the limiting factor. It would be a mistake to assume that larger budgets automatically speed up the attainment of scientific breakthroughs.

I shall stop now, and if Dr. Kantrowitz will give me a chance to speak again, I should like to make some critical accusations. While fulfilling my role as the economist member of this panel, some thoughts have occurred to me that I would like to present.

DR. ARTHUR KANTROWITZ: That was really eloquent. I think that we have been subject to a tremendous amount of slanderous propaganda in this "bankruptcy" business, and it is refreshing to hear a professional economist give us information to put the thing in perspective again.

I would like now to ask our news representative, Mr. F. Clarke Newlon of "Missiles & Rockets" Magazine, to say a few words about how it would help us to have more money in our space program. Just what would it give us? Are we really held back by lack of money, or is it that we just don't know how to do things?

MR. F. CLARKE NEWLON: Part of the job of the staff of the magazine I work for is to cover the Washington scene and to try to get a feeling for the attitudes of the Administration space agencies, sometimes the military, and Congress. We have noted very forcibly in the past few months that there seems to be an almost complete lack of concern in the Administration--even in the space agencies (though I might say I suspect this is compulsory some times)--over our space program. When you get this coming down from the top, it seeps down to the man on the street--you can feel it. Congress seems less concerned about our progress in the race for space and how we do. I don't think this is true of the military, because I think we do very well there. But certainly in our civilian space program we could do a lot more.

I would like to diverge a minute on this to postulate a theory that won't be new to some of us--as we keep going forward in the present state of military standoff, whereby we can clobber the enemy and he can clobber us (and this incidentally, is known sometimes as the concept of clobberation), it is becoming quite apparent to all concerned that there really isn't any point in an all-out war.

It just is not going to be. It's possible the Russians may have realized this now. So, you move from there to another plane of what happens next. You might say this will be an attempt to gain control of man's mind somehow, or what would be an easier, more readily available avenue, the control of space. I have no real idea--maybe General Boushey could tell us--what we would attempt in the way of military weapons if we controlled space. Maybe it would not have to be military; maybe it could be an economic weapon. But, this much I am sure of: If any one country can control space, they will very surely find a way to use it to dominate the world.

Now, to get back to the original point of Dr. Kantrowitz's introduction on how I think we could use more money. A budget for our civilian space agency of $485,000,000, less $28,000,000 which Congress cut off, is pretty ridiculously small when you figure what this means. For instance, in September NASA and the Navy attempted to put up a transit or navigational satellite, and had a routine failure in the booster. This is something that might have happened once out of ten; it was a pretty well proven booster. It now is delayed until next March. There was no back-up program.

We had programmed a moon probe early in October which, had it been successful, would have accomplished approximately the same thing the Russian satellite is doing now. The booster in this case, which also is a fairly well proven weapon, burned up in static test. Right now NASA is frantically trying to borrow a booster and to borrow a launching pad, because they have no back-up program on this. The reason they do not have a back-up program is they do not have the money for it.

I do not think the Russians put out one vehicle when they try a firing. I will bet they put out half a dozen. If the first three fail, they have the fourth. The way we are going we miss and wait seven months or more before we have another one.

DR. ARTHUR KANTROWITZ: I think this is a clear statement of how we could use more money. And I think that provides an appropriate setting, perhaps, for any criticisms you may have, Dr. Gilbert.

DR. HORACE N. GILBERT: My criticisms are not directed specifically to the points Mr. Newlon has just made. There is a point of contact, however, in that to get more money from Congress to support what is being discussed at this Symposium, a better job of selling has to be done. General Holzman has used the expression, I believe, that we must "improve the climate" relating to the support of advances in propulsion. It is in this connection that I make the following accusations:

1. The programs which you are carrying on and which you wish to expand have already resulted in a serious disruption of the market for technically trained people. The organizations which most of you represent have bid up salaries and have hired away scientists and engineers from industries not in these government programs. There is hard feeling on the part of these concerns, and many of them have as good relationships with their Congressmen as you do. You are also doing serious injury to the teaching profession by taking away at various technical levels those who normally would teach in our secondary schools and in our institutions of higher education.

2. Many scientists and engineers in the programs described at this Symposium are seriously under-utilized, with serious impairment of their morale and possibly permanent damage to their employment attitudes. Workloads commonly fluctuate widely, especially because of unavoidable discontinuity in contracts. If there are thousands of people affected in this way, and if their families live in a climate of frustration, unfavorable impressions spread. Congressmen get the idea that the responsible services do not spend their monies wisely.

3. Where the organizational units engaged in the work being described at this Symposium are large and complex, and many of them are, conditions of work develop to which many creative people are allergic. A few administrative methods are being tried that are intended to reduce this difficulty, but the frustration coefficient tends to be high. I have talked with people in the aircraft industry about this problem. Their response is that the design, development and production of today's high performance aircraft are complex jobs requiring the use of complete teams in many technical fields. Undoubtedly this is so, but the result is great expense and record-long times to get jobs done. Thus far our great aircraft companies have won out following this formula. In the new space-age problems we are facing, it may be that we shall not be so successful. In certain vital parts of our programs we must emphasize conditions favorable to creativity, not big budgets.

4. My last criticism is this: Some of our greatest cost-conscious production teams that turned in such phenomenal production records during World War II are being ruined. Some of you come from these companies, although you are probably not members of the production groups. It is important, however, that we should be aware of what is going on. The decline of conventional weapons and devices, before the new systems to replace them are ready for series production, is causing a serious gap. The revolution is so radical, in fact, that there is a fair prospect that conventional production teams no longer will be needed.

Thank you, Dr. Kantrowitz, for giving me the opportunity to set forth these blasts!

DR. ARTHUR KANTROWITZ: I think this is wonderful. As I understand it, you made four points. I would like to answer the first of these and then get other people to comment. The first point was that the defense industry constitutes an unfair competition to the commercial industry of the country for technically trained people. It seems to me that there are two points that make defense industries attractive. The first is that salaries are higher and that the market price for engineering talent is going up rapidly. I feel that this is a healthy development, and I think that the thing that can be said here is: Play to satisfy the beast; that which is honored in a country will be cultivated there. It has been said many times that in this country a man's salary level has a good deal to do with his standing in his community. Now, if we want to cultivate our technical skill, I think that we can do nothing better than to raise the salary levels of engineering and scientific people to the levels that are widespread among, say, physicians or attorneys.

The second thing that attracts people to defense industries is that, in my opinion, they are extremely progressive by comparison with the rest of American industry. This, I think, stems from the fact that the Government--in particular the military services--has been able to take a long view toward technical progress, has been able to exhibit far more foresight than company managements, and has been able to make these defense industries more progressive and thus more attractive for first-class scientific and technical people. I think this, again, is to the good; so I think this competition that has been created by defense industries for technically trained people is one of the healthiest things that has happened to this country.

Now, I believe that it is important to hear other people talk to the other points that were raised by Dr. Gilbert. His next point was the problem of non-utilization of technical personnel.

BRIGADIER GENERAL BENJAMIN G. HOLZMAN: I would only say that I think Dr. Gilbert has a point here. There is an instability in contracting that fluctuates with the military climate and so I cannot help but feel he is right here.

DR. ARTHUR KANTROWITZ: I think we have to concede that such an effect certainly exists, that it is something that everybody, of course, is against, and that it is a difficult problem with which to cope. It has something to do with the fluctuation of the loads.

The next person I would like to call on is Dr. Smith of the University of Oklahoma. Dr. Smith is a historian of science, and I think it is particularly valuable to have his feelings toward the problem that I would like to build a little discussion on--how to stimulate America to a more adventurous policy in research.

DR. THOMAS SMITH: Speaking as a member of an "impractical" discipline, I find myself agreeing with both Dr. Gilbert and Dr. Kantrowitz with regard to this trend toward increasing salaries. You see, historians are not being called away from university campuses. If the science and engineering staffs are getting higher salaries to keep them on the campuses, so also, by a trickle-down process, will the historians receive salary increases.

I have a couple of ideas I would like to toss out here regarding the more efficient use we can make of the more money we would like to see spent on space research and development. Specifically, I am going to discuss a couple of obstacles in our traditional thinking that ought to be removed. The first of these obstacles will be appreciated if we look back at the good old days of the propeller-driven airplane when we had experts called "aircraft engineers." Then if we look at the environment of today, we discover the experts are called in the newspapers "space scientists."

To describe this apparent change in another way, I notice that we hear a great deal about the need for more "pure science." But we don't hear very much about the need for more "pure engineering." I think we are victims of an old tradition that places the thinker on one plane and the doer on another--and the doer is definitely on the lower level. Then we proceed to the conclusions, rather uncritically, that the best science is pure and that normally it is to be found in its best

form in a free society dedicated to the welfare and dignity of every individual. Well, speaking as a historian of science, I can only say, "Balderdash!" because the history of science provides a massive, documented denial of these weird presumptions of the character of science and the character of engineering.

Nevertheless, we continue to accept the traditional images out of a kind of cultural inertia. They are images that let us set up a neat distinction between basic research on the one hand and applied research on the other. Science versus engineering! "Longhaired egghead" versus nuts-and-bolts "do-it-yourselfer!" What a misleading dichotomy that is! A Platonic fallacy, so to speak. And the history of science and technology shows it to be a fallacy over and over again.

The second obstacle to our thinking is another traditional idea, the concept of the "creative genius." Curiously, the mystifying creative genius is about the only engineer who is capable of competing with the scientist for popular prestige and reverence. We all know about Thomas Edison and James Watt. I recall in a book I had as a boy a picture of James Watt as a child. He was contemplating a teakettle lid that was bouncing up and down because of the steam inside. Child prodigy preparing for his future! So romantically appealing--and so inaccurate.

Then there is Newton and his falling apple that touched him like a fairy's wand. Or the Wright brothers and their childhood fascination with kites. I think it was Wilbur Wright who indeed said they did have this interest in kites. Surely they weren't the first or the only boy experts with kites, yet the episode becomes important, after they have won fame.

Consider Galileo: There he is, where tradition has placed him, up on top of the tower with cannon balls in hand--an unsupported story that no scientist would accept if he applied the standards of verification required in his professional work. If we accept such stories and such simplified descriptions of creativity and invention we are victims of fraud.

With such mistaken notions abroad about the character of the inventive process and about the difference between pure and applied research, it was, I am sorry to say, natural in the course of events that one of the President's Cabinet Secretaries in the past could disdain publicly any interest in why potatoes turn brown when fried.

I am sure you remember the days in recent research and development activities when "space" was a bad word and "Far Side" (referring to the now-photographed backside of the moon) was taboo. And there was a period when basic research had to masquerade as development in order to be carried on with federal funds. My reason for making these remarks comes down to this: Research and development, as it is practiced and as it is performed, does not correspond to many of our judgments about it that we have inherited. Had the Cabinet Secretary realized this, he might not have been trapped by his own acceptance of the Platonic fallacy into disdaining the question of why fried potatoes turn brown.

Research and development--the creative process--deserves to be better understood than it commonly is. As it becomes better understood, the rate of advance in advanced propulsion and in many other areas is going to increase, and research and development will become more efficient. It will become more efficient because many of our engineering schools are placing more emphasis

upon technical knowledge of a fundamental nature. They are converting the engineer into more of a "thinker," but they are continuing to emphasize the necessity that he must do as well as think. More instruction in mathematics and more powerful use of mathematics are being encouraged.

Among administrators and business management, research was never in higher repute than it is today. And it was never more highly subsidized. This is a trend that is only just getting started in the long-run history of science and technology. Among administrators, there will be less concern with such superficial problems as wasteful duplication--whatever that is--in research. There will be more concern to keep every technical man as fully and widely informed as possible in his own field and in any other field that appears relevant. Wasted effort will be most efficiently avoided when good men work in an environment that encourages the widest exchange of information.

Executives will continue to speak publicly, I am sure, about requirements and schedules and expectations, but in their supported programs and their allocation of funds, requirements and political needs will dominate their judgment less, while operative functional analysis of the path along which they wish the work to progress will provide more effective guidance. They will increasingly recognize and avoid frustrating expectations. We take it for granted that today's executive does not expect his Boxer pup to start talking; he is not frustrated about it. As affairs progress, he won't expect, say, the director of ARPA, of Research and Engineering and of the Guided Missiles Committee to state explicitly where their functions stop overlapping in the Department of Defense. As affairs progress, every executive will speedily perceive, for example, that the policy for a national space program that President Eisenhower publicly described within the first six weeks after the first Sputnik went up is the same policy he has followed ever since. Every executive will recognize that this policy and the persisting desire of the President to balance the budget provide the best key to the major events that have occurred at the national level in the allocation of funds and authority for the national space program.

The creative process is not a compartmentalized activity. It is not applied research versus basic research. It is one continuous spectrum, ranging from intellectual abstractions at one extreme to concrete tools at the other. The best research and development organization will be the one staffed with the diversity of personnel and the diversity of personal talents that will enable it to scan the research and development spectrum continuously from end to end and--this is essential--then communicate the resulting insights throughout its staff, from end to end.

If a research and development organization disabuses itself of the Platonic fallacy that I have described, and if it disabuses itself of the mistaken notions that prevail about the nature of inventive genius--well, I still must admit that a firm can go broke. But, of those that don't go broke, the most advanced will be utilizing the entire spectrum of the creative process, and we shall be moving out into the reaches of space far more rapidly than we are at present.

DR. ARTHUR KANTROWITZ: That was a beautiful statement. I think that here, again, when you listen to Platonic fallacies it is good to remember this quotation I like so much. "What is honored in the country will be cultivated there." One of the things really important is to see to it that in this country engineering is more honored than it now is.

One of the vital aspects of our space program is the business of whether or not it is really an urgent task to put man in space at the earliest time. This is a critical question, because if it is not urgent, if there is no point in having manned space vehicles, our space program immediately becomes much cheaper. If it is really a critical point, then our space program can indeed use more money.

One of the important positions that has been taken in defense of this country's space program, that I, at least, regard as currently inadequate, is that man in space is not terribly important. I would like to ask General Boushey to talk to this point.

BRIGADIER GENERAL HOMER A. BOUSHEY: The title of this panel I see is "Progress in Propulsion." First, as the No. Seven panelist I suggest we change the title to "Seven Angry Men." Then I would like to go on to make five points, trying to keep within four minutes, plus one minute of grace and a minute of peace.

Someone recently said we might wake up to the tragedy of losing the next war. If I can go back in a serious vein, perhaps that is not what we, as Americans, are really concerned about. We would not worry so much about losing the next war; we might be worried about losing our refrigerators, the second car in the garage, and those things that we really seem to value. As whoever said it: "Give honor to things you really think are important,"--that is my first point. I think we do face a tragic situation if we do not change our ways.

The second point is trying to decide what the military thinks are the military requirements in space. I would just like to put down four things that I call axioms or corollaries of Air Force policies. Maybe the last one is a little of my own; I won't blame the Air Force for it. The four go this way: "Space is a location, not a function." I am sure you have heard this. Next, "It is an indivisible medium which goes up." It is not like the sea where there is an "under" the sea, "surface" of the sea, and an "above" the sea. There is no clear plane of demarcation which separates the air from space. It is a gradual thing. I can visualize man going into space. Suddenly he realizes he is no longer being supported; he has been changed over and is supported by other laws--Kepler's, Newton's--that don't apply the same way as in the atmosphere. The third axiom, if I can use the corollary, would be in the military, "Well, let's not use space unless there is some good reason to use it." It must do something better than another medium, another location. For example, maybe we can use an underwater cable to transmit messages from here to there better than a communication satellite. We may even want some redundance. But, just because space happens to be glamorous, let's not go out of our way to do it by space means when other means are better. My last axiom is "Man will find a very useful role in space." If we don't believe that, why are we making this tremendous effort, which, in the final analysis, is to get man off this planet?

Point No. 3. Here, again, is this angry man stuff--science versus the military--and the thinking (that is, the military mind of thinking): "Is everybody a Colonel Blimp just because he happens to wear a uniform and is there a conflict between military aims and scientific aims?" I don't think so. I think, historically, science and the military have been joined hand-in-hand. I will give you two or three examples. . . . . The Lewis and Clark expedition; Admiral Byrd's expeditions to the North and South Poles; and Captain Cooke and his South Sea discoveries. These were all military-scientific combined missions. I think we can help each other.

All branches of the military have a great deal to offer science, and science has a great deal to offer the military. Why argue about it. Let's get on with the job.

To give you an idea of this, Dr. Gilbert mentioned the upheaval which dollar competition is creating in industry. What do you think it does to our military boys? Some of them have 18 or 19 years' service, and you may keep them on another year until they can retire. But you don't have a very good chance, with military pay, of keeping a man with a Masters or Ph. D. in the service with these attractive offers.

And, next: "What is there about a military mind that is any different than anyone else's?"

The other day we had a meeting in the Pentagon and one chap was a lieutenant colonel. He was in uniform, but I guess they thought they would impress us. They introduced him as "doctor" rather than "lieutenant colonel." Someone said, "You know what this means?" "Yeah," I said, "I know." "Well, I'll tell you anyway." I listened and he had a good point. But a doctorate means that sometime, probably in the past, he did something and they gave him a doctorate. Now, a lieutenant colonel doesn't mean it was 20 years ago, or 25. He had to go through the grades of a second lieutenant, first, captain, major, and lieutenant colonel; and yet, they thought they were impressing the audience by calling this man "doctor" instead of "lieutenant colonel."

Item No. 4. A long time ago I was an engineer. I do not pretend I could even work a slide rule now; but there are different ways of thinking, and I say there is an advantage to instinctive thinking. It often gets you in trouble, but sometimes it brings results where even the computer won't. I think it is just as valid to extrapolate from the impression to our natural senses as it is to extrapolate a formula from a vague hypothesis.

Now let me get to my next-to-the-last point. Let me, on past experience--personal, if you will--try to extrapolate into space, using intuitive feelings. The first thing you will say, I am sure, is: "How can you be intuitive about space? You ain't been there." Granted, no one has. But, then, neither have the engineers, scientists, and philosophers. However, every pilot and everyone who has ridden an airplane has experienced, almost without exception, everything you can think of in space, to a lesser degree, such as short periods of weightlessness (I have had about 15 seconds) and high g forces (I've been up to 10), and, also, a person can get air sick. I think it will be much the same as space sickness, only I expect a space-sick guy is going to be much sicker. Airplanes fly fast, they fly high, they fly far. A satellite goes higher, it goes faster, and it goes further; but it is more or less of the same--more of the higher, faster, further, but less of the density and less of the bumps. So, let's think of these things.

I don't think getting into space is going to be such a terrific problem. The one thing your natural senses will not tell you is whether or not you are being radiated to death. They might tell you if you are getting a fast lethal dose; but at a lower rate, you can't even tell it in the dentist's x-ray room. Generally, though, I think one can extrapolate intuitively and visualize a space environment--which brings me to my last point.

Will man be useful in space? My own view is very definite. Let me give you a few reasons. One, he is a thinking animal. Even octopuses think; and man in space will think. And in my opinion, he can think better than these confounded

machines that are, you know, complicated idiots. Next, he is curious, and he has judgment; and he, above all things, can add to reliability. I won't repeat the joke about the large source of material from unskilled labor, but for a hundred fifty pounds, you get a pretty good computing machine, and, if you only give it a little oxygen, water, food, and so forth, he can fix the transistor, change the tube, and keep the thing going and reliable. I just shudder when I think of millions of dollars fired into space, having people look at it as a monument eternally, and saying, "if only that damn tube hadn't blown, wouldn't that be wonderful." Send a man along--and I hope it will be an Air Force man.

DR. ARTHUR KANTROWITZ: Thank you very much. I like the notion that we constitute seven angry men, seven men with something to be angry about: I think it would be a wonderful thing if someone would figure out a mechanism of making a hundred seventy million angry people, people that are angry about being second in a race, too.

I would like now to ask General Holzman to make a few remarks, closing the meeting.

BRIGADIER GENERAL BENJAMIN G. HOLZMAN: We, at the Air Force Office of Scientific Research hold many symposia throughout the year. I sincerely believe in these symposia. I feel we must get together and get our attention together, orient ourselves on what the latest developments are; stimulate our own scientists to get on with the job.

I want to express my sincere appreciation to the Avco-Everett Research Laboratory for acting as host for the Symposium, especially Dr. Kantrowitz and his staff who helped put it on. I want to thank Paul Atkinson, Milton Slawsky, and others. This has been a first-class symposium. I hope to see you all at our Third Symposium. Thank you very, very much.

AUTHOR INDEX

VOLUME I

VOLUME II

Farber, M.
Fluorine Containing Solid Propellants

Gross, R. A.
A Detonation Wave Hypersonic Ramjet, by W. H. Sargent and R. A. Gross

Huff, G. F.
A Novel Thermochemical Approach to High Impulse

Mager, A.
On Efficient Utilization of Supersonic Combustion in Ramjets, by A. Mager and J. Baker

Mann, David J.
Boron Containing Solid Propellants

Ritchey, H. W.
Design and Cost Estimate for a 10,000,000 – pound Thrust, 60 – second Duration Solid Propellant Booster

Sargent, W. H.
A Detonation Wave Hypersonic Ramjet, by W. H. Sargent and R. A. Gross

Sprenger, D. F.
Large Solid Propellant Rockets

Weber, Richard J.
Comments on Hypersonic Airbreathing Propulsion Papers

VOLUME III

Fairweather, Stephen H.
Space Power Supply Systems

Fraas, A. P.
Fission Reactors as a Source of Electrical Power in Space

Larson, John W.
Nuclear Liquid Metal Cycle Propulsion

Leverett, M. C.
Direct Cycle Nuclear Turbojet

Reynolds, Harry L.
Nuclear Powered Ramjets

Savage, W. F.
Direct Cycle Nuclear Turbojet

Schreiber, R. E.
Nuclear Powered Rockets

Taylor, T. B.
Project Orion

U.S. GOVERNMENT PRINTING OFFICE: 1960 O - 574071